Electroweak Decay of Mesons with Charm

Andreas Pierre Thörn

Thesis submitted for the degree of
Master of Physics

Department of Physics
University of Oslo

June 2006

Acknowledgements

First of all I would like to thank my supervisor professor Jan Olav Eeg for accepting me as a master student, and for all the help with the problems and questions that turned up underway. Many of the question marks that has appeared during the work with this thesis, has been removed or stretched out to exclamation marks, and I am thankful for all the help I've got in trying to understand this, sometimes complicated, matter.

I would also like to give a thank to some of the professors I've had here at the university for their inspiration and for their way of making physics both exciting and interesting. I would especially like to mention professor Carsten Lütken for his inspiring and well explained lectures in quantum field theory.

Secondly, I would like to say that it was not my intension to make this thesis as long as it is. That is rather a logical consequence of the large number of diagram calculations that have been computed in this thesis, and not because of unnecessary long and complicated discussions.

Andreas Thörn

Borgen, May 2006

Preface

This thesis has been written in Microsoft Word, and most of the figures have been drawn in the CAD program DeltaCAD. For the calculations of the Feynman diagrams we have used the analytical program FORM. A program example with some explanation of the program structure is given in the appendix B. For a more detailed explanation of FORM's possibilities see ref. [9]. Most numerical calculations and graphs in the thesis have been calculated using Maple.

In the calculations natural units ($h = c = 1$) have been used, and this also applies for the most part to the discussion of the general theory and models, as we have tried to keep ourselves to the units used in original articles. Only occasionally does $h \neq 1$ and $c \neq 1$ occur, but then it is clear from the context what we mean.

The thesis is organized as follows: we start with a short introduction to some elementary particle physics to refresh some of the concepts and language used, and then move on to a discussion of the Standard model and problems connected with it. We then move into effective field theory, describing Fermi theory, heavy quark effective field theory, chiral perturbation theory and heavy light chiral perturbation theory, which are models either being used directly or leading to models being used. In the next chapter we go through the chiral quark models for light quarks, introduce the gluon condensate, and expand the chiral quark model to also include the vector mesons. This is followed by the heavy light chiral quark model, which includes both the heavy quark effective field theory and the chiral quark model, and end up with the full heavy light chiral quark model Lagrangian. Our next chapter looks into the Feynman rules for the process $D \to V\gamma$, and gives the couplings and effective propagators used in the calculations of the diagrams, and gives an introduction into how we should calculate the diagrams. We then start on the calculations and uses first the Vacuum Saturation Approach to split the diagram in two parts; one part where we have annihilation of the D-meson and one where we have creation of the vector meson. Each of these diagrams are then calculated including different configurations of photons and gluons attached to the loops. Finally they are again combined to give the full diagrams. The results we get form these calculations are then used to f. ex. calculate the decay widths, which we then compare to experimental data.

Abstract

From the time of its introduction, the standard model has become a very well established model in particle physics. In fact, no experiment so far has shown any violation of this model. Still, there are some unsatisfying aspects and open questions that this model cannot explain. For instance, the standard model requires as many as 21 input parameters, depending on your counting scheme [1]. Among these are the coefficients of the Cabibbo-Kobayashi-Maskawa matrix. This is a 3×3 matrix, where the square of the absolute value of its matrix elements, $\left|V_{qq'}\right|^2$, is proportional to the probability for a transition from a quark of flavour q to a quark of flavour q'. We can get information about this matrix by comparing theoretical calculations of decay probabilities to different final states with experimental data from decay of particles containing a heavy quark, for example a D-meson.

What we have done in this thesis is to look at the decay process $D \to V\gamma$, and calculated the amplitudes and decay widths for the process, including the gluon condensate to first order. D is here a heavy-light D-meson, containing a heavy c-quark and one light quark (u, d or s). γ is a photon and V is a vector meson consisting of only light quarks (i.e. V = ρ, ω, φ or K^*). In order to do these calculations we used the heavy light chiral quark model and the chiral quark model for vector mesons. In these models we treated the c-quark as a heavy particle, and disregarded terms including $1/m_c$, as these where considered being small in the theory. As the mass of the c-quark is in the range 1,15 – 1,35 GeV and our energy cutoff was chosen to be Λ = 1 GeV, this could give rise to uncertainties and inaccuracies in the theory.

We then turned to a specific process; $D^0 \to \bar{K}^{*0}\gamma$. This process we approximated as a point interaction using Fermi theory, and using Wilson coefficients to account for the effects of the heavy particle. From this we found that the non-factorizable part of the decay process was slightly dominating over the factorizable one. We next used the VSA factorization limit to split the $D^0 \to \bar{K}^{*0}\gamma$ process to two parts; one which annihilated the D-meson and one which created the vector meson. We then calculated $M = i\mathcal{L}$ for these two types of diagrams separately, with gluons and photons coupled to them when necessary. This gave nine diagrams of the annihilation type and 26 of the creation type. Later these two types of diagrams were combined into a total of 33 full diagrams, and from these we calculated the amplitudes and decay widths, and compared them to experimental values.

What we found from these calculations was that our results for the decay widths where too low (from a factor 137 to 30 times lower) compared to the experimental values. An attempt to adjust any of the parameters used to gain a better value of the decay width, did only result in unphysical values of the adjusted parameters for the process we were looking at. One reason for this, that we discussed, was the value of the factor h_V and how the decay width was affected by the use of the formula for h_V compared to using only the numerical value for it. Apparently the decay width became very sensitive to the value of the gluon condensate when using the equation for h_V, and a slight change in the gluon condensate value (within its uncertainty limits) gave the correct value for the specific process that we were looking at. However, although it also gave clearly less deviation in the decay widths for the other processes we studied ($D^0 \to \rho^0\gamma$ and $D^0 \to \omega\gamma$), it did not gave the correct values, probably meaning that the problem is more complex. The same situation occurred when we looked specifically at the decay width as a function of the constituent quark mass.

An attempt to combine the two, i.e. finding the optimal values of the gluon condensate and the constituent quark mass, by plotting the decay width as a function of these two, showed that it was not possible. Using our data and numerical values of the other parameters, it seemed that we were only able to adjust one of the parameters (condensate or quark mass) once the other had been specified, if we wanted the correct value of the decay width when using the formula for h_V. These small adjustments in the gluon condensate or the mass to get the experimentally correct decay width, was not possible to do when the value for h_V was explicitly put equal to 6.

We also looked at the Cabibbo-Kobayashi-Maskawa matrix elements, and tried in different ways to extract their values from our results. One of these ways was to calculate the ratio between different CKM matrix elements. This approach turned out to give results that agreed quite well with experimental values. Unfortunately, lack of experimental data reduced the number of ratios we could calculate.

Contents

Chapter 1

Introduction

We will start this thesis with a quick summary of some of the elementary parts and concepts used in particle physics and the standard model. The standard model will be studied more closely in chapter 2.

We have 4 fundamental forces; the gravitational, the electromagnetic, the weak and the strong force. Gravitation is usually neglected in particle physics, since its effect on the particles involved is so small. However, theories that do contain the gravitational interactions are being studied. One possible theory of this kind may be sting theory, which incorporates the so called super symmetry (fermions and bosons are being super symmetric partners of the same elementary particle). We will not go any further into that in this thesis, but just continue to disregard gravitational effects.

All of these fundamental forces are mediated by exchange of vector bosons; gravitation by the graviton (which has not yet been found), the electromagnetic force by the photon γ, the weak force by the heavy particles $W^{\pm}$ and Z^0 (depending on whether there is a change in charge in the exchange or not) and the strong force by the gluons g. Table 1.1 [1] gives some of the properties of these exchange bosons.

Table 1.1 Some of the properties of the strong, electromagnetic and weak interactions and their exchange particles.

Interaction	**Couples to**	**Exchange particle(s)**	**Mass (GeV/c^2)**	**Spin and parity (J^P)**
Strong	Colour charge	8 gluons (g)	0	1^-
Electromagnetic	Electric charge	Photon (γ)	0	1^-
Weak	Weak charge	$W^{\pm}$ and Z^0	$\approx 10^2$	1

The photon is electrical neutral and has no mass. The electromagnetic force therefore has an infinite range. The $W^{\pm}$ and Z^0 bosons on the other hand have a mass around 100 GeV/c^2, and consequently have a much smaller range. Furthermore, the $W^{\pm}$ and Z^0 bosons also have a weak charge, which also shortens the range of the weak force. The gluons are, like the photons, massless, but have in addition a charge called colour. This means that the gluons can couple not only to quarks (which also have colour charge), but also to them selves. This give rise to the possibility of having self interaction diagrams like the ones shown in figure 1.1, and it also limits the range of the strong force.

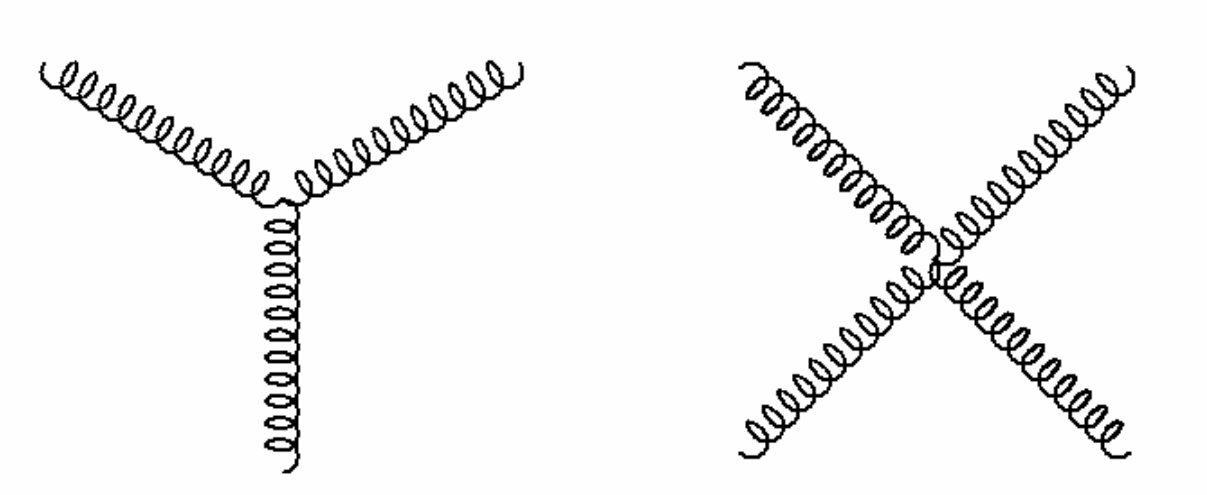

Figure 1.1 Gluon self interaction. Gluons carry colour charge and can therefore couple to each other, as well as quarks.

In addition to the exchange bosons there also exists two other types of fundamental particles according to the standard model, namely leptons and quarks. The reason for classifying quarks and leptons as fundamental particles, comes from the fact that there is no experimental evidence of compositeness (that the particles should be composed of smaller components), such as exited states or form factors associated with an intrinsic structure for these particles.

The two types of particles are both fermions with spin ½. They are grouped in 3 types, families or generations (or any other synonym that one can come up with) according to their mass, and each has its own antiparticle with opposite electric charge, colour and third component of the isospin (or isotopic spin), but with otherwise equal properties as their counter particles. Isospin is a quantum number coming from the fact that certain groups, or multiplets, of particles behave identically with respect to the strong or weak force. Particles belonging to such a multiplet can be described as different states of the same particle. These states are characterized by the quantum number isospin. Table 1.2 shows some of the quarks and leptons properties [1].

Table 1.2 Properties of the quarks and leptons, and their grouping into families.

Fermions	Family			Electrical charge (e)	Colour	Weak isospin, T		Spin
	1	2	3			Left handed	Rigth handed	
Leptons	ν_e	ν_μ	ν_τ	0	-	1/2	-	1/2
	e	μ	τ	-1	-	1/2	0	1/2
Quarks	u	c	t	+2/3	r, b, g	1/2	0	1/2
	d	s	b	-1/3		1/2	0	1/2

As one can see from the table above, unlike the leptons, quarks do not appear uncharged. The different types of quarks (u, d, s, etc) are usually referred to as flavours.

As mentioned earlier quarks have colour charge, which is necessary for the Pauli principle to be fulfilled. We can see this by looking at the Δ^{++} resonance. The Δ^{++} consists of 3 u-quarks and has a total spin of 3/2 and positive parity, it is in fact the lightest baryon (particles consisting of 3 quarks) with $J^p = 3/2^+$. We can therefore assume that its orbital angular momentum is $l = 0$, so its spatial wave function is symmetric. In order to get total spin $J = 3/2$ all the quarks spins must be parallel, and that gives a spin wave function which also is

symmetric. In addition, if we exchange two quarks the situation will not change, so the wave function is symmetric under the interchange of two quarks, and the resultant total wave function seem to be symmetric, in conflict with the Pauli principle. By including the colour charge of the quarks, that is, giving each quark its own colour (usually called red (r), green (g) and blue (b)) the Pauli principle can be fulfilled. For antiparticles we get same situation but with anti-colours.

A weak interaction can transform a lepton into its family neutrino as well as transforming quarks of one flavour into quarks of another flavour, f. ex. a d-quark transforming into a u-quark, as is the case in β-decay. In all such processes the identity of the lepton or quark changes, as well as its charge by +1e or -1e. Such reactions are described by the term *charged currents*. This was for a long time the only known sort of weak interaction. We now know that weak interactions also can proceed via the exchange of the electrical neutral Z^0 bosons. In that case the leptons or quarks are not changed, and we refer to this as *neutral currents*.

When describing a process involving charged currents, one usually refers to it as being leptonic, semi-leptonic or non-leptonic. A leptonic process is one where the W boson only couples to leptons, a semi-leptonic process is one where it couples to both leptons and quarks, and a non-leptonic process is one where the W boson couples only to quarks. The process we will look at, $D \rightarrow V\gamma$, is of this latter type. This does not mean, however, that processes involving charged currents are the only type of processes we can have for $D \rightarrow V\gamma$. We can also have processes involving neutral currents. However, these are more exotic and will not be studied in this thesis.

Chapter 2

The Standard Model

The standard model (SM) describes the fundamental particles in nature and their interactions, and has become well established in particle physics. In fact, no experiment so far has shown any violation of this model. However, there are some unsatisfying aspects and open questions that this model cannot explain. We will mention some of these at the end of this chapter.

The SM is a $SU(3)\times SU(2)\times U(1)$ gauge theory which combines the electroweak theory and quantum chromodynamics (QCD). The SU(3) is the colour symmetry group, while $SU(2)\times U(1)$ is the weak isospin and weak hypercharge symmetry. The gauge groups describes all possible local symmetry transformations that the theory can be exposed to and still keep the Lagrangian invariant. Thereof the name "gauge". The Lagrangian must also be globally Lorentz invariant, in order to use relativistic mechanics in the description.

2.1 Electroweak theory

The electroweak theory is a combined theory for the electromagnetic and weak interactions, as two sides of the same interaction. It was first introduced in the 1960's by Sheldon Glashow, Steven Weinberg and Abdus Salam, and is therefore also called the Glashow-Weinberg-Salam (GWS) theory for weak interactions. It is the experimentally correct spontaneous broken gauge theory that describes the weak interactions.

If we group the quarks into families according to mass and charge, and look specifically at quark transitions in weak decays, we will see that transitions are mainly within the family, and to a much lesser degree to other families.

$$\begin{pmatrix} u \\ d \end{pmatrix} \quad \begin{pmatrix} c \\ s \end{pmatrix} \quad \begin{pmatrix} t \\ b \end{pmatrix} \tag{2.1}$$

An explanation for this was first given by Nicola Cabibbo in 1963, before the introduction of quarks. Cabibbo gave here an explanation of why we get a lower value of the coupling constant in the process s → u (20 times lower) than in the process u → d, in semi-leptonic hadron decays [1].

We look at Cabibbo's explanation from a more modern point of view, and chose to define a state $|\mathrm{d}'\rangle$, as a "partner" of the flavour eigenstate $|\mathrm{u}\rangle$. This state $|\mathrm{d}'\rangle$ is a linear combination of the states $|\mathrm{d}\rangle$ and $|\mathrm{s}\rangle$. We also define a similar "partner" state for the c-quark as a linear

combination of $|s\rangle$ and $|d\rangle$, orthogonal to $|d'\rangle$, called $|s'\rangle$. These states, $|d'\rangle$ and $|s'\rangle$, are actually quark states in the basis that diagonalize their Higgs coupling. This basis is also the physical one, since it diagonalizes the mass matrix (a matrix whose eigenvalues gives the physical mass of the quarks). But more on that later.

By looking at the quark eigenstates $|d'\rangle$ and $|s'\rangle$ of W exchange, we will see that these are related to $|d\rangle$ and $|s\rangle$ of the strong interaction by a rotation through an angle θ_C, the Cabibbo angle. Written as a matrix it becomes:

$$\begin{pmatrix} |d'\rangle \\ |s'\rangle \end{pmatrix} = \begin{pmatrix} \cos\theta_C & \sin\theta_C \\ -\sin\theta_C & \cos\theta_C \end{pmatrix} \cdot \begin{pmatrix} |d\rangle \\ |s\rangle \end{pmatrix} \tag{2.2}$$

The experimental value of θ_C, which can be determined by comparing the lifetimes and branching ratios of some leptonic and hadronic decays of different particles (see figure 2.1), gives

$$\sin\theta_C \approx 0,22 \quad \text{and} \quad \cos\theta_C \approx 0,98 \tag{2.3}$$

From these values we can see that for example the transitions c ↔ d or s ↔ u (outside family) compared to c ↔ s or d ↔ u (inside family) are being suppressed by a factor of

$$\frac{\sin^2\theta_C}{\cos^2\theta_C} \approx \frac{1}{20} \tag{2.4}$$

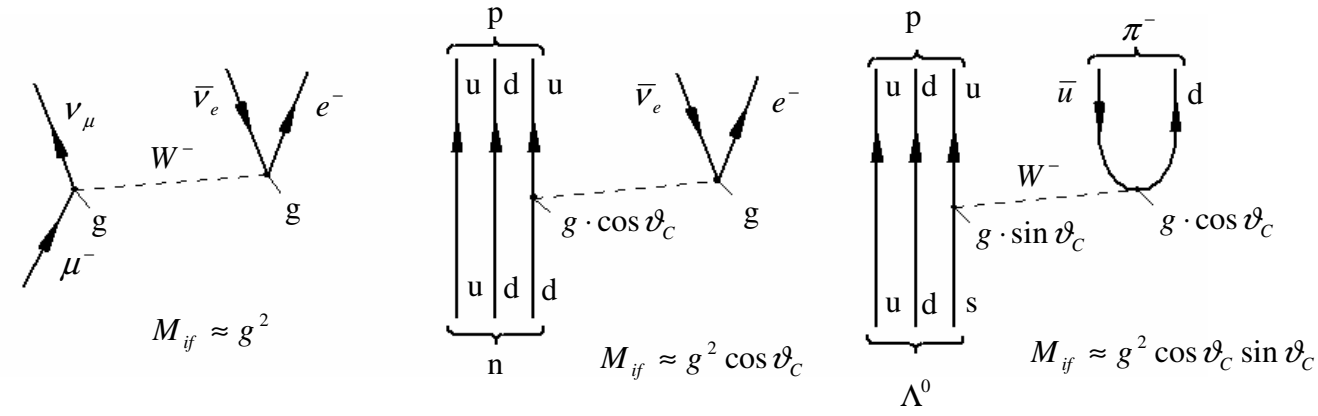

Figure 2.1 Different leptonic and hadronic decay processes used in determining the Cabibbo angle.

If we add a third generation of quarks $\begin{pmatrix} t \\ b \end{pmatrix}$ the 2x2 matrix in equation (2.2) is being replaced by a 3x3 matrix. This matrix is called the Cabibbo-Kobayashi-Maskawa matrix or the CKM-matrix, and has the following form

$$\begin{pmatrix} |d'\rangle \\ |s'\rangle \\ |b'\rangle \end{pmatrix} = \begin{pmatrix} V_{ud} & V_{us} & V_{ub} \\ V_{cd} & V_{cs} & V_{cb} \\ V_{td} & V_{ts} & V_{tb} \end{pmatrix} \cdot \begin{pmatrix} |d\rangle \\ |s\rangle \\ |b\rangle \end{pmatrix} \tag{2.5}$$

The square of the absolute value of a matrix element, $|V_{qq'}|^2$, is proportional to the probability for a transition from a quark of flavour q to a quark of flavour q'.

The matrix is unitary (meaning that $VV^{\dagger} = 1$) so all the matrix elements are correlated. By allowing for a phase redefinition of the quark fields, the number of parameters is reduced from nine to four. This convenient parameterization was proposed by Wolfenstein, and uses the fact that $V_{us} = \lambda \approx 0{,}22$ is small, to rewrite the CKM-matrix to order λ^3 [6]

$$V = \begin{pmatrix} 1-\frac{1}{2}\lambda^2 & \lambda & \lambda^3 A(\rho - i\eta) \\ -\lambda & 1-\frac{1}{2}\lambda^2 & \lambda^2 A \\ \lambda^3 A(1-\rho-i\eta) & -\lambda^2 A & 1 \end{pmatrix} \tag{2.6}$$

where $A \approx 0{,}85$ from experiments. The four parameters are now three angles and one imaginary phase (proportional to η). A picture called the unitary triangle is often used to show the correlation between the parameters. From the fact that the CKM-matrix is unitary, one can construct a rescaled relation from the first and third column

$$\frac{V_{ud}V_{ub}^*}{V_{cd}V_{cb}^*} + \frac{V_{cd}V_{cb}^*}{V_{cd}V_{cb}^*} + \frac{V_{td}V_{tb}^*}{V_{cd}V_{cb}^*} = 0 \tag{2.7}$$

If we insert Wolfenstein's parameterization we get

$$(\rho + i\eta) + (-1) + (1 - \rho + i\eta) + O(\lambda^4) = 0 \tag{2.8}$$

This equation can then be represented as a triangle in the complex plane, as shown in figure 2.2 [2].

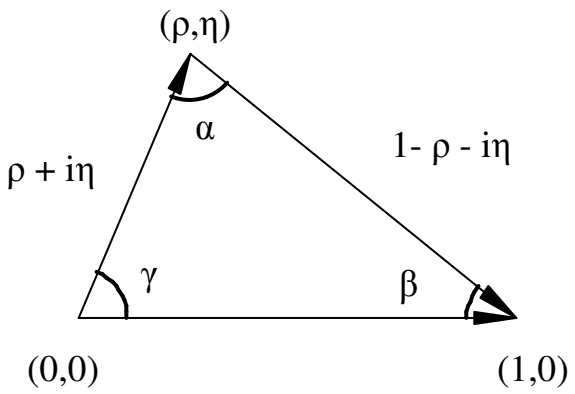

Figure 2.2 The unitary triangle.

The imaginary phase is an indication of a broken CP invariance. CP invariance means that both charge and parity are conserved during a process or decay. Parity transforms a left handed particle into a right handed one, and charge conjugation transforms a particle into an anti-particle. The combination of these two gives the transformation of a left handed particle into a right handed anti-particle. In 1964 it was shown [1] that the CP invariance was broken in neutral kaon decay. Neutral kaons can decay to either two or three pions. The two pion's final state must have positive parity, while the three pions must have negative parity. That means that a CP eigenstate only decays to two pions if and only if CP = +1, and only to three pions if and only if CP = -1.

Experimentally two neutral K-mesons are observed in K^0 decays; K^0_S (for short, referring to the particles short lifetime) and K^0_L (for long). (The lifetimes differ in fact by a factor of 580.) K^0_S decays dominantly to two pions, while K^0_L decays to three pions. In 1964 it was shown that K^0_L also decays to two pions, which means that the same state (CP = -1) decays both to three and two pions. In other words CP invariance is not conserved! It has later been shown that also K^0_S decays to three pions.

Numerical the CKM-matrix can be written [1]

$$\left(\left|V_{ij}\right|\right) = \begin{pmatrix} 0,9745...0,9760 & 0,217...0,224 & 0,0018...0,0045 \\ 0,217...0,224 & 0,9737...0,9753 & 0,036...0,042 \\ 0,004...0,013 & 0,036...0,042 & 0,9991...0,9994 \end{pmatrix} \qquad (2.9)$$

within 90%-confidence limits. The numbers along the diagonal are close to one, as these numbers describe transitions within the family. As we can see, transitions from the first $\begin{pmatrix} u \\ d \end{pmatrix}$ to the third $\begin{pmatrix} t \\ b \end{pmatrix}$ family are highly suppressed.

Weak quark decays, i.e. change of quark flavour (for example c → u), does only proceed through W exchange. Neutral flavour changing currents has never been observed.

According to the electroweak theory the particles or fields (from a quantum field theoretical point of view) are being organized differently in SU(2), depending on if they are left- or right-handed (having spins that are anti-parallel or parallel to the direction of the particles motion). Left handed fermion fields are being organized in doublets, while right-handed fermions end up as singlets. Also the value of Y (U(1) charge) and the third component of the weak isospin, T^3, are different in the two cases. Right-handed fermions get $T^3 = 0$ and Y = the electrical charge, while left-handed fermions gets $T^3 = \pm ½$. Since left- and right-handed fermions exists in different representations of the same gauge group (SU(2)), we consider the components to be different, distinct particles, but as being mixed due to the introduction of the fermion mass fields.

$$\begin{aligned} \begin{pmatrix} \nu_l \\ l^- \end{pmatrix} &\rightarrow \begin{pmatrix} \nu_l \\ l^- \end{pmatrix}_L, (l^-)_R, \ (\nu)_R \\ \begin{pmatrix} q \\ q' \end{pmatrix} &\rightarrow \begin{pmatrix} q \\ q' \end{pmatrix}_L, (q)_R, (q')_R \end{aligned} \tag{2.10}$$

where l = e, μ, τ for the leptons and q = u, c, t and q' = d, s, b for the quarks. As seen form eq. (2.10) we have also included right-handed neutrinos. This is because studies of solar neutrinos indicate that flavour oscillations take place [1]. This would then indicate that the neutrino have a tiny, yet non-vanishing, mass.

2.2 Spontaneous Symmetry Breaking

Symmetries are in general a very important concept in the SM, since they, for example, can be used to extract and organize physical predictions of the theory, and often makes the results (even if the theory has been solved exactly) more comprehensible. In specific, the concept of spontaneous symmetry breaking (SSB) is very important in GWS theory and we will therefore have a closer look at what it means.

If we look at quantum field theory (QFT) and statistical mechanics we will find that there are some analogies between them, for example a scalar field theory can be seen as a continuum description of a system that allows second order phase transitions, for example a ferro-magnet. If we continue this analogue, the QFT system, like the statistical system, might therefore have a field that has non-zero global value (for the magnet it is the direction of the magnetic field). As this global field might also have a direction, it will then violate the symmetry of the Lagrangian. Look for example at the condensation of hot matter into a solid. A collection of gaseous iron atoms will interact randomly because of collisions with no preferred direction. As this iron gas is cooled and allowed to condense into a solid, magnetic crystals will form, where each crystal has its north- and south-pole. This coupling of the atoms introduces a preferred direction in space. In such a case the symmetry is said to be broken or hidden.

As an example of SSB in QFT lets look at a φ^4 theory, which has the Lagrangian

$$\mathcal{L} = \frac{1}{2}\left(\partial_\mu \varphi\right)^2 + \frac{1}{2}\mu^2\varphi^2 - \frac{\lambda}{4!}\varphi^4 \tag{2.11}$$

where the usual m^2 has been replaced by $-\mu^2$. Equation (2.11) has a discrete symmetry; it is invariant under the exchange $\varphi \rightarrow -\varphi$. The corresponding Hamiltonian is

$$H = \int d^3x \left[\frac{1}{2}\pi^2 + \frac{1}{2}\left(\nabla\varphi\right)^2 - \frac{1}{2}\mu^2\varphi^2 + \frac{\lambda}{4!}\varphi^4 \right] \tag{2.12}$$

Classically, the configuration with minimal energy is one with a uniform field $\varphi(x) = \varphi_0$, where φ_0 is chosen in such a way that the following potential is minimized

$$V(\varphi) = -\frac{1}{2}\mu^2\varphi^2 + \frac{\lambda}{4!}\varphi^4 \tag{2.13}$$

The potential is shown in figure 2.3. The minimum occurs when

$$\varphi_0 = \pm v = \pm\sqrt{\frac{6}{\lambda}\mu} \tag{2.14}$$

v is usually called the expectation value of φ.

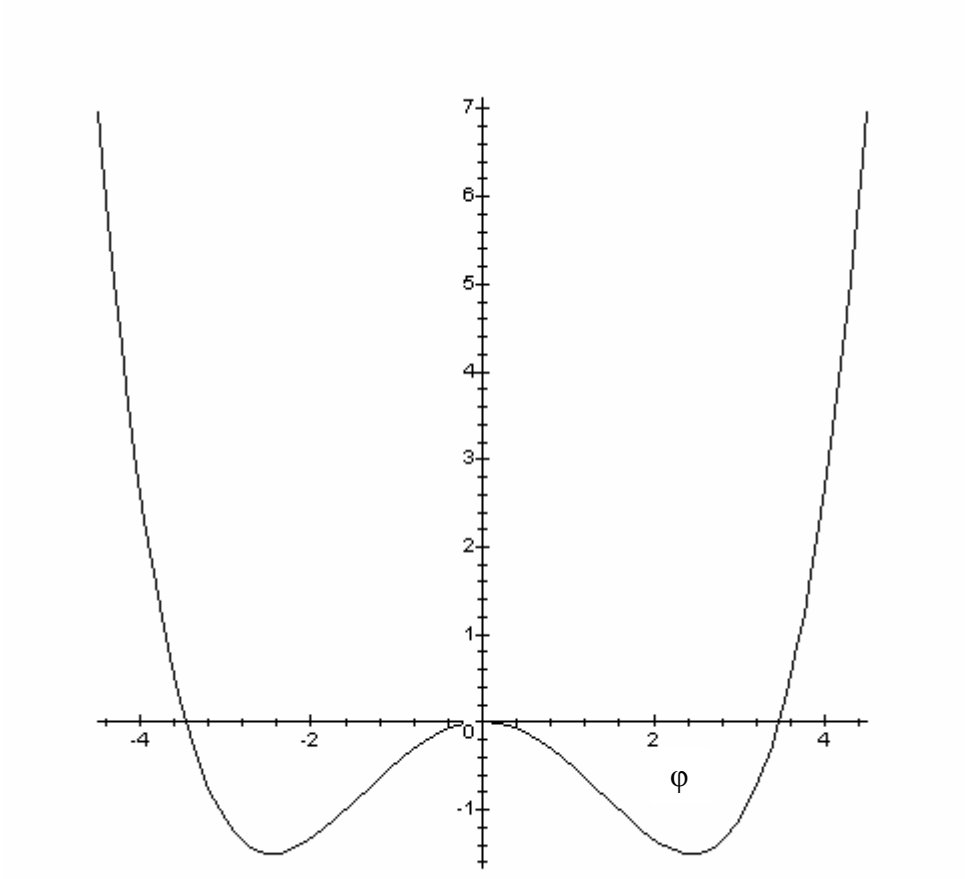

Figure 2.3 The graph shows the shape of the potential V(φ). μ^2 and λ are set equal to 1 for simplicity.

We now suppose that the system is close to its positive minimum. We then choose to write

$$\varphi(x) = v + \sigma(x) \tag{2.15}$$

and rewrites the Lagrangian in terms of σ(x). This gives

$$\mathcal{L} = \frac{1}{2}\left(\partial_\mu \sigma\right)^2 - \frac{1}{2}\left(2\mu^2\right)\sigma^2 - \sqrt{\frac{\lambda}{6}}\mu\sigma^3 - \frac{\lambda}{4!}\sigma^4 \tag{2.16}$$

when we disregard constants. This Lagrangian describes a simple scalar field with mass $\sqrt{2}\mu$ and σ^3 and σ^4 interactions. The symmetry $\varphi \rightarrow -\varphi$ is no longer apparent. Still, the symmetry is there through the special combination of the two parameters v and σ. This is what is called spontaneous symmetry breaking. One can say that the potential hides the symmetry at low energy.

If the symmetry that is broken is a continuous symmetry, then we will have an appearance of massless particles. This is Goldstones theorem, and the massless particles that appear are called Goldstone bosons. If this continuous symmetry is global, the Goldstone bosons will be massless, but if it is a local symmetry, they will be "eaten" by the gaugebosons and become heavy ($W^{\pm}$, Z^0). The fact that SSB generates a mass for the gauge bosons is called the Higgs mechanism.

Now back to the GWS theory. If we start with a theory with SU(2) gauge symmetry (three dimensional rotational symmetry) and introduce a *scalar* field to spontaneously break the symmetry (a spinor representation of SU(2)), we will get a system without massless bosons, but with three massive gauge bosons, as can be seen from the following.

We look at a SU(2) gauge field coupled to a scalar field φ that transforms as a spinor of SU(2). The covariant derivative of this scalar is

$$D_\mu \varphi = (\partial_\mu - igA_\mu^a t^a)\varphi \tag{2.17}$$

where $t^a = \sigma^a/2$, and where σ^a are the usual Pauli matrices. If φ gets a vacuum expectation value this can generally be written as

$$\langle\varphi\rangle = \frac{1}{\sqrt{2}}\begin{pmatrix} 0 \\ v \end{pmatrix} \tag{2.18}$$

The square of eq. (2.17) gives the field's kinetic energy term, and the gauge boson masses arises from this expression when $\varphi = \langle\varphi\rangle$.

$$\left|D_\mu \varphi\right|^2 = \frac{1}{2}g^2 (0 \quad v) t^a t^b \begin{pmatrix} 0 \\ v \end{pmatrix} A_\mu^a A^{b\mu} + \ldots \tag{2.19}$$

By interchanging a and b, and introducing $\{t^a, t^b\} = 1/2\,\delta^{ab}$ we can symmetrize the matrix product and get the mass terms

$$\Delta\mathcal{L} = \frac{g^2 v^2}{8} A_\mu^a A^{a\mu} \tag{2.20}$$

All the three gauge bosons now get the same mass

$$m_A = \frac{gv}{2} \tag{2.21}$$

If we instead had transformed the field φ after a *vector* representation of SU(2), we would have got two gauge bosons with the same mass (W bosons) and one with zero mass (the photon) [7]. One might think that this is a combined model of weak and electromagnetic interaction, but it is not the case since we are missing the Z-boson.

Instead we return to GWS theory. We now know that if we spontaneous break the symmetry by introducing a scalar field that transforms as a spinor of SU(2), this leads to a system with three massive gauge bosons, but with no massless bosons. We therefore introduce a U(1) gauge symmetry in addition. The scalar field gets a charge Y = +1/2 under the U(1) symmetry, and the complete gauge transformation is now

$$\varphi \to e^{i\alpha^a t^a} e^{i\beta/2} \varphi \tag{2.22}$$

If the field φ once again has a vacuum expectation value

$$\langle \varphi \rangle = \frac{1}{\sqrt{2}} \begin{pmatrix} 0 \\ v \end{pmatrix} \tag{2.23}$$

then a gauge transformation with

$$\alpha^1 = \alpha^2 = 0,\ \alpha^3 = \beta \tag{2.24}$$

will make $\langle \varphi \rangle$ invariant, i.e. the theory will contain a massless boson that correspond to this special combination of generators. The other three bosons acquire mass from the Higgs mechanism.

The covariant derivative of the field φ is

$$D_\mu \varphi = \left(\partial_\mu - igA_\mu^a t^a - i\frac{1}{2} g' B_\mu \right) \varphi \tag{2.25}$$

where A_μ^a and B_μ are SU(2) and U(1) gauge bosons, respectively. The coupling constants are called g and g'. The square of eq. (2.25) at the fields vacuum expectation value gives once again the boson mass terms

$$\Delta\mathcal{L} = \frac{1}{2}\frac{v^2}{4}\left[g^2 \left(A_\mu^1\right)^2 + g^2 \left(A_\mu^2\right)^2 + (-gA_\mu^3 + g'B_\mu)^2 \right] \tag{2.26}$$

where we have used $t^a = \sigma^a/2$. There are three massive vector bosons

$$\begin{aligned} W_\mu^\pm &= \frac{1}{\sqrt{2}}\left(A_\mu^1 \mp iA_\mu^2\right) \quad \text{with masses } m_W = g\frac{v}{2} \\ Z_\mu^0 &= \frac{1}{\sqrt{g^2 + g'^2}}(gA_\mu^3 - g'B_\mu) \quad \text{with mass } m_Z = \sqrt{g^2 + g'^2}\,\frac{v}{2} \end{aligned} \tag{2.27}$$

The fourth vector field remains massless

$$A_\mu = \frac{1}{\sqrt{g^2 + g'^2}}(g'A_\mu^3 + gB_\mu) \quad \text{with mass } m_A = 0 \tag{2.28}$$

We associate this field with the electromagnetic vector potential. The covariant derivative can now be written in terms of these expressions, and gives us an expression for the electrical charge and its quantum number.

$$e = \frac{gg'}{\sqrt{g^2 + g'^2}}, \quad Q = T^3 + Y \tag{2.29}$$

We can also define the weak mixing angle, or the Weinberg angle, θ_W, which appears in the expression when we change basis from (A^3, B) to (Z^0, A), i.e. SSB introduces a mixing of the neutral gauge bosons. In addition to give an expression for the coupling constants and the mass relation between m_W and m_Z, this angle also describes the coupling of all the weak bosons using only e and θ_W.

2.2.1 Mass Terms of Fermion Fields and the CKM Matrix

Up to now, we have neglected the mass terms of the fermions. As the GWS theory treats left-handed and right-handed fermion fields differently, we cannot simply put the usual mass terms into the Lagrangian; the different (left-/right-handed) fields have different gauge quantum numbers, so the gauge invariance is broken if we just put in the usual mass terms. From equation (2.29) it follows that once we have specified the value of T^3, the value of Y will follow, meaning that the value of Y will be different for the left- and right-handed components of the quarks and leptons. Also, only left-handed components of the fermion fields couple to the W bosons in GWS theory. So how do we involve the mass terms? The answer lies in SSB.

As we have seen, by assuming that a scalar field φ has a vacuum expectation value we got the mass of the W and Z bosons. This field was a spinor under SU(2), with charge Y = +1/2. Using these quantum numbers we can now link e_L, e_R and φ in a gauge invariant coupling

$$\Delta\mathcal{L}_e = -\lambda_e \overline{E}_L \varphi \cdot e_R + ... \tag{2.30}$$

E_L is here a doublet $\begin{pmatrix} \nu_L \\ e_L \end{pmatrix}$ and λ_r is a dimensionless coupling constant. All the U(1) charges Y sum to zero for the fields. If we now replace φ with φ_0 we get

$$\Delta\mathcal{L}_e = -\frac{1}{\sqrt{2}} \lambda_e v \overline{e}_L e_R + ... \tag{2.31}$$

Where the mass term of the electron is

$$m_e = \lambda_e \frac{v}{\sqrt{2}} \tag{2.32}$$

This is actually a general expression, and since the masses are dependent on v, we expect $m_e \approx m_W$. However, $m_e/m_W \approx 6 \cdot 10^{-6}$, and although the GWS theory allows a small m_e, the difference cannot be explained by this theory.

We can write the mass terms for the quark fields in the same manner. The terms are invariant under SU(2) and have total Y = 0.

$$\Delta\mathcal{L}_q = -\lambda_d \overline{Q}_L \varphi \cdot d_R - \lambda_u \varepsilon^{ab} \overline{Q}_{La} \varphi_b^+ u_R + ... \tag{2.33}$$

with $\varphi = \frac{1}{\sqrt{2}} \begin{pmatrix} 0 \\ v \end{pmatrix}$ we get the masses

$$m_d = \lambda_d \frac{v}{\sqrt{2}}, \quad m_u = \lambda_u \frac{v}{\sqrt{2}} \tag{2.34}$$

Totally we now have the following expression for the mass terms

$$\mathcal{L}_{mass} = -\lambda_e^i \overline{E}_L^i \varphi \cdot e_R^i - \lambda_\nu^i \overline{E}_{La}^i \varepsilon^{ab} \varphi_b^+ \nu_R^i - \lambda_d \overline{Q}_L \varphi \cdot d_R - \lambda_u \varepsilon^{ab} \overline{Q}_{La} \varphi_b^+ u_R \tag{2.35}$$

where i = e, υ, τ, and where the general expression for the mass is

$$m_x = \lambda_x \frac{v}{\sqrt{2}} \tag{2.36}$$

If we now bring further generations of quarks into the picture, we can have further couplings that mix the generations. Alternatively we can diagonalize the Higgs coupling by choosing a new basis for the quark fields. Let

$$u_L^i = (u_L, c_L, t_L), \quad d_L^i = (d_L, s_L, b_L) \tag{2.37}$$

be up and down type quarks in their original basis, and u'^i_L and d'^i_L be quarks in the basis that diagonalizes their Higgs coupling. This basis is the physical one since it diagonalizes the mass matrix. The two bases are related through

$$u^i_L = U^{ij}_u u'^j_L, \qquad d^i_L = U^{ij}_d d'^j_L \tag{2.38}$$

In this new basis the W current gets the following form

$$J^{\mu+}_W = \frac{1}{\sqrt{2}} \bar{u}^i_L \gamma^\mu d^i_L = \frac{1}{\sqrt{2}} \bar{u}'^i_L \gamma^\mu \left(U^+_u U_d \right)_{ij} d'^i_L \tag{2.39}$$

where $\left(U^+_u U_d \right)_{ij} = V_{ij}$ is the unitary CKM-matrix. In SU(2) this is a real rotation

$$V_{ij} = \begin{pmatrix} \cos\theta_C & \sin\theta_C \\ -\sin\theta_C & \cos\theta_C \end{pmatrix}_{ij} \tag{2.40}$$

where the angle θ_C is the Cabibbo angle.

2.3 Quantum Chromodynamics

The most natural candidate for a model of strong interactions is the non-Abelian gauge theory with gauge group SU(3) (an Abelian group is one where all its elements are commuting, in a non-Abelian group they are not), coupled to fermions (quarks) in the fundamental representation. This theory is known as quantum chromodynamics, QCD.

The theoretical picture of the strong interaction began with the identification of the elementary quarks (u and d) making up the proton and neutron. As their properties became better understood, the interactions between the fermions became constrained. This led to the construction of a unique theory, describing the strong interaction between the quarks.

In 1963 Gell-Mann and Zweig presented a model that explained the spectrum of the strongly interacting particles in terms of elementary constituents, the quarks. From this model the mesons was described as a quark-antiquark system, and this was also confirmed to be the case; mesons are spin 0 and spin 1 states with odd parity, as expected from fermion-antifermion states. Baryons became states consisting of three quarks.

To be able to explain electric charge and other quantum numbers, Gell-Mann and Zweig proposed three types of quarks; up (u), down (d) and strange (s). As additional hadrons have been discovered, more types of quarks have been required. These are the charm (c), bottom (b) and top (t) quarks (the last two are sometimes also called beauty and truth). The quark types are referred to as quark flavours.

Since the baryons have integer charge, the quarks need to have fractions of the electric charge; u, s, and t all have charge +2/3 e, while the quarks d, c and b all have charge -1/3 e

(where e equals the absolute value of the electron charge). The numerical values of the charges for u and d, comes from the fact that the hadron with the largest positive charge is Δ^{++}, having charge +2e, and consisting of three u-quarks, while the most negative charged hadron is Δ^{-}, having a charge of -1e, consisting of three d-quarks.

The theory presented by Gell-Mann and Zweig had great success in predicting new hadronic states and in explaining the strengths of electromagnetic and weak-interaction transitions among the hadrons. The quark model naturally incorporates the most important symmetry relations among strongly interacting particles. If one assumes that the u- and d-quarks have equal masses and interactions, then the SU(2) symmetry group that acts as a unitary rotation of u- and d-states, should be a symmetry of the strong interactions. Indeed, both in nuclear and elementary particle physics the quantum states form multiplets of this SU(2) symmetry, called isotopic spin or isospin, as mentioned in the introduction. Since the s-quark is only a little heavier than u- and d-quarks, it makes sense to consider the symmetry of unitary transformations of the triplett (u, d, s). Gell-Mann and Ne'eman showed that the elementary particles naturally fill out irridusible representations of this SU(3) symmetry.

Despite the phenomenological success of the original quark model, two major problems remained: free particles with a fraction charge had not been found, and the total wavefunction of the quark states was symmetric, in conflict with Paulis principle.

As explained also in the introduction, the problem with Pauli's principle was solved by introducing colour to the quarks, i.e. the quarks are assigned to a fundamental representation of a new internal SU(3) global symmetry. If we now disregard spin and flavour, and postulates that all hadron wavefunctions should be invariant under the SU(3) symmetry transformation, the following allowed combinations of quarks appear: $\bar{q}^i q_i$, $\varepsilon^{ijk} q_i q_j q_k$ and $\varepsilon^{ijk} \bar{q}^i \bar{q}^j \bar{q}^k$. Here q is a quark, $\bar{q}$ is an antiquark and i, j, k runs over the colours. This gives that the physical hadrons are singlets under colour, and the only possible light hadrons are mesons, baryons and antibaryons. However, more exotic combinations are possible; for example the pentaquark ($q\bar{q}qqq$) or the tetraquark ($q\bar{q}q\bar{q}$). The reason that colour charges are not seen in free particles is that the three (anti-)colour charges ((anti-)red, (anti-)green and (anti-)blue), as well as a colour and its anti-colour, all sum up to zero colour charge.

But why should quarks have this colour property, and what makes the hadron wavefuntions colour singlets? The answer comes partly from deep inelastic scattering and the discovery of non-Abelian gauge theories having the property of asymptotic freedom (see further down). In deep inelastic scattering no coloured states were observed, and yet we knew that the colour charge had to exist in order for the Pauli principle to be fulfilled. The colour symmetry was identified with the gauge group, and the colour with the gauge quantum numbers of the quarks. This led to a model of the strong interaction as a system of quarks of different flavours, each assigned to the fundamental representation of the local gauge group SU(3). The quanta of this SU(3) gauge field are the gluons, and the theory is called quantum chromodynamics (QCD).

QCD is a theory of strong interactions (the strong sector of the SM), much like QED being a theory of electromagnetic interactions. Like QED, QCD have an effective coupling constant that changes with energy. However, the running of this coupling constant in QCD is the direct opposite of the running of the coupling constant in QED, i.e. while the photon sees more of the change when the energy increases, the gluon sees less of the change.

In QED the running of the coupling constant is due to an effect called screening. Here the vacuum becomes polarized, i.e. real, virtual electron-positron pair creates a cloud of charged pairs that screens the bare charge. The e^+e^--pairs makes the vacuum behave like a dielectric medium, making the bare charge look smaller than it is, at large distances. As the energy increases, we move closer to the bare charge, penetrating the polarization cloud, and sees the bare charge. The effective charge increases as the distance gets smaller. This gives a running coupling constant, which can be shown graphically as a function of distance, as shown in figure 2.4.

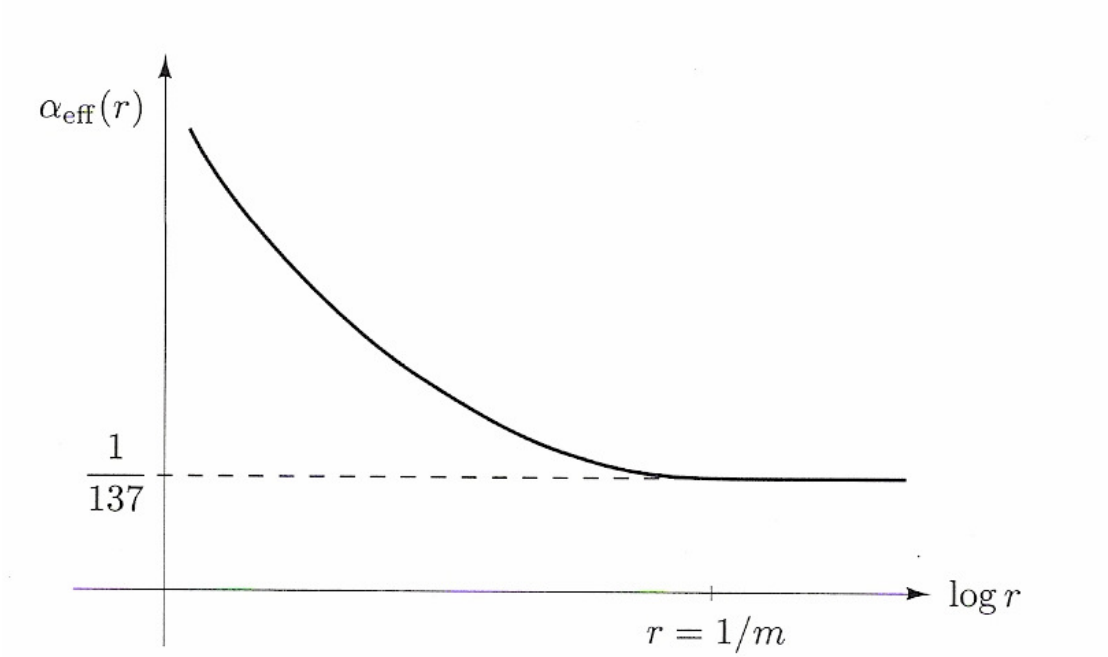

Figure 2.4 A sketch of the effective electromagnetic coupling constant as a function of distance.

In QCD we have in a way the opposite effect, naturally called antiscreening. Like the situation in QED we have virtual particle pairs screening the bare colour charge. In QCD these pairs consists of quark-antiquark pairs. In addition, we have gluons that carry colour charge themselves. The effect of these gluons is, in opposition to the situation in QED, to amplify the field rather than to reduce it, at low energy. The effective colour charge decreases as the distance gets smaller.

But one could ask: shouldn't the $q\bar{q}$-pairs screen the colour charge, like the case in QED? Yes, but the contribution from the gluons dominates. In fact, the antiscreening effect due to the gluons turns out be 12 times [7] as large as the screening effect due to the $q\bar{q}$-pairs. At high enough energy the decreasing of the coupling constant α_S causes the quarks and gluons to behave almost as non-interacting particles, giving the property called asymptotic freedom.

QCD exhibits colour confinement; i.e. the only finite-energy asymptotic states of the theory are those that are singlets of the colour SU(3). This turns out to be a consequence of the non-Abelian gauge theory coupling to colour. It is in a way an opposite property of asymptotic freedom, because at low energy α_S is large and increases with distance. This gives a potential that increases with distance. Separation of colour singlets into colour components is therefore

impossible. If we for example look at a meson and try to separate the two quarks, this will generate a tube of a field between the quarks (see figure 2.5). In non-Abelian gauge theories with strong enough coupling the tube has a fixed radius and energy density, giving an energy cost proportional to the separation. This explains why no free quarks (or free colour charges) are observed.

That does not mean, however, that quarks cannot be separated from each other. As the quarks are pulled further apart the energy in the field is rising, giving, at large enough distance (around 1-2 fm [1]) or energy, rise to the formation of two new quarks that couples to the old ones, forming two new quark pairs or hadrons. This process belong to the type of processes called hadronization.

Figure 2.5 The strong force field between two quarks.

The Lagrangian for QCD is of Yang-Mills type, as QCD is a non-Abelian gauge theory. It has the following form

$$\mathcal{L}_{QCD} = \sum \bar{q}\left(i\gamma_\mu D^\mu - m_q\right)q - \frac{1}{4}G^a_{\mu\nu}G^{a,\mu\nu} \tag{2.41}$$

where the sum goes over quark flavours. D^μ is the covariant derivative

$$D^\mu = \partial^\mu - ig_S t^a A^{a,\mu} \tag{2.42}$$

where t^a are the colour matrices ($t^a = \frac{\lambda^a}{2}$ where λ^a are 3×3 Gell-Mann matrices) and $A^{a,\mu}$ are the gauge fields. The gluonic field tensor

$$G^a_{\mu\nu} = \partial_\mu A^a_\nu - \partial_\nu A^a_\mu + g_S\left[t^a, t^b\right]A^a_\mu A^b_\nu \tag{2.43}$$

gets a third term due to the non-Abelian property of QCD (in Yang-Mills theory this third term comes from the fact that the commutator of, there, the Dirac matrices, are not equal to zero). This is not the case in QED, which is an Abelian field theory, where the electro-magnetic field tensor only has two terms

(2.44)

$$F_{\mu\nu} = \partial_\mu A_\nu - \partial_\nu A_\mu$$

From the third factor of the gluonic field tensor we also get terms in the Lagrangian that correspond to the four gluon self-coupling vertex

$$-\frac{1}{4} g_S^2 \left(f^{ebc} A_\mu^a A_\nu^b \right) \left(f^{ecd} A^{c,\mu} A^{d,\nu} \right) \tag{2.45}$$

and the three gluon self-coupling vertex

$$-g_S f^{abc} \left(\partial_\mu A_\nu^a \right) A^{b,\mu} A^{c,\nu} \tag{2.46}$$

as was mentioned and shown (figure 1.1) in the introduction.

Even though the SM has had great success in many aspects, it is still unsatisfactory in others. We will just mention a few of these. The number of parameters required by the SM is quite large; up to 21 parameters depending on your counting scheme. Some of these parameters are the fermion and boson masses, the coupling constants for the interactions and the matrix elements in the CKM-matrix. These are not given by the SM, but have to be experimentally determined and incorporated ad hoc into the model. The SM also leaves a lot of open questions, such as: why is it exactly three fermion families? Does the Higgs boson exists? What is the origin of the masses of fermions and the Z- and W-bosons? What is the origin of the CP violation? What is the origin of the mixing of quark families, as described by the CKM-matrix? Why do we have just four interactions? These are questions that the SM doesn't answer, and shows that, although the SM gives a very good description of the elementary particles and forces in Nature, it is not a complete model.

Chapter 3

Effective Field Theory

In the case of processes where the energy scales are widely separated, such as in the case of a heavy hadron decaying to lighter mesons, we can look at the low energy behaviour independent of the high energy. We do this by putting large parameters (compared to a relevant energy scale Λ for the theory) to infinity. Infinity means here very large compared to the energy scale Λ. This gives an approximation that can be further corrected by use of small perturbations. In the case where we are looking at the process $D \rightarrow V\gamma$, we let the mass of the heavy c-quark go to infinity, $m_c \rightarrow \infty$ or $1/m_c \rightarrow 0$.

In processes of the type above, several different scales are involved, f. ex. the mass of the decaying D-meson ($m_D \sim 2$ GeV/c^2) and the mass of the exchange boson involved in the process ($m_W \sim 90$ GeV/c^2). The different scales are also often well separated ($m_W >> m_D$). This is the case in many hadronic decay processes, and leads to the fact that different techniques to theoretically calculate the decays, enters at different energy scales.

Effective field theories are theories of the type just described, where low energy physics, i.e. low compared to some characteristic energy scale or cutoff Λ, are being described by a simplified model, rather than a complete theory. Also, we don't even have to know the high energy Lagrangian in order to calculate the low energy dynamics, which makes effective field theories such a powerful tool.

In our calculations the cutoff or energy scale Λ will be 1 GeV, and only relevant degrees of freedom (particles with mass below the cutoff Λ) will be important in these calculations. The higher excitations or heavy scales (particles with mass above Λ, i.e. the c-quark) will be integrated out and contained in the Wilson coefficients (see more about these coefficients in the next paragraph). Using this we can get an effective field theory to describe the interactions of the u-, d-, and s-quarks with the c-quark, which is exactly what we need to study the process $D \rightarrow V\gamma$.

We have to notice though, that all the heavy particle interactions are replaced with local interactions between the relevant degrees of freedom (the light quarks), i.e. the heavy fields are not included in the Lagrangian, but their virtual effects are represented by various couplings between the light fields. The infrared behaviour is retained, but the ultraviolet behaviour will be changed, as these high energy levels are unavailable to our theory. The accuracy of the theory will depend on various parameters, like the energy level we are working in and the mass of the heavy quarks involved.

Effective field theory is a very popular way to describe theories at certain energy levels and is used widely, each being a valid representation of the full standard model in its relevant energy level. One could in fact call older theories without quarks for effective field theories, as these

gives a good description of the interactions at lower energy levels, but becomes less accurate at higher energy levels.

This line of reasoning leads to a philosophical question, namely if it ever will be possible to have a theory that is working on all scales. I will not discuss this question, but only quote a statement made by professor Lütken during a lecture about the renormalization group: *"Quantum field theories without cutoff is nonsense."*, meaning that every theory has some cutoff, beyond where it's not valid any more, and to therefore think that we can get a theory that works on *all* energy scales is perhaps a bit too optimistic. Look for example at Newtonian mechanics. It is only valid as long as the velocity of the bodies involved are less then around 1/10 of the speed of light in vacuum. Above this limit, relativistic mechanics has to be applied in order to get the correct results. The same situation occurs for gravitation; Newton's gravitational laws works fine for apples falling to the ground and other earthbound situations, but when f. ex. calculating exact orbits of planets going around the sun, general theory of relativity has to be applied. When dealing with even more massive phenomena like black holes, and the physics beyond the horizon of the black hole, the general theory of relativity has to be supplied with quantum mechanics in order to give correct results.

3.1 Operator Product Expansion

We continue to look at the general form of effective field theories. Any EFT can be written on operator product expansion form [8]

$$\mathcal{L} = \sum_i C_i O_i \tag{3.1}$$

where O_i are the operators constructed out of the light fields, and the couplings C_i contains all the heavy degrees of freedom (high energy effects above our Λ). These coefficients are referred to as Wilson coefficients, from the physicist Kenneth G. Wilson, the man who's behind this way of formulating EFT's and one of the men behind the renormalization group.

According to Wilson's picture all the parameters in a renormalizible theory can be thought of as being scale dependent quantities. (If one introduces a cut-off, which goes to infinity at the end of the calculation, when calculating divergent integrals in a theory and the physical observables given by the theory are independent of the cut-off, then the theory is called renormalizible.) This dependence is described by simple differential equations called renormalization group equations. Solutions of these equations leads, under certain circumstances, to that the correlation functions of the quantum field having unusual, but computable scaling laws as function of their coordinates.

This means that by introducing a cutoff in the theory we are looking at, we can rewrite the correlation function using an efficient Lagrangian, $\mathcal{L}_{\text{eff}}$, instead of the full Lagrangian, $\mathcal{L}_0$, that we had before the introduction of the cutoff. We usually say that the terms in $\mathcal{L}_{\text{eff}}$ is a set of local operators, O_i, that can be added as perturbations to $\mathcal{L}_0$.

Using a combination of integration over high-momentum degrees of freedom with a rescaling of the parameters in $\mathcal{L}_0$, the operation can be rewritten as a transformation of the Lagrangian.

By continuing the procedure we can integrate further over another shell of momentum space and transform the Lagrangian further. As the shells of momentum space become infinitesimal (as we approach the cutoff), the transformation becomes continuous. The result of the integrations over high-momentum degrees of freedom of a field theory can then be described as a flow in space of all possible Lagrangians. This is of historical reasons referred to as the renormalization group.

If the operators have coefficients that grow under the recursion we call the coefficients relevant (operators with dimension $d_i < 4$). Coefficients that die away are irrelevant ($d_i > 4$), while those not changing are marginal ($d_i = 4$). The dimension d_i of the operators O_i then determines the dimension of the couplings C_i. This gives, and this is an important point, that the irrelevant operators are also irrelevant for low energy EFT's, while they are relevant at higher energy scales (when energy $>> \Lambda$). Therefore one can neglect the contributions from the irrelevant operators and only take relevant and marginal operators into account.

We therefore begin with a theory where the low energy dynamics are separated from the high energy by a chosen energy scale. Depending on what scale we are working on we can use different techniques for our calculations; at high energy we can put the low energy scales to zero, and when working at low scales we put the heavy scales to infinity. The non-local heavy interactions are then replaced with local non-renormalizable interactions. As mentioned before, we still have the infrared behaviour at low scales, but the ultraviolet behaviour will be changed as these levels are not available, and the high energy dynamics will be imbedded in the low energy couplings.

3.2 Fermi theory

Let's now look at an example of how this approach can be used. In the standard model weak decays proceed via exchange of a heavy $W^{\pm}$ boson between two left-handed currents (one incoming and one outgoing). In Fermi theory, on the other hand, the mass of the boson goes to infinity which reduces the $W^{\pm}$ interaction to a point interaction between the particles involved. This was actually the original description of the weak interaction before the idea of W and Z bosons was introduced. In fact, it was first proposed by Fermi in 1934 to describe the nuclear β-process

$$n \rightarrow p + e^{-} + \bar{\nu}_e \tag{3.2}$$

A standard weak decay in the SM is the process $D \rightarrow K\pi$. It is shown both in the full standard model description and in low energy effective field theory in figure 3.1.

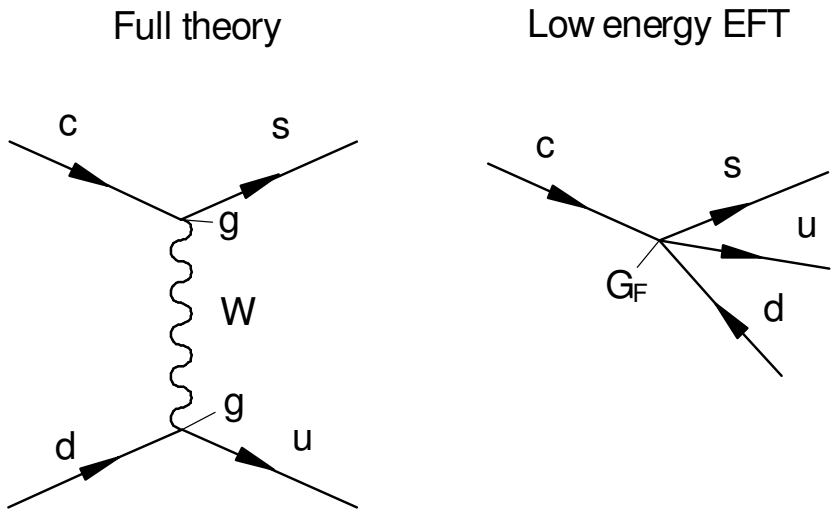

Figure 3.1 Same process both in the full standard model description and in low energy effective field theory.

The strength of the coupling of this low energy interaction is described by the Fermi constant G_F, which satisfies the relation

$$\frac{G_F}{\sqrt{2}} = \frac{g^2}{8m_W{}^2} \tag{3.3}$$

We can use the contact interaction since the momentum transfer carried by $W^{\pm}$ is much smaller that the mass of the boson, $q^2 << m_W{}^2$. In addition, we do not include the W field at low energies (low compared to m_W) since $W^{\pm}$ cannot be produced at such energies. The propagator also changes because of this to

$$\frac{-g_{\mu\nu} + q_\mu q_\nu / m_W{}^2}{q^2 - m_W{}^2} \underset{q^2<<m_W{}^2}{\rightarrow} \frac{g_{\mu\nu}}{m_W{}^2} \tag{3.4}$$

and for an interaction of this type, the effective Lagrangian becomes

$$\mathcal{L}_{\text{Fermi}} = -\frac{G_F}{\sqrt{2}} J^\mu J^\dagger{}_\mu \tag{3.5}$$

where the currents J_μ are the charged weak currents

$$J_\mu = \bar{d}\gamma_\mu(1-\gamma_5)u \tag{3.6}$$

Here d and u are representatives for their families, i.e. u = u, s or t and d = d, c or b. We look at the four particle process in figure 3.1, $c \rightarrow su\bar{d}$. In the limit $q^2 << m_W{}^2$ the propagator is being changed to

$$\frac{1}{p^2 - {m_W}^2} \to -\frac{1}{{m_W}^2} \tag{3.7}$$

In a weak non-leptonic process the Lagrangian is written as

$$\Delta\mathcal{L} = \frac{G_F}{\sqrt{2}} \cos\theta \sin\theta (\bar{s}\gamma^\mu (1-\gamma_5)c)(\bar{u}\gamma_\mu (1-\gamma_5)d) \tag{3.8}$$

But we know that the quarks with charge +2/3e (u, s, t) couples to the quarks with charge $-1/3$ e (d, c, b) by a unitary rotation given by the CKM-matrix. This allows us to write the following expression

$$\Delta\mathcal{L} = \frac{G_F}{\sqrt{2}} V_{ud} V^*_{cs} (\bar{s}\gamma^\mu (1-\gamma_5)c)(\bar{u}\gamma_\mu (1-\gamma_5)d) \tag{3.9}$$

The amplitude now becomes

$$\begin{aligned} A(c \to su\bar{d}) &= i\frac{g^2}{8} V^*_{cs} V_{ud} \frac{1}{p^2 - {m_W}^2} (\bar{s}\gamma^\mu (1-\gamma_5)c)(\bar{u}\gamma^\mu (1-\gamma_5)d) \\ &= i\frac{G_F}{\sqrt{2}} V^*_{cs} V_{ud} (\bar{s}\gamma^\mu (1-\gamma_5)c)(\bar{u}\gamma^\mu (1-\gamma_5)d) + O\left(\frac{p^2}{{m_W}^2}\right) \end{aligned} \tag{3.10}$$

As the mass of the W boson is approximately 80,4 GeV/c^2, we see that the transferred momentum has to be significant in order to give any contribution.

What about our process; D → Vγ? This is also a non-leptonic process, but the decay is here only to one massive particle and not two. If we look specifically at the process D^0 ($c\bar{u}$) → $\bar{K}^{*0}$ ($s\bar{d}$) + γ, we will get the following form for the effective Lagrangian

$$\mathcal{L}_{eff} = -\frac{G_F}{\sqrt{2}} V^*_{cs} V_{ud} [C_1 O_1 + C_2 O_2] \tag{3.11}$$

where the operators O_1 and O_2 has the following form

$$\begin{aligned} O_1 &= (\bar{u}\gamma^\mu (1-\gamma_5)c)(\bar{d}\gamma_\mu (1-\gamma_5)s) \\ O_2 &= (\bar{d}\gamma^\mu (1-\gamma_5)c)(\bar{u}\gamma_\mu (1-\gamma_5)s) \end{aligned} \tag{3.12}$$

and C_1 and C_2 are the Wilson coefficients being of order 10^{-1} and 10^0, respectively. Also note that while O_1 and O_2 are having dimension 6, the Lagrangian in eq. 3.11 has dimension 4 (since G_F has dimension -2). If we now perform a Fierz transformation, using the Fierz identity

$$\delta_{\alpha\beta}\delta_{\rho\sigma} = 2t^a_{\alpha\sigma}t^a_{\rho\beta} + \frac{1}{N_C}\delta_{\alpha\sigma}\delta_{\rho\beta} \tag{3.13}$$

on O_2, which with indices will have the following form

$$O_{2,\alpha\beta\rho\sigma} = (\bar{d}_\alpha \gamma^\mu (1-\gamma_5) c_\beta)(\bar{u}_\rho \gamma_\mu (1-\gamma_5) s_\sigma) \tag{3.14}$$

we get

$$\begin{aligned} O_2^{\text{Fierz}} &= 2(\bar{u} t^a \gamma^\mu (1-\gamma_5) c)(\bar{d} t^a \gamma_\mu (1-\gamma_5) s) \\ &\quad + \frac{1}{N_C}(\bar{u}\gamma^\mu (1-\gamma_5) c)(\bar{d}\gamma_\mu (1-\gamma_5) s) \\ &= 2\tilde{O}_1 + \frac{1}{N_C} O_1 \end{aligned} \tag{3.15}$$

where

$$\tilde{O}_1 = (\bar{u} t^a \gamma^\mu (1-\gamma_5) c)(\bar{d} t^a \gamma_\mu (1-\gamma_5) s) \tag{3.16}$$

If we now insert the Fierz transformed operator O_2^{Fierz} into the effective Lagrangian we get the following expression

$$\begin{aligned} \mathcal{L}_{\text{eff}} &= -\frac{G_F}{\sqrt{2}} V^*_{cs} V_{ud} \left[C_1 O_1 + C_2 O_2^{\text{Fierz}} \right] \\ &= -\frac{G_F}{\sqrt{2}} V^*_{cs} V_{ud} \left[\left(C_1 + \frac{C_2}{N_C} \right) O_1 - 2 C_2 \tilde{O}_1 \right] \end{aligned} \tag{3.17}$$

Using this expression, together with the expressions for the operators O_1 (eq. 3.12) and $\tilde{O}_1$ (eq. 3.16), we can write the amplitude of the process $D^0 \to \bar{K}^{*0} + \gamma$ including the gluon condensate

$$\begin{aligned} \left\langle \bar{K}^{*0}\gamma \middle| \mathcal{L}_{\text{eff}} \middle| D^0 \right\rangle = \frac{G_F}{\sqrt{2}} V^*_{cs} V_{ud} \{ & \left(C_1 + \frac{C_2}{N_C} \right) \cdot \\ & [\left\langle \bar{K}^{*0}\gamma g g \middle| (\bar{d}\gamma^\mu (1-\gamma_5) s) \middle| 0 \right\rangle \left\langle 0 \middle| (\bar{u}\gamma_\mu (1-\gamma_5) c) \middle| D^0 \right\rangle \\ & + \left\langle \bar{K}^{*0}\gamma \middle| (\bar{d}\gamma^\mu (1-\gamma_5) s) \middle| 0 \right\rangle \left\langle g g \middle| (\bar{u}\gamma_\mu (1-\gamma_5) c) \middle| D^0 \right\rangle \\ & + \left\langle \bar{K}^{*0} g g \middle| (\bar{d}\gamma^\mu (1-\gamma_5) s) \middle| 0 \right\rangle \left\langle \gamma \middle| (\bar{u}\gamma_\mu (1-\gamma_5) c) \middle| D^0 \right\rangle \\ & + \left\langle \bar{K}^{*0} \middle| (\bar{d}\gamma^\mu (1-\gamma_5) s) \middle| 0 \right\rangle \left\langle \gamma g g \middle| (\bar{u}\gamma_\mu (1-\gamma_5) c) \middle| D^0 \right\rangle] \\ & + 2C_2 [\left\langle \bar{K}^{*0}\gamma g \middle| (\bar{d} t^a \gamma^\mu (1-\gamma_5) s) \middle| 0 \right\rangle \left\langle g \middle| (\bar{u} t^a \gamma_\mu (1-\gamma_5) c) \middle| D^0 \right\rangle \\ & + \left\langle \bar{K}^{*0} g \middle| (\bar{d} t^a \gamma^\mu (1-\gamma_5) s) \middle| 0 \right\rangle \left\langle \gamma g \middle| (\bar{u} t^a \gamma_\mu (1-\gamma_5) c) \middle| D^0 \right\rangle] \} \end{aligned} \tag{3.18}$$

Here we have actually gone in advance of things a bit, by using the so called VSA factorized limit, which more or less lets us split the total process $D \to V\gamma$ into an annihilation process of

the D-meson and a creation process of the vector particle. We will look more into this in chapter 6.

As one can see from eq. 3.18, the expression is separated in two parts; one factorizable part with a factor $C_1 + \frac{C_2}{N_C}$ in front, and one non-factorizable with a factor $2C_2$ in front. The non-factorizable part is made quasi-factorizable with the use of the colour matrix t^a. In order to see which one of the two parts (the factorizable or the non-factorizable) that is dominant, we have to know the values of the Wilson coefficients C_1 and C_2. These are given from [8, 10] at an energy level $\mu = 1$ GeV, and gives us the following relation

$$\frac{C_1 + \frac{C_2}{N_C}}{2C_2} = \frac{(-0,06) + \frac{1,10}{3}}{2 \cdot 1,10} \approx 0,139 \qquad (3.19)$$

Here we can see that the non-factorizable part is contributing mostly; about a factor seven over the factorizable part. This domination of the non-factorizable part was also found for the B-decay in [5], however, in that case the domination was much larger. The non-factorizable part was dominating about 117 times over the factorizable part. Furthermore, in non-leptonic D-decays (in the charmed sector) the coefficient C_2's dependence on renormalization scheme is much stronger than in B-decays, and both C_1 and C_2 depends much more on renormalization scheme and cutoff $\mu = \Lambda$, than the coefficients in the B-sector. This is due to the larger QCD coupling involved.

However, if we look at the situation in figure 3.1 we see that Fermi theory gives only one operator (see eq. 3.10). This then suggest that at tree level, where $m_W \to \infty$, one of the Wilson coefficients will be equal to 1 and the other equal to 0. As we are working at lower energy levels, we see that this fits reasonably the values of our Wilson coefficients above.

Also note that we cannot use the so called effective values for C_1 and C_2, as one sometimes sees in the literature, because in that case the non-factorizable effects are taken into account in a phenomenological way, i.e. the effects are included in the coefficients. Since these are the effects we are trying to calculate, the effective values for C_1 and C_2 cannot be used.

3.3 Heavy Quark Effective Field Theory

Heavy quark effective field theory (HQEFT) is an effective field theory describing processes where a heavy quark interacts with light degrees of freedom (i.e. the light quarks u, d, s) through low energy gluons, i.e. gluons within the energy range $\Lambda < |p| < m_Q$, where p is the gluon's four-momentum and m_Q is the mass of the heavy quark. For us this means $|p| < m_c$, since the c-quark is the heavy quark in our process.

An important concept in this theory is heavy quark symmetry, which is a property that light hadronic constituents in a system ignore the flavour and spin orientation of the heavy quark in the system, since the heavy quark is surrounded by a cloud of light quarks and gluons. From

this, the properties of the heavy-light meson become independent of the mass and spin of the heavy quark. This symmetry arises when the mass of the heavy quark m_Q goes to infinity, or $\Lambda/m_Q << 1$. Using this we can write an effective field theory at low energies for the heavy quark in inverse powers of m_Q (since $1/m_Q \to 0$ as $m_Q \to \infty$).

A combination of chiral symmetry ($m_q \to 0$, where m_q is the mass of the light quark) and the heavy quark symmetry ($1/m_Q \to 0$), allows us to write an effective field theory which combines the light and heavy quarks. The symmetries of these effective field theories will then restrict the possible interactions between the quarks, giving a combined theory for the heavy-light mesons. In this theory a heavy quark can be annihilated, but not created, as the energy we are working in is too low for the heavy quark to be produced ($|p| < m_Q$).

At low energies, as we are looking at now, and for very large quark masses ($m_Q = m_c \to \infty$), the heavy quark's momentum can be written as $p = m_Q v + k$, where v is the four-velocity of the heavy quark ($v = (1, 0, 0, 0)$) and $k << m_Q$ is the residual momentum. This phenomenon (the rewriting of the momentum) is known as heavy quark velocity super-selection, and basically means that the velocity of the (heavy-light) meson is unchanged by QCD interactions. As the heavy quarks velocity always is equal to the velocity of the meson [5], the heavy quarks velocity is also unchanged by QCD interactions. In addition we have $v \cdot v = 1$.

If we look at the usual propagator for the Dirac theory

$$S(p) = \frac{\gamma \cdot p + m}{p^2 - m^2} \tag{3.20}$$

we will get the following transformation in the heavy mass limit

$$\begin{aligned} S_{HQ}(p) = \left.\frac{\gamma \cdot v + m_Q}{p^2 - m_Q{}^2}\right|_{p = m_Q v + k} &= \frac{\gamma \cdot m_Q v + \gamma \cdot k + m_Q}{k^2 + 2 m_Q v \cdot k} \\ &\underset{k << m_Q}{\to} \frac{\gamma \cdot v + 1}{2 v \cdot k} = \frac{P_+(v)}{v \cdot k} \end{aligned} \tag{3.21}$$

where the projection operators $P_\pm$ is defined as

$$P_\pm = \frac{1}{2}(1 \pm \gamma \cdot v) \tag{3.22}$$

From this one can see that the heavy quark projection operator is independent of flavour and mass of the quark, and thus have the heavy quarks flavour symmetry, as mentioned earlier. The spin symmetry can be seen from the following relation

$$P_+ \gamma^\mu P_+ = P_+ v^\mu P_+ = v^\mu P_+ \tag{3.23}$$

which in turn leads to the transformation of the quark-gluon vertex

$$ig \frac{\lambda^a}{2} \gamma^\mu \to ig \frac{\lambda^a}{2} v^\mu \tag{3.24}$$

So the interaction is independent of the spin of the heavy quark.

Since the heavy quark field doesn't have enough energy to create heavy quarks, we can split the field Q in two parts, Q_v and R_v.

$$Q(x) = (P_+ + P_-)Q(x) = e^{-im_Q v\cdot x}(Q_v(x) + R_v(x)) \tag{3.25}$$

where

$$Q_v(x) = e^{im_Q v\cdot x}P_+Q(x) \quad \text{and} \quad R_v(x) = e^{im_Q v\cdot x}P_-Q(x) \tag{3.26}$$

Q_v is the part we gain from splitting of the large mass of the field. From the equation of motion for the heavy quark field we have $\gamma\cdot vQ_v = Q_v$ and $\gamma\cdot vR_v = -R_v$, or in terms of the projection operators $P_+Q_v = Q_v$ and $P_+R_v = 0$. The term Q_v is called the large component field or the reduced field. This field annihilates a heavy quark with velocity v. The term R_v is called the small component field and creates a heavy anti-quark with the same velocity v. For a heavy anti-quark we have

$$\begin{aligned}\bar{Q}_v(x) &= e^{im_Q v\cdot x}P_-Q(x)\\ \bar{R}_v(x) &= e^{im_Q v\cdot x}P_+Q(x)\end{aligned} \tag{3.27}$$

Since heavy (on shell) quarks cannot be created at this level of energy, the R_v field can be integrated out. If we use the Euler-Lagrange equation

$$\partial_\mu\left(\frac{\partial\mathcal{L}}{\partial(\partial_\mu\varphi)}\right) - \frac{\partial\mathcal{L}}{\partial\varphi} = 0 \tag{3.28}$$

for the fields, we get the following equation of motion when we take $\varphi = Q$

$$(i\gamma\cdot D - m_Q)Q(x) = 0 \tag{3.29}$$

for the Dirac field Q. If we now only use the reduced quark field Q_v instead, we end up with the following equation of motion

$$v\cdot DQ_v = 0 \tag{3.30}$$

instead of eq. 3.29. Using this equation of motion and the energy propagators, we can express the term R_v as

$$\begin{aligned}R_v &= \frac{1}{2m_Q + i(v\cdot D)}i(\gamma\cdot D_\perp)Q_v\\ &= \frac{i(\gamma\cdot D_\perp)}{2m_Q}\left(1 + \mathcal{O}\left(\frac{1}{m_Q}\right)\right)Q_v\end{aligned} \tag{3.31}$$

where we have defined

$$D_{\perp}^{\mu} = D^{\mu} - v^{\mu}(v \cdot D) \tag{3.32}$$

which is the part of the Dirac operator orthogonal to the velocity v.

In order to find the Lagrangian for the theory, we start with the heavy-quark Lagrangian

$$\mathcal{L}_{\text{eff}} = \bar{Q}(i\gamma \cdot D - m_Q)Q \tag{3.33}$$

To this expression we insert the expression for R_v, and get the following Lagrangian

$$\mathcal{L}_{\text{eff}} = \bar{Q}_v i(v \cdot D)Q_v + \bar{Q}_v i(v \cdot D_{\perp}) \frac{1}{2m_Q + i(v \cdot D)} i(v \cdot D_{\perp})Q_v \tag{3.34}$$

We can further expand the Lagrangian in powers of D/m_Q by using

$$\begin{aligned} P_+ i(\gamma \cdot D_{\perp}) i(\gamma \cdot D_{\perp}) P_+ &= P_+ \left\{ (i(\gamma \cdot D_{\perp}))^2 + \frac{1}{2}\left[i(\gamma \cdot D_{\perp}), i(\gamma \cdot D_{\perp}) \right] \right\} P_+ \\ &= P_+ \left\{ (i(\gamma \cdot D_{\perp}))^2 + \frac{g_s}{2}\sigma^{\mu\nu} G_{\mu\nu} \right\} P_+ \end{aligned} \tag{3.35}$$

where

$$G_{\mu\nu} = \frac{\lambda^a}{2} G_{\mu\nu}^a = t^a G_{\mu\nu}^a \tag{3.36}$$

is the gluonic field tensor and the colour matrix, so that $\sigma \cdot G = \sigma^{\mu\nu} G_{\mu\nu}^a t^a$. We now end up with the heavy quark effective field theory Lagrangian, that satisfies both the heavy quark spin and flavour symmetry

$$\begin{aligned} \mathcal{L}_{\text{HQEFT}} &= \bar{Q}_v i(v \cdot D)Q_v + \frac{1}{2m_Q}\bar{Q}_v (i\gamma \cdot D_{\perp})^2 Q_v + \frac{g_s}{4m_Q}\bar{Q}_v \sigma \cdot G Q_v + \mathcal{O}(\frac{1}{m_Q}) \\ &= \bar{Q}_v i(v \cdot D)Q_v + \mathcal{O}_{\text{kin}} + \mathcal{O}_{\text{mag}} + \mathcal{O}(\frac{1}{m_Q}) \end{aligned} \tag{3.37}$$

where

$$\mathcal{O}_{\text{kin}} = \frac{1}{2m_Q}\bar{Q}_v (i\gamma \cdot D_{\perp})^2 Q_v \quad \text{and} \quad \mathcal{O}_{\text{mag}} = \frac{g_s}{4m_Q}\bar{Q}_v \sigma \cdot G Q_v \tag{3.38}$$

are the kinetic and magnetic operators, respectively.

We can now write the full heavy quark field Q(x) as a function of only the reduced field Q_v by eliminating R_v using equation 3.31. This gives the full field

$$\begin{aligned} Q(x) &= e^{-im_Q v\cdot x}(Q_v(x)+R_v(x)) \\ &= e^{-im_Q v\cdot x}\left(1+\frac{1}{2m_Q+i(v\cdot D)}i(\gamma\cdot D_\perp)\right)Q_v(x) \\ &= e^{-im_Q v\cdot x}\left(1+\frac{i(\gamma\cdot D_\perp)}{2m_Q}+\mathcal{O}\left(\frac{1}{m_Q{}^2}\right)\right)Q_v(x) \end{aligned} \tag{3.39}$$

3.4 Chiral Perturbation Theory

Quarks are the fundamental building blocks for hadrons. However, these are not the particles we observe in nature (due to confinement). We only observe the particles built out of the quarks, namely baryons and mesons. In the sector of the lowest pseudoscalar mesons (K, η, π) the interactions can be described in terms of an effective field theory, the chiral Lagrangian, that only include these light states. The chiral Lagrangian and the chiral perturbation theory provide a useful representation of this sector of the standard model, after the quark and gluon degrees of freedom have been integrated out. The form of this effective field theory and all its possible terms are determined by $SU(3)_L \otimes SU(3)_R$ chiral invariance and Lorentz invariance. Terms that explicitly break the chiral invariance are introduced in terms of the quarks mass matrix, M_q. By using hadronic states to describe QCD dynamics instead of using quarks and gluons, we can solve the difficulty of confinement of quarks and gluons at low energy levels, although it brings in a number of undetermined constants. Figure 3.2 gives an illustration of the different energy levels and their corresponding theories.

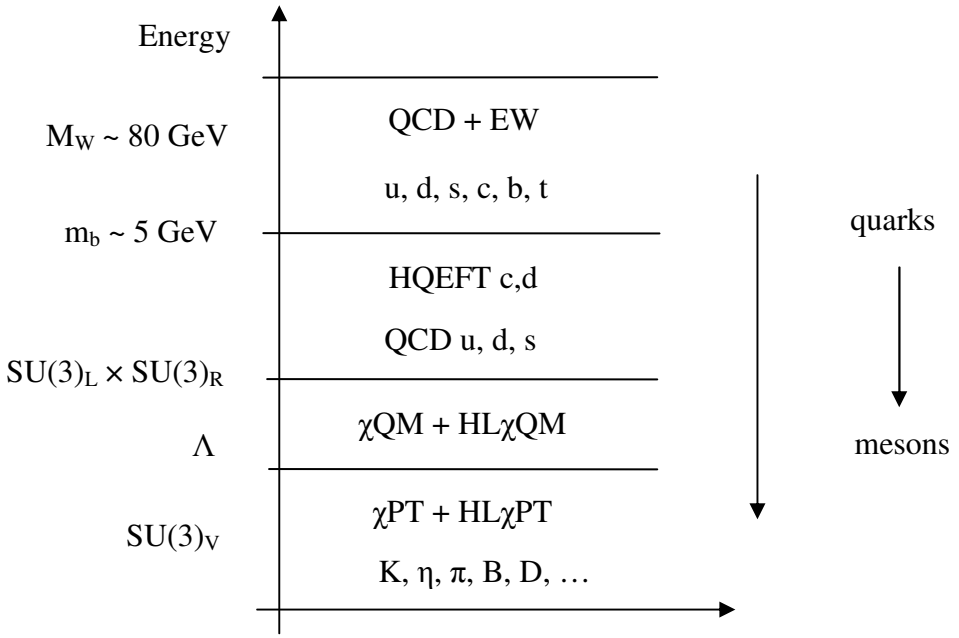

Figure 3.2 Different energy levels and their corresponding theories.

The chiral symmetry is a global $SU(3)_L \otimes SU(3)_R$ symmetry, and it is the symmetry of QCD when the quarks are massless. This is an approximate symmetry of strong interactions in the light quark sector due to the relatively small mass of the quarks (u, d, s).

The term chirality can be explained as follows. A particle's helicity is a quantity determined by whether the particle's spin is in the direction of its momentum, or if it is in the opposite direction. It is defined as

$$h = \frac{\vec{s} \bullet \vec{p}}{|\vec{s}| \cdot |\vec{p}|} \tag{3.40}$$

This quantity can change depending on the position of the observer. The usual way to show this is to say that the observer is located in an inertial system, having a velocity that is greater than the velocity of the particle we are observing. As the observer passes the particle the helicity changes, as the particle's momentum reverses according to the observer. As the mass of the particle goes to zero, f. ex. a photon, we can no longer find an inertial system that moves faster than that particle. We refer to the helicity of this massless particle as chirality, which is either left or right.

If we now neglect the quark masses of the light sector, we will get a QCD Lagrangian of the form

$$\mathcal{L}_{QCD} = -\frac{1}{4} G^a_{\mu\nu} G^{a,\mu\nu} + i\bar{q}_L \gamma^\mu D_\mu q_L + i\bar{q}_R \gamma^\mu D_\mu q_R \tag{3.41}$$

where we now have left- and right-handed components of the quark field behaving as independent fields, and without the Dirac massterm from the Dirac equation 2.41

$$\mathcal{L}_{\text{Dirac}} = \sum \bar{q}(i\gamma^{\mu}D_{\mu} - m_{q})q - \frac{1}{4}G^{a}_{\mu\nu}G^{a,\mu\nu} \tag{3.42}$$

This $\mathcal{L}_{QCD}$ is then invariant under global $SU(3)_L \otimes SU(3)_R$ transformation, with the following transformation of the left- and right-handed components of the quark fields

$$q_L \rightarrow g_L q_L \quad \text{and} \quad q_R \rightarrow g_R q_R \tag{3.43}$$

where

$$g_{L,R} \in SU(n_f)_{L,R} \tag{3.44}$$

Here n_f represents the number of quarks flavours, in this case three (u, d, s).

The approximate chiral symmetry ($m_{u,\,d,\,s} \rightarrow 0$) is not seen in the hadronic sector. While hadrons are classified in $SU(3)_V$ representations (a subgroup of $SU(3)_L \otimes SU(3)_R$ where $g_L = g_R$), opposite parity multiplets (as should exist if they transformed under $SU(3)_L \otimes SU(3)_R$) are not observed experimentally. The octet of pseudoscalar mesons (k, π and η_8) is also much lighter than other hadrons (such as vector mesons), but they are not massless, suggesting that the ground state of the theory should not be symmetric under the chiral group.

This means that the $SU(3)_L \otimes SU(3)_R$ symmetry is spontaneously broken down to $SU(3)_{L+R}$ symmetry, and from Goldstone's theorem an octet of massless (approximate massless compared to other hadronic states) pseudoscalar bosons appear, namely π^0, $\pi^{\pm}$, K^0, $K^{\pm}$, $\bar{K}^0$, $\bar{K}^{\pm}$ and η_8. That there are 8 and not 16 bosons arises from the fact that the number of generators is reduced form 16 to 8 (n^2 -1 from each $SU(n)_{L,R}$ group). The eight pseudo-Goldstone bosons (or would-be Goldstone bosons) coming from the symmetry breaking appears encoded in the exponential representation of the $SU(3)_L \otimes SU(3)_R$ field Σ

$$\Sigma = \xi \cdot \xi = e^{2i\Pi/f} \tag{3.45}$$

or

$$\xi = e^{i\Pi/f} \tag{3.46}$$

where Π is pseudoscalar octet

$$\Pi = \frac{1}{\sqrt{2}} \begin{pmatrix} \frac{1}{\sqrt{2}}\pi^0 + \frac{1}{\sqrt{6}}\eta_8 & \pi^+ & K^+ \\ \pi^- & -\frac{1}{\sqrt{2}}\pi^0 + \frac{1}{\sqrt{6}}\eta_8 & K^0 \\ K^- & \bar{K}^0 & -\frac{2}{\sqrt{6}}\eta_8 \end{pmatrix} \tag{3.47}$$

and f is, to lowest order, equal to the pion decay constant f_π = 93 MeV.

The most general Lagrangian, both respecting chiral symmetry and taken into account the fact that there are strong constrains on the interactions of the would-be Goldstone bosons, has the following form [3]

$$\mathcal{L}^{(2)}_{\text{Strong}} = \frac{f^2}{4}\text{Tr}(D_\mu \Sigma D^\mu \Sigma^\dagger) + \frac{f^2}{2} B_0 \text{Tr}(\mathcal{M}_q \Sigma^\dagger + \Sigma \mathcal{M}_q^\dagger) \tag{3.48}$$

to order $\left(iD_\mu\right)^2$. D_μ is the usual covariant derivative $D_\mu = \partial_\mu - ieA_\mu$ containing the photon field A_μ, and $\mathcal{M}_q$ is the quark mass matrix containing the chiral symmetry breaking quark mass terms

$$\mathcal{M}_q = \begin{pmatrix} m_u & 0 & 0 \\ 0 & m_d & 0 \\ 0 & 0 & m_s \end{pmatrix} \tag{3.49}$$

The quantity B_0, from eq. 3.48, is defined through the quark condensate $\langle \bar{q}q \rangle$ by

$$\langle \bar{q}_i q_j \rangle = -f^2 B_0 \delta_{ij} \tag{3.50}$$

where

$$(m_s + m_d)\langle \bar{q}q \rangle = -f_K^2 m_K^2 \quad , \quad (m_u + m_d)\langle \bar{q}q \rangle = -f_\pi^2 m_\pi^2 \tag{3.51}$$

The field Σ is the same as we had before (eq. 3.45), and it is also unitary ($\Sigma^\dagger \Sigma = I$).

As mentioned in the start of this chapter we get a number of undetermined constants by using hadronic states to describe QCD dynamics instead of using quarks and gluons. To order $\left(iD_\mu\right)^4$ we get a Lagrangian $\mathcal{L}^4$ [2] that contains ten additional coupling constants L_i plus two constants that do not correspond to any physical quantities. These higher order terms of the Lagrangian are those consistent with chiral symmetry.

3.5 Heavy Light Chiral Perturbation Theory

Heavy light chiral perturbation theory (HLχPT) is an application of chiral perturbation theory studied in the last section, to mesons consisting of one light and one heavy quark. This effective field theory is then in turn based on HQEFT.

We start by introducing a meson field, that is, a field that describes the light and heavy quarks in the heavy-light meson in the theory. Let H and $\bar{H}$ represent the mesons in the vertices of the Feynman diagrams. We introduce a ground state vector $P_\mu^{A\bar{a}}$ and pseudoscalar $P_5^{A\bar{a}}$ fields

that annihilates mesons with a heavy quark of flavour A and a light quark of flavour $\bar{a}$. The 4×4 bispinor field that annihilates such a meson can now be written

$$H_{A\bar{a}} = \frac{(1+\gamma\cdot v)}{2}\left(P_\mu^{A\bar{a}}\gamma^\mu - iP_5^{A\bar{a}}\gamma_5\right) \tag{3.52}$$

and is containing a spin zero pseudoscalar boson $P_5^{A\bar{a}}$ ($J^P = 0^-$) and a spin one vector boson $P_\mu^{A\bar{a}}$ ($J^P = 1^-$). The bispinor field that creates a meson with the same flavour configuration as above is

$$\bar{H}_{A\bar{a}} = \gamma^0 H_{A\bar{a}}^\dagger \gamma^0 = \left[(P_\mu^{A\bar{a}})^\dagger \gamma^\mu - i(P_5^{A\bar{a}})^\dagger \gamma_5\right]\frac{(1+\gamma\cdot v)}{2} \tag{3.53}$$

Here $(P_\mu^{A\bar{a}})^\dagger$ represents a spin one vector meson and $(P_5^{A\bar{a}})^\dagger$ a spin zero pseudoscalar meson. By using these two equations (eq. 3.52 and 3.53) one can describe the heavy-light mesons in loop vertices in Feynman diagrams. For anti-particles the degrees of freedom have been integrated out in the HQEFT, so these fields has to be included wherever they might appear.

Fields that destroy or create anti-mesons with the flavour configuration $\bar{A}a$ are $P_\mu^{\bar{A}a}$ for vector (spin 1) mesons and $P_5^{\bar{A}a}$ for scalar (spin 0) mesons. This gives the following bispinors

$$\begin{aligned} H_{\bar{A}a} &= \left(P_\mu^{\bar{A}a}\gamma^\mu - iP_5^{\bar{A}a}\gamma_5\right)\frac{(1+\gamma\cdot v)}{2} \\ \bar{H}_{\bar{A}a} &= \gamma^0 H_{\bar{A}a}^\dagger \gamma^0 = \frac{(1+\gamma\cdot v)}{2}\left[(P_\mu^{\bar{A}a})^\dagger \gamma^\mu - i(P_5^{\bar{A}a})^\dagger \gamma_5\right] \end{aligned} \tag{3.54}$$

In the process we are looking at, $D \to V\gamma$, we will get a very simple expression since we only have an annihilation of a D-meson, which is a pseudoscalar meson. This gives an expression

$$H_{C\bar{q}} = \frac{(1+\gamma\cdot v)}{2}\left(-iP_5^{C\bar{q}}\gamma_5\right) = -i\frac{(1+\gamma\cdot v)}{2}P_5\gamma_5 \tag{3.55}$$

where $\bar{q} = \bar{u}$, $\bar{d}$ or $\bar{s}$. For the creation of the vector particle V, we will not use any of these expressions since it only contains light quarks. The vector particle creation will be discussed in chapter 4 and 5.

With the meson fields now in place, we can write the chiral Lagrangian to lowest order (taken into account heavy quark and chiral symmetry)

$$\begin{aligned} \mathcal{L}_{Strong} = &\pm Tr\left[\bar{H}_{vk}^{(\pm)}(iv\cdot D_{hk})H_{vh}^{(\pm)}\right] \\ &-g_A Tr\left[\bar{H}_{vk}^{(\pm)}H_{vh}^{(\pm)}\gamma_\mu\gamma_5 A_{hk}^\mu\right] \\ &+2\lambda_1 Tr\left[\bar{H}_{vk}^{(\pm)}H_{vh}^{(\pm)}(\tilde{M}_q^V)_{hk}\right] \\ &+\frac{e\beta}{4}Tr\left[\bar{H}_{vk}^{(\pm)}H_{vh}^{(\pm)}\sigma\cdot F(Q_q^\xi)_{hk}\right]+... \end{aligned} \tag{3.56}$$

We have used $H^{(\pm)}$ here to refer to both particles (+) and antiparticles (-). k and h are $SU(3)_L$ triplet indices and v is the four-velocity of the meson. g_A is the strong axial coupling, while λ_1 and β are unknowns in HLχPT, but can be determined in HLχQM. Q_q^ξ and $\tilde{M}_q^V$ are quantities that we will study later, while V^μ and A^μ are vector and axial fields. F is the electromagnetic field tensor.

In addition to the terms above there also exists $1/m_Q$ terms like

$$\Delta\mathcal{L}_{\text{Strong}}^{(2)} = \frac{\lambda_2}{m_Q}\text{Tr}\left[\bar{H}_v\sigma^{\mu\nu}H_v\sigma_{\mu\nu}\right]+... \tag{3.57}$$

coming from the chromo-magnetic operator (i.e. a spin-spin interaction due to the quark colour charges). However, to our calculations these terms are irrelevant as we will only look at leading order terms.

Chapter 4

Chiral Quark Models

We start by looking at the chiral quark model, and then continue with the gluon condensate that the heavy light chiral quark model (HLχQM) includes in the description of a process like $D \to V\gamma$. We will then study the chiral quark model where we include vector mesons, which is an essential part of out process.

4.1 The Chiral Quark Model in the Light Sector

The chiral quark model (χQM) is a mean field approximation of the Nambu-Jona-Lasinio (NJL) quark model, which is a low energy quark model for the light sector, where the light quarks couple to the would-be Goldstone bosons (K, π, η_8) in such a way that the resulting theory is chiral invariant. In this model, a four-quark interaction Lagrangian is added to the QCD Lagrangian. As it works on scales $\Lambda << m_Q$, we can replace the heavy quark field Lagrangian with a kinetic term from HQEFT, giving a Lagrangian of the form

$$\mathcal{L}_{NJL} = \bar{q}(i\gamma^\mu D_\mu - \mathcal{M}_q)q + \bar{Q}_v(iv\cdot D)Q_v + \mathcal{L}_{int} \tag{4.1}$$

where

$$\mathcal{L}_{int} = -\frac{\kappa}{2}\bar{\psi}\gamma^\mu t_c^a \psi \bar{\psi} t_c^a \psi \tag{4.2}$$

is the four-interaction Lagrangian. By use of various Fierz transformations this interaction can be altered into combinations of scalar, pseudo-scalar, vector or pseudo-vector operators. This is done by introducing auxiliary fields (i.e. fields with no kinetic terms), which are identified as Goldstone bosons, heavy-light mesons, vector and axial vector mesons of QCD, which enable us to integrate out the quarks. When this is done, kinetic and interaction terms appear between the mesons. In this way the interaction can be altered to include combinations of scalars, pseudo-scalars, vectors or pseudo-vectors, depending on what's needed.

Chiral invariance of the chiral quark model means that $SU(3)_L \times SU(3)_R$ symmetry of the light quark sector (u, d, s) still holds in this model. This symmetry makes sure that there still are a small number of parameters in this model, and that we only need the quarks condensate, gluon condensate and the light constituent quark mass to calculate couplings and other terms in the model.

In the Lagrangian of the χQM we will find the usual QCD term $\bar{q}(i\gamma^\mu D_\mu - \mathcal{M}_q)q$ as well as an additional term describing the interaction between chiral quarks and the Goldstone bosons. The quarks q (u, d, s) are now also in the form of two separate components q_L and q_R, transforming under $SU(3)_L$ and $SU(3)_R$, respectively. The resulting Lagrangian has the following form [3]

$$\begin{aligned}\mathcal{L}_{\chi QM} = {} & \bar{q}_L(i\gamma^\mu D_\mu)q_L + \bar{q}_R(i\gamma^\mu D_\mu)q_R - \bar{q}_L\mathcal{M}_q q_R - \bar{q}_R\mathcal{M}_q^\dagger q_L \\ & -m(\bar{q}_R\Sigma^\dagger q_L + \bar{q}_L\Sigma q_R)\end{aligned} \tag{4.3}$$

$\mathcal{M}_q$ is the quark mass matrix, as in eq. 3.49, m is the constituent light quark mass we use for the light quark sector (of order 10^{-1} GeV) and Σ is the 3×3 matrix in eq 3.45.

We can also get the Lagrangian of the chiral quark model in a more transparent way within the "rotated version" of the χQM. Here we have flavour rotated quark fields χ given by

$$\chi_L = \xi^\dagger q_L \quad \text{and} \quad \chi_R = \xi q_R \tag{4.4}$$

and where

$$\xi \cdot \xi = \Sigma, \quad \xi = e^{i\Pi/f} \tag{4.5}$$

as before. The constituent quark fields χ_L and χ_R now transforms in the following way under $SU(3)_V$

$$\chi_L \to U\chi_L, \quad \chi_R \to U\chi_R \tag{4.6}$$

instead of transforming as

$$q_L \to g_L q_L \quad \text{and} \quad q_R \to g_R q_R \tag{4.7}$$

where

$$g_{L,R} \in SU(n_f)_{L,R} \tag{4.8}$$

U is defined from the $SU(3)_L \times SU(3)_R$ chiral transformation

$$\xi \to L\xi U^\dagger = U\xi R^\dagger \tag{4.9}$$

We now get the following Lagrangian

$$\mathcal{L}_{\chi QM,R} = \bar{\chi}\left[\gamma^\mu(iD_\mu + \mathcal{V}_\mu + \gamma_5\mathcal{A}_\mu) - m\right]\chi - \bar{\chi}\tilde{\mathcal{M}}_q\chi \tag{4.10}$$

which is invariant under $SU(3)_V$. The unknown terms are here the vector field $\mathcal{V}_\mu$

$$\mathcal{V}_\mu \equiv \frac{i}{2}(\xi^\dagger \partial_\mu \xi - \xi \partial_\mu \xi^\dagger) \tag{4.11}$$

and the axial vector field $\mathcal{A}_\mu$

$$\mathcal{A}_\mu \equiv -\frac{i}{2}(\xi^\dagger \partial_\mu \xi - \xi \partial_\mu \xi^\dagger) \tag{4.12}$$

$\mathcal{A}_\mu$ can also found to be of the form

$$\mathcal{A}_\mu = \frac{1}{f}\partial_\mu \Pi + \mathcal{O}\left(\frac{1}{f^2}\right) \tag{4.13}$$

where $f \approx f_\pi$. The term $\tilde{\mathcal{M}}_q$ has the following form

$$\tilde{\mathcal{M}}_q = \tilde{\mathcal{M}}_q{}^V + \tilde{\mathcal{M}}_q{}^A \gamma_5 \tag{4.14}$$

and is the rotated current quark matrix, where

$$\begin{aligned} \tilde{\mathcal{M}}_q{}^V &= \frac{1}{2}(\xi^\dagger \mathcal{M}_q{}^\dagger \xi^\dagger + \xi \mathcal{M}_q \xi) \\ \tilde{\mathcal{M}}_q{}^A &= -\frac{1}{2}(\xi^\dagger \mathcal{M}_q{}^\dagger \xi^\dagger - \xi \mathcal{M}_q \xi) \end{aligned} \tag{4.15}$$

where $\mathcal{M}_\mu$ is again the same quark matrix as we had before (eq 3.49).

By comparing the Lagrangians, the rotated (eq 4.10) and the original one (eq 4.3), we see that the chiral interactions in the original Lagrangian (terms three and four) are incorporated into the term $\bar{\chi}\tilde{\mathcal{M}}_q\chi$, while interaction terms proportional to m (last term in the original Lagrangian) become a pure constituent mass term.

4.1.1 The Gluon Condensate

We now introduce the gluon condensate

$$\left\langle \frac{\alpha}{\pi} G^2 \right\rangle = \left\langle 0 \left| \frac{\alpha_S}{\pi} G^a_{\mu\nu} G^a_{\mu\nu} \right| 0 \right\rangle \tag{4.16}$$

where $|0\rangle$ = vacuum state and a is a colour octet index. This gluon condensate was along with the quark condensate

$$\langle \bar{q}q \rangle = \langle 0 | \bar{q}q | 0 \rangle \tag{4.17}$$

introduced as parameters in QCD sum rules as a way of parametrizing the vacuum effects effecting the process. However, the exact structure of the fluctuating vacuum fields are irrelevant to us since everything is parametrized by the gluon and quark condensates that describe the vacuum characteristics. So why do we introduce the gluon condensate now? The reason is that we need to estimate the long distance (low energy) gluon interactions in the non-leptonic decay, which are parametrized by the gluon condensate. As we are only interested in the effects at lowest order to estimate non-factorizable effects, we neglect higher order gluon condensate. That is, we truncate the gluon condensate expansion at the first order gluon condensate $\left\langle g_S{}^2 G^2 \right\rangle$ and disregard all higher gluon condensate contributions, $\left\langle g_S{}^3 G^3 \right\rangle$, $\left\langle g_S{}^4 G^4 \right\rangle$, etc.

As we take the first order gluon condensate into account in the process, we will get two gluons in the Feynman diagrams to represent it. The reason for this can be seen from the expression for the gluon condensate, which contains two gluonic field tensors. The gluons couple only to the light quarks in the meson, since the long distance gluon couplings of the heavy quark are suppressed by a factor $1/m_Q$, where as before m_Q is the mass of the heavy quark. In χQM the hard gluons are being integrated out, leaving us only with the degrees of freedom coming from the low energy gluons. The effect of these gluons coupling to the light quarks is then parametrized by the gluon condensate in the model.

We introduce the gluon condensate, $\left\langle \frac{\alpha}{\pi} G^2 \right\rangle$, into the calculations of the Feynman diagrams by making the following replacement in the diagrams for the soft gluon couplings [4]

$$g_S^2 G^a_{\mu\nu} G^b_{\alpha\beta} \to \frac{4\pi^2}{(N_C{}^2 - 1)} \delta^{ab} \frac{1}{12} \left\langle \frac{\alpha}{\pi} G^2 \right\rangle (g_{\mu\alpha} g_{\nu\beta} - g_{\mu\beta} g_{\nu\alpha}) \tag{4.18}$$

This expression simplifies to

$$g_S^2 G^a_{\mu\nu} G^a_{\alpha\beta} \to 4\pi^2 \frac{1}{12} \left\langle \frac{\alpha}{\pi} G^2 \right\rangle (g_{\mu\alpha} g_{\nu\beta} - g_{\mu\beta} g_{\nu\alpha}) \tag{4.19}$$

when a = b and we sum over a (as the Kronecker delta becomes equal $N_C{}^2$ -1.) We will use these expressions later in our diagram calculations.

We have two important divergent loop integrals, I_1 (quadratic divergent) and I_2 (logarithmic divergent)

$$I_1 = \int \frac{d^d p}{(2\pi)^d} \frac{1}{p^2 - m^2} \tag{4.20}$$

$$I_2 = \int \frac{d^d p}{(2\pi)^d} \frac{1}{(p^2 - m^2)^2} \tag{4.21}$$

which we will use throughout the calculations for the diagrams later on. In the light sector these are related to the gluon condensate and the quark condensate through the following expressions

$$f_\pi^2 = -4im^2 N_C I_2 + \frac{1}{24m^2}\left\langle \frac{\alpha}{\pi} G^2 \right\rangle \tag{4.22}$$

$$\langle \bar{q}q \rangle = -4imN_C I_1 - \frac{1}{12m}\left\langle \frac{\alpha}{\pi} G^2 \right\rangle \tag{4.23}$$

These relations are obtained from calculations of various simple Feynman diagrams. Using these relations, combined with other ($I_{3/2}$ for example), we can determine the value of many of the parameters within the heavy light chiral quark model using only a few input parameters.

The vacuum effects are, as we can see, not only of the form of external gluon lines coupled to the light quarks, but also in the divergent loop integrals themselves.

4.1.2 Chiral Quark Model Including Vector Mesons

We now wish to include vector mesons, and not only pseudoscalar mesons, in the chiral perturbation theory. An important difference compared to the chiral quark model for pseudoscalar mesons, besides the spin, is the mass of the vector mesons, which are now in the range 0,8 to 1 GeV. Our starting point is the following Lagrangian [2]

$$\mathcal{L} = \mathcal{L}_{mass} + \mathcal{L}_{\chi QM} + \mathcal{L}_{IVA} \tag{4.24}$$

where

$$\mathcal{L}_{mass} = m_V^2 Tr[V_\mu V^\mu] + m_A^2 Tr[A_\mu A^\mu] \tag{4.25}$$

is the bare mass term. V is here given as Π in eq. 3.47, but with π replaced by ρ etc. We get a similar exchange for the axial vector field A. (These vector and axial vector fields should not be confused with the fields $\mathcal{V}$ and $\mathcal{A}$ in eq. 4.11 and 4.12, as they are now having a much greater mass than these pseudoscalar fields we looked at earlier.) After integrating out the quarks, the masses are modified and identified as the physical ones. Then we can also find a kinetic term

$$\mathcal{L}_{kin} = -\frac{1}{2}\left[V_{\mu\nu} V^{\mu\nu} \right] - \frac{1}{2}\left[A_{\mu\nu} A^{\mu\nu} \right] \tag{4.26}$$

where

$$X_{\mu\nu} = \nabla_\mu X_\nu - \nabla_\nu X_\mu \tag{4.27}$$

with X = V or A. Here ∇ is a covariant derivative including the Goldstone bosons.

(4.28)

$$\nabla_\mu X_\nu \equiv \partial_\mu X_\nu + i[X_\mu, X_\nu]$$

Now, for the left-handed current for the process vac → X, we find the SU(3) octet current

$$J_\mu^n(\text{vac} \to X) = \frac{1}{2} k_X \text{Tr}[\Lambda^n X_\mu] \tag{4.29}$$

where Λ^n is given from bosonization of the weak currents by

$$\begin{gathered} \bar{q}_L \gamma^\mu \lambda^n q_L = \bar{\chi}_L \gamma^\mu \Lambda^n \chi_L; \\ \Lambda^n \equiv \xi^\dagger \lambda^n \xi \end{gathered} \tag{4.30}$$

For our process we have

$$J_\mu^n(\text{vac} \to V) = \frac{1}{2} k_V \text{Tr}[\Lambda^n V_\mu] \tag{4.31}$$

The Lagrangian $\mathcal{L}_{\chi QM}$ is the usual chiral quark model Lagrangian, namely

$$\mathcal{L}_{\chi QM} = \bar{\chi}\left[\gamma^\mu (iD_\mu + V_\mu + \gamma_5 A_\mu) - m\right]\chi - \bar{\chi}\tilde{\mathcal{M}}_q \chi \tag{4.32}$$

The important term in eq. 4.24 is, however, the last one; $\mathcal{L}_{IVA}$. This is the interaction Lagrangian between the quarks and the vectors and axial vectors, and it has the following form in this model

$$\mathcal{L}_{IVA} = \bar{\chi}\left[h_V \gamma^\mu V_\mu + h_A \gamma^\mu \gamma_5 A_\mu\right]\chi \tag{4.33}$$

From this expression we can later determine the vertex factor when quarks are coupled to a vector particle. Normalization of the kinetic energy terms gives

$$\frac{f^2 h_V^2}{3m^2}\left[1 - \frac{1}{15m^2 f^2}\left\langle \frac{\alpha_S}{\pi} G^2 \right\rangle\right] = 1 \tag{4.34}$$

where $h_A = h_V$ before chiral corrections. This is an implicit expression for the coefficient h_V. For the currents, we get the relation for the vector case

$$k_V = \frac{1}{2} h_V \left(-\frac{\langle \bar{q}q \rangle}{m} + f^2 - \frac{1}{8m^2}\left\langle \frac{\alpha_S}{\pi} G^2 \right\rangle \right) \tag{4.35}$$

and in the same way for the axial case

$$k_A = \frac{1}{2} h_A \left(-\frac{\langle \bar{q}q \rangle}{m} - 3f^2 + \frac{1}{8m^2}\left\langle \frac{\alpha_S}{\pi} G^2 \right\rangle \right) \tag{4.36}$$

4.2 Heavy Light Chiral Quark Model

The heavy light chiral quark model (HLχQM) is a quark model that combines both the heavy quark effective field theory (where $1/m_Q \to 0$) and the chiral quark model (where $m_q \to 0$) to a theory that includes elements from both of these theories. In other words, the chiral quark model is extended from the light to the heavy sector where we use the HQEFT to describe the particles. The resulting theory is a theory for the combined particles consisting of both a heavy quark and a light quark. These are the so called heavy-light mesons. They are any meson with one heavy quark of flavour c, b or t, and one light quark of flavour u, d or s. In our process HLχQM will play an important role in the annihilation of the D-meson. By combining the spin-flavour heavy quark symmetry and chiral quark symmetry, the HLχQM will describe the low energy strong interactions between the heavy-light mesons and the would-be Goldstone bosons, and also include the coupling to the electromagnetic field.

Just like in the heavy quark effective field theory, the heavy quark field in the HLχQM will be replaced by a reduced field Q_v (for quarks) and R_v (for anti-quarks), just like in section 3.3.

We now introduce the Lagrangian containing both quark fields and mesonic fields

$$\mathcal{L}_{HL\chi QM} = \mathcal{L}_{HQEFT} + \mathcal{L}_{\chi QM} + \mathcal{L}_{int} \tag{4.37}$$

Both $\mathcal{L}_{HQEFT}$ and $\mathcal{L}_{\chi QM}$ we have seen before in sections 3.3 and 4.1, but the Lagrangian $\mathcal{L}_{int}$ is new. It is a generalization of the interactions of the $\mathcal{L}_{\chi QM}$ in eq. 4.10 to the interactions between heavy meson field and heavy quarks, and has the following form [4]

$$\mathcal{L}_{int} = -G_H\left[\bar{\chi}_a \bar{H}_c^a Q_v + \bar{Q}_v H_c^a \chi_a\right] + \frac{1}{2G_3}\mathrm{Tr}\left[\bar{H}_c^a H_c^a\right] \tag{4.38}$$

G_H is here the effective coupling for the vertices, and can be expressed as a function of f_π, m, g_A and the gluon condensate $\left\langle \frac{\alpha_S}{\pi} G^2 \right\rangle$

$$G_H^2 = \frac{m(1+3g_A)}{2f_\pi^2 + \frac{m^2 N_C}{4\pi} - \frac{\pi}{32m^2}\left\langle \frac{\alpha_S}{\pi} G^2 \right\rangle} \tag{4.39}$$

G_H has to be of this form since it is the only way to keep the HLχQM consistent with obtaining the first two terms in the Lagrangian in eq. 3.56. $\bar{H}_c^a$ and H_c^a represents, as in the section on chiral perturbation effective field theory, meson fields; creation and annihilation, respectively. The term $\frac{1}{2G_3}\mathrm{Tr}\left[\bar{H}_c^a H_c^a\right]$ of the interaction Lagrangian is a self interaction with G_3 as the coupling constant.

As we see, the Lagrangian in eq 4.37 is divided in three parts; the chiral quark model Lagrangian $\mathcal{L}_{\chi QM}$, describing the light sector, the heavy quark effective field theory

Lagrangian $\mathcal{L}_{HQEFT}$, describing the heavy sector, and finally the interaction Lagrangian $\mathcal{L}_{int}$, describing the mesons and the heavy/light quarks or meson vertices. The Lagrangian then covers both the heavy and light sector as well as the mesons, like the D-meson in our case. The c-quark is treated as a heavy quark by this model, though its mass is only 1,15 – 1,35 GeV. This is close to the cutoff scale Λ = 1 GeV, and could lead to inaccuracies when the $1/m_Q$ corrections are neglected, as we will do.

If we recall the constant λ_1 from eq. 3.56, we said that it could not be determined in the HLχPT, but within the HLχQM it can, and will have the following form

$$\lambda_1 = \frac{1}{4}(3g_A + 1) - \frac{(9\pi - 16)\mu_G^2}{768\eta_2 m^2} \tag{4.40}$$

where the g_A is the strong axial coupling, m is the constituent light quark mass and μ_G is the chromo-magnetic operator having the following form

$$\mu_G^2(H) = \frac{1}{2M_H} C_M(\mu) \langle H | \bar{Q}_v \frac{1}{2} \sigma \cdot G Q_v | H \rangle \tag{4.41}$$

If we put $\mu = \Lambda$ we get

$$\mu_G^2 = \eta_2 \frac{G_H^2}{m} \left\langle \frac{\alpha_S}{\pi} G^2 \right\rangle \tag{4.42}$$

with

$$\eta_2 = \frac{(\pi + 2)}{32} C_M(\Lambda) \tag{4.43}$$

The constant $C_M(\mu)$ contains high energy effects down to the energy scale μ, and has been calculated to $C_M^c(\Lambda) = 1{,}15$ in the D-sector [4].

4.3 The Full HLχQM Lagrangian

Let us now collect all the relevant Lagrangians to see the shape of the full Lagrangian $\mathcal{L}_{HL\chi QM}$. From eq 4.10 we had the rotated chiral quark model Lagrangian

$$\mathcal{L}_{\chi QM,R} = \bar{\chi}\left[\gamma^\mu (iD_\mu + \mathcal{V}_\mu + \gamma_5 \mathcal{A}_\mu) - m\right]\chi - \bar{\chi}\tilde{\mathcal{M}}_q\chi \tag{4.44}$$

and from eq 3.37 we had the heavy quark effective field theory Lagrangian that had the following form

$$\mathcal{L}_{\text{HQEFT}} = \bar{Q}_v i(v\cdot D)Q_v + \frac{1}{2m_Q}\bar{Q}_v(i\gamma\cdot D_\perp)^2 Q_v + \frac{g_s}{4m_Q}\bar{Q}_v\sigma\cdot GQ_v + \mathcal{O}(\frac{1}{m_Q}) \qquad (4.45)$$

We also had the interaction Lagrangian in eq 4.38 of the form

$$\mathcal{L}_{\text{int}} = -G_H\left[\bar{\chi}_a\bar{H}_c^a Q_v + \bar{Q}_v H_c^a \chi_a\right] + \frac{1}{2G_3}\text{Tr}\left[\bar{H}_c^a H_c^a\right] \qquad (4.46)$$

Figure 4.1 shows a heavy-light meson loop described within the HLχQM. From the interaction Lagrangian one can see that the vertex factor to the left in this diagram is $iG_H H_v^a$, where the i-factor comes from the relation $\mathcal{L} = -iM$, and where what we call the vertex factor is what we use in $M = i\mathcal{L}$. The upper double line in the diagram is the heavy quark Q_v with velocity v, and the lower single line is the light quark χ_a, where a is the light quark flavour. The solid and dashed double line to the left represents the meson field, while × is the weak vertex and has the form $\xi^\dagger\gamma^\mu L$ for "annihilation" diagrams like the one in figure 4.1.

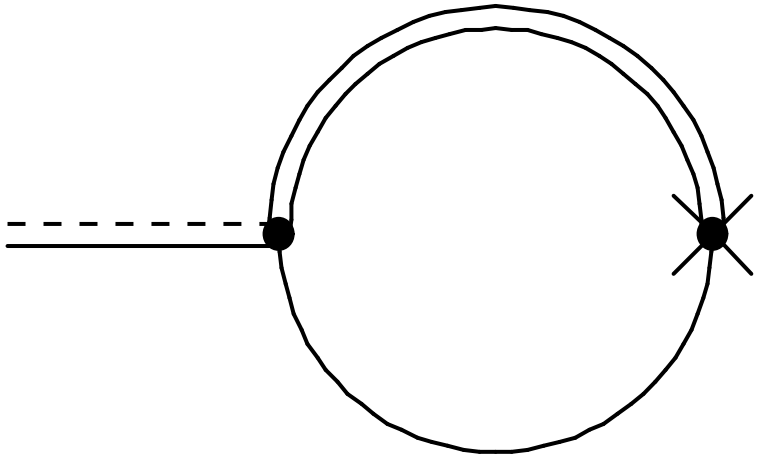

Figure 4.1 A heavy-light meson loop diagram described within the HLχQM.

For non-factorizable diagrams, i.e. diagrams with one single gluon coupling to it, we will add a colour matrix t^a to the weak vertex in order to make the full diagrams quasi-factorizable.

We now have the three Lagrangians and putting them together will give the full Lagrangian to first order

$$\begin{aligned}\mathcal{L}_{\text{HL}\chi\text{QM}} &= \bar{\chi}\left[\gamma^\mu(iD_\mu + \mathcal{V}_\mu + \gamma_5\mathcal{A}_\mu) - m\right]\chi - \bar{\chi}\tilde{\mathcal{M}}_q\chi \\ &+\bar{Q}_v i(v\cdot D)Q_v + \frac{1}{2m_Q}\bar{Q}_v(i\gamma\cdot D_\perp)^2 Q_v + \frac{g_s}{4m_Q}\bar{Q}_v\sigma\cdot GQ_v \\ &-G_H\left[\bar{\chi}_a\bar{H}_c^a Q_v + \bar{Q}_v H_c^a\chi_a\right] + \frac{1}{2G_3}\text{Tr}\left[\bar{H}_c^a H_c^a\right]\end{aligned} \qquad (4.47)$$

This Lagrangian now includes light chiral quarks, heavy quarks and mesons. The first line of this Lagrangian describes the light sector (π, K and η), the second line the heavy quark sector, and the third line is a bridge between the two, describing the heavy-light sector, like the heavy-light meson D. In addition we have the Lagrangian for the vector mesons given in eq. 4.24.

Chapter 5

Feynman Rules for D → Vγ

Up until now we have been studying the different quark models being valid at different energy levels, and has come to a model describing heavy and light quarks and their interactions; the HLχQM. We started with a general description of the standard model, then moved on to low energy effective field theories, i.e. approximations of the standard model, and finally ended up with the chiral quark model, including the chiral quark model with vector mesons, thereby reducing the generality and the energy region we work in. What is left for us to do now before we start with the calculations of the Feynman diagrams describing the process D → Vγ, is to find the couplings and the so called effective propagators. These effective propagators are expressions for propagators of the light quarks in the meson loops that includes any external particles (photon or gluons) that they may couple to. If we for example wish to describe an external photon line coupled to the light quark, it will not be necessary for us to first include the light quark propagator, then a photon coupling and then again the light quark propagator after the photon coupling. Instead we insert the correct effective propagator into a Feynman diagram. These effective propagators will be used in both the calculation of the annihilation of the D-meson and the creation of a vector particle.

The path-integral method, or functional method (since it is based on generating functionals), is a very useful method for calculating propagators. This is since it is based on the Lagrangian, rather then the Hamiltonian, which gives us the possibility to read off the vertex factors right out of the Lagrangian of the field theory. An example of this is the rotated chiral Lagrangian in eq 4.10, where we have a term of the following form

$$\bar{\chi}\gamma^{\mu}\gamma_5 \mathcal{A}_{\mu}\chi \tag{5.1}$$

This describes the interaction of an axial vector $\mathcal{A}_{\mu}$ coupling to a chiral quark χ, and this gives a vertex contribution $i\gamma^{\mu}\gamma_5$ to the Feynman diagram. The i comes from $M = i\mathcal{L}$, where M is what we calculate from the diagrams. Another example is the interaction Lagrangian (eq 4.38) which gives a vertex factor $-iG_H H_v^a$. This is shown in figure 5.1.

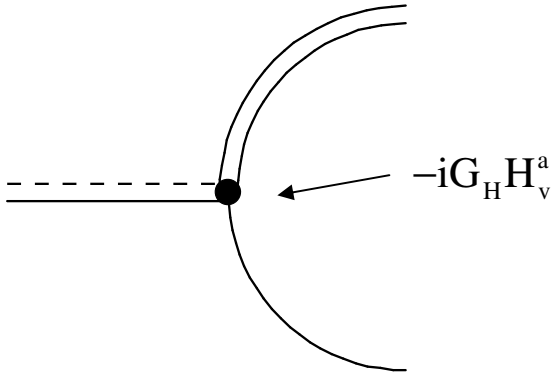

Figure 5.1 The vertex factor in the HLχQM.

5.1 Couplings and Effective Propagators

Now we would like to express the external gauge field A_μ in powers of the gluon field strength tensor G. We can then use this to calculate the vertex factors for processes like qg → q, or emission of a photon (but then using the electromagnetic field strength tensor instead). By expressing the gluons using the gluon field strength tensor G instead of the field A_μ, we can use the expression we had in eq 4.18

$$g_S^2 G_{\mu\nu}^a G_{\alpha\beta}^b \to \frac{4\pi^2}{(N_C{}^2 - 1)} \delta^{ab} \frac{1}{12} \left\langle \frac{\alpha}{\pi} G^2 \right\rangle (g_{\mu\alpha} g_{\nu\beta} - g_{\mu\beta} g_{\nu\alpha}) \tag{5.2}$$

to go from gluons to the gluon condensate.

We can do this by imposing a gauge condition on the field. This makes no difference as the correlation function (which can be calculated using the path-integral method) is gauge invariant. We use here the Fock-Schwinger gauge to simplify the calculations. The gauge condition is

$$(x^\mu - x_0^\mu) A_\mu^0(x) = 0 \tag{5.3}$$

As x_0 will cancel out of the calculations, we can simply put $x_0 = 0$ without loss of generality. The reason for this is that the Fock-Schwinger gauge condition expressly breaks translational invariance, (breaking of translational invariance means that $S(x,0) \neq S(0,-x)$, where $S_{\alpha\beta}(x,y) = \langle 0 | T \int \psi_\alpha(x) \bar{\psi}_\beta(y) | 0 \rangle$) and the symmetry would restore itself naturally. Doing so will leave us with the condition $x^\mu A_\mu = 0$. Nevertheless, in the Fock-Schwinger gauge it is important to include all the diagrams in order to get the correct answer. Leaving a diagram out, will most likely lead to infinities or zero.

To get the external field expressed by the gluon field tensors, we use the derivative identity

$$A_\mu(x) = \frac{\partial}{\partial x_\mu}(A_\nu(x)x_\nu) - x_\nu \frac{\partial}{\partial x_\mu} A_\nu(x) \tag{5.4}$$

and the Fock-Schwinger gauge condition. The last term in eq. 5.4 can be written

$$-x_\nu \frac{\partial}{\partial x_\mu} A_\nu(x) \to -x_\nu G_{\mu\nu} - x_\nu \frac{\partial}{\partial x_\nu} A_\mu(x) \tag{5.5}$$

where we used $G_{\mu\nu} = \partial_\mu A_\nu - \partial_\nu A_\mu$. By substituting $x \to \alpha x$ and integrating we get the following expression

$$A^a_\mu(x) = \int_0^1 dx \alpha G^a_\mu(\alpha x) = \frac{1}{2} x^\nu G^a_{\mu\nu}(0) + \frac{1}{3} x^\beta x^\nu (D_\beta G^a_{\nu\mu}(0)) + ... \tag{5.6}$$

Fourier transforming this expression to first order gives

$$A^a_\mu(k) = \int_0^1 dz e^{ikz} A^a_\mu(z) = -\frac{i}{2}(2\pi)^4 G^a_{\rho\mu}(0) \frac{\partial}{\partial k_\rho} \delta^{(4)}(0) + ... \tag{5.7}$$

This gives the first-order vertex factor for the coupling of a gluon to a quark

$$-i\gamma^\mu t^a A^a_\mu = -\frac{1}{2} t^a \gamma^\mu G^a_{\mu\nu}(0) \frac{\partial}{\partial k_\nu} |_{k_\nu = 0} + ... \tag{5.8}$$

This is shown in figure 5.2.

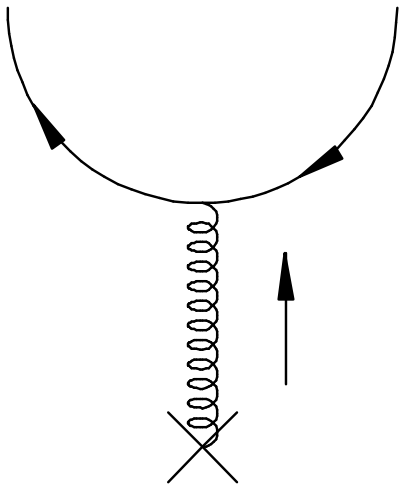

Figure 5.2 The first-order vertex factor for the coupling of a gluon to a quark.

In the same way we can get the vertex factor for a process $q\gamma \to q$, where a photon couples to a light quark, as shown in figure 5.3.

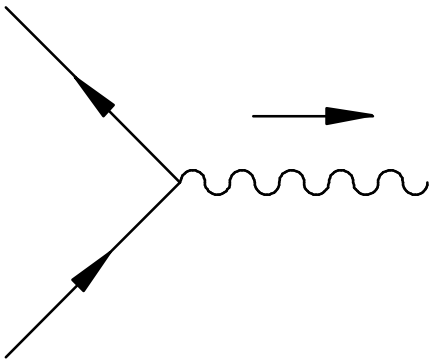

Figure 5.3 The coupling of a photon to a light quark.

The electromagnetic coupling to light quarks is $e\tilde{Q}_\xi^V \gamma^\mu A_\mu^{em}$, and we get the electromagnetic field

$$A_\mu^{em} = -\frac{i}{2} F_{\nu\mu}(0) \frac{\partial}{\partial k_\nu} (2\pi)^4 \delta^{(4)}(k) \tag{5.9}$$

using the same procedure as with the gluon vertex. The vertex factor, to first order, is then

$$\frac{1}{2} \gamma^\mu e \tilde{Q}_\xi^V F_{\mu\nu}(0) \frac{\partial}{\partial k_\nu} |_{k_\nu = 0} + ... \tag{5.10}$$

The term $\tilde{Q}_\xi^V$ used above is related to the SU(3) quark charge matrix Q

$$\tilde{Q}_\xi^V = \frac{1}{2}(\xi^\dagger Q \xi + \xi Q \xi^\dagger) \tag{5.11}$$

$$Q = \begin{pmatrix} 2/3 & 0 & 0 \\ 0 & -1/3 & 0 \\ 0 & 0 & -1/3 \end{pmatrix} \tag{5.12}$$

The full electromagnetic current is of the form

$$J_\mu^{em} = \bar{\chi} \tilde{Q}_\xi^V \gamma_\mu \chi + \bar{\chi} \tilde{Q}_\xi^A \gamma_\mu \gamma_5 \chi \tag{5.13}$$

But as the photon is a vector boson, we only use the first term. The term $\tilde{Q}_\xi^A$ would have the form

$$\tilde{Q}_\xi^A = \frac{1}{2}(\xi^\dagger Q \xi - \xi Q \xi^\dagger) \tag{5.14}$$

For a reverse process, i.e. $q \rightarrow q\gamma$, we simply reverse the momentum of the photon $k_\nu \rightarrow -k_\nu$. If we use the identity

$$\frac{\partial}{\partial k_\nu} S(p+k)\,|_{k_\nu=0} = -S(p)\gamma^\nu S(p) \tag{5.15}$$

also for the reverse process, we get

$$\frac{\partial}{\partial k_\nu} S(p-k)\,|_{k_\nu=0} = S(p)\gamma^\nu S(p) \tag{5.16}$$

If we now include the quark propagators in the process shown in figure 5.2, we get an expression of the form

$$\begin{aligned} iS(p)\left[\frac{1}{2}\gamma^\mu e\tilde{Q}_\xi^V F_{\mu\nu}\frac{\partial}{\partial k_\nu}\right] iS(p+k)\,|_{k_\nu=0} &= -\frac{1}{2}e\tilde{Q}_\xi^V F_{\mu\nu} S(p)\gamma^\mu S(p)\gamma^\nu S(p) \\ &= -\frac{1}{2}e\tilde{Q}_\xi^V F_{\mu\nu} R^{\mu\nu}\frac{1}{(p^2-m^2)^3} \end{aligned} \tag{5.17}$$

where we have defined

$$R^{\mu\nu} = (\gamma\cdot p+m)\gamma^\mu(\gamma\cdot p+m)\gamma^\nu(\gamma\cdot p+m) \tag{5.18}$$

If we use the gamma matrix anti-commutator $\{\gamma^\mu,\gamma^\nu\} = 2g^{\mu\nu}$ and the identity $\gamma^\mu\gamma^\nu = g^{\mu\nu} - i\sigma^{\mu\nu}$, where $\sigma^{\mu\nu} = \frac{i}{2}\left[\gamma^\mu,\gamma^\nu\right]$, we can get an expression of the following form

$$\begin{aligned} 2R^{\mu\nu} &= 2(\gamma\cdot p+m)\left[p^\mu\gamma^\nu + \gamma^\mu p^\nu\right](\gamma\cdot p+m) \\ &-(m^2-p^2)\left[g^{\mu\nu}(\gamma\cdot p+m) - i\sigma^{\mu\nu}(\gamma\cdot p+m) + (\gamma\cdot p+m)g^{\mu\nu} - (\gamma\cdot p+m)i\sigma^{\mu\nu}\right] \end{aligned} \tag{5.19}$$

We only look at the anti-symmetric part of this expression, since the process must be anti-symmetric in μ and ν. We are then left with the term

$$R^{\mu\nu}_{asym} = \frac{i}{2}(m^2-p^2)\left\{\sigma^{\mu\nu},(\gamma\cdot p+m)\right\} \tag{5.20}$$

We now end up with an "effective" propagator S_l^F for one photon emitted from a light quark, $q\gamma \rightarrow q$

$$\begin{aligned} iS_l^F &= -\frac{i}{4}e\tilde{Q}_\xi^V F_{\mu\nu}\frac{1}{(p^2-m^2)^2}\left\{\sigma^{\mu\nu},(\gamma\cdot p+m)\right\} \\ &= -\frac{i}{4}e\frac{1}{(p^2-m^2)^2}\left\{\tilde{Q}_\xi^V\sigma\cdot F,(\gamma\cdot p+m)\right\} \end{aligned} \tag{5.21}$$

In the same manner we can arrive at an "effective" propagator for one gluon emitted from a light quark qg → q.

$$\begin{aligned} iS_1^G &= \frac{i}{4} g_s t^b G_{\mu\nu}^b \frac{1}{(p^2 - m^2)^2} \{\sigma^{\mu\nu}, (\gamma \cdot p + m)\} \\ &= \frac{i}{4} g_s \frac{1}{(p^2 - m^2)^2} \{\sigma \cdot G, (\gamma \cdot p + m)\} \end{aligned} \tag{5.22}$$

where $\sigma \cdot G = \sigma^{\mu\nu} t^a G_{\mu\nu}^a$.

We can also construct effective propagators for the processes ggq → q, gq → q → qγ and qgg → q → qγ. These processes are shown in figure 5.4.

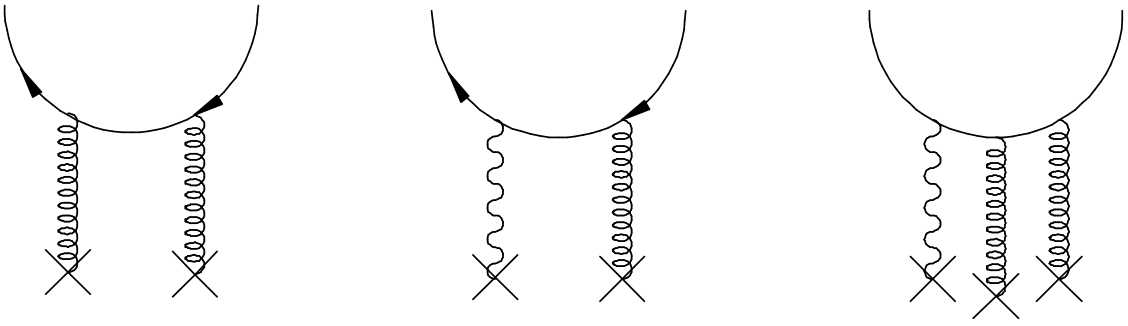

Figure 5.4 Gluons and photons coupling to light quarks.

We look at the first process and uses the soft gluon g as an incoming particle. For this process we have

$$iS_2^{GG} = \left\{ iS(p) \left[-\frac{1}{2} g_s t^a \gamma^\mu G_{\mu\nu}^a \frac{\partial}{\partial q_{1,\nu}} \right] iS(p - q_1) \left[-\frac{1}{2} g_s t^b \gamma^\alpha G_{\alpha\beta}^b \frac{\partial}{\partial q_{2,\beta}} \right] iS(p - q_1 - q_2) \right\}_{q_1 = q_2 = 0} \tag{5.23}$$

By using eq. 5.2 we get

$$iS_2^{GG} = \frac{i\pi^2}{12} t^a t^b \left\langle \frac{\alpha}{\pi} G^2 \right\rangle (2SRSRS - 2S\gamma^\mu SRS\gamma_\mu S) \tag{5.24}$$

where S is the propagator $S = \frac{\gamma \cdot p + m}{p^2 - m^2}$ and R is defined $R = \gamma^\mu S \gamma_\mu$. We find that

$$
\begin{aligned}
2SRSRS - 2S\gamma^{\mu}SRS\gamma_{\mu}S &= 2\frac{4}{(p^2-m^2)^5}\left\{(\gamma\cdot p)(p^4-5p^2m^2+8m^4)+m(-p^4+p^2m^2+4m^4)\right\} \\
&\quad -2\frac{4}{(p^2-m^2)^5}\left\{(\gamma\cdot p)(p^4-2p^2m^2+5m^4)+2m(p^4-p^2m^2+2m^4)\right\} \\
&= -\frac{24m}{(p^2-m^2)^4}\left[m(\gamma\cdot p)+p^2\right]
\end{aligned}
\tag{5.25}
$$

giving finally the effective propagator for two gluons coupling to a light quark

$$
iS_2^{GG} = i2\pi^2 t^a t^a \left\langle \frac{\alpha}{\pi} G^2 \right\rangle \frac{m}{(p^2-m^2)^4}\left[m(\gamma\cdot p)+p^2\right] \tag{5.26}
$$

The other two propagators, S_2^{FG} and S_2^{GF}, can be written

$$
iS_2^{FG} = \frac{i}{4} e g_s Q F_{\mu\nu} t^a G^a_{\alpha\beta} R^{\mu\nu\alpha\beta} \tag{5.27}
$$

$$
iS_2^{GF} = \frac{i}{4} e g_s Q F_{\alpha\beta} t^a G^a_{\mu\nu} R^{\mu\nu\alpha\beta} \tag{5.28}
$$

where

$$
\begin{aligned}
R^{\mu\nu\alpha\beta} &= S(p)\gamma^{\beta}S(p)\gamma^{\nu}S(p)\gamma^{\mu}S(p)\gamma^{\alpha}S(p) \\
&\quad +S(p)\gamma^{\iota}S(p)\gamma^{\beta}S(p)\gamma^{\mu}S(p)\gamma^{\alpha}S(p) \\
&\quad +S(p)\gamma^{\nu}S(p)\gamma^{\mu}S(p)\gamma^{\beta}S(p)\gamma^{\alpha}S(p)
\end{aligned}
\tag{5.29}
$$

As for the propagators S_3^{FGG}, S_3^{GFG} and S_3^{GGF} we have

$$
iS_3^{FGG} = \frac{\pi^2}{24} e Q F_{\mu\nu} t^a t^a \left\langle \frac{\alpha}{\pi} G^2 \right\rangle (g_{\alpha\rho}g_{\beta\sigma} - g_{\alpha\sigma}g_{\beta\sigma}) T^{\mu\nu\alpha\beta\sigma\rho} \tag{5.30}
$$

$$
iS_3^{GFG} = \frac{\pi^2}{24} e Q F_{\alpha\beta} t^a t^a \left\langle \frac{\alpha}{\pi} G^2 \right\rangle (g_{\mu\rho}g_{\nu\sigma} - g_{\mu\sigma}g_{\nu\rho}) T^{\mu\nu\alpha\beta\sigma\rho} \tag{5.31}
$$

$$
iS_3^{GGF} = \frac{\pi^2}{24} e Q F_{\upsilon\sigma} t^a t^a \left\langle \frac{\alpha}{\pi} G^2 \right\rangle (g_{\mu\alpha}g_{\nu\beta} - g_{\mu\beta}g_{\nu\alpha}) T^{\mu\nu\alpha\beta\sigma\rho} \tag{5.32}
$$

where $T^{\mu\nu\alpha\beta\sigma\rho}$ is a huge expression, still in simplified form,

$$
\begin{aligned}
T^{\mu\nu\alpha\beta\sigma\rho} = {} & S\gamma^{\sigma}S\gamma^{\beta}S\gamma^{\nu}S\gamma^{\mu}S\gamma^{\alpha}S\gamma^{\rho}S + S\gamma^{\beta}S\gamma^{\sigma}S\gamma^{\nu}S\gamma^{\mu}S\gamma^{\alpha}S\gamma^{\rho}S \\
& + S\gamma^{\beta}S\gamma^{\nu}S\gamma^{\sigma}S\gamma^{\mu}S\gamma^{\alpha}S\gamma^{\rho}S + S\gamma^{\beta}S\gamma^{\nu}S\gamma^{\mu}S\gamma^{\sigma}S\gamma^{\alpha}S\gamma^{\rho}S \\
& + S\gamma^{\beta}S\gamma^{\nu}S\gamma^{\mu}S\gamma^{\alpha}S\gamma^{\sigma}S\gamma^{\rho}S + S\gamma^{\sigma}S\gamma^{\nu}S\gamma^{\beta}S\gamma^{\mu}S\gamma^{\alpha}S\gamma^{\rho}S \\
& + S\gamma^{\nu}S\gamma^{\sigma}S\gamma^{\beta}S\gamma^{\mu}S\gamma^{\alpha}S\gamma^{\rho}S + S\gamma^{\nu}S\gamma^{\beta}S\gamma^{\sigma}S\gamma^{\mu}S\gamma^{\alpha}S\gamma^{\rho}S \\
& + S\gamma^{\nu}S\gamma^{\beta}S\gamma^{\mu}S\gamma^{\sigma}S\gamma^{\alpha}S\gamma^{\rho}S + S\gamma^{\nu}S\gamma^{\beta}S\gamma^{\mu}S\gamma^{\alpha}S\gamma^{\sigma}S\gamma^{\rho}S \\
& + S\gamma^{\sigma}S\gamma^{\nu}S\gamma^{\mu}S\gamma^{\beta}S\gamma^{\alpha}S\gamma^{\rho}S + S\gamma^{\nu}S\gamma^{\sigma}S\gamma^{\mu}S\gamma^{\beta}S\gamma^{\alpha}S\gamma^{\rho}S \\
& + S\gamma^{\nu}S\gamma^{\mu}S\gamma^{\sigma}S\gamma^{\beta}S\gamma^{\alpha}S\gamma^{\rho}S + S\gamma^{\nu}S\gamma^{\mu}S\gamma^{\beta}S\gamma^{\sigma}S\gamma^{\alpha}S\gamma^{\rho}S \\
& + S\gamma^{\nu}S\gamma^{\mu}S\gamma^{\beta}S\gamma^{\alpha}S\gamma^{\sigma}S\gamma^{\rho}S
\end{aligned}
\tag{5.33}
$$

where $S = \dfrac{\gamma \cdot p + m}{p^2 - m^2}$ is simplified to S. Although it is not very easy to see at first glimpse, $T^{\mu\nu\alpha\beta\sigma\rho}$ can be divided into three parts, each having five terms, where σ moves from left to the second last on the right in each part, while the other indices are unchanged.

5.2 The Couplings for the Vector Particles

The diagrams with the creation of a vector particle consist of a loop with two light quarks, i.e. a quark and an anti-quark. The difference between these diagrams and the annihilation diagrams of a D-meson, is that here we can have couplings of photons and gluons to both light quarks, and not only to one of them. While the coupling to one quark line give nine different diagrams for the D-annihilation loop, it gives 26 possible diagrams to calculate for the V-creation loop, when we have the possibility of coupling up to one photon and two gluons to the light quarks. Luckily, we can use the same effective propagators for the diagrams where we have a creation of a vector particle as for the diagrams where we had an annihilation of a D-meson.

What we need to find, however, are the vertex couplings. This can be quite easily done since we have the Lagrangian from eq. 4.33. As in the first section of this chapter, the vertex factor can now be read right out of this Lagrangian. This gives us

$$
ih_V \gamma_\mu V^\mu, \tag{5.34}
$$

h_V is here a coupling constant, and can be expressed through eq. 4.34. Eq. 5.34 is the meson vertex coupling between the vector particle, i.e. the light vector meson and the light quarks, as shown in figure 5.5.

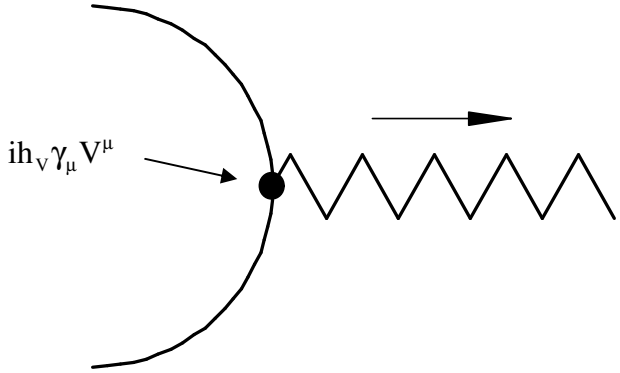

Figure 5.5 The vertex factor for the meson vertex in the creation of a vector particle.

For the vertex factor shown in figure 5.6, we get the following expression [3]

$$\Lambda^n\gamma^\mu L \tag{5.35}$$

where Λ^n is given in eq. 4.30 and L equals $(1-\gamma_5)/2$.

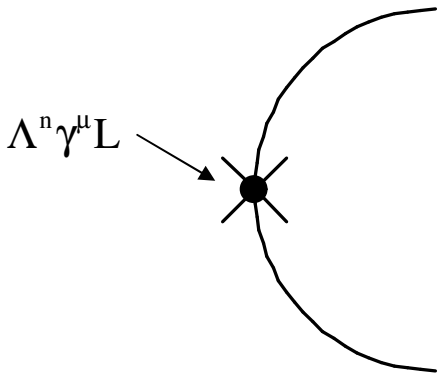

Figure 5.6 The weak vertex factor for the creation of a light quark/anti-quark loop.

Chapter 6

Calculations of $D \to V\gamma$

We are now going to do the calculations for the process $D \to V\gamma$, where D may be D^+ ($c\bar{d}$), D^- ($\bar{c}d$), D^0 ($c\bar{u}$), $\bar{D}^0$ ($\bar{c}u$), D_s^+ ($c\bar{s}$) or D_s^- ($\bar{c}s$). V is a vector meson consisting of only light quarks (u, d, s), giving the nine possibilities ρ^+, ρ^-, ρ^0, ϖ, φ, K^{*+}, K^{*-}, K^{*0} or $\bar{K}^{*0}$, and γ is a photon as usual. We will here calculate the expression $M = i\mathcal{L}$ for those diagrams where a heavy-light meson is annihilated, and those where a vector particle is created. That is, we will split the process in two; one part where a heavy-light meson is annihilated, and one part where a light meson is created, with photons and gluons coupling to the diagrams where necessary. We will call the two types of diagrams for *annihilation* and *creation* diagrams, respectively, which points to the annihilation process of the D-meson and the creation process of the vector particle, when looking at the total decay process $D \to V\gamma$. The annihilation diagrams will be $\langle 0|Q_{v_c}\gamma_\mu\bar{q}_L|D\rangle$ with photons and gluons coupling to it, and the creation diagrams will be $\langle V|J_\mu^{n,L}|0\rangle = \langle V|\bar{q}_{1,L}\lambda^n\gamma_\mu q_{2,L}|0\rangle$, also with photons and gluons coupling to it. As mentioned before, external (photon or gluon) lines will only couple to the light quarks in the meson loops, since the contributions for a connection to a heavy quark is suppressed by a factor m_Q.

In order for us to split the full diagram into two parts, we use the Vacuum Saturation Approach (VSA) factorized limit (as was mentioned in chapter 3) for the weak vertices, where we insert a vacuum state between the D-annihilation and the V-creation. The diagrams can then be bosonized, i.e. we integrate out the quark fields, separately and multiply the two diagrams afterwards. We can say that the annihilation and creation occurs at the same point. The VSA factorization limit is valid in the limit $1/N_c \to 0$. As we have only $N_c = 3$, this becomes a very naïve factorization, and we will therefore not put $N_c = 3$ explicitly in the calculations (until the calculations of the final results). The approximation neglects short distance QCD effects and long distance hadronic effects, and it is also very sensitive to vacuum effects such as those parametrized by the gluon condensate. The gluon contribution has therefore to be taken into consideration.

Using the VSA factorization limit for our process we get

$$\langle V|\mathcal{L}_{eff}|D\rangle \to \langle V|\bar{q}_{1,L}\lambda^n\gamma_\mu q_{2,L}|0\rangle\langle 0|Q_{v_c}\gamma_\mu\bar{q}_L|D\rangle \qquad (6.1)$$

where we have ignored the numerical factors coming from the Fermi theory for the moment. We will include these in the numerical calculations in chapter 7. If we also take the photon into consideration we get the following two separate permutations

$$\langle V|\mathcal{L}_{eff}|D\rangle \to \langle V\gamma|\bar{q}_{1,L}\lambda^n\gamma_\mu q_{2,L}|0\rangle\langle 0|Q_{v_c}\gamma_\mu\bar{q}_L|D\rangle$$
$$\langle V|\mathcal{L}_{eff}|D\rangle \to \langle V|\bar{q}_{1,L}\lambda^n\gamma_\mu q_{2,L}|0\rangle\langle\gamma|Q_{v_c}\gamma_\mu\bar{q}_L|D\rangle$$

depending on which meson loop the photon couples to. Using the Fierz transformation and the Fermi theory, this then gives us the expressions in eq. 3.18.

Parametrizing the vacuum effects with the gluon condensate to first order gives two gluons in the diagrams, in addition to the photon. This, together with the diagrams without any external lines, gives 33 different diagrams for the full $D \to V\gamma$ process. The full diagrams with gluon condensate to first order are shown in figure 6.1, where the diagrams on the right hand side are the diagrams that can be combined with the diagrams on the left hand side. The numbers to the left are the number of possible complete diagrams in each row.

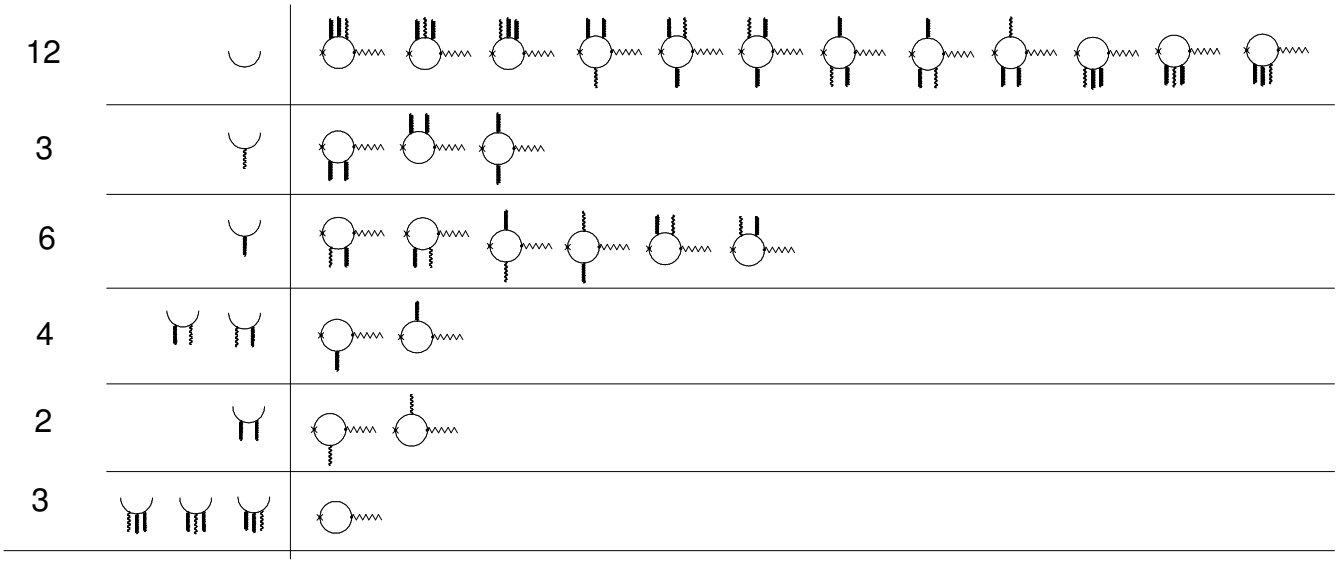

Figure 6.1 All the possible full diagrams for the process $D \to V\gamma$, with gluon condensate to first order.

As mentioned before, we get nine possible annihilation diagrams and 26 possible creation diagrams to calculate. These are sketched in figure 6.2 and figure 6.3. We then have to glue together those diagrams that belong together (as shown in figure 6.1). For us, this means that the full diagram must have one external photon line, and if it has external gluon lines, then the full diagram must have two of these.

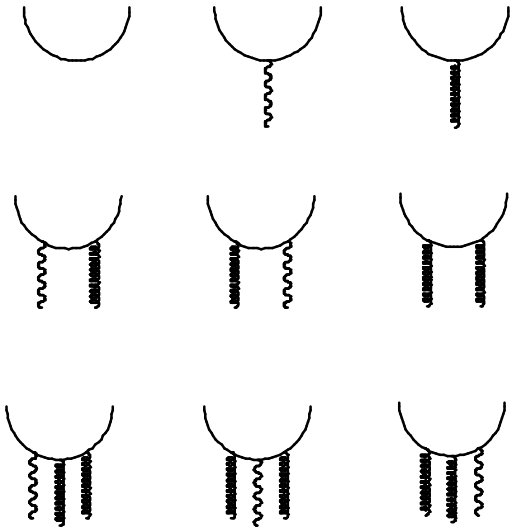

Figure 6.2 Sketch of all the possible annihilation diagrams for the process $D \rightarrow V\gamma$.

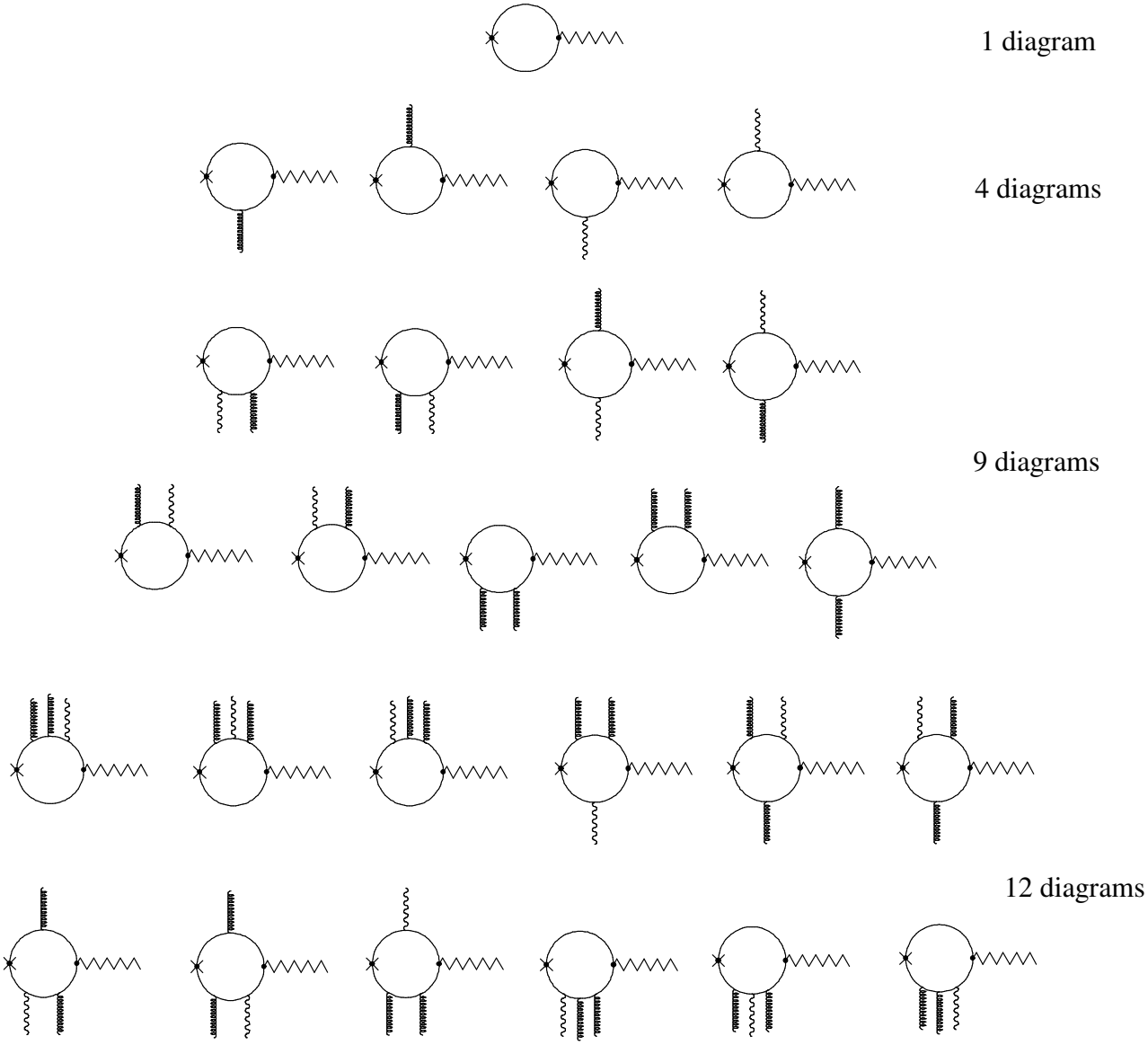

Figure 6.3 Sketch of all the possible creation diagrams for the process $D \rightarrow V\gamma$.

6.1 Partial Diagram Calculations

We will now calculate all partial diagrams, that is, nine of annihilation type $\langle 0|Q_{v_c}\gamma_\mu\bar{q}_L|D\rangle$ and 26 of creation type $\langle V|\bar{q}_{1,L}\lambda^n\gamma_\mu q_{2,L}|0\rangle$, with photons and gluons coupled to them when necessary. These are the diagrams sketched in the figures 6.2 and 6.3, and arise in the VSA factorization limit when the full Feynman diagram is split in two parts.

In the calculations of the diagrams we will use the effective propagators from section 5.2 for external photon and gluon lines. We will also use the heavy quark propagator

$$\frac{iP_+}{v\cdot p} \tag{6.3}$$

where v is the velocity of the heavy c-quark. In addition, we get a factor

$$-iG_H H \tag{6.4}$$

for the meson vertex for the annihilation diagrams, and the weak vertices will give a factor $\xi^\dagger\Gamma^\mu$, where the factor $\xi^\dagger$ comes from the rotation $\bar{q}_L = \bar{\chi}\xi^\dagger$. The form of Γ^μ turns out to be

$$\Gamma^\mu = \gamma^\mu L \tag{6.5}$$

as the factors C_γ and C_v in the general expression for $\Gamma^\alpha = C_\gamma(\mu)\gamma^\alpha L + C_v(\mu)v^\alpha R$ in perturbative QCD, are close to one and zero, respectively. Another simplification that we will sometimes use is

$$T(p) = \gamma\cdot p + m \tag{6.6}$$

to simplify the expressions.

For the creation diagrams we will use the factor

$$ih_V\gamma^\mu V_\mu \tag{6.7}$$

for the meson vertex, where we have two light quarks and the vector particle, and the factor

$$\Lambda^n\gamma_\mu L \tag{6.8}$$

for the vertex where the quarks couple to the weak current. We will also be using some tricks and rules for calculating gamma matrices. These are summarized below

$$\gamma^\mu\gamma^\nu\gamma_\mu = (2-D)\gamma^\nu \tag{6.9}$$

$$\gamma^\mu p_\mu \gamma^\nu \gamma^\sigma p_\sigma \underset{\text{Integration over p}}{\rightarrow} (2-D)\frac{p_\mu p_\sigma}{D} g_{\mu\sigma}\gamma^\nu \tag{6.10}$$

$$R\gamma^\mu\gamma\cdot p\gamma^\nu\gamma\cdot p\sigma^{\alpha\beta} \underset{\text{Integration over p}}{\rightarrow} \frac{(2-D)}{D} p^2 R\gamma^\mu\gamma^\nu\sigma^{\alpha\beta} \tag{6.11}$$

$$\begin{aligned} R\gamma^\mu\gamma\cdot p\gamma^\nu\sigma^{\alpha\beta}\gamma\cdot p &\underset{\text{Integration over p}}{\rightarrow} \gamma\cdot pR\gamma^\mu\gamma\cdot p\gamma^\nu\sigma^{\alpha\beta} \\ &= L\gamma\cdot p\gamma^\mu\gamma\cdot p\gamma^\nu\sigma^{\alpha\beta} \\ &= \frac{(2-D)}{D} p^2 L\gamma^\mu\gamma^\nu\sigma^{\alpha\beta} \end{aligned} \tag{6.12}$$

$$\text{Tr[odd number of } \gamma] \underset{\text{Integration over p}}{\rightarrow} 0 \tag{6.13}$$

$$\gamma_\mu L = R\gamma_\mu, \quad \text{where } L = \frac{1}{2}(1-\gamma_5) \text{ and } R = \frac{1}{2}(1+\gamma_5) \tag{6.14}$$

In addition, we will use the general expression I_n,

$$I_n = \int \frac{d^d p}{(2\pi)^d} \frac{1}{(p^2 - m^2)^n} \tag{6.15}$$

where n = 1, 2, 3, …, in the partial diagram calculations. It is, however, only when n = 1 or 2 that we get integrals that are divergent. For $n \geq 3$ we get integrals that can be calculated, as is done in the appendix.

6.1.1 Calculations of the Annihilation Diagrams

In this section we will do the calculations of the annihilation diagrams $\langle 0 | Q_{v_c} \gamma_\mu \bar{q}_L | D \rangle$, which are the diagrams for the annihilation of a D-meson. It turns out that these are the same diagrams as the ones that have already been calculated in [5]. We will, however, not only write down the results from these calculations, but also give some explanation to them, as much of the same procedure will be used in the calculation of the creation diagrams (and since some errors have been found in the calculations done in [5]).

We start with the simplest diagram for this process. This is shown in figure 6.4.

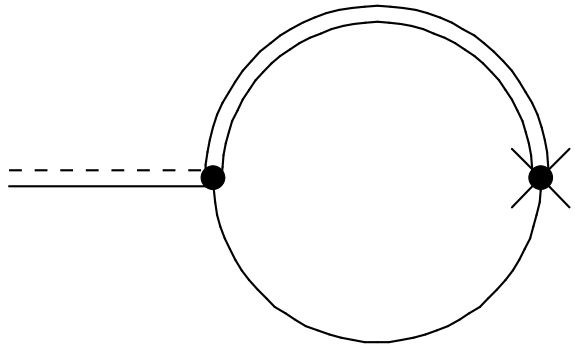

Figure 6.4 $\langle 0|\bar{q}\gamma^{\mu}LQ_{v_c}|D\rangle$ *- The simplest D-meson annihilation diagram with no photons or gluons coupling to it.*

This is a very strait forward diagram, as it doesn't contain any external photon or gluon lines coupled to it. To get an expression for the diagram we simply use the Feynman rules. First of all we note that this diagram contains a loop, giving us a minus sign, as well as the trace of a product of Dirac matrices. Since we are dealing with quarks, that have the property colour, we also have to multiply with the trace of the colour unit matrix, Tr $\mathbf{1}_c$, which is equal to N_c. In addition we have to integrate over the loop momenta p: $\int \frac{d^4p}{(2\pi)^4}$. Looking at our diagram in figure 6.4, we see that we have a weak vertex factor $\xi^{\dagger}\Gamma^{\mu}$, where $\Gamma^{\mu} = \gamma^{\mu}L$, as well as a meson vertex factor $-iG_H H$, which contains the annihilation operator for the heavy-light meson. Together with the heavy quark propagator and the effective propagator for this diagram we end up with the following expression

$$M^{\mu} = -N_c \int \frac{d^4p}{(2\pi)^4} \mathrm{Tr}[\xi^{\dagger}\gamma^{\mu}L \frac{iP_+}{v\cdot p}(-iG_H H) iS(p)] \tag{6.16}$$

The propagator S(p) is here just the simple propagator $\frac{\gamma\cdot p + m}{p^2 - m^2}$, since we don't have any external photon or gluon lines. We can calculate this expression, that is, do the integration using dimensional regularization. This procedure is described in the appendix, section A.2. We get

$$\begin{aligned} M^{\mu} &= -N_c \int \frac{d^4p}{(2\pi)^4} \mathrm{Tr}\left[\xi^{\dagger}\gamma^{\mu}L \frac{iP_+}{v\cdot p}(-iG_H H) iS(p) \right] \\ &= -iN_c G_H \mathrm{Tr}[\xi^{\dagger}\gamma^{\mu}LH \int \frac{d^4p}{(2\pi)^4} \frac{1}{v\cdot p} \frac{\gamma\cdot p + m}{p^2 - m^2}] \\ &= -iN_c G_H \mathrm{Tr}[\xi^{\dagger}\gamma^{\mu}LH((\gamma\cdot v)I_1 + mI_{3/2})] \\ &= -iN_c G_H [mI_{3/2} - I_1]\mathrm{Tr}[\xi^{\dagger}\gamma^{\mu}LH] \end{aligned} \tag{6.17}$$

We can now in principle follow the same procedure for all annihilation diagrams, only changing the effective propagator and adding a colour matrix t^a in the weak vertex when an external gluon line is added.

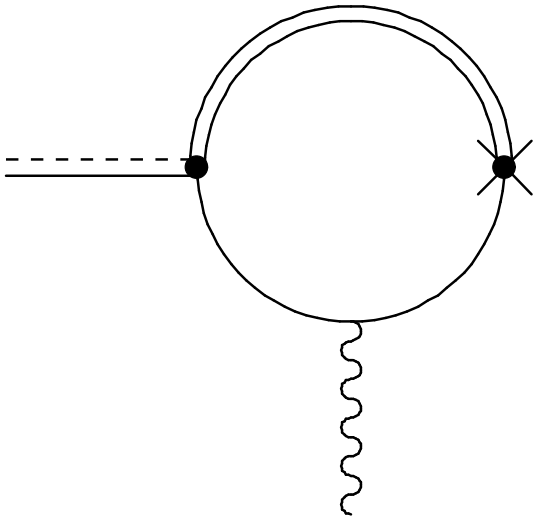

Figure 6.5 $\langle\gamma|\bar{q}\gamma^{\mu}LQ_{v_c}|D\rangle$ *- An annihilation diagram for the D-meson with a photon coupled to it.*

In the second diagram, shown in figure 6.5, we have a photon coupling to the light quark in the loop. This is the only difference between this diagram and the one we had in figure 6.4. Instead of writing down the vertex factor for the electromagnetic interaction vertex and the quark propagators before and after the interaction, we simply use the effective propagator from section 5.2, iS_1^F, where the subscript 1 means that one particle is coupling to the quark, and the superscript F indicates a photon. We now get the following expression

$$\begin{aligned}
M^{\mu} &= -N_c\int\frac{d^4p}{(2\pi)^4}\mathrm{Tr}\left[\xi^{\dagger}\gamma^{\mu}L\frac{iP_+}{v\cdot p}(-iG_H H)iS_1^F\right] \\
&= -N_c G_H\int\frac{d^4p}{(2\pi)^4}\mathrm{Tr}\left[\xi^{\dagger}\gamma^{\mu}L\frac{1}{v\cdot p}H\times\left(-\frac{i}{4}e\tilde{Q}_{\xi}^{V}F_{\alpha\beta}\frac{1}{(p^2-m^2)^2}\{T(p),\sigma^{\alpha\beta}\}\right)\right] \\
&= \frac{iN_c G_H e}{4}\mathrm{Tr}\left[\xi^{\dagger}\gamma^{\mu}LH\tilde{Q}_{\xi}^{V}F_{\alpha\beta}\int\frac{d^4p}{(2\pi)^4}\frac{1}{v\cdot p}\frac{1}{(p^2-m^2)^2}\times\left(\{\gamma\cdot p,\sigma^{\alpha\beta}\}+2m\sigma^{\alpha\beta}\right)\right] \\
&= \frac{N_c G_H e}{4}\mathrm{Tr}\left[\xi^{\dagger}\gamma^{\mu}LH\left(iI_2\{\gamma\cdot v,\sigma\cdot F\tilde{Q}_{\xi}^{V}\}+\frac{1}{8\pi}\sigma\cdot F\tilde{Q}_{\xi}^{V}\right)\right]
\end{aligned} \tag{6.18}$$

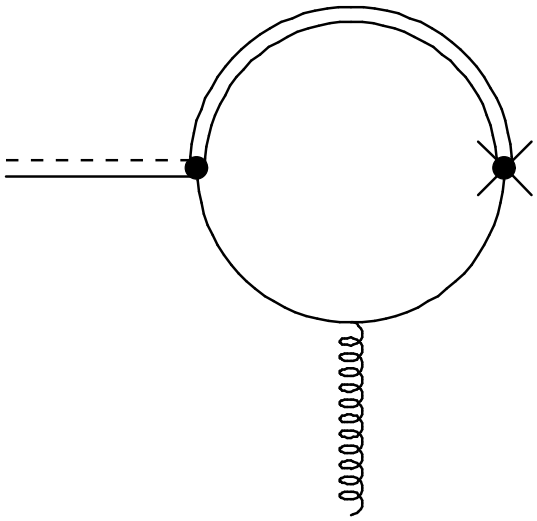

Figure 6.6 $\langle g|\bar{q}\gamma^{\mu}Lt^{a}Q_{v_c}|D\rangle$ *- An annihilation diagram for the D-meson with a gluon coupled to it.*

The third of the annihilation diagrams is one with a gluon coupled to the light quark on the loop. This is a non-factoriable diagram (having one external gluon line coupled to the loop) and has to be connected to another non-factorizable partial diagram also with a colour matrix t^a. By inserting this colour matrix in the weak vertex (together with the coloured current $\bar{q}\gamma^{\mu}Lt^{a}Q$ from the Fierz transformation) the full Feynman diagrams made up of partial diagrams like this one, becomes quasi-factorizable. This can be done since we only include the gluon condensate to lowest order with only two gluons coupling to the light quarks in the process. Here we also have to note that the trace of the colour unit matrix disappears; a consequence of including the colour matrix t^a in the weak vertex.

$$\begin{aligned}
M^{\mu} &= -\int \frac{d^4p}{(2\pi)^4}\mathrm{Tr}\left[\xi^{\dagger}\gamma^{\mu}Lt^{a}\,\frac{iP_{+}}{v\cdot p}(-iG_{H}H)iS_{l}^{G}\right] \\
&= -G_{H}\int \frac{d^4p}{(2\pi)^4}\mathrm{Tr}\left[\xi^{\dagger}\gamma^{\mu}Lt^{a}\,\frac{1}{v\cdot p}H\times\left(\frac{i}{4}g_{s}t^{a}G^{a}_{\alpha\beta}\,\frac{1}{(p^2-m^2)^2}\{T(p),\sigma^{\alpha\beta}\}\right)\right] \\
&= -\frac{iG_{H}g_{s}}{4}\mathrm{Tr}\left[\xi^{\dagger}\gamma^{\mu}LHt^{a}t^{a}G_{\alpha\beta}\int \frac{d^4p}{(2\pi)^4}\,\frac{1}{v\cdot p}\,\frac{1}{(p^2-m^2)^2}\times\left(\{\gamma\cdot p,\sigma^{\alpha\beta}\}+2m\sigma^{\alpha\beta}\right)\right] \\
&= -\frac{G_{H}g_{s}}{8}\mathrm{Tr}\left[\xi^{\dagger}\gamma^{\mu}LH\left(iI_{2}\{\gamma\cdot v,\sigma\cdot G\}+\frac{1}{8\pi}\sigma\cdot G\right)\right]
\end{aligned} \tag{6.19}$$

where we have used the identity $\mathrm{Tr}[t^{a}t^{a}]=\frac{1}{2}$.

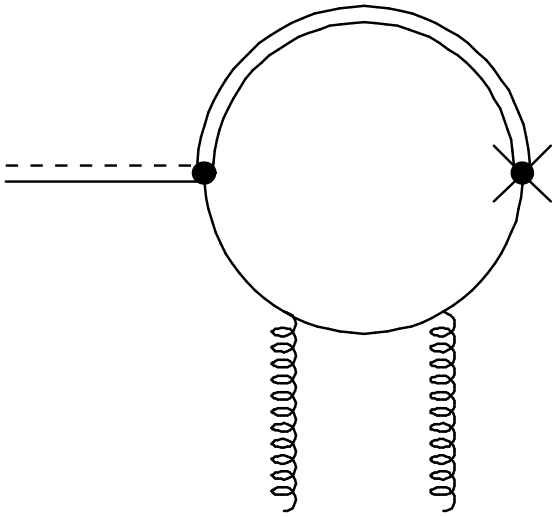

Figure 6.7 $\langle gg|\bar{q}\gamma^{\mu}LQ_{v_c}|D\rangle$ *- An annihilation diagram for the D-meson with two gluons coupled to it.*

Our next diagram will be the one shown in figure 6.7, where two gluons are coupled to the light quark in the loop. In the calculation of this diagram we use the expression for the quark condensate expansion (eq. 4.18) as well as the effective propagator for two external gluon lines.

$$\begin{aligned}
M^{\mu} &= -\int \frac{d^4p}{(2\pi)^4}\mathrm{Tr}\left[\xi^{\dagger}\gamma^{\mu}L\frac{iP_+}{v\cdot p}(-iG_H H)iS_2^{GG}\right] \\
&= -G_H\int \frac{d^4p}{(2\pi)^4}\mathrm{Tr}\left[\xi^{\dagger}\gamma^{\mu}L\frac{1}{v\cdot p}H\times 2i\pi^2 t^a t^a\left\langle\frac{\alpha_s}{\pi}G^2\right\rangle\frac{1}{(p^2-m^2)^4}(m(\gamma\cdot p)+p^2)\right] \\
&= -i\frac{2\pi^2 m G_H}{2}\left\langle\frac{\alpha_s}{\pi}G^2\right\rangle\mathrm{Tr}\left[\xi^{\dagger}\gamma^{\mu}LH\int\frac{d^4p}{(2\pi)^4}\frac{1}{v\cdot p}\frac{p^2+m(\gamma\cdot p)}{(p^2-m^2)^4}\right] \\
&= G_H\left\langle\frac{\alpha_s}{\pi}G^2\right\rangle\mathrm{Tr}\left[\xi^{\dagger}\gamma^{\mu}LH\left(\frac{\pi}{128m^2}+\frac{-1}{96m^2}\right)\right] \\
&= \frac{3\pi-4}{384m^2}G_H\left\langle\frac{\alpha_s}{\pi}G^2\right\rangle\mathrm{Tr}\left[\xi^{\dagger}\gamma^{\mu}LH\right]
\end{aligned} \tag{6.20}$$

In the diagrams that follow, we have not integrated out the momentum. This will be done later when annihilation and creation diagrams are multiplied to give the full Feynman diagrams.

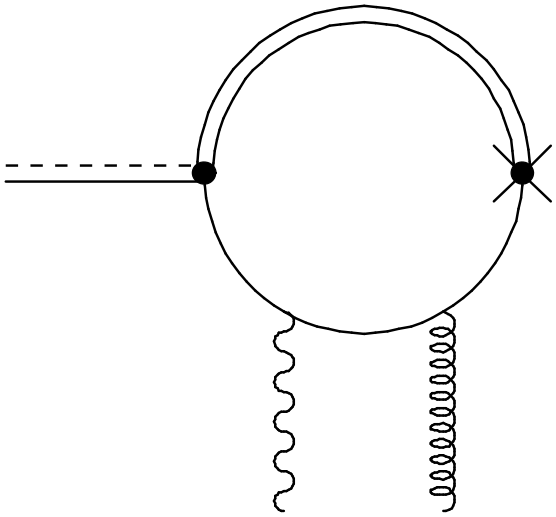

Figure 6.8 $\langle \gamma g | \bar{q}\gamma^{\mu} L t^{a} Q_{v_c} | D \rangle$ *- An annihilation diagram for the D-meson with one photon and one gluon coupled to it.*

We look at the diagram in figure 6.8. This is a diagram with one external photon line and one external gluon line coupled to the loop. With the replacement iS_2^{FG} instead of iS_2^{GG} that we had in the last calculation and with only one colour matrix, we get

$$\begin{aligned} M^{\lambda} &= -\int \frac{d^4p}{(2\pi)^4} \mathrm{Tr}\left[\xi^{\dagger}\gamma^{\lambda} L t^{a} \frac{iP_+}{v\cdot p}(-iG_H H) iS_2^{FG} \right] \\ &= \int \frac{d^4p}{(2\pi)^4} \mathrm{Tr}\left[\xi^{\dagger}\gamma^{\lambda} L t^{a} \frac{1}{v\cdot p} G_H H \times \left(\frac{i}{4} e g_s Q F_{\mu\nu} t^{a} G^{a}_{\alpha\beta} R^{\mu\nu\alpha\beta} \right) \right] \\ &= i\frac{G_H e g_s}{8} \int \frac{d^4p}{(2\pi)^4} \mathrm{Tr}\left[\xi^{\dagger}\gamma^{\lambda} L \frac{1}{v\cdot p} H \times Q F_{\mu\nu} G^{a}_{\alpha\beta} R^{\mu\nu\alpha\beta} \right] \end{aligned} \tag{6.21}$$

where we have used the term

$$\begin{aligned} R^{\mu\nu\alpha\beta} &= S(p)\gamma^{\beta}S(p)\gamma^{\nu}S(p)\gamma^{\mu}S(p)\gamma^{\alpha}S(p) \\ &+ S(p)\gamma^{\nu}S(p)\gamma^{\beta}S(p)\gamma^{\mu}S(p)\gamma^{\alpha}S(p) \\ &+ S(p)\gamma^{\nu}S(p)\gamma^{\mu}S(p)\gamma^{\beta}S(p)\gamma^{\alpha}S(p) \end{aligned} \tag{6.22}$$

This expression will also be used in the next calculation. Note also that we have here changed the index in the superscript of M to λ. This is just so that we can keep the indices used in the effective propagator.

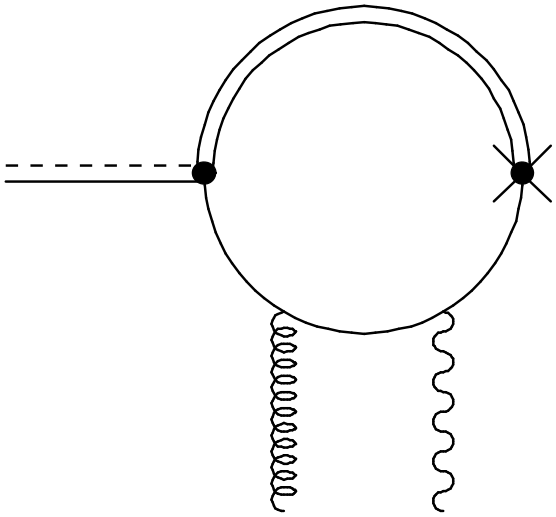

Figure 6.9 $\langle g\gamma|\bar{q}\gamma^{\mu}Lt^{a}Q_{v_c}|D\rangle$ *- An annihilation diagram for the D-meson with one gluon and one photon coupled to it.*

The diagram in figure 6.9 is almost the same as the one we had in figure 6.8, only that the photon and gluon lines has switched places. In fact, the only difference will be that the indices in the gluonic and electromagnetic field tensors are changed. We get

$$\begin{aligned} M^{\lambda} &= -\int \frac{d^4p}{(2\pi)^4} \mathrm{Tr}\left[\xi^{\dagger}\gamma^{\lambda} L t^{a} \frac{iP_{+}}{v\cdot p}(-iG_{H}H) iS_2^{GF} \right] \\ &= \int \frac{d^4p}{(2\pi)^4} \mathrm{Tr}\left[\xi^{\dagger}\gamma^{\lambda} L t^{a} \frac{1}{v\cdot p} G_{H} H \times \left(\frac{i}{4} e g_s t^{a} G^{a}_{\mu\nu} Q F_{\alpha\beta} R^{\mu\nu\alpha\beta} \right) \right] \\ &= i\frac{G_H e g_s}{8} \int \frac{d^4p}{(2\pi)^4} \mathrm{Tr}\left[\xi^{\dagger}\gamma^{\lambda} L \frac{1}{v\cdot p} H \times G^{a}_{\mu\nu} Q F_{\alpha\beta} R^{\mu\nu\alpha\beta} \right] \end{aligned} \tag{6.23}$$

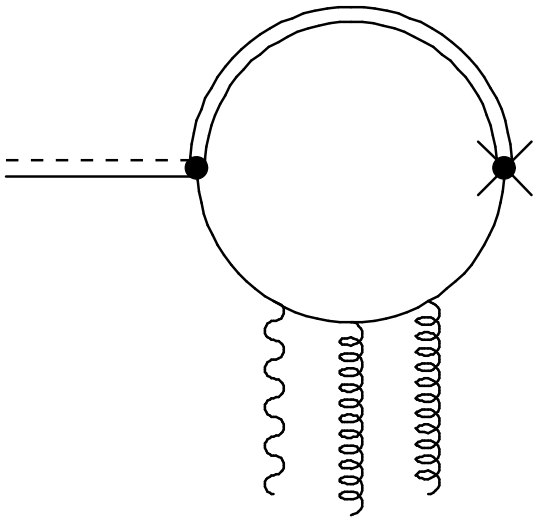

Figure 6.10 $\langle \gamma gg | \bar{q}\gamma^{\mu} L Q_{v_c} | D \rangle$ *- An annihilation diagram for the D-meson with one external photon line and two external gluon lines coupled to it.*

For the last three diagrams we will get the same situation as for the two diagrams just calculated, namely that the only difference between them will be a change in indices, coming from the different effective propagators. In figure 6.10 we have a diagram with one external photon line and two external gluon lines coupling to the loop. This gives

$$\begin{aligned} M^{\lambda} &= -\int \frac{d^4p}{(2\pi)^4} \mathrm{Tr}\left[\xi^{\dagger}\gamma^{\lambda} L \frac{iP_+}{v\cdot p}(-iG_H H) iS_3^{FGG} \right] \\ &= \int \frac{d^4p}{(2\pi)^4} \mathrm{Tr}\left[\xi^{\dagger}\gamma^{\lambda} L \frac{1}{v\cdot p} G_H H \times \frac{\pi^2}{24} eQF_{\mu\nu} t^a t^a \left\langle \frac{\alpha_s}{\pi} G^2 \right\rangle \left(g_{\alpha\rho}g_{\beta\sigma} - g_{\alpha\sigma}g_{\beta\rho} \right) T^{\mu\nu\alpha\beta\sigma\rho} \right] \\ &= \frac{eG_H}{48} \left\langle \frac{\alpha_s}{\pi} G^2 \right\rangle \int \frac{d^4p}{(2\pi)^4} \mathrm{Tr}\left[\xi^{\dagger}\gamma^{\lambda} L \frac{1}{v\cdot p} H \times QF_{\mu\nu} \left(g_{\alpha\rho}g_{\beta\sigma} - g_{\alpha\sigma}g_{\beta\rho} \right) T^{\mu\nu\alpha\beta\sigma\rho} \right] \end{aligned} \tag{6.24}$$

where $T^{\mu\nu\alpha\beta\sigma\rho}$ is the same as the expression given in eq. 5.33. This expression we will use in the next two calculations as well.

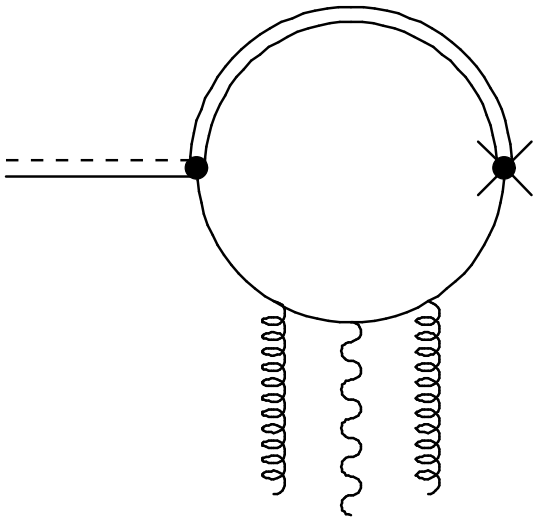

Figure 6.11 $\langle g\gamma g|\bar{q}\gamma^{\mu}LQ_{v_c}|D\rangle$ *- An annihilation diagram for the D-meson with one external photon line and two external gluon lines coupled to it.*

The next diagram, shown in figure 6.11, differs from the one we had only by a change of effective propagator; iS_3^{GFG} instead of iS_3^{FGG}. Since we don't do the integrations, the only difference in the result of the calculation will be a change in indices.

$$\begin{aligned} M^{\lambda} &= -\int \frac{d^4p}{(2\pi)^4} Tr\left[\xi^{\dagger}\gamma^{\lambda}L\frac{iP_+}{v\cdot p}(-iG_H H)iS_3^{GFG}\right] \\ &= \int \frac{d^4p}{(2\pi)^4} Tr\left[\xi^{\dagger}\gamma^{\lambda}L\frac{1}{v\cdot p}G_H H\times\frac{\pi^2}{24}eQF_{\alpha\beta}t^a t^a\left\langle\frac{\alpha_s}{\pi}G^2\right\rangle\left(g_{\mu\rho}g_{\nu\sigma}-g_{\mu\sigma}g_{\nu\rho}\right)T^{\mu\nu\alpha\beta\sigma\rho}\right] \\ &= \frac{eG_H}{48}\left\langle\frac{\alpha_s}{\pi}G^2\right\rangle\int\frac{d^4p}{(2\pi)^4}Tr\left[\xi^{\dagger}\gamma^{\lambda}L\frac{1}{v\cdot p}H\times QF_{\alpha\beta}\left(g_{\mu\rho}g_{\nu\sigma}-g_{\mu\sigma}g_{\nu\rho}\right)T^{\mu\nu\alpha\beta\sigma\rho}\right] \end{aligned} \tag{6.25}$$

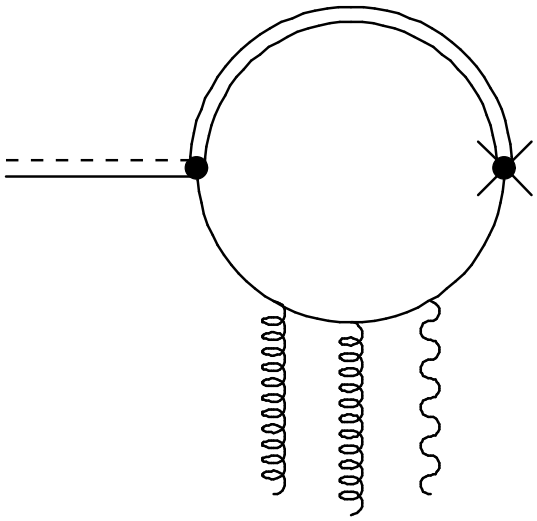

Figure 6.12 $\langle gg\gamma|\bar{q}\gamma^{\mu}LQ_{v_c}|D\rangle$ *- An annihilation diagram for the D-meson with one external photon line and two external gluon lines coupled to it.*

Finally, the last annihilation diagram as shown in figure 6.12. Here we use the effective propagator iS_3^{GGF} and it gives us

$$\begin{aligned} M^{\lambda} &= -\int \frac{d^4p}{(2\pi)^4} Tr\left[\xi^{\dagger}\gamma^{\lambda}L\frac{iP_+}{v\cdot p}(-iG_H H)iS_3^{GGF}\right] \\ &= \int \frac{d^4p}{(2\pi)^4} Tr\left[\xi^{\dagger}\gamma^{\lambda}L\frac{1}{v\cdot p}G_H H\times\frac{\pi^2}{24}eQF_{\rho\sigma}t^a t^a\left\langle\frac{\alpha_s}{\pi}G^2\right\rangle\left(g_{\mu\alpha}g_{\nu\beta}-g_{\mu\beta}g_{\nu\alpha}\right)T^{\mu\nu\alpha\beta\sigma\rho}\right] \\ &= \frac{eG_H}{48}\left\langle\frac{\alpha_s}{\pi}G^2\right\rangle\int\frac{d^4p}{(2\pi)^4}Tr\left[\xi^{\dagger}\gamma^{\lambda}L\frac{1}{v\cdot p}H\times QF_{\rho\sigma}\left(g_{\mu\alpha}g_{\nu\beta}-g_{\mu\beta}g_{\nu\alpha}\right)T^{\mu\nu\alpha\beta\sigma\rho}\right] \end{aligned} \tag{6.26}$$

As we can see, the only difference between the last three diagrams are the indices, similar to the two diagrams with one external photon line and one external gluon line, as mentioned before. These last three diagrams must couple to the same type of diagram, so we do not expect much variation between them.

6.1.2 Calculations of the Creation Diagrams

We start with the simplest diagram, namely the one shown in figure 6.13. Here we have a loop with two light quarks, and no external photon or gluon lines.

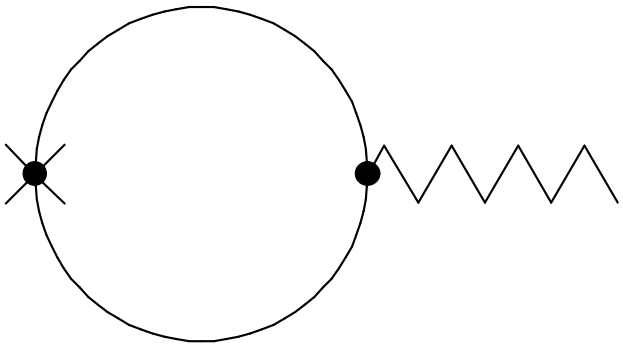

Figure 6.13 $\langle V|\bar{\chi}\Lambda^n\gamma_\mu L\chi|0\rangle$ *- A creation diagram for a vector particle with no external photon- or gluon-lines.*

Since this is the first creation diagram, we will do a more extensive calculation than we have done earlier. As the diagrams become more and more complex, however, we will sketch the procedure and write down the final results.

Since the diagram do not contain any external lines, the quark propagators will just be the ordinary S(p), and we get the following expression

$$\begin{aligned} M^\mu &= -N_C \int \frac{d^D p}{(2\pi)^D} \mathrm{Tr}\Big[\big(\Lambda^n \gamma^\mu L\big) iS(p) \big(ih_V \gamma_\nu V^\nu\big) iS(p)\Big] \\ &= iN_C h_V \mathrm{Tr}_F\Big[\Lambda^n V^\nu\Big] \int \frac{d^D p}{(2\pi)^D} \mathrm{Tr}\Big[R\gamma^\mu S(p)\gamma_\nu S(p)\Big] \\ &= iN_C h_V \mathrm{Tr}_F\Big[\Lambda^n V^\nu\Big] T_{\mu\nu} \end{aligned} \tag{6.27}$$

Here Tr_F is the trace over flavour matrices and Tr without any subscript is the trace over Dirac matrices. We have also used the general space-time dimension D here, but we will put this equal to four in the final result.

$$
\begin{aligned}
T_{\mu\nu} &= \int \frac{d^D p}{(2\pi)^D} \mathrm{Tr}\left[R\gamma^\mu S(p)\gamma_\nu S(p) \right] \\
&= \int \frac{d^D p}{(2\pi)^D} \frac{1}{\left(p^2 - m^2\right)^2} \mathrm{Tr}\left[R\gamma^\mu (\gamma\cdot p + m)\gamma_\nu (\gamma\cdot p + m) \right] \\
&= \int \frac{d^D p}{(2\pi)^D} \frac{1}{\left(p^2 - m^2\right)^2} \mathrm{Tr}\left[R\gamma^\mu \gamma\cdot p\gamma_\nu \gamma\cdot p + m^2 R\gamma^\mu\gamma_\nu \right], \qquad \text{since Tr[odd number of } \gamma] = 0 \\
&= \int \frac{d^D p}{(2\pi)^D} \frac{1}{\left(p^2 - m^2\right)^2} \mathrm{Tr}\left[R\gamma^\mu (2-D)\frac{p^2}{D}\gamma_\nu + m^2 R\gamma^\mu\gamma_\nu \right] \qquad (6.28) \\
&= \int \frac{d^D p}{(2\pi)^D} \frac{1}{\left(p^2 - m^2\right)^2} \left[\frac{2-D}{D} p^2 + m^2 \right] \mathrm{Tr}\left[R\gamma^\mu\gamma_\nu \right] \\
&= \int \frac{d^D p}{(2\pi)^D} \frac{1}{\left(p^2 - m^2\right)^2} \left[\frac{2-D}{D} p^2 + m^2 \right] 2g_{\mu\nu}
\end{aligned}
$$

Here we use a small trick to remove p^2 in the numerator

$$
\begin{aligned}
T_{\mu\nu} &= \int \frac{d^D p}{(2\pi)^D} \frac{1}{\left(p^2 - m^2\right)^2} \left[\frac{2-D}{D} \left\{ (p^2 - m^2) + m^2 \right\} + m^2 \right] 2g_{\mu\nu} \\
&= \int \frac{d^D p}{(2\pi)^D} \frac{1}{\left(p^2 - m^2\right)^2} \left[\frac{2-D}{D} (p^2 - m^2) + m^2 \left(1 + \frac{2-D}{D} \right) \right] 2g_{\mu\nu} \qquad (6.29) \\
&= \left[\left(\frac{2-D}{D} \right) I_1 + m^2 \left(1 + \frac{2-D}{D} \right) I_2 \right] 2g_{\mu\nu}
\end{aligned}
$$

where I_1 and I_2 are the divergent integrals given in the appendix. This trick we will use frequently in the calculations that follows. If we put this result into our expression for M, we get the final result

$$
\begin{aligned}
M^\mu &= iN_C h_V \mathrm{Tr}_F\left[\Lambda^n V^\nu \right] \left[\left(\frac{2-D}{D} \right) I_1 + m^2 \left(1 + \frac{2-D}{D} \right) I_2 \right] 2g_{\mu\nu} \\
&\underset{D\to 4}{\to} iN_C h_V \mathrm{Tr}_F\left[\Lambda^n V^\nu \right] \left[m^2 I_2 - I_1 \right] g_{\mu\nu}
\end{aligned} \qquad (6.30)
$$

In the same manner we can continue to calculate the other creation diagrams.

The next type of diagrams are the ones where we have a coupling of one photon or one gluon to one of the quarks. We have four of these, as shown in figure 6.3. We start with the one shown in figure 6.14, where we have a photon coupled to the upper light quark.

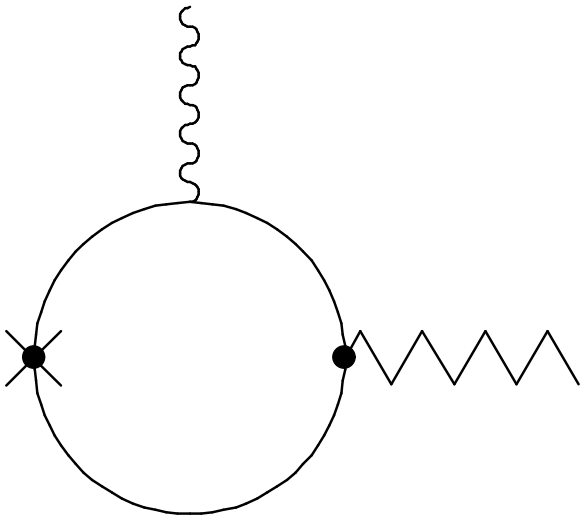

Figure 6.14 $\langle V\gamma|\bar{\chi}\Lambda^n\gamma_\mu L\chi|0\rangle$ *- A creation diagram for a vector particle with one external photon line.*

The calculation of this diagram will be like the calculation we had above, but with the change of one the propagators into the effective propagator iS_1^F. The calculation will, however, be much longer then the calculation above, but we will still go through it in some detail as some of the diagrams coming after will be similar. We get

$$\begin{aligned} M^\mu &= -N_c \int \frac{d^D p}{(2\pi)^D} \mathrm{Tr}\left[(\Lambda^n \gamma^\mu L) i S_1^F (i h_\nu \gamma_\nu V^\nu) i S(p) \right] \\ &= i N_c h_\nu \mathrm{Tr}_F \left[\Lambda^n V^\nu \right] \int \frac{d^D p}{(2\pi)^D} \mathrm{Tr}\left[\gamma^\mu L S_1^F \gamma_\nu S(p) \right] \\ &= i N_c h_\nu \mathrm{Tr}_F \left[\Lambda^n V^\nu \right] T_{\mu\nu} \end{aligned} \tag{6.31}$$

where

$$\begin{aligned} T_{\mu\nu} &= \int \frac{d^D p}{(2\pi)^D} \mathrm{Tr}\left[R\gamma^\mu \left(-\frac{e}{4} \frac{1}{\left(p^2 - m^2\right)^2} \left\{ \tilde{Q}_\xi^\nu \sigma \cdot F, (\gamma \cdot p + m) \right\} \right) \gamma_\nu \frac{\gamma \cdot p + m}{p^2 - m^2} \right] \\ &= -\frac{e}{4} \int \frac{d^D p}{(2\pi)^D} \frac{1}{\left(p^2 - m^2\right)^3} \mathrm{Tr}\left[R\gamma^\mu \left\{ \tilde{Q}_\xi^\nu \sigma \cdot F, (\gamma \cdot p + m) \right\} \gamma_\nu (\gamma \cdot p + m) \right] \\ &= -\frac{e}{4} \int \frac{d^D p}{(2\pi)^D} \frac{1}{\left(p^2 - m^2\right)^3} A \end{aligned} \tag{6.32}$$

where

$$
\begin{aligned}
A &= \mathrm{Tr}\left[R\gamma^{\mu} \left\{ \tilde{Q}_{\xi}^{\nu}\sigma\cdot F, (\gamma\cdot p + m) \right\} \gamma_{\nu} (\gamma\cdot p + m) \right] \\
&= \mathrm{Tr}\left[R\gamma^{\mu} \left(\tilde{Q}_{\xi}^{\nu}\sigma\cdot F(\gamma\cdot p + m) + (\gamma\cdot p + m)\tilde{Q}_{\xi}^{\nu}\sigma\cdot F \right) \gamma_{\nu} (\gamma\cdot p + m) \right] \\
&= \mathrm{Tr}\left[R\gamma^{\mu} \left(\tilde{Q}_{\xi}^{\nu}\sigma\cdot F\gamma\cdot p + 2m\tilde{Q}_{\xi}^{\nu}\sigma\cdot F + \gamma\cdot p\tilde{Q}_{\xi}^{\nu}\sigma\cdot F \right) \gamma_{\nu} (\gamma\cdot p + m) \right] \\
&= \mathrm{Tr}[R\gamma^{\mu} (\tilde{Q}_{\xi}^{\nu}\sigma\cdot F\gamma\cdot p\gamma_{\nu}\gamma\cdot p + 2m\tilde{Q}_{\xi}^{\nu}\sigma\cdot F\gamma_{\nu}\gamma\cdot p + \gamma\cdot p\tilde{Q}_{\xi}^{\nu}\sigma\cdot F\gamma_{\nu}\gamma\cdot p + \\
&\quad m\tilde{Q}_{\xi}^{\nu}\sigma\cdot F\gamma\cdot p\gamma_{\nu} + 2m^2\tilde{Q}_{\xi}^{\nu}\sigma\cdot F\gamma_{\nu} + m\gamma\cdot p\tilde{Q}_{\xi}^{\nu}\sigma\cdot F\gamma_{\nu})] \\
&= \mathrm{Tr}\left[R\gamma^{\mu} \left(\tilde{Q}_{\xi}^{\nu}\sigma\cdot F\gamma\cdot p\gamma_{\nu}\gamma\cdot p + \gamma\cdot p\tilde{Q}_{\xi}^{\nu}\sigma\cdot F\gamma_{\nu}\gamma\cdot p + 2m^2\tilde{Q}_{\xi}^{\nu}\sigma\cdot F\gamma_{\nu} \right) \right] \\
&= \mathrm{Tr}\left[(R\gamma^{\mu}\tilde{Q}_{\xi}^{\nu}\sigma\cdot F)\gamma\cdot p\gamma_{\nu}\gamma\cdot p + R\gamma^{\mu}\gamma\cdot p(\tilde{Q}_{\xi}^{\nu}\sigma\cdot F\gamma_{\nu})\gamma\cdot p + 2m^2 R\gamma^{\mu}\tilde{Q}_{\xi}^{\nu}\sigma\cdot F\gamma_{\nu} \right] \\
&= \mathrm{Tr}\left[\frac{(2-D)}{D} p^2 R\gamma^{\mu}\tilde{Q}_{\xi}^{\nu}\sigma\cdot F\gamma_{\nu} + \gamma\cdot pR\gamma^{\mu}\gamma\cdot p(\tilde{Q}_{\xi}^{\nu}\sigma\cdot F\gamma_{\nu}) + 2m^2 R\gamma^{\mu}\tilde{Q}_{\xi}^{\nu}\sigma\cdot F\gamma_{\nu} \right] \qquad (6.33) \\
&= \mathrm{Tr}\left[\frac{(2-D)}{D} p^2 R\gamma^{\mu}\tilde{Q}_{\xi}^{\nu}\sigma\cdot F\gamma_{\nu} + L\gamma\cdot p\gamma^{\mu}\gamma\cdot p\tilde{Q}_{\xi}^{\nu}\sigma\cdot F\gamma_{\nu} + 2m^2 R\gamma^{\mu}\tilde{Q}_{\xi}^{\nu}\sigma\cdot F\gamma_{\nu} \right] \\
&= \mathrm{Tr}\left[\frac{(2-D)}{D} p^2 R\gamma^{\mu}\tilde{Q}_{\xi}^{\nu}\sigma\cdot F\gamma_{\nu} + \frac{(2-D)}{D} p^2 L\gamma^{\mu}\tilde{Q}_{\xi}^{\nu}\sigma\cdot F\gamma_{\nu} + 2m^2 R\gamma^{\mu}\tilde{Q}_{\xi}^{\nu}\sigma\cdot F\gamma_{\nu} \right] \\
&= \mathrm{Tr}\left[\left(\frac{(2-D)}{D} p^2 (R+L) + 2m^2 R \right) \gamma^{\mu}\tilde{Q}_{\xi}^{\nu}\sigma\cdot F\gamma_{\nu} \right] \\
&= \mathrm{Tr}\left[\left(\frac{(2-D)}{D} p^2 + 2m^2 R \right) \gamma^{\mu}\tilde{Q}_{\xi}^{\nu}\sigma\cdot F\gamma_{\nu} \right] \\
&= \mathrm{Tr}\left[\left(\frac{(2-D)}{D} p^2 + 2m^2 \frac{1}{2}(1+\gamma_5) \right) \gamma^{\mu}\tilde{Q}_{\xi}^{\nu}\sigma\cdot F\gamma_{\nu} \right] \\
&= \mathrm{Tr}\left[\left(\frac{(2-D)}{D} p^2 + m^2 (1+\gamma_5) \right) \gamma^{\mu}\tilde{Q}_{\xi}^{\nu}\sigma\cdot F\gamma_{\nu} \right]
\end{aligned}
$$

Putting this expression into $T_{\mu\nu}$ we get

$$
\begin{aligned}
T_{\mu\nu} &= -\frac{e}{4}\int \frac{d^D p}{(2\pi)^D} \frac{1}{\left(p^2 - m^2\right)^3} \mathrm{Tr}\left[\left(\frac{(2-D)}{D} p^2 + m^2 (1+\gamma_5) \right) \gamma^{\mu}\tilde{Q}_{\xi}^{\nu}\sigma\cdot F\gamma_{\nu} \right] \\
&= -\frac{e}{4}\mathrm{Tr}\left[\left(\frac{(2-D)}{D} I_2 + m^2 \left(1 + \gamma_5 + \frac{(2-D)}{D} \right) I_3 \right) \gamma^{\mu}\tilde{Q}_{\xi}^{\nu}\sigma\cdot F\gamma_{\nu} \right]
\end{aligned} \qquad (6.34)
$$

But I_3 is not a divergent integral, so we can insert its calculated value (given in the in the appendix). This gives the final result

$$
\begin{aligned}
M^{\mu} &= -\frac{ieN_c h_{\nu}}{4} \mathrm{Tr}_F\left[\Lambda^n V^{\nu} \right] \mathrm{Tr}\left[\left(\frac{(2-D)}{D} I_2 + m^2 \left(1 + \gamma_5 + \frac{(2-D)}{D} \right) \left(\frac{-i}{32\pi^2 m^2} \right) \right) \gamma^{\mu}\tilde{Q}_{\xi}^{\nu}\sigma\cdot F\gamma_{\nu} \right] \\
&\underset{D\to 4}{\longrightarrow} -\frac{ieN_c h_{\nu}}{8} \mathrm{Tr}_F\left[\Lambda^n V^{\nu} \right] \mathrm{Tr}\left[\left(\left(\frac{-i}{32\pi^2} \right) (2\gamma_5 + 1) - I_2 \right) \gamma^{\mu}\tilde{Q}_{\xi}^{\nu}\sigma\cdot F\gamma_{\nu} \right]
\end{aligned} \qquad (6.35)
$$

As one can see, the calculations can be rather long, and we will therefore try to just sketch the calculations for diagram calculations that give similar results.

We now look at the diagram in figure 6.15, which is the same type of diagram that we had, only with the external photon line moved to the lower quark line in the loop.

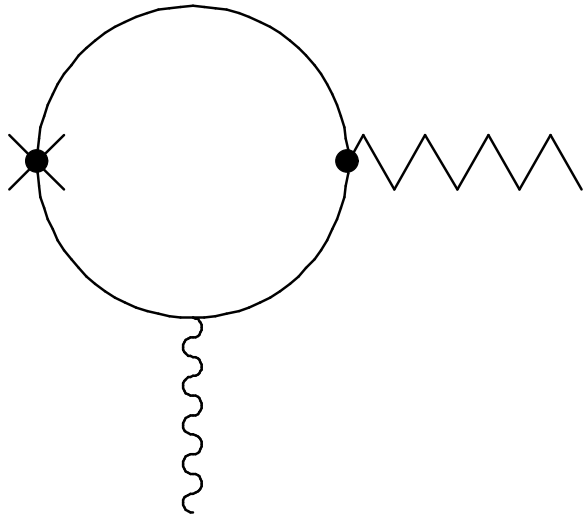

Figure 6.15 $\langle V\gamma|\bar{\chi}\Lambda^n\gamma_\mu L\chi|0\rangle$ *- Also a creation diagram for a vector particle with one external photon line.*

For our calculations this simply means that the two propagators switch place in the expression for M above (eq. 6.35), and we expect that the calculation of this diagram should not differ very much from the one we had above.

$$
\begin{aligned}
M^\mu &= -N_c\int\frac{d^Dp}{(2\pi)^D}\mathrm{Tr}\left[(\Lambda^n\gamma^\mu L)iS(p)(ih_v\gamma_v V^v)iS_1^F\right] \\
&= iN_c h_v \mathrm{Tr}_F\left[\Lambda^n V^v\right]\int\frac{d^Dp}{(2\pi)^D}\mathrm{Tr}\left[\gamma^\mu LS(p)\gamma_v S_1^F\right] \\
&= -\frac{ieN_c h_v}{4}\mathrm{Tr}_F\left[\Lambda^n V^v\right]\int\frac{d^Dp}{(2\pi)^D}\mathrm{Tr}\left[R\gamma^\mu\left(\frac{\gamma\cdot p+m}{p^2-m^2}\right)\gamma_v\left(-\frac{e}{4}\frac{1}{\left(p^2-m^2\right)^2}\left\{\tilde{Q}_\xi^v\sigma\cdot F,(\gamma\cdot p+m)\right\}\right)\right] \\
&= -\frac{ieN_c h_v}{4}\mathrm{Tr}_F\left[\Lambda^n V^v\right]\mathrm{Tr}\left[\left(\frac{(2-D)}{D}I_2+m^2\left(1+\gamma_5+\frac{(2-D)}{D}\right)\left(\frac{-i}{32\pi^2m^2}\right)\right)\gamma^\mu\gamma_v\tilde{Q}_\xi^v\sigma\cdot F\right] \\
&\underset{D\to4}{\to} -\frac{ieN_c h_v}{8}\mathrm{Tr}_F\left[\Lambda^n V^v\right]\mathrm{Tr}\left[\left(\left(\frac{-i}{32\pi^2}\right)(2\gamma_5+1)-I_2\right)\gamma^\mu\gamma_v\tilde{Q}_\xi^v\sigma\cdot F\right]
\end{aligned}
\tag{6.36}
$$

We see here that the only change from eq 6.35 is the order of the Dirac matrices in the trace.

Our next calculation will be of the diagram in figure 6.16, where we have an external gluon line instead of a photon line. This simply means that we exchange the propagator iS_1^F with the

propagator with one external gluon line, iS_1^G. However, we also have to include a colour matrix t^a in the weak vertex factor, in order to make the diagram quasi-factorizable.

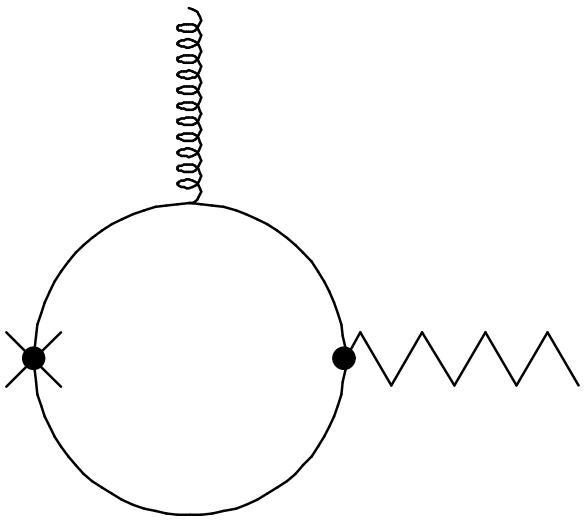

Figure 6.16 $\langle Vg|\bar{\chi}\Lambda^n\gamma_\mu t^a L\chi|0\rangle$ *- A creation diagram for a vector particle with one external gluon line coupled to the upper quark.*

We get

$$\begin{aligned} M^\mu &= -\int \frac{d^D p}{(2\pi)^D} Tr\left[(\Lambda^n \gamma^\mu L t^a) i S_1^G (i h_\nu \gamma_\nu V^\nu) i S(p) \right] \\ &= i h_\nu Tr_F\left[\Lambda^n V^\nu\right] \int \frac{d^D p}{(2\pi)^D} Tr\left[\gamma^\mu L t^a S_1^G \gamma_\nu S(p)\right] \\ &= i h_\nu Tr_F\left[\Lambda^n V^\nu\right] T_{\mu\nu} \end{aligned} \tag{6.37}$$

where

$$\begin{aligned} T_{\mu\nu} &= \int \frac{d^D p}{(2\pi)^D} Tr\left[R\gamma^\mu t^a t^a G^a_{\alpha\beta} \left(\frac{g_s}{4} \frac{1}{\left(p^2 - m^2\right)^2} \left\{\sigma^{\alpha\beta}, (\gamma\cdot p + m)\right\} \right) \gamma_\nu \left(\frac{\gamma\cdot p + m}{p^2 - m^2} \right) \right] \\ &= \frac{g_s}{8} \int \frac{d^D p}{(2\pi)^D} \frac{1}{\left(p^2 - m^2\right)^3} Tr\left[R\gamma^\mu G_{\alpha\beta} \left\{\sigma^{\alpha\beta}, (\gamma\cdot p + m)\right\} \gamma_\nu (\gamma\cdot p + m) \right] \\ &= \frac{g_s}{8} \int \frac{d^D p}{(2\pi)^D} \frac{1}{\left(p^2 - m^2\right)^3} Tr\left[\frac{2-D}{D} p^2 \gamma^\mu \sigma^{\alpha\beta} G_{\alpha\beta} \gamma_\nu + m^2 \left(1 + \gamma_5\right) \gamma^\mu \sigma^{\alpha\beta} G_{\alpha\beta} \gamma_\nu \right] \\ &= \frac{g_s}{8} Tr\left[\left(\frac{2-D}{D} I_2 + m^2 \left(1 + \gamma_5 + \frac{2-D}{D} \right) I_3 \right) \gamma^\mu \sigma^{\alpha\beta} G_{\alpha\beta} \gamma_\nu \right] \end{aligned} \tag{6.38}$$

Which gives the final result

$$M^{\mu} = \frac{ih_v g_s}{8} Tr_F\left[\Lambda^n V^v\right] Tr\left[\left(\frac{2-D}{D} I_2 + m^2\left(1+\gamma_5+\frac{2-D}{D}\right)\left(\frac{-i}{32\pi^2 m^2}\right)\right)\gamma^{\mu}\sigma^{\alpha\beta}G_{\alpha\beta}\gamma_v\right]$$
$$\underset{D\to 4}{\to} \frac{ih_v g_s}{16} Tr_F\left[\Lambda^n V^v\right] Tr\left[\left(\left(\frac{-i}{32\pi^2}\right)(2\gamma_5+1) - I_2\right)\gamma^{\mu}\sigma^{\alpha\beta}G_{\alpha\beta}\gamma_v\right] \quad (6.39)$$

For the diagram in figure 6.17 we will get, in the same way as with the photon coupled to the quark, almost the same result.

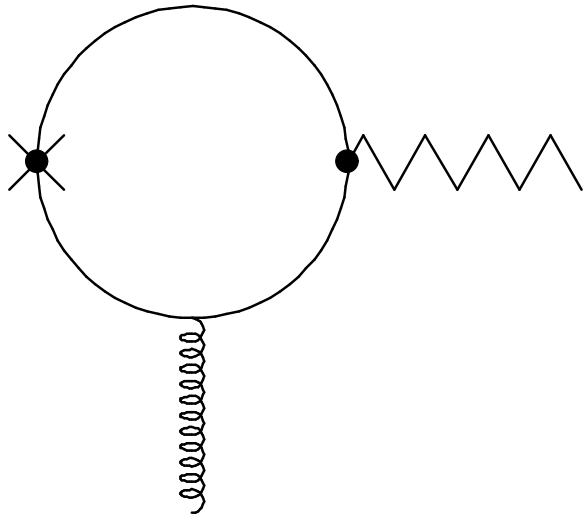

Figure 6.17 $\langle Vg|\bar{\chi}\Lambda^n\gamma_\mu t^a L\chi|0\rangle$ *- Another creation diagram for a vector particle with one external gluon line coupled to the lower quark.*

$$\begin{aligned}
M^{\mu} &= -\int \frac{d^D p}{(2\pi)^D} Tr\left[(\Lambda^n\gamma^{\mu} L t^a) iS(p)(ih_v\gamma_v V^v) iS_1^G\right] \\
&= ih_v Tr_F\left[\Lambda^n V^v\right]\int \frac{d^D p}{(2\pi)^D} Tr\left[\gamma^{\mu} L t^a S(p)\gamma_v S_1^G\right] \\
&= ih_v Tr_F\left[\Lambda^n V^v\right]\int \frac{d^D p}{(2\pi)^D} Tr\left[R\gamma^{\mu} t^a\left(\frac{\gamma\cdot p+m}{p^2-m^2}\right)\gamma_v t^a G^a_{\alpha\beta}\left(\frac{g_s}{4}\frac{1}{\left(p^2-m^2\right)^2}\left\{\sigma^{\alpha\beta},(\gamma\cdot p+m)\right\}\right)\right] \\
&= \frac{ih_v g_s}{8} Tr_F\left[\Lambda^n V^v\right] Tr\left[\left(\frac{2-D}{D} I_2 + m^2\left(1+\gamma_5+\frac{2-D}{D}\right)\left(\frac{-i}{32\pi^2 m^2}\right)\right)\gamma^{\mu}\gamma_v\sigma^{\alpha\beta}G_{\alpha\beta}\right] \\
&\underset{D\to 4}{\to} \frac{ih_v g_s}{16} Tr_F\left[\Lambda^n V^v\right] Tr\left[\left(\left(\frac{-i}{32\pi^2}\right)(2\gamma_5+1) - I_2\right)\gamma^{\mu}\gamma_v\sigma^{\alpha\beta}G_{\alpha\beta}\right]
\end{aligned} \quad (6.40)$$

The only difference compared to eq. 6.39 is the position of the Dirac matrix γ_v, just like in the case of the photon.

Now we move on to the diagrams with two external lines, i.e. either one photon line and one gluon line, or two gluon lines. As seen from figure 6.3, we have here nine diagrams of this type. These diagrams are also more complicated, as we have to deal with two effective propagators.

We will, however, start with the ones that only contain one effective propagator, and our first diagram will be the one shown in figure 6.18. This diagram contains one photon- and one gluon-line coupled to the upper quark. As in the case of the annihilation diagrams, we will not do the momentum integrations for the following four diagrams, but wait until we combine the annihilation and creation diagrams.

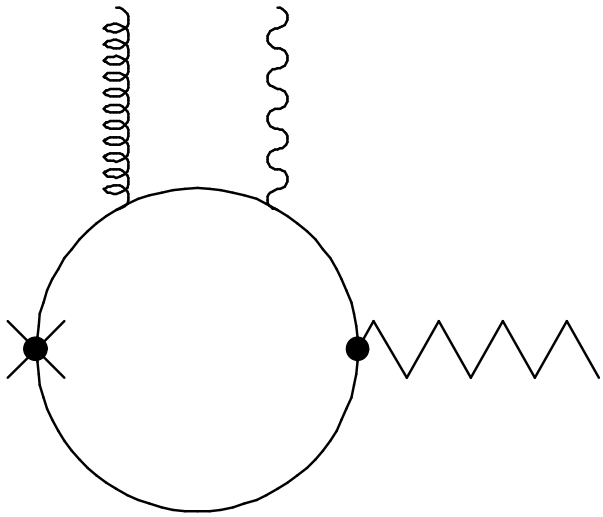

Figure 6.18 $\langle V\gamma g|\bar{\chi}\Lambda^n\gamma_\mu t^a L\chi|0\rangle$ *- A creation diagram for a vector particle with one external photon line and one external gluon line coupled to the upper quark.*

We get the following expression for this diagram

$$\begin{aligned} M^\mu &= -\int \frac{d^D p}{(2\pi)^D} Tr\left[\Lambda^n \gamma^\mu L t^a i S_2^{GF} i h_V \gamma_\nu V^\nu i S(p)\right] \\ &= i h_V Tr_F\left[\Lambda^n V^\nu\right] \int \frac{d^D p}{(2\pi)^D} Tr\left[\gamma^\mu L t^a S_2^{GF} \gamma_\nu S(p)\right] \\ &= i h_V Tr_F\left[\Lambda^n V^\nu\right] \int \frac{d^D p}{(2\pi)^D} Tr\left[R\gamma^\mu t^a \frac{e g_S}{4} Q F_{\alpha\beta} t^a G^a_{\sigma\rho} R^{\sigma\rho\alpha\beta} \gamma_\nu S(p)\right] \\ &= \frac{i h_V e g_S}{16} Tr_F\left[\Lambda^n V^\nu\right] \int \frac{d^D p}{(2\pi)^D} Tr\left[\left(1+\gamma_5\right)\gamma^\mu Q F_{\alpha\beta} G_{\sigma\rho} R^{\sigma\rho\alpha\beta} \gamma_\nu S(p)\right] \end{aligned} \tag{6.41}$$

where

$$
\begin{aligned}
R^{\sigma\rho\alpha\beta} &= S(p)\gamma^{\beta}S(p)\gamma^{\rho}S(p)\gamma^{\sigma}S(p)\gamma^{\alpha}S(p) \\
&+S(p)\gamma^{\rho}S(p)\gamma^{\beta}S(p)\gamma^{\sigma}S(p)\gamma^{\alpha}S(p) \\
&+S(p)\gamma^{\rho}S(p)\gamma^{\sigma}S(p)\gamma^{\beta}S(p)\gamma^{\alpha}S(p)
\end{aligned}
\tag{6.42}
$$

as before. We will use this expression in the following three diagrams.

The next diagram we will be looking at is the one in figure 6.19, where the photon- and gluon-line just switched places compared to the last diagram in figure 6.18.

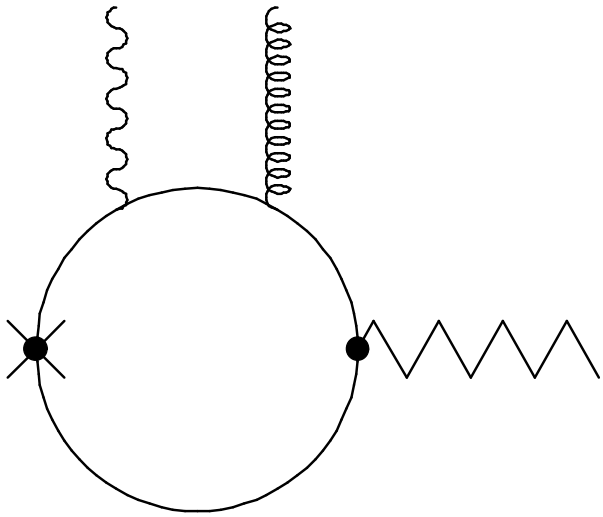

Figure 6.19 $\langle Vg\gamma|\bar{\chi}\Lambda^{n}\gamma_{\mu}t^{a}L\chi|0\rangle$ *- A creation diagram for a vector particle with one external gluon line and one external photon line coupled to the upper quark.*

For this diagram we get

$$
\begin{aligned}
M^{\mu} &= -\int\frac{d^{D}p}{(2\pi)^{D}}Tr\left[\Lambda^{n}\gamma^{\mu}Lt^{a}iS_{2}^{FG}ih_{V}\gamma_{v}V^{v}iS(p)\right] \\
&= ih_{V}Tr_{F}\left[\Lambda^{n}V^{v}\right]\int\frac{d^{D}p}{(2\pi)^{D}}Tr\left[\gamma^{\mu}Lt^{a}S_{2}^{FG}\gamma_{v}S(p)\right] \\
&= ih_{V}Tr_{F}\left[\Lambda^{n}V^{v}\right]\int\frac{d^{D}p}{(2\pi)^{D}}Tr\left[R\gamma^{\mu}t^{a}\frac{eg_{S}}{4}QF_{\sigma\rho}t^{a}G_{\alpha\beta}^{a}R^{\sigma\rho\alpha\beta}\gamma_{v}S(p)\right] \\
&= \frac{ih_{V}eg_{S}}{16}Tr_{F}\left[\Lambda^{n}V^{v}\right]\int\frac{d^{D}p}{(2\pi)^{D}}Tr\left[\left(1+\gamma_{5}\right)\gamma^{\mu}QF_{\sigma\rho}G_{\alpha\beta}R^{\sigma\rho\alpha\beta}\gamma_{v}S(p)\right]
\end{aligned}
\tag{6.43}
$$

Next diagram in line is the one in figure 6.20.

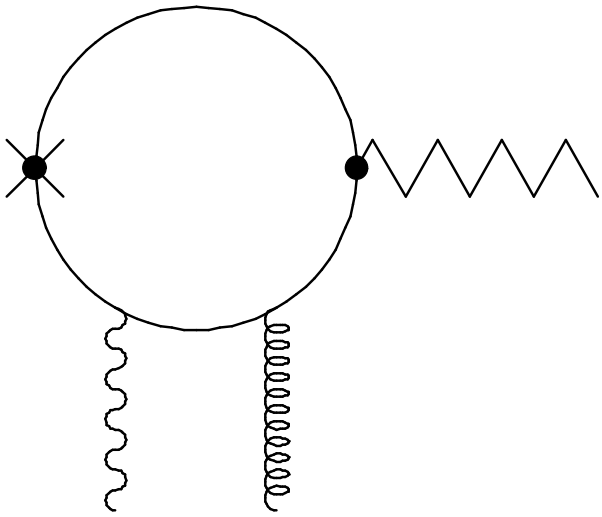

Figure 6.20 $\langle V\gamma g|\bar{\chi}\Lambda^n\gamma_\mu t^a L\chi|0\rangle$ *- A creation diagram for a vector particle with one external photon line and one external gluon line coupled to the lower quark.*

Compared to eq. 6.43 the only difference is the order of propagators. We get the following

$$\begin{aligned} M^\mu &= -\int \frac{d^D p}{(2\pi)^D} \mathrm{Tr}\left[\Lambda^n \gamma^\mu L t^a i S(p) i h_V \gamma_\nu V^\nu i S_2^{GF}\right] \\ &= i h_V \mathrm{Tr}_F\left[\Lambda^n V^\nu\right] \int \frac{d^D p}{(2\pi)^D} \mathrm{Tr}\left[\gamma^\mu L t^a S(p) \gamma_\nu S_2^{GF}\right] \\ &= i h_V \mathrm{Tr}_F\left[\Lambda^n V^\nu\right] \int \frac{d^D p}{(2\pi)^D} \mathrm{Tr}\left[R\gamma^\mu t^a S(p)\gamma_\nu \frac{e g_S}{4} Q F_{\sigma\rho} t^a G^a_{\alpha\beta} R^{\sigma\rho\alpha\beta}\right] \\ &= \frac{i h_V e g_S}{16} \mathrm{Tr}_F\left[\Lambda^n V^\nu\right] \int \frac{d^D p}{(2\pi)^D} \mathrm{Tr}\left[(1+\gamma_5)\gamma^\mu S(p)\gamma_\nu Q F_{\sigma\rho} G_{\alpha\beta} R^{\sigma\rho\alpha\beta}\right] \end{aligned} \tag{6.44}$$

The last of the diagrams with one photon- and one gluon-line connected to one of the light quarks is the one in figure 6.21.

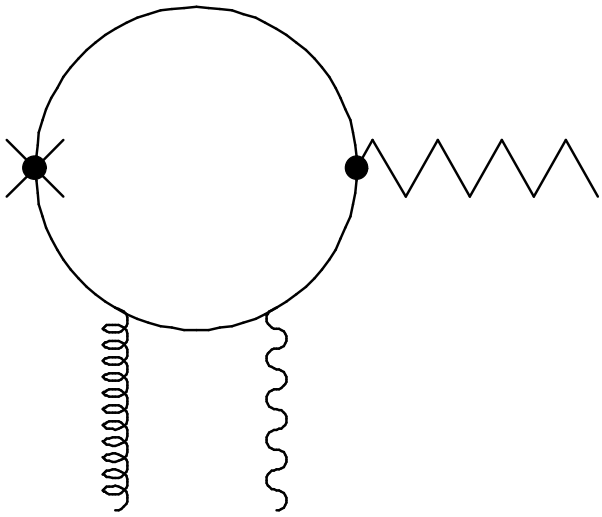

Figure 6.21 $\langle Vg\gamma|\bar{\chi}\Lambda^n\gamma_\mu t^a L\chi|0\rangle$ *- A creation diagram for a vector particle with one external gluon line and one external photon line coupled to the lower quark.*

Once again only the order of the propagators has to be changed in order to get an expression for this diagram.

$$\begin{aligned} M^\mu &= -\int \frac{d^D p}{(2\pi)^D} Tr\left[\Lambda^n \gamma^\mu L t^a i S(p) i h_V \gamma_\nu V^\nu i S_2^{FG}\right] \\ &= i h_V Tr_F\left[\Lambda^n V^\nu\right] \int \frac{d^D p}{(2\pi)^D} Tr\left[\gamma^\mu L t^a S(p) \gamma_\nu S_2^{FG}\right] \\ &= i h_V Tr_F\left[\Lambda^n V^\nu\right] \int \frac{d^D p}{(2\pi)^D} Tr\left[R\gamma^\mu t^a S(p)\gamma_\nu \frac{e g_S}{4} Q F_{\sigma\rho} t^a G^a_{\alpha\beta} R^{\sigma\rho\alpha\beta}\right] \\ &= \frac{i h_V e g_S}{16} Tr_F\left[\Lambda^n V^\nu\right] \int \frac{d^D p}{(2\pi)^D} Tr\left[(1+\gamma_5)\gamma^\mu S(p)\gamma_\nu Q F_{\alpha\beta} G_{\sigma\rho} R^{\sigma\rho\alpha\beta}\right] \end{aligned} \tag{6.45}$$

In some of the following calculations of the diagrams we can integrate out the momentum. This will give us a bit simpler final results than the last four above, but with a bit longer calculations. Our first diagram will be the one in figure 6.22.

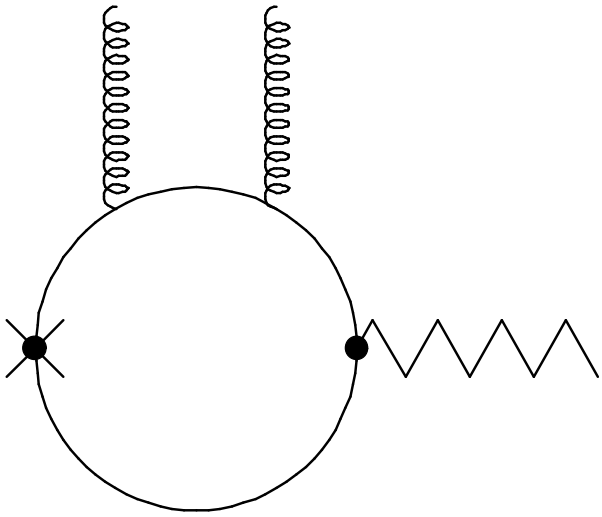

Figure 6.22 $\langle \mathrm{Vgg}|\bar{\chi}\Lambda^n\gamma_\mu L\chi|0\rangle$ *- A creation diagram for a vector particle with two external gluon lines coupled to the upper quark.*

The calculation goes as follows

$$
\begin{aligned}
M &= -\int \frac{d^D p}{(2\pi)^D}\mathrm{Tr}\left[\Lambda^n\gamma^\mu \mathrm{Li}S_2^{GG} i h_V \gamma_\nu V^\nu i S(p)\right] \\
&= i h_V \mathrm{Tr}_F\left[\Lambda^n V^\nu\right]\int \frac{d^D p}{(2\pi)^D}\mathrm{Tr}\left[R\gamma^\mu S_2^{GG}\gamma_\nu S(p)\right] \\
&= i h_V \mathrm{Tr}_F\left[\Lambda^n V^\nu\right]\int \frac{d^D p}{(2\pi)^D}\mathrm{Tr}\left[R\gamma^\mu 2\pi^2 t^a t^a \left\langle\frac{\alpha}{\pi}G^2\right\rangle \frac{m}{(p^2-m^2)^4}\left[m(\gamma\cdot p)+p^2\right]\gamma_\nu \frac{\gamma\cdot p+m}{p^2-m^2}\right] \qquad (6.46) \\
&= \pi^2 i h_V \left\langle\frac{\alpha}{\pi}G^2\right\rangle \mathrm{Tr}_F\left[\Lambda^n V^\nu\right]\int \frac{d^D p}{(2\pi)^D}\frac{1}{(p^2-m^2)^5}\mathrm{Tr}\left[R\gamma^\mu m\left[m(\gamma\cdot p)+p^2\right]\gamma_\nu(\gamma\cdot p+m)\right] \\
&= \pi^2 i h_V \left\langle\frac{\alpha}{\pi}G^2\right\rangle \mathrm{Tr}_F\left[\Lambda^n V^\nu\right] T_{\mu\nu}
\end{aligned}
$$

where

$$
\begin{aligned}
T_{\mu\nu} &= \int \frac{d^D p}{(2\pi)^D} \frac{1}{(p^2 - m^2)^5} \mathrm{Tr}\left[R\gamma^\mu m\left[m(\gamma\cdot p) + p^2 \right]\gamma_\nu(\gamma\cdot p + m)\right] \\
&= \int \frac{d^D p}{(2\pi)^D} \frac{1}{(p^2 - m^2)^5} \mathrm{Tr}\left[R\gamma^\mu \left[m^2\gamma\cdot p\gamma_\nu\gamma\cdot p + m^2 p^2\gamma_\nu \right]\right] \\
&= \int \frac{d^D p}{(2\pi)^D} \frac{1}{(p^2 - m^2)^5} \mathrm{Tr}\left[R\gamma^\mu m^2\left[\frac{2-D}{D} p^2\gamma_\nu + p^2\gamma_\nu \right]\right] \\
&= \int \frac{d^D p}{(2\pi)^D} \frac{1}{(p^2 - m^2)^5} \mathrm{Tr}\left[R\gamma^\mu m^2\gamma_\nu\left[(p^2 - m^2)\left(\frac{2-D}{D} + 1 \right) + m^2\left(\frac{2-D}{D} + 1 \right)\right]\right] \\
&= \left(\frac{2-D}{D} + 1 \right)(I_4 + m^2 I_5)\mathrm{Tr}\left[R\gamma^\mu\gamma_\nu \right]
\end{aligned}
\tag{6.47}
$$

Putting this into the expression for M gives

$$
\begin{aligned}
M &= \pi^2 i h_V m^2 \left\langle \frac{\alpha}{\pi} G^2 \right\rangle \mathrm{Tr}_F\left[\Lambda^n V^v \right]\left(\frac{2-D}{D} + 1 \right)\left(\frac{i}{96\pi^2 m^4} + \frac{-i}{384\pi^2 m^4} \right)\mathrm{Tr}\left[R\gamma^\mu\gamma_\nu \right] \\
&= 2\pi^2 i h_V m^2 \left\langle \frac{\alpha}{\pi} G^2 \right\rangle \mathrm{Tr}_F\left[\Lambda^n V^v \right]\left(\frac{2-D}{D} + 1 \right)\left(\frac{i}{128\pi^2 m^4} \right) g_{\mu\nu} \\
&\underset{D\to 4}{\rightarrow} -\frac{h_V}{128 m^2}\left\langle \frac{\alpha}{\pi} G^2 \right\rangle \mathrm{Tr}_F\left[\Lambda^n V^v \right] g_{\mu\nu}
\end{aligned}
\tag{6.48}
$$

We now turn to the diagram in figure 6.23, which is the same as we had above only with the gluons now connected to the lower quark.

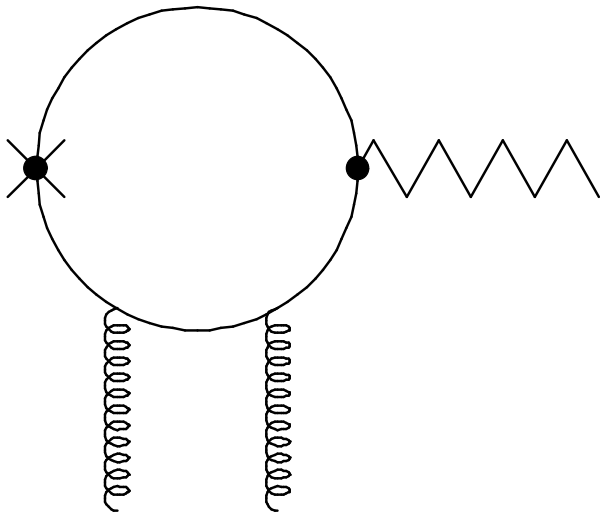

Figure 6.23 $\langle \mathrm{Vgg}|\bar{\chi}\Lambda^n\gamma_\mu L\chi|0\rangle$ *- A creation diagram for a vector particle with two external gluon lines coupled to the lower quark.*

The calculations for this diagram turn out to be

$$
\begin{aligned}
M &= -\int \frac{d^D p}{(2\pi)^D} \mathrm{Tr}\left[\Lambda^n \gamma^\mu \mathrm{LiS}(p) i h_V \gamma_\nu V^\nu i S_2^{GG}\right] \\
&= i h_V \mathrm{Tr}_F\left[\Lambda^n V^\nu\right] \int \frac{d^D p}{(2\pi)^D} \mathrm{Tr}\left[R\gamma^\mu S(p)\gamma_\nu S_2^{GG}\right] \\
&= i h_V \mathrm{Tr}_F\left[\Lambda^n V^\nu\right] \int \frac{d^D p}{(2\pi)^D} \mathrm{Tr}\left[R\gamma^\mu \frac{\gamma\cdot p + m}{p^2 - m^2}\gamma_\nu 2\pi^2 t^a t^a \left\langle \frac{\alpha}{\pi} G^2 \right\rangle \frac{m}{(p^2-m^2)^4}\left[m(\gamma\cdot p) + p^2\right]\right] \\
&= \pi^2 i h_V \left\langle \frac{\alpha}{\pi} G^2 \right\rangle \mathrm{Tr}_F\left[\Lambda^n V^\nu\right] \int \frac{d^D p}{(2\pi)^D} \frac{1}{(p^2-m^2)^5} \mathrm{Tr}\left[R\gamma^\mu (\gamma\cdot p + m)\gamma_\nu m\left[m(\gamma\cdot p) + p^2\right]\right] \\
&= \pi^2 i h_V \left\langle \frac{\alpha}{\pi} G^2 \right\rangle \mathrm{Tr}_F\left[\Lambda^n V^\nu\right] T_{\mu\nu}
\end{aligned}
\tag{6.49}
$$

where

$$
\begin{aligned}
T_{\mu\nu} &= \int \frac{d^D p}{(2\pi)^D} \frac{1}{(p^2-m^2)^5} \mathrm{Tr}\left[R\gamma^\mu (\gamma\cdot p + m)\gamma_\nu m\left[m(\gamma\cdot p) + p^2\right]\right] \\
&= \int \frac{d^D p}{(2\pi)^D} \frac{1}{(p^2-m^2)^5} \mathrm{Tr}\left[R\gamma^\mu \left[\gamma\cdot p\gamma_\nu m^2 \gamma\cdot p + m^2\gamma_\nu((p^2-m^2)+m^2)\right]\right] \\
&= \int \frac{d^D p}{(2\pi)^D} \frac{1}{(p^2-m^2)^5} \mathrm{Tr}\left[R\gamma^\mu m^2\gamma_\nu\left[\frac{2-D}{D}p^2 + (p^2-m^2) + m^2\right]\right] \\
&= \int \frac{d^D p}{(2\pi)^D} \frac{1}{(p^2-m^2)^5} \mathrm{Tr}\left[R\gamma^\mu m^2\gamma_\nu\left[(p^2-m^2)\left(\frac{2-D}{D}+1\right) + m^2\left(\frac{2-D}{D}+1\right)\right]\right] \\
&= m^2\left(\frac{2-D}{D}+1\right)(I_4 + m^2 I_5)\mathrm{Tr}\left[R\gamma^\mu\gamma_\nu\right]
\end{aligned}
\tag{6.50}
$$

which is exactly what we got in the last calculation (eq. 6.48)! The result is therefore

$$
\begin{aligned}
M &= \pi^2 i h_V m^2 \left\langle \frac{\alpha}{\pi} G^2 \right\rangle \mathrm{Tr}_F\left[\Lambda^n V^\nu\right]\left(\frac{2-D}{D}+1\right)\left(\frac{i}{96\pi^2 m^4} + \frac{-i}{384\pi^2 m^4}\right)\mathrm{Tr}\left[R\gamma^\mu\gamma_\nu\right] \\
&\underset{D\to 4}{\to} -\frac{h_V}{128 m^2}\left\langle \frac{\alpha}{\pi} G^2 \right\rangle \mathrm{Tr}_F\left[\Lambda^n V^\nu\right] g_{\mu\nu}
\end{aligned}
\tag{6.51}
$$

Next, we look at the situation where we have one gluon coupling to each of the upper and lower quarks. This is shown in figure 6.24.

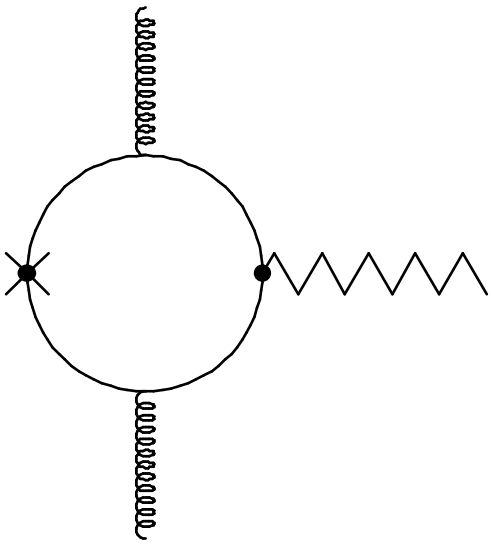

Figure 6.24 $\langle \mathrm{Vgg}|\bar{\chi}\Lambda^n\gamma_\mu \mathrm{L}\chi|0\rangle$ *- A creation diagram for a vector particle with two external gluon lines coupled both to the upper and lower quarks.*

The calculation for this diagram goes as follows

$$
\begin{aligned}
M^\lambda &= -\int \frac{d^D p}{(2\pi)^D} \mathrm{Tr}\left[(\Lambda^n \gamma^\lambda \mathrm{L}) i S_1^G (i h_v \gamma_\delta V^\delta) i S_1^G\right] \\
&= i h_v \mathrm{Tr}_F\left[\Lambda^n V^\delta\right] \int \frac{d^D p}{(2\pi)^D} \mathrm{Tr}\left[\gamma^\lambda \mathrm{L} S_1^G \gamma_\delta S_1^G\right] \\
&= i h_v \mathrm{Tr}_F\left[\Lambda^n V^\delta\right] \int \frac{d^D p}{(2\pi)^D} \mathrm{Tr}[R\gamma^\lambda \left(\frac{1}{4} g_s t^a G^a_{\alpha\beta} \frac{1}{\left(p^2 - m^2\right)^2} \left\{\sigma^{\alpha\beta}, (\gamma \cdot p + m)\right\}\right) \gamma_\delta \times \\
&\left(\frac{1}{4} g_s t^a G^a_{\sigma\rho} \frac{1}{\left(p^2 - m^2\right)^2} \left\{\sigma^{\sigma\rho}, (\gamma \cdot p + m)\right\}\right)] \qquad (6.52) \\
&= -\frac{i\pi^2 h_v}{768} \mathrm{Tr}_F\left[\Lambda^n V^\delta\right] \times \int \frac{d^D p}{(2\pi)^D} \frac{1}{\left(p^2 - m^2\right)^4} \\
&\mathrm{Tr}\left[(1+\gamma_5)\gamma^\lambda \left\{\left[\gamma^\alpha, \gamma^\beta\right] G_{\alpha\beta}, (\gamma \cdot p + m)\right\} \gamma_\delta \left\{\tilde{Q}_\xi^V \left[\gamma^\sigma, \gamma^\rho\right] F_{\sigma\rho}, (\gamma \cdot p + m)\right\}\right] \\
&= -\frac{i\pi^2 h_v}{768} \left\langle \frac{\alpha_s}{\pi} G^2 \right\rangle \left(g_{\alpha\sigma} g_{\beta\rho} - g_{\alpha\rho} g_{\beta\sigma}\right) \mathrm{Tr}_F\left[\Lambda^n V^\delta\right] \int \frac{d^D p}{(2\pi)^D} \frac{1}{\left(p^2 - m^2\right)^4} \\
&\mathrm{Tr}\left[(1+\gamma_5)\gamma^\lambda \left(\left\{\left[\gamma^\alpha, \gamma^\beta\right], \gamma \cdot p\right\} \gamma_\delta \left\{\left[\gamma^\sigma, \gamma^\rho\right], \gamma \cdot p\right\} + 4m^2 \left[\gamma^\alpha, \gamma^\beta\right] \gamma_\delta \left[\gamma^\sigma, \gamma^\rho\right]\right)\right]
\end{aligned}
$$

Now, finally the last two diagrams of the type with two external lines. These are diagrams with one photon line coupled to one quark and one gluon line coupled to the other quark, and their calculations are very similar to the one we just calculated (eq. 6.52). We start with the diagram in figure 6.25.

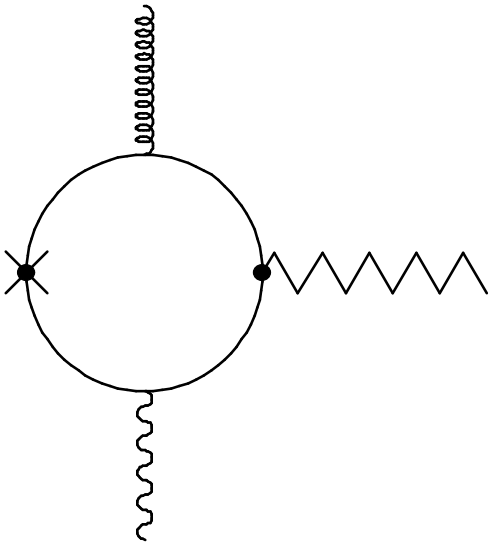

Figure 6.25 $\langle Vg\gamma|\bar{\chi}\Lambda^n t^a \gamma_\mu L\chi|0\rangle$ *- A creation diagram for a vector particle with one external gluon line and one external photon line coupled both to the upper and lower quarks.*

The calculation will be

$$
\begin{aligned}
M^\lambda &= -\int \frac{d^D p}{(2\pi)^D} \mathrm{Tr}\left[(\Lambda^n \gamma^\lambda L t^a) i S_1^G (i h_v \gamma_\delta V^\delta) i S_1^F\right] \\
&= i h_v \mathrm{Tr}_F\left[\Lambda^n V^\delta\right] \int \frac{d^D p}{(2\pi)^D} \mathrm{Tr}[R\gamma^\lambda t^a \left(\frac{1}{4} g_s t^a G^a_{\alpha\beta} \frac{1}{\left(p^2 - m^2\right)^2}\left\{\sigma^{\alpha\beta}, (\gamma\cdot p + m)\right\}\right)\gamma_\delta \times \\
&\left(-\frac{1}{4} e\tilde{Q}^V_\xi F_{\sigma\rho} \frac{1}{\left(p^2 - m^2\right)^2}\left\{\sigma^{\sigma\rho}, (\gamma\cdot p + m)\right\}\right)] \\
&= \frac{i h_v e g_s}{256} \mathrm{Tr}_F\left[\Lambda^n V^\delta\right] \int \frac{d^D p}{(2\pi)^D} \frac{1}{\left(p^2 - m^2\right)^4} \\
&\mathrm{Tr}\left[(1+\gamma_5)\gamma^\lambda \left(\left\{\left[\gamma^\alpha, \gamma^\beta\right] G_{\alpha\beta}, \gamma\cdot p\right\}\gamma_\delta \left\{\tilde{Q}^V_\xi \left[\gamma^\sigma, \gamma^\rho\right] F_{\sigma\rho}, \gamma\cdot p\right\} + 4m^2 \left[\gamma^\alpha, \gamma^\beta\right] G_{\alpha\beta}\gamma_\delta \tilde{Q}^V_\xi \left[\gamma^\sigma, \gamma^\rho\right] F_{\sigma\rho}\right)\right]
\end{aligned}
\tag{6.53}
$$

We get almost the same result for the diagram in figure 6.26.

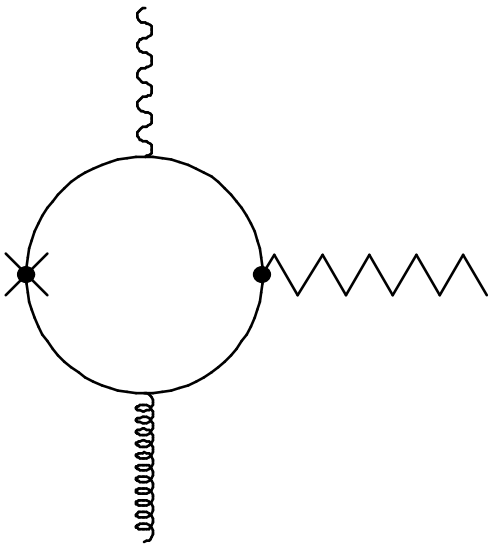

Figure 6.26 $\langle V\gamma g|\bar{\chi}\Lambda^n t^a \gamma_\mu L\chi|0\rangle$ *- A creation diagram for a vector particle with one external photon line and one external gluon line coupled both to the upper and lower quarks.*

Calculations for this diagram will be as follows

$$
\begin{aligned}
M^\lambda &= -\int \frac{d^D p}{(2\pi)^D} \mathrm{Tr}\left[(\Lambda^n \gamma^\lambda L t^a) i S_l^F (i h_v \gamma_\delta V^\delta) i S_l^G\right] \\
&= i h_v \mathrm{Tr}_F\left[\Lambda^n V^\delta\right] \int \frac{d^D p}{(2\pi)^D} \mathrm{Tr}[R\gamma^\lambda t^a \left(-\frac{1}{4} e \tilde{Q}_\xi^V F_{\sigma\rho} \frac{1}{\left(p^2 - m^2\right)^2} \left\{\sigma^{\sigma\rho}, (\gamma \cdot p + m)\right\}\right) \gamma_\delta \times \qquad (6.54) \\
&\left(\frac{1}{4} g_s t^a G^a_{\alpha\beta} \frac{1}{\left(p^2 - m^2\right)^2} \left\{\sigma^{\alpha\beta}, (\gamma \cdot p + m)\right\}\right)] \\
&= \frac{i h_v e g_s}{256} \mathrm{Tr}_F\left[\Lambda^n V^\delta\right] \int \frac{d^D p}{(2\pi)^D} \frac{1}{\left(p^2 - m^2\right)^4} \\
&\mathrm{Tr}\left[(1+\gamma_5)\gamma^\lambda \left(\left\{\tilde{Q}_\xi^V \left[\gamma^\sigma, \gamma^\rho\right] F_{\sigma\rho}, \gamma \cdot p\right\} \gamma_\delta \left\{\left[\gamma^\alpha, \gamma^\beta\right] G_{\alpha\beta}, \gamma \cdot p\right\} + 4m^2 \tilde{Q}_\xi^V \left[\gamma^\sigma, \gamma^\rho\right] F_{\sigma\rho} \gamma_\delta \left[\gamma^\alpha, \gamma^\beta\right] G_{\alpha\beta}\right)\right]
\end{aligned}
$$

Lastly we have the diagrams with two gluon lines and one photon line coupled to the loop. From figure 6.3 we can see that there are twelve of these, and, as suspected, in only a few of them can we do the integration over the momentum. Except in these few cases, we will be very sketchy in the calculations of the diagrams.

We start with the diagram in figure 6.27.

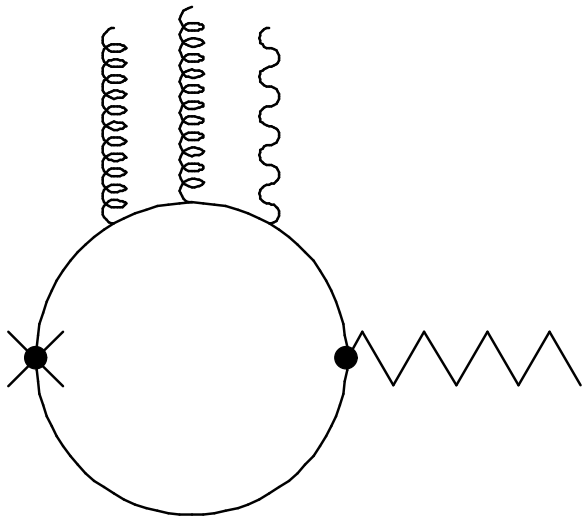

Figure 6.27 $\langle V\gamma gg|\bar{\chi}\Lambda^n\gamma_\mu L\chi|0\rangle$ *- A creation diagram for a vector particle with one external photon line and two external gluon lines coupled to the upper quark.*

Here the calculation will be the following

$$\begin{aligned}
M^\lambda &= -\int \frac{d^D p}{(2\pi)^D} Tr\left[\Lambda^n \gamma^\lambda L i S_3^{GGF} i h_V \gamma_\delta V^\delta i S(p)\right] \\
&= h_V Tr_F\left[\Lambda^n V^\delta\right] \int \frac{d^D p}{(2\pi)^D} Tr\left[R\gamma^\lambda i S_3^{GGF} \gamma_\delta S(p)\right] \\
&= h_V Tr_F\left[\Lambda^n V^\delta\right] \int \frac{d^D p}{(2\pi)^D} Tr\left[R\gamma^\lambda \frac{\pi^2}{24} eQF_{\rho\sigma} t^a t^a \left\langle \frac{\alpha}{\pi} G^2 \right\rangle \left(g_{\mu\alpha} g_{\nu\beta} - g_{\mu\beta} g_{\nu\alpha}\right) T^{\mu\nu\alpha\beta\sigma\rho} \gamma_\delta S(p)\right] \\
&= \frac{\pi^2 h_V e}{96} \left\langle \frac{\alpha}{\pi} G^2 \right\rangle Tr_F\left[\Lambda^n V^\delta\right] \int \frac{d^D p}{(2\pi)^D} Tr\left[\left(1+\gamma_5\right)\gamma^\lambda Q F_{\rho\sigma} \left(g_{\mu\alpha} g_{\nu\beta} - g_{\mu\beta} g_{\nu\alpha}\right) T^{\mu\nu\alpha\beta\sigma\rho} \gamma_\delta S(p)\right]
\end{aligned} \tag{6.55}$$

Here $T^{\lambda\eta\alpha\beta\sigma\rho}$ is the same as we had in chapter 5, section 5.2, but with μ and ν replaced with λ and η.

$$\begin{aligned}
T^{\lambda\eta\alpha\beta\sigma\rho} = {} & S\gamma^\sigma S\gamma^\beta S\gamma^\eta S\gamma^\lambda S\gamma^\alpha S\gamma^\rho S + S\gamma^\beta S\gamma^\sigma S\gamma^\eta S\gamma^\lambda S\gamma^\alpha S\gamma^\rho S \\
& + S\gamma^\beta S\gamma^\eta S\gamma^\sigma S\gamma^\lambda S\gamma^\alpha S\gamma^\rho S + S\gamma^\beta S\gamma^\eta S\gamma^\lambda S\gamma^\sigma S\gamma^\alpha S\gamma^\rho S \\
& + S\gamma^\beta S\gamma^\eta S\gamma^\lambda S\gamma^\alpha S\gamma^\sigma S\gamma^\rho S + S\gamma^\sigma S\gamma^\eta S\gamma^\beta S\gamma^\lambda S\gamma^\alpha S\gamma^\rho S \\
& + S\gamma^\eta S\gamma^\sigma S\gamma^\beta S\gamma^\lambda S\gamma^\alpha S\gamma^\rho S + S\gamma^\eta S\gamma^\beta S\gamma^\sigma S\gamma^\lambda S\gamma^\alpha S\gamma^\rho S \\
& + S\gamma^\eta S\gamma^\beta S\gamma^\lambda S\gamma^\sigma S\gamma^\alpha S\gamma^\rho S + S\gamma^\eta S\gamma^\beta S\gamma^\lambda S\gamma^\alpha S\gamma^\sigma S\gamma^\rho S \\
& + S\gamma^\sigma S\gamma^\eta S\gamma^\lambda S\gamma^\beta S\gamma^\alpha S\gamma^\rho S + S\gamma^\eta S\gamma^\sigma S\gamma^\lambda S\gamma^\beta S\gamma^\alpha S\gamma^\rho S \\
& + S\gamma^\eta S\gamma^\lambda S\gamma^\sigma S\gamma^\beta S\gamma^\alpha S\gamma^\rho S + S\gamma^\eta S\gamma^\lambda S\gamma^\beta S\gamma^\sigma S\gamma^\alpha S\gamma^\rho S \\
& + S\gamma^\eta S\gamma^\lambda S\gamma^\beta S\gamma^\alpha S\gamma^\sigma S\gamma^\rho S
\end{aligned} \tag{6.56}$$

The next diagram is the one shown in figure 6.28.

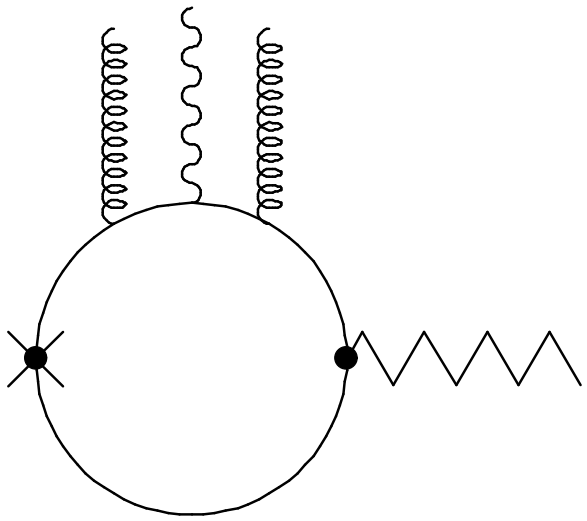

Figure 6.28 $\langle Vg\gamma g|\bar{\chi}\Lambda^n\gamma_\mu L\chi|0\rangle$ *- A creation diagram for a vector particle with one external photon line and two external gluon lines coupled to the upper quark.*

It is calculated as follows

$$\begin{aligned}
M^\lambda &= -\int \frac{d^D p}{(2\pi)^D} \mathrm{Tr}\left[\Lambda^n \gamma^\lambda L i S_3^{GFG} i h_V \gamma_\delta V^\delta i S(p)\right] \\
&= h_V \mathrm{Tr}_F\left[\Lambda^n V^\delta\right] \int \frac{d^D p}{(2\pi)^D} \mathrm{Tr}\left[R\gamma^\lambda i S_3^{GFG} \gamma_\delta S(p)\right] \\
&= h_V \mathrm{Tr}_F\left[\Lambda^n V^\delta\right] \int \frac{d^D p}{(2\pi)^D} \mathrm{Tr}\left[R\gamma^\lambda \frac{\pi^2}{24} eQF_{\alpha\beta} t^a t^a \left\langle \frac{\alpha}{\pi} G^2 \right\rangle \left(g_{\mu\rho} g_{\nu\sigma} - g_{\mu\sigma} g_{\nu\rho}\right) T^{\mu\nu\alpha\beta\sigma\rho} \gamma_\delta S(p)\right] \\
&= \frac{\pi^2 h_V e}{96} \left\langle \frac{\alpha}{\pi} G^2 \right\rangle \mathrm{Tr}_F\left[\Lambda^n V^\delta\right] \int \frac{d^D p}{(2\pi)^D} \mathrm{Tr}\left[\left(1+\gamma_5\right)\gamma^\lambda Q F_{\alpha\beta} \left(g_{\mu\rho} g_{\nu\sigma} - g_{\mu\sigma} g_{\nu\rho}\right) T^{\mu\nu\alpha\beta\sigma\rho} \gamma_\delta S(p)\right]
\end{aligned} \tag{6.57}$$

The diagram in figure 6.29,

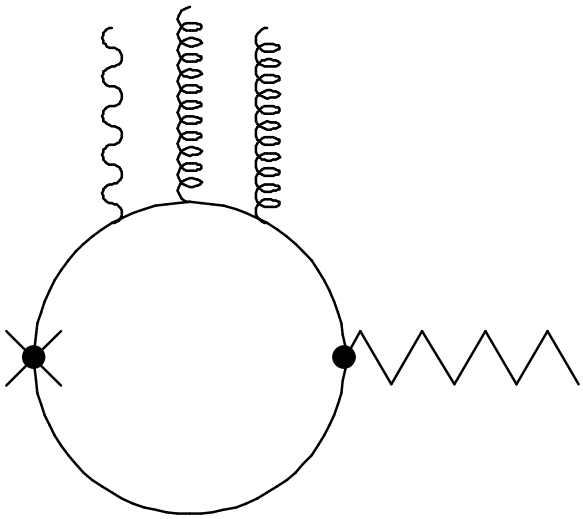

Figure 6.29 $\langle Vgg\gamma|\bar{\chi}\Lambda^n\gamma_\mu L\chi|0\rangle$ *- A creation diagram for a vector particle with one external photon line and two external gluon lines coupled to the upper quark.*

becomes

$$\begin{aligned}
M^\lambda &= -\int \frac{d^D p}{(2\pi)^D} Tr\left[\Lambda^n \gamma^\lambda L i S_3^{FGG} i h_V \gamma_\delta V^\delta i S(p)\right] \\
&= h_V Tr_F\left[\Lambda^n V^\delta\right] \int \frac{d^D p}{(2\pi)^D} Tr\left[R\gamma^\lambda i S_3^{FGG} \gamma_\delta S(p)\right] \\
&= h_V Tr_F\left[\Lambda^n V^\delta\right] \int \frac{d^D p}{(2\pi)^D} Tr\left[R\gamma^\lambda \frac{\pi^2}{24} eQF_{\mu\nu} t^a t^a \left\langle \frac{\alpha}{\pi} G^2 \right\rangle \left(g_{\alpha\rho} g_{\beta\sigma} - g_{\alpha\sigma} g_{\beta\rho}\right) T^{\mu\nu\alpha\beta\sigma\rho} \gamma_\delta S(p)\right] \\
&= \frac{\pi^2 h_V e}{96} \left\langle \frac{\alpha}{\pi} G^2 \right\rangle Tr_F\left[\Lambda^n V^\delta\right] \int \frac{d^D p}{(2\pi)^D} Tr\left[\left(1+\gamma_5\right)\gamma^\lambda Q F_{\mu\nu} \left(g_{\alpha\rho} g_{\beta\sigma} - g_{\alpha\sigma} g_{\beta\rho}\right) T^{\mu\nu\alpha\beta\sigma\rho} \gamma_\delta S(p)\right]
\end{aligned} \tag{6.58}$$

The next three diagrams are the same as the three above, but with the external lines coupled to the lower quark instead. For the first of these diagram, as shown in figure 6.30,

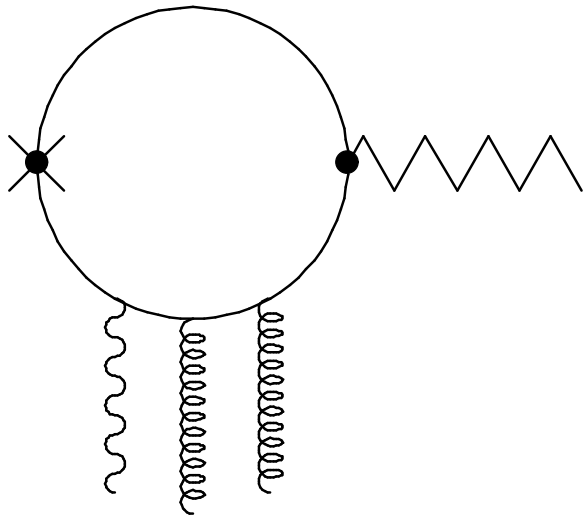

Figure 6.30 $\langle V\gamma gg|\bar{\chi}\Lambda^n\gamma_\mu L\chi|0\rangle$ *- A creation diagram for a vector particle with one external photon line and two external gluon lines coupled to the lower quark.*

we get

$$\begin{aligned}
M^\lambda &= -\int \frac{d^D p}{(2\pi)^D} \mathrm{Tr}\left[\Lambda^n\gamma^\lambda L i S(p) i h_V \gamma_\delta V^\delta i S_3^{GGF}\right] \\
&= h_V \mathrm{Tr}_F\left[\Lambda^n V^\delta\right]\int \frac{d^D p}{(2\pi)^D} \mathrm{Tr}\left[R\gamma^\lambda S(p)\gamma_\delta i S_3^{GGF}\right] \\
&= h_V \mathrm{Tr}_F\left[\Lambda^n V^\delta\right]\int \frac{d^D p}{(2\pi)^D} \mathrm{Tr}\left[R\gamma^\lambda S(p)\gamma_\delta \frac{\pi^2}{24} eQF_{\rho\sigma} t^a t^a \left\langle \frac{\alpha}{\pi} G^2 \right\rangle \left(g_{\mu\alpha}g_{\nu\beta} - g_{\mu\beta}g_{\nu\alpha}\right) T^{\mu\nu\alpha\beta\sigma\rho}\right] \\
&= \frac{\pi^2 h_V e}{96}\left\langle \frac{\alpha}{\pi} G^2 \right\rangle \mathrm{Tr}_F\left[\Lambda^n V^\delta\right]\int \frac{d^D p}{(2\pi)^D} \mathrm{Tr}\left[\left(1+\gamma_5\right)\gamma^\lambda S(p)\gamma_\delta Q F_{\rho\sigma}\left(g_{\mu\alpha}g_{\nu\beta} - g_{\mu\beta}g_{\nu\alpha}\right) T^{\mu\nu\alpha\beta\sigma\rho}\right]
\end{aligned} \tag{6.59}$$

The next diagram, shown in figure 6.31,

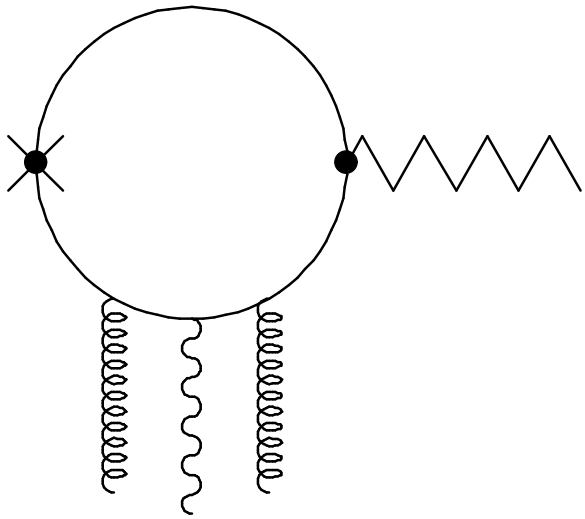

Figure 6.31 $\langle Vg\gamma g|\bar{\chi}\Lambda^n\gamma_\mu L\chi|0\rangle$ *- A creation diagram for a vector particle with one external photon line and two external gluon lines coupled to the lower quark.*

gives

$$
\begin{aligned}
M^\lambda &= -\int \frac{d^D p}{(2\pi)^D} \mathrm{Tr}\left[\Lambda^n \gamma^\lambda L i S(p) i h_V \gamma_\delta V^\delta i S_3^{GFG}\right] \\
&= h_V \mathrm{Tr}_F\left[\Lambda^n V^\delta\right] \int \frac{d^D p}{(2\pi)^D} \mathrm{Tr}\left[R\gamma^\lambda S(p)\gamma_\delta i S_3^{GFG}\right] \\
&= h_V \mathrm{Tr}_F\left[\Lambda^n V^\delta\right] \int \frac{d^D p}{(2\pi)^D} \mathrm{Tr}\left[R\gamma^\lambda S(p)\gamma_\delta \frac{\pi^2}{24} eQF_{\alpha\beta} t^a t^a \left\langle \frac{\alpha}{\pi} G^2 \right\rangle \left(g_{\mu\rho}g_{\nu\sigma} - g_{\mu\sigma}g_{\nu\rho}\right) T^{\mu\nu\alpha\beta\sigma\rho}\right] \\
&= \frac{\pi^2 h_V e}{96} \left\langle \frac{\alpha}{\pi} G^2 \right\rangle \mathrm{Tr}_F\left[\Lambda^n V^\delta\right] \int \frac{d^D p}{(2\pi)^D} \mathrm{Tr}\left[\left(1+\gamma_5\right)\gamma^\lambda S(p)\gamma_\delta QF_{\alpha\beta}\left(g_{\mu\rho}g_{\nu\sigma} - g_{\mu\sigma}g_{\nu\rho}\right) T^{\mu\nu\alpha\beta\sigma\rho}\right]
\end{aligned}
\tag{6.60}
$$

Finally, the third of these diagrams, shown in figure 6.32,

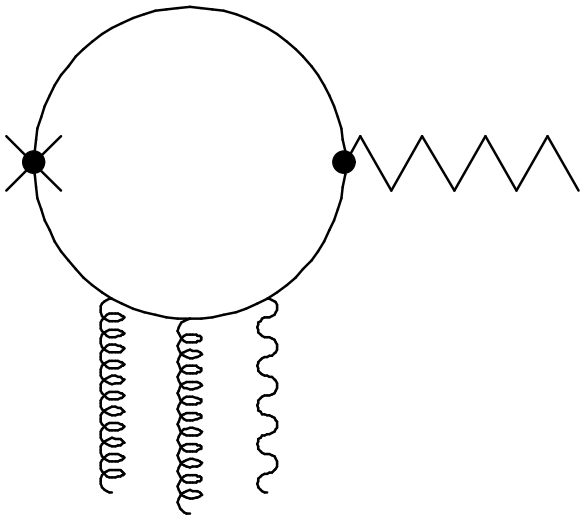

Figure 6.32 $\langle \mathrm{Vgg}\gamma|\bar{\chi}\Lambda^{n}\gamma_{\mu}\mathrm{L}\chi|0\rangle$ *- A creation diagram for a vector particle with one external photon line and two external gluon lines coupled to the lower quark.*

gives

$$
\begin{aligned}
M^{\lambda} &= -\int \frac{d^{D}p}{(2\pi)^{D}} \mathrm{Tr}\left[\Lambda^{n}\gamma^{\lambda}\mathrm{LiS}(p)\mathrm{ih}_{V}\gamma_{\delta}V^{\delta}\mathrm{iS}_{3}^{FGG}\right] \\
&= h_{V}\mathrm{Tr}_{F}\left[\Lambda^{n}V^{\delta}\right]\int \frac{d^{D}p}{(2\pi)^{D}} \mathrm{Tr}\left[R\gamma^{\lambda}S(p)\gamma_{\delta}\mathrm{iS}_{3}^{FGG}\right] \\
&= h_{V}\mathrm{Tr}_{F}\left[\Lambda^{n}V^{\delta}\right]\int \frac{d^{D}p}{(2\pi)^{D}} \mathrm{Tr}\left[R\gamma^{\lambda}S(p)\gamma_{\delta}\frac{\pi^{2}}{24}eQF_{\mu\nu}t^{a}t^{a}\left\langle\frac{\alpha}{\pi}G^{2}\right\rangle\left(g_{\alpha\rho}g_{\beta\sigma}-g_{\alpha\sigma}g_{\beta\rho}\right)T^{\mu\nu\alpha\beta\sigma\rho}\right] \\
&= \frac{\pi^{2}h_{V}e}{96}\left\langle\frac{\alpha}{\pi}G^{2}\right\rangle\mathrm{Tr}_{F}\left[\Lambda^{n}V^{\delta}\right]\int \frac{d^{D}p}{(2\pi)^{D}} \mathrm{Tr}\left[\left(1+\gamma_{5}\right)\gamma^{\lambda}S(p)\gamma_{\delta}QF_{\mu\nu}\left(g_{\alpha\rho}g_{\beta\sigma}-g_{\alpha\sigma}g_{\beta\rho}\right)T^{\mu\nu\alpha\beta\sigma\rho}\right]
\end{aligned}
\tag{6.61}
$$

The last six diagrams have external lines coupled to both quarks, and the first of these that we will look at is the one shown in figure 6.33.

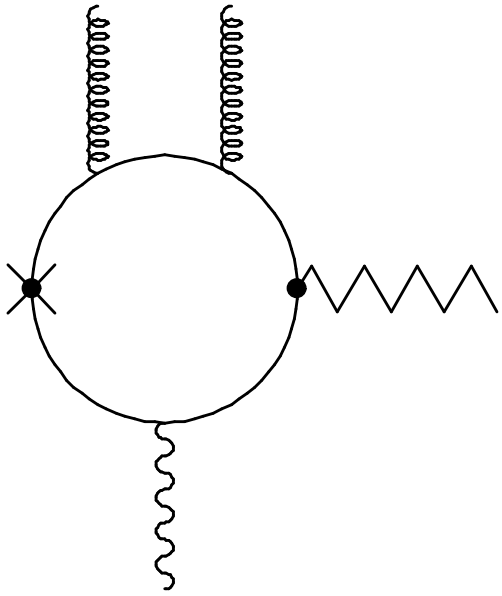

Figure 6.33 $\langle \mathrm{Vgg}\gamma|\bar{\chi}\Lambda^{n}\gamma_{\mu}\mathrm{L}\chi|0\rangle$ *- A creation diagram for a vector particle with two external gluon lines coupled to the upper quark and one external photon line coupled to the lower quark.*

This diagram has two gluons coupled to the upper quark and one photon coupled to the lower quark. This is also a diagram in which we can do the integration over the momenta, and it gives us

$$
\begin{aligned}
M^{\lambda} &= -\int \frac{d^{D}p}{(2\pi)^{D}} \mathrm{Tr}\left[\Lambda^{n}\gamma^{\lambda}\mathrm{Li}S_{2}^{GG}ih_{V}\gamma_{\delta}V^{\delta}iS_{1}^{F}\right] \\
&= ih_{V}\mathrm{Tr}_{F}\left[\Lambda^{n}V^{\delta}\right]\int \frac{d^{D}p}{(2\pi)^{D}} \mathrm{Tr}\left[R\gamma^{\lambda}S_{2}^{GG}\gamma_{\delta}S_{1}^{F}\right] \\
&= ih_{V}\mathrm{Tr}_{F}\left[\Lambda^{n}V^{\delta}\right]\int \frac{d^{D}p}{(2\pi)^{D}} \mathrm{Tr}[R\gamma^{\lambda}2\pi^{2}t^{a}t^{a}\left\langle\frac{\alpha}{\pi}G^{2}\right\rangle\frac{m}{(p^{2}-m^{2})^{4}}\left[m(\gamma\cdot p)+p^{2}\right]\gamma_{\delta}\times \\
&\left(-\frac{e}{4}\tilde{Q}_{\xi}^{V}F_{\sigma\rho}\right)\frac{1}{\left(p^{2}-m^{2}\right)^{2}}\left\{\sigma^{\sigma\rho},(\gamma\cdot p+m)\right\}] \\
&= -\frac{ih_{V}e\pi^{2}m}{4}\left\langle\frac{\alpha}{\pi}G^{2}\right\rangle\mathrm{Tr}_{F}\left[\Lambda^{n}V^{\delta}\right]\int \frac{d^{D}p}{(2\pi)^{D}}\frac{1}{(p^{2}-m^{2})^{6}}\mathrm{Tr}\left[R\gamma^{\lambda}\left[m(\gamma\cdot p)+p^{2}\right]\gamma_{\delta}\tilde{Q}_{\xi}^{V}F_{\sigma\rho}\left\{\sigma^{\sigma\rho},(\gamma\cdot p+m)\right\}\right] \\
&= -\frac{ih_{V}e\pi^{2}m}{4}\left\langle\frac{\alpha}{\pi}G^{2}\right\rangle\mathrm{Tr}_{F}\left[\Lambda^{n}V^{\delta}\right]T_{\lambda\delta}
\end{aligned}
\tag{6.62}
$$

Calculating $T_{\lambda\delta}$ gives

$$
\begin{aligned}
T_{\lambda\delta} &= \int \frac{d^D p}{(2\pi)^D} \frac{1}{(p^2-m^2)^6} \mathrm{Tr}\Big[R\gamma^\lambda \Big[m(\gamma\cdot p) + p^2 \Big] \gamma_\delta \tilde{Q}_\xi^V F_{\sigma\rho} \left\{ \sigma^{\sigma\rho}, (\gamma\cdot p + m) \right\} \Big] \\
&= \int \frac{d^D p}{(2\pi)^D} \frac{1}{(p^2-m^2)^6} \mathrm{Tr}\Big[R\gamma^\lambda \left(m(\gamma\cdot p) + p^2 \right) \gamma_\delta \tilde{Q}_\xi^V F_{\sigma\rho} \left(\sigma^{\sigma\rho}(\gamma\cdot p + m) + (\gamma\cdot p + m)\sigma^{\sigma\rho} \right) \Big] \\
&= \int \frac{d^D p}{(2\pi)^D} \frac{1}{(p^2-m^2)^6} \mathrm{Tr}\Big[R\gamma^\lambda \left(m(\gamma\cdot p) + p^2 \right) \gamma_\delta \tilde{Q}_\xi^V F_{\sigma\rho} \left(\sigma^{\sigma\rho}(\gamma\cdot p) + 2m\sigma^{\sigma\rho} + (\gamma\cdot p)\sigma^{\sigma\rho} \right) \Big] \\
&= \int \frac{d^D p}{(2\pi)^D} \frac{1}{(p^2-m^2)^6} \mathrm{Tr}\Big[R\gamma^\lambda \left(m(\gamma\cdot p)\gamma_\delta \tilde{Q}_\xi^V \sigma\cdot F(\gamma\cdot p) + m(\gamma\cdot p)\gamma_\delta \tilde{Q}_\xi^V F_{\sigma\rho}(\gamma\cdot p)\sigma^{\sigma\rho} + 2mp^2 \gamma_\delta \tilde{Q}_\xi^V \sigma\cdot F \right) \Big] \\
&= m\int \frac{d^D p}{(2\pi)^D} \frac{1}{(p^2-m^2)^6} \mathrm{Tr}\left[\left(\frac{2-D}{D} \right) p^2 \gamma^\lambda \gamma_\delta \tilde{Q}_\xi^V \sigma\cdot F + 2p^2 R\gamma^\lambda \gamma_\delta \tilde{Q}_\xi^V \sigma\cdot F \right] \qquad (6.63) \\
&= m\int \frac{d^D p}{(2\pi)^D} \frac{p^2}{(p^2-m^2)^6} \mathrm{Tr}\left[\left(\frac{2-D}{D} + 2R \right) \gamma^\lambda \gamma_\delta \tilde{Q}_\xi^V \sigma\cdot F \right] \\
&= m(I_5 + m^2 I_6)\mathrm{Tr}\left[\left(\frac{2-D}{D} + 2R \right) \gamma^\lambda \gamma_\delta \tilde{Q}_\xi^V \sigma\cdot F \right]
\end{aligned}
$$

And the final result becomes

$$
\begin{aligned}
M^\lambda &= -\frac{ih_V e\pi^2 m^2}{4} \left\langle \frac{\alpha}{\pi} G^2 \right\rangle \mathrm{Tr}_F\left[\Lambda^n V^\delta \right] \left(\frac{-i}{384\pi^2 m^6} + \frac{i}{1920\pi^2 m^6} \right) \mathrm{Tr}\left[\left(\frac{2-D}{D} + 2R \right) \gamma^\lambda \gamma_\delta \tilde{Q}_\xi^V \sigma\cdot F \right] \qquad (6.64) \\
&\underset{D\to 4}{\to} -\frac{ih_V e\pi^2 m^2}{4} \left\langle \frac{\alpha}{\pi} G^2 \right\rangle \mathrm{Tr}_F\left[\Lambda^n V^\delta \right] \left(\frac{-i}{480\pi^2 m^6} \right) \mathrm{Tr}\left[\left(-\frac{1}{2} + (1+\gamma_5) \right) \gamma^\lambda \gamma_\delta \tilde{Q}_\xi^V \sigma\cdot F \right] \\
&= -\frac{h_V e}{3840 m^4} \left\langle \frac{\alpha}{\pi} G^2 \right\rangle \mathrm{Tr}_F\left[\Lambda^n V^\delta \right] \mathrm{Tr}\left[(2\gamma_5 + 1)\gamma^\lambda \gamma_\delta \tilde{Q}_\xi^V \sigma\cdot F \right]
\end{aligned}
$$

The next diagram is the following, shown in figure 6.34.

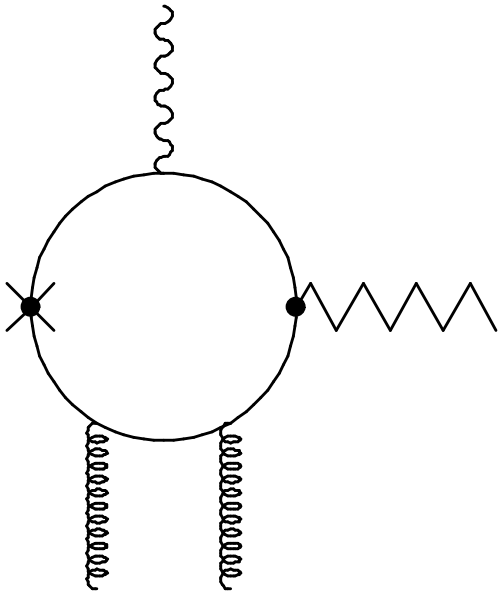

Figure 6.34 $\langle V\gamma gg|\bar{\chi}\Lambda^n\gamma_\mu L\chi|0\rangle$ *- A creation diagram for a vector particle with one external photon line coupled to the upper quark and two external gluon lines coupled to the lower quark.*

The calculation for this diagram will be like the one above, but where the effective propagators have switched places. This gives

$$\begin{aligned}
M^\lambda &= -\int\frac{d^D p}{(2\pi)^D}\mathrm{Tr}\left[\Lambda^n\gamma^\lambda L i S_1^F i h_V\gamma_\delta V^\delta i S_2^{GG}\right] \\
&= i h_V \mathrm{Tr}_F\left[\Lambda^n V^\delta\right]\int\frac{d^D p}{(2\pi)^D}\mathrm{Tr}[R\gamma^\lambda\left(-\frac{e}{4}\tilde{Q}_\xi^V F_{\sigma\rho}\right)\frac{1}{\left(p^2-m^2\right)^2}\left\{\sigma^{\sigma\rho},(\gamma\cdot p+m)\right\}\gamma_\delta\times \\
&\quad 2\pi^2 t^a t^a\left\langle\frac{\alpha}{\pi}G^2\right\rangle\frac{m}{(p^2-m^2)^4}\left[m(\gamma\cdot p)+p^2\right]] \\
&= -\frac{i h_V e\pi^2 m^2}{4}\left\langle\frac{\alpha}{\pi}G^2\right\rangle\mathrm{Tr}_F\left[\Lambda^n V^\delta\right](I_5+m^2 I_6)\mathrm{Tr}\left[\left(\frac{2-D}{D}+2R\right)\gamma^\lambda\tilde{Q}_\xi^V\sigma\cdot F\gamma_\delta\right] \\
&\underset{D\to 4}{\to} -\frac{h_V e}{3840 m^4}\left\langle\frac{\alpha}{\pi}G^2\right\rangle\mathrm{Tr}_F\left[\Lambda^n V^\delta\right]\mathrm{Tr}\left[(2\gamma_5+1)\gamma^\lambda\tilde{Q}_\xi^V\sigma\cdot F\gamma_\delta\right]
\end{aligned} \tag{6.65}$$

We will not be able to integrate out the momentum in the last four diagrams, and the only difference between them will be in the indices. We start with the diagram shown in figure 6.35.

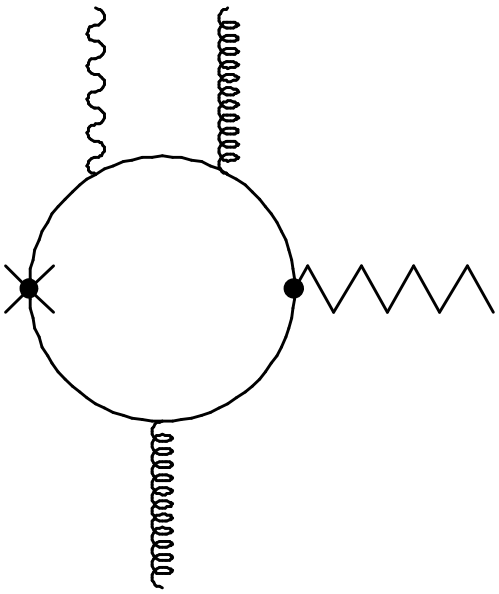

Figure 6.35 $\langle \mathrm{Vg\gamma g}|\bar{\chi}\Lambda^{n}\gamma_{\mu}\mathrm{L}\chi|0\rangle$ *- A creation diagram for a vector particle with one external gluon line and one external photon line coupled to the upper quark and one external gluon line coupled to the lower quark.*

Calculation of this diagram gives

$$
\begin{aligned}
M^{\lambda} &= -\int \frac{d^{D}p}{(2\pi)^{D}} \mathrm{Tr}\left[\Lambda^{n}\gamma^{\lambda}\mathrm{LiS}_{2}^{FG}\mathrm{ih}_{V}\gamma_{\delta}V^{\delta}\mathrm{iS}_{l}^{G}\right] \\
&= \mathrm{ih}_{V}\mathrm{Tr}_{F}\left[\Lambda^{n}V^{\delta}\right]\int \frac{d^{D}p}{(2\pi)^{D}} \mathrm{Tr}\left[R\gamma^{\lambda}\left(\frac{eg_{S}}{4}QF_{\mu\nu}t^{a}G_{\alpha\beta}^{a}R^{\mu\nu\alpha\beta}\right)\gamma_{\delta}\left(\frac{g_{S}}{4}t^{a}G_{\sigma\rho}^{a}\frac{1}{(p^{2}-m^{2})^{2}}\left\{\sigma^{\sigma\rho},(\gamma\cdot p+m)\right\}\right)\right] \\
&= \frac{\mathrm{ih}_{V}eg_{S}^{2}}{32}\mathrm{Tr}_{F}\left[\Lambda^{n}V^{\delta}\right]\int \frac{d^{D}p}{(2\pi)^{D}}\frac{1}{(p^{2}-m^{2})^{2}}\mathrm{Tr}\left[R\gamma^{\lambda}QF_{\mu\nu}G_{\alpha\beta}R^{\mu\nu\alpha\beta}\gamma_{\delta}G_{\sigma\rho}\left\{\sigma^{\sigma\rho},(\gamma\cdot p+m)\right\}\right] \qquad (6.66) \\
&= -\frac{\mathrm{h}_{V}e\pi^{2}}{384}\left\langle\frac{\alpha_{s}}{\pi}G^{2}\right\rangle\left(g_{\alpha\sigma}g_{\beta\rho}-g_{\alpha\rho}g_{\beta\sigma}\right)\mathrm{Tr}_{F}\left[\Lambda^{n}V^{\delta}\right]\times \\
&\int \frac{d^{D}p}{(2\pi)^{D}}\frac{1}{(p^{2}-m^{2})^{2}}\mathrm{Tr}\left[\left(1+\gamma_{5}\right)\gamma^{\lambda}QF_{\mu\nu}R^{\mu\nu\alpha\beta}\gamma_{\delta}\left\{\left[\gamma^{\sigma},\gamma^{\rho}\right],(\gamma\cdot p+m)\right\}\right]
\end{aligned}
$$

The next diagram is the one in figure 6.36.

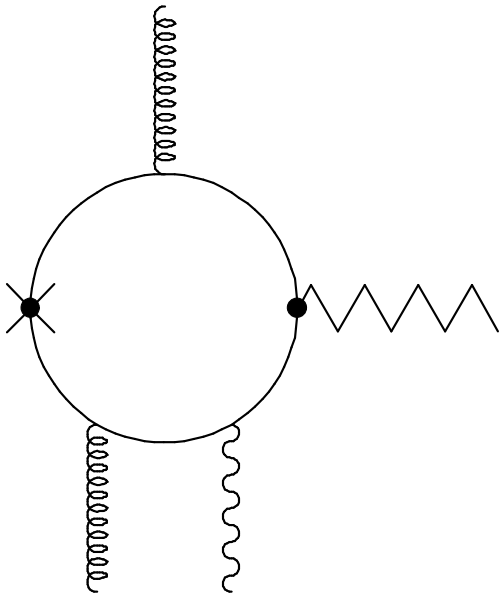

Figure 6.36 $\langle \mathrm{Vg\gamma g}|\bar{\chi}\Lambda^{n}\gamma_{\mu}\mathrm{L}\chi|0\rangle$ *- A creation diagram for a vector particle with one external gluon line coupled to the upper quark, and one external gluon line and one external photon line coupled to the lower quark.*

The calculation will not differ much from the one above, as the only change is a switch of the two effective propagators as usual.

$$
\begin{aligned}
M^{\lambda} &= -\int \frac{d^{D}p}{(2\pi)^{D}} \mathrm{Tr}\left[\Lambda^{n}\gamma^{\lambda}\mathrm{L}iS_{1}^{G}ih_{V}\gamma_{\delta}V^{\delta}iS_{2}^{FG}\right] \\
&= ih_{V}\mathrm{Tr}_{F}\left[\Lambda^{n}V^{\delta}\right]\int \frac{d^{D}p}{(2\pi)^{D}} \mathrm{Tr}\left[R\gamma^{\lambda}\left(\frac{g_{S}}{4}t^{a}G_{\sigma\rho}^{a}\frac{1}{(p^{2}-m^{2})^{2}}\left\{\sigma^{\sigma\rho},(\gamma\cdot p+m)\right\}\right)\gamma_{\delta}\left(\frac{eg_{S}}{4}QF_{\mu\nu}t^{a}G_{\alpha\beta}^{a}R^{\mu\nu\alpha\beta}\right)\right] \\
&= \frac{ih_{V}eg_{S}^{2}}{32}\mathrm{Tr}_{F}\left[\Lambda^{n}V^{\delta}\right]\int \frac{d^{D}p}{(2\pi)^{D}}\frac{1}{(p^{2}-m^{2})^{2}} \mathrm{Tr}\left[R\gamma^{\lambda}G_{\sigma\rho}\left\{\sigma^{\sigma\rho},(\gamma\cdot p+m)\right\}\gamma_{\delta}QF_{\mu\nu}G_{\alpha\beta}R^{\mu\nu\alpha\beta}\right] \qquad (6.67) \\
&= -\frac{h_{V}e\pi^{2}}{384}\left\langle\frac{\alpha_{s}}{\pi}G^{2}\right\rangle\left(g_{\sigma\alpha}g_{\rho\beta}-g_{\sigma\beta}g_{\rho\alpha}\right)\mathrm{Tr}_{F}\left[\Lambda^{n}V^{\delta}\right]\times \\
&\int \frac{d^{D}p}{(2\pi)^{D}}\frac{1}{(p^{2}-m^{2})^{2}} \mathrm{Tr}\left[\left(1+\gamma_{5}\right)\gamma^{\lambda}\left\{\left[\gamma^{\sigma},\gamma^{\rho}\right],(\gamma\cdot p+m)\right\}\gamma_{\delta}QF_{\mu\nu}R^{\mu\nu\alpha\beta}\right]
\end{aligned}
$$

The next diagram will be the one shown in figure 6.37.

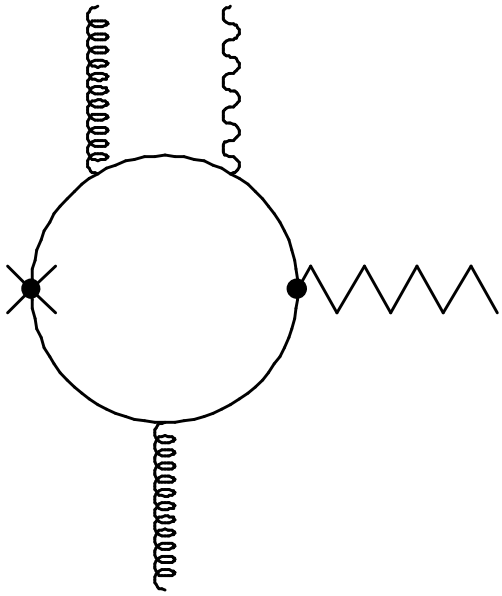

Figure 6.37 $\langle V\gamma gg|\bar{\chi}\Lambda^n\gamma_\mu L\chi|0\rangle$ *- A creation diagram for a vector particle with one external photon line and one external gluon coupled to the upper quark, and one external gluon line coupled to the lower quark.*

A calculation for this diagram gives

$$
\begin{aligned}
M^\lambda &= -\int \frac{d^D p}{(2\pi)^D} \mathrm{Tr}\left[\Lambda^n \gamma^\lambda L i S_2^{GF} i h_V \gamma_\delta V^\delta i S_1^G\right] \\
&= i h_V \mathrm{Tr}_F\left[\Lambda^n V^\delta\right] \int \frac{d^D p}{(2\pi)^D} \mathrm{Tr}\left[R\gamma^\lambda\left(\frac{e g_S}{4} Q F_{\alpha\beta} t^a G^a_{\mu\nu} R^{\mu\nu\alpha\beta}\right)\gamma_\delta\left(\frac{g_S}{4} t^a G^a_{\sigma\rho} \frac{1}{(p^2-m^2)^2}\left\{\sigma^{\sigma\rho},(\gamma\cdot p+m)\right\}\right)\right] \\
&= \frac{i h_V e g_S^2}{32} \mathrm{Tr}_F\left[\Lambda^n V^\delta\right] \int \frac{d^D p}{(2\pi)^D} \frac{1}{(p^2-m^2)^2} \mathrm{Tr}\left[R\gamma^\lambda Q F_{\alpha\beta} G_{\mu\nu} R^{\mu\nu\alpha\beta}\gamma_\delta G_{\sigma\rho}\left\{\sigma^{\sigma\rho},(\gamma\cdot p+m)\right\}\right] \qquad (6.68) \\
&= -\frac{h_V e \pi^2}{384}\left\langle\frac{\alpha_s}{\pi}G^2\right\rangle\left(g_{\mu\sigma}g_{\nu\rho}-g_{\mu\rho}g_{\nu\sigma}\right)\mathrm{Tr}_F\left[\Lambda^n V^\delta\right]\times \\
&\quad \int \frac{d^D p}{(2\pi)^D} \frac{1}{(p^2-m^2)^2} \mathrm{Tr}\left[\left(1+\gamma_5\right)\gamma^\lambda Q F_{\alpha\beta} R^{\mu\nu\alpha\beta}\gamma_\delta\left\{\left[\gamma^\sigma,\gamma^\rho\right],(\gamma\cdot p+m)\right\}\right]
\end{aligned}
$$

And finally the last of the creation type diagrams, shown in figure 6.38.

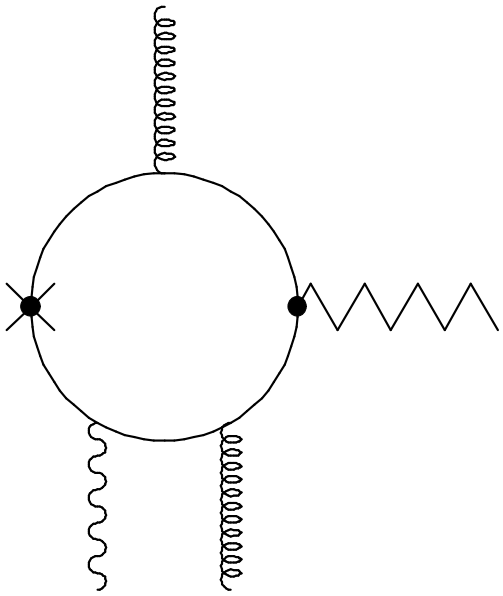

Figure 6.38 $\langle \mathrm{Vgg}\gamma|\bar{\chi}\Lambda^{n}\gamma_{\mu}\mathrm{L}\chi|0\rangle$ *- A creation diagram for a vector particle with one external gluon line coupled to the upper quark, and one external photon line and one external gluon line coupled to the lower quark.*

The calculation for this diagram will be as follows

$$
\begin{aligned}
M^{\lambda} &= -\int \frac{d^{D}p}{(2\pi)^{D}} \mathrm{Tr}\left[\Lambda^{n}\gamma^{\lambda}\mathrm{L}iS_{1}^{G}ih_{V}\gamma_{\delta}V^{\delta}iS_{2}^{GF}\right] \\
&= ih_{V}\mathrm{Tr}_{F}\left[\Lambda^{n}V^{\delta}\right]\int \frac{d^{D}p}{(2\pi)^{D}} \mathrm{Tr}\left[R\gamma^{\lambda}\left(\frac{g_{S}}{4}t^{a}G_{\sigma\rho}^{a}\frac{1}{(p^{2}-m^{2})^{2}}\left\{\sigma^{\sigma\rho},(\gamma\cdot p+m)\right\}\right)\gamma_{\delta}\left(\frac{eg_{S}}{4}QF_{\alpha\beta}t^{a}G_{\mu\nu}^{a}R^{\mu\nu\alpha\beta}\right)\right] \\
&= \frac{ih_{V}eg_{S}^{2}}{32}\mathrm{Tr}_{F}\left[\Lambda^{n}V^{\delta}\right]\int \frac{d^{D}p}{(2\pi)^{D}}\frac{1}{(p^{2}-m^{2})^{2}}\mathrm{Tr}\left[R\gamma^{\lambda}G_{\sigma\rho}\left\{\sigma^{\sigma\rho},(\gamma\cdot p+m)\right\}\gamma_{\delta}QF_{\alpha\beta}G_{\mu\nu}R^{\mu\nu\alpha\beta}\right] \qquad (6.69) \\
&= -\frac{h_{V}e\pi^{2}}{384}\left\langle\frac{\alpha_{s}}{\pi}G^{2}\right\rangle\left(g_{\sigma\mu}g_{\rho\nu}-g_{\sigma\nu}g_{\rho\mu}\right)\mathrm{Tr}_{F}\left[\Lambda^{n}V^{\delta}\right]\times \\
&\int \frac{d^{D}p}{(2\pi)^{D}}\frac{1}{(p^{2}-m^{2})^{2}}\mathrm{Tr}\left[\left(1+\gamma_{5}\right)\gamma^{\lambda}\left\{\left[\gamma^{\sigma},\gamma^{\rho}\right],(\gamma\cdot p+m)\right\}\gamma_{\delta}QF_{\alpha\beta}R^{\mu\nu\alpha\beta}\right]
\end{aligned}
$$

This was all the 26 *creation* diagrams, where we have a creation of a vector particle with the possibility of having one photon and/or one/two gluons coupled to the quark loop. It now remains to combine the annihilation and creation diagrams to get the total or complete diagrams for the process $D \rightarrow V\gamma$.

6.2 The Total Diagrams

Here we will combine our annihilation and creation diagram calculations from the last two paragraphs into complete diagrams describing the full process $D \rightarrow V\gamma$. We will use the analytical program FORM to do the multiplication and integration of the traces. An example of such a program is given in the appendix B. Also, in this section we will look specifically at the process $D^0 \rightarrow \bar{K}^{*0}\gamma$, when doing the calculations.

A general matrix element for an electromagnetic current from a pseudoscalar state (like the D-meson) to a vector state (like the vector particle), is described by the Lorentz invariant form factor of the form [5, and references therein]

$$\left\langle p',\varepsilon' \middle| J^{\mu}(0) \middle| p \right\rangle = -ig(q^2)\varepsilon^{\mu\nu\alpha\beta}\varepsilon'_{\nu}\, p'_{\alpha}\, p_{\beta} \tag{6.70}$$

For a weak decay with emission of a photon (a $0^- \rightarrow 1^- + \gamma$ process) the parity conserving amplitude will have the same form as above, but with a polarization vector for the photon, $\varepsilon(\gamma)$, in addition. For our process the term q will be equal to $(p'- p) = k$, which is the photon's 4-momentum. ε' is the vector particle's polarization vector, p' its 4-momentum and p the 4-momentum of the D-meson. p will be replaced by v, as this is what is used in the calculations.

Looking at an on-shell decay, that is $k^2 = 0$, we have $g(q^2 = k^2 = 0) = e\beta$. In addition, the spin 1 photon has the transverse polarisation vector $\varepsilon(\gamma)$, and the vector particle has the polarization vector $\varepsilon'(V)$. Neglecting coefficients, the general form factor for on-shell decay including the photon emission gets the following form

$$\varepsilon^{\mu\nu\alpha\beta}\varepsilon_{\mu}(\gamma)\varepsilon'_{\nu}(V)p'_{\alpha}\, v_{\beta} \tag{6.71}$$

By using the following equation relating the momentums in the process

$$p' = m_D v - k \tag{6.72}$$

we can write the general form factor as

$$\varepsilon^{\mu\nu\alpha\beta}\varepsilon_{\mu}(\gamma)\varepsilon'_{\nu}(V)k_{\alpha}v_{\beta} \tag{6.73}$$

Some juggling with indices gives further

$$\varepsilon^{\mu\nu\alpha\beta}v_{\mu}\varepsilon'_{\nu}(V)k_{\alpha}\varepsilon_{\beta}(\gamma) \tag{6.74}$$

The parity conserving terms will be proportional to this result, and the way FORM writes this expression is through e_(v,y,z,V). (Actually $e\_(v,y,z,V) = i\varepsilon^{\mu\nu\alpha\beta}v_{\mu}\varepsilon'_{\nu}(V)k_{\alpha}\varepsilon_{\beta}(\gamma)$, but since we have neglected coefficients above, we don't write the i-factor. It will however be important in the final results.) y and z are here the momentum and polarization vector of the photon as they appear in the electromagnetic tensor

$$F_{\mu\nu} = k_\mu \varepsilon_\nu(\gamma) - k_\nu \varepsilon_\mu(\gamma) = y(\mu)z(\nu) - y(\nu)z(\mu) \tag{6.75}$$

As weak decays break the parity, also the parity violating terms must be included in the result. These are proportional to $F_{\mu\nu} v^\mu V^\nu$, and will in FORM's notation be terms of the type v.y*z.V and v.z*y.V. This we can see from

$$\begin{aligned} F_{\mu\nu} v^\mu V^\nu &= (y(\mu)z(\nu) - z(\mu)y(\nu)) v^\mu V^\nu \\ &= (y \cdot v)(z \cdot V) - (z \cdot v)(y \cdot V) \end{aligned} \tag{6.76}$$

However, in many of the calculations these terms will cancel when the total diagram calculations are summed.

It would be useful to get all the answers on a general form, especially later when we are going to do a summation over the diagrams. We expect the general result to be of the form

$$\mathcal{L} = A^{(+)} i\varepsilon^{\mu\nu\alpha\beta} \Phi_D v_\mu \varepsilon'_\nu(V) k_\alpha \varepsilon_\beta(\gamma) + A^{(-)} \Phi_D F_{\mu\nu} v^\mu V^\nu \tag{6.77}$$

where Φ_D is the pseudoscalar part of the D-meson field. The factors $A^{(\pm)}$ may be expressed through the decay width

$$\Gamma(D \to V\gamma) \sim \left(\left|A^{(+)}\right|^2 + \frac{\left|A^{(-)}\right|^2}{4} \right) \times \frac{M_D^2 \left(1 - \left(\frac{m_V}{M_D}\right)^2\right)^4}{\frac{72}{\pi}\left(1 + \left(\frac{m_V}{M_D}\right)^2\right)} \tag{6.78}$$

where the factor 4 under $A^{(-)}$ is a normalization factor, M_D is the mass of the D-meson and m_V is the mass of the vector meson. We will look more into this in the last chapter.

In order to save some space, we will use the expression on the left side of eq. 6.76 ($F_{\mu\nu} v^\mu V^\nu$) together with the FORM expression e_(v,y,z,V) in the results. This may look inconsistent, but since these terms will not be part of the $A^{(\pm)}$ factors, and therefore will not be part of the numerical calculations in the final chapter, we will write the results like this.

6.2.1 Calculation of the Total Diagrams

We start with the simplest of the combined diagrams, namely the ones without vacuum effects on the form of external gluon lines. These diagrams have only an external photon line, which can couple to either of the light quarks. We therefore get three diagrams of this type.

Our first total diagram will be the one in figure 6.39, which consists of the two partial diagrams from figure 6.5 and figure 6.13.

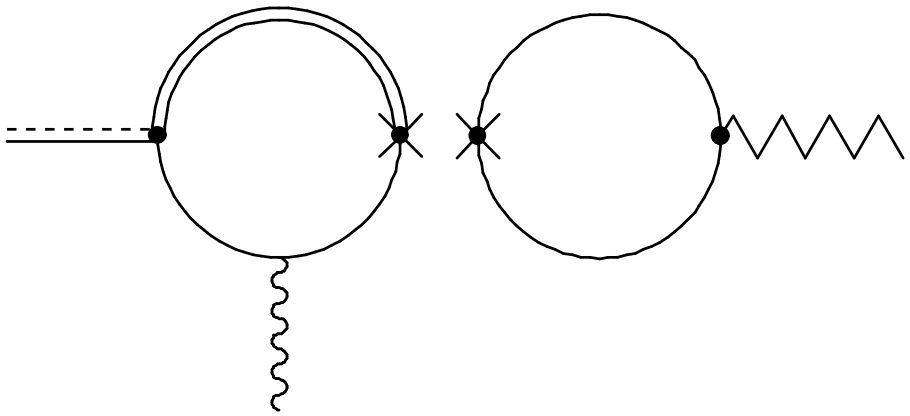

Figure 6.39 A combined diagram for the process $\langle V|\bar{\chi}\Lambda^n\gamma_\mu L\chi|0\rangle\langle\gamma|\bar{q}\gamma^\mu LQ_{v_c}|D\rangle$.

These two partial diagrams has the following expressions for M

$$M^\mu = \frac{N_c G_H e}{4}\mathrm{Tr}\left[\xi^\dagger\gamma^\mu LH\left(iI_2\{\gamma\cdot v,\sigma\cdot F\tilde{Q}_\xi^V\}+\frac{1}{8\pi}\sigma\cdot F\tilde{Q}_\xi^V\right)\right] \tag{6.79}$$

and

$$M = iN_C h_V \mathrm{Tr}_F\left[\Lambda^n V^v\right]\left[m^2 I_2 - I_1\right]g_{\mu v} \tag{6.80}$$

Multiplying these two expressions will give us

$$\begin{aligned} DfV &= \frac{iN_c{}^2 G_H h_V e}{4}\left[m^2 I_2 - I_1\right]g_{\mu v}\mathrm{Tr}_F\left[\Lambda^n V^v\right]\mathrm{Tr}\left[\xi^\dagger\gamma^\mu LH\left(iI_2\{\gamma\cdot v,\sigma\cdot F\tilde{Q}_\xi^V\}+\frac{1}{8\pi}\sigma\cdot F\tilde{Q}_\xi^V\right)\right] \\ &= \frac{iN_c{}^2 G_H h_V e Q_d\sqrt{M_D}}{32}\left[m^2 I_2 - I_1\right]g_{\mu v}\mathrm{Tr}_F\left[\Lambda^n V^v\right]\times \\ &\mathrm{Tr}\left[\gamma^\mu(1-\gamma_5)(1+\gamma\cdot v)\gamma_5\left(iI_2\{\gamma\cdot v,\left[\gamma^\sigma,\gamma^\rho\right]\cdot F_{\sigma\rho}\}+\frac{1}{8\pi}\left[\gamma^\sigma,\gamma^\rho\right]\cdot F_{\sigma\rho}\right)\right] \end{aligned} \tag{6.81}$$

where we have used that $\xi^\dagger = 1$ and substituted P_5 in the momentum space with the square root of the mass of the D-meson. Since $\xi^\dagger = 1$ (since we're not dealing with pseudo-scalar mesons, see eq. 3.46), Λ^n simply becomes equal to λ^n. When then taking the trace over $\Lambda^n V^v$, we will get a vector field, containing a polarization vector of the spin one vector particle. We will continue to call this field for V in the calculations. So, in eq 6.81 there is more or less just one trace to calculate, and using FORM we get the following answer

$$\begin{aligned} DfV = &\frac{iN_c{}^2 G_H h_V e Q_d\sqrt{M_D}}{32}\left[m^2 I_2 - I_1\right]\times \\ &\left(\frac{2}{\pi}*v\cdot y*z\cdot V-\frac{2}{\pi}*v\cdot z*y\cdot V-\frac{2}{\pi}*e\_(v,y,z,V)+32i\cdot I_2*e\_(v,y,z,V)\right) \end{aligned} \tag{6.82}$$

If we now use eq. 6.76, we can rewrite this expression on a more universal and shorter form

$$DfV = \frac{iN_c{}^2 G_H h_V e Q_d \sqrt{M_D}}{16}\left[m^2 I_2 - I_1\right]\times\left(\frac{1}{\pi}F_{\mu\nu}v^\mu V^\nu + \left(16i\cdot I_2 - \frac{1}{\pi}\right)e\_(v,y,z,V)\right) \qquad (6.83)$$

The notion DfV in eq. 6.81 and the following is a short hand notation for the process just described, that is $\langle V|\bar{\chi}\Lambda^n\gamma_\mu L\chi|0\rangle\,\langle\gamma|\bar{q}\gamma^\mu LQ_{v_c}|D\rangle$, where f stands for photon. A g would indicate a gluon. In this notation everything standing before V is coupled to the light quark in the D-meson loop and everything after is coupled to the V-loop. In the simple diagrams without gluon condensate it is usually clear where the external line is coupled, but this may not the case when the gluon condensate is included. This is because in the creation type diagrams we have the possibility of having external lines coupled to both the upper and lower quark in the loop, so it has to be specified in the notation to which quark the line is connected. We will do this by putting a subscript d (for down) or u (for up) on the f (photon) or g (gluon). F. ex. the notion $DgVf_ug_d$ is a short hand notation for the process $\langle V\gamma g|\bar{\chi}\Lambda^n\gamma_\mu t^b L\chi|0\rangle$ $\langle g|\bar{q}\gamma^\mu Lt^a Q_{v_c}|D\rangle$, i.e. a D-meson loop with a gluon coupled to the light quark, and a vector particle loop with a photon coupled to the upper light quark and a gluon coupled to the lower light quark in the loop. This is now indicated by the subscript u (up) on the f and the subscript d (down) on the g.

The next full diagram that we will look at is the one in figure 6.40 below. The only difference between this diagram and the one we just calculated is the position of the external photon line, which now is connected to the lower quark in the loop in the creation diagram.

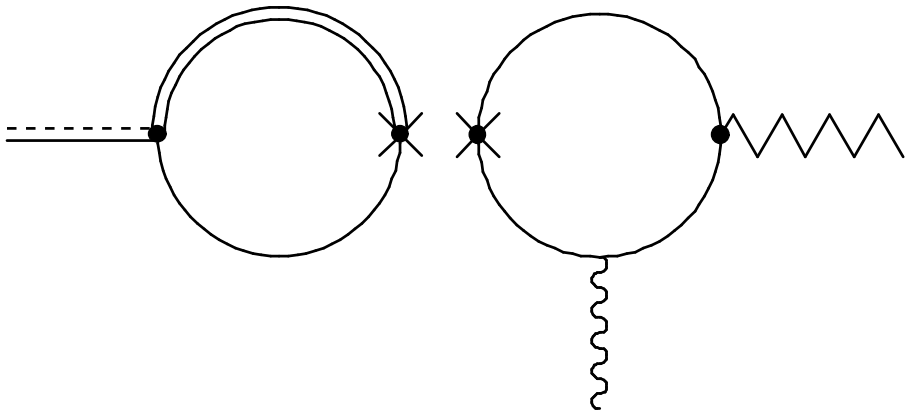

Figure 6.40 A combined diagram for the process $\langle V|\bar{\chi}\Lambda^n\gamma_\mu L\chi|\gamma\rangle\,\langle 0|\bar{q}\gamma^\mu LQ_{v_c}|D\rangle$.

The expression for M for the creation diagram is given from eq. 6.36

$$M^\mu = -\frac{ieN_c h_v}{8}Tr_F\left[\Lambda^n V^v\right]Tr\left[\left(\left(\frac{-i}{32\pi^2}\right)(2\gamma_5+1) - I_2\right)\gamma^\mu\gamma_v\tilde{Q}_\xi^v\sigma\cdot F\right] \qquad (6.84)$$

while eq. 6.16 gives us the expression for M for the annihilation diagram.

$$M^{\mu} = -iN_c G_H [mI_{3/2} - I_1] Tr[\xi^{\dagger}\gamma^{\mu} LH] \tag{6.85}$$

Multiplying these two expressions gives us

$$\begin{aligned} DVf_d &= -\frac{N_c{}^2 G_H h_v e}{8}[mI_{3/2} - I_1] Tr_F\left[\Lambda^n V^v\right] Tr[\xi^{\dagger}\gamma^{\mu} LH] Tr\left[\left(\left(\frac{-i}{32\pi^2}\right)(2\gamma_5 + 1) - I_2\right)\gamma^{\mu}\gamma_v \tilde{Q}_{\xi}^{v}\sigma\cdot F\right] \\ &= -\frac{N_c{}^2 G_H h_v e Q_u \sqrt{M_D}}{64}[mI_{3/2} - I_1] Tr_F\left[\Lambda^n V^v\right]\times \\ &\quad Tr[\gamma^{\mu}(1-\gamma_5)(1+\gamma\cdot v)\gamma_5] Tr\left[\left(\left(\frac{-i}{32\pi^2}\right)(2\gamma_5 + 1) - I_2\right)\gamma^{\mu}\gamma_v\sigma\cdot F\right] \end{aligned} \tag{6.86}$$

Using FORM to calculate the product of the traces we end up with the following result

$$\begin{aligned} DVf_d = &-\frac{N_c{}^2 G_H h_v e Q_u \sqrt{M_D}}{64}[mI_{3/2} - I_1]\times \\ &(64*v\cdot y*z\cdot V*I_2 + 6*v\cdot y*z\cdot V*\frac{i}{\pi^2} - 64*v\cdot z*y\cdot V*I_2 \\ &-6*v\cdot z*y\cdot V*\frac{i}{\pi^2} - 64*e\_(v,y,z,V)*I_2 - 6*e\_(v,y,z,V)*\frac{i}{\pi^2}) \end{aligned} \tag{6.87}$$

Using again eq. 6.76, this can be rewritten to

$$DVf_d = \frac{N_c{}^2 G_H h_v e Q_u \sqrt{M_D}}{32}[mI_{3/2} - I_1]\left(32I_2 + \frac{3i}{\pi^2}\right)\left(-F_{\mu v} v^{\mu} V^{v} + e\_(v,y,z,V)\right) \tag{6.88}$$

Following the same procedure for the full diagram in figure 6.41,

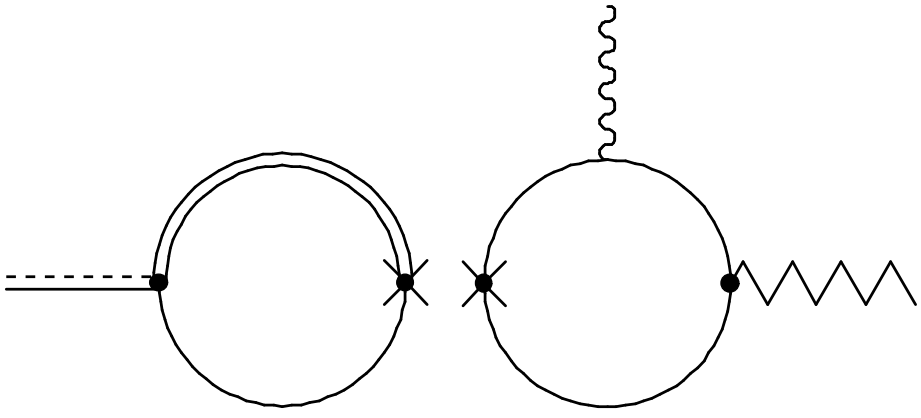

Figure 6.41 A combined diagram for the process $\langle V|\bar{\chi}\Lambda^n\gamma_{\mu}L\chi|\gamma\rangle\langle 0|\bar{q}\gamma^{\mu}LQ_{v_c}|D\rangle$.

which has the following expression for M for the creation diagram

$$M^{\mu} = -\frac{ieN_c h_v}{8} Tr_F\left[\Lambda^n V^v\right] Tr\left[\left(\left(\frac{-i}{32\pi^2}\right)(2\gamma_5+1) - I_2\right)\gamma^{\mu}\tilde{Q}_{\xi}^{v}\sigma\cdot F\gamma_v\right] \tag{6.89}$$

gives us the result

$$DVf_u = \frac{N_c{}^2 G_H h_v e Q_u \sqrt{M_D}}{32}[mI_{3/2} - I_1]\left(32I_2 + \frac{3i}{\pi^2}\right)\left(F_{\mu\nu}v^{\mu}V^{\nu} + e\_(v,y,z,V)\right) \tag{6.90}$$

As we can see, the parity violating terms from this expression will cancel the parity violating terms from eq. 6.88, when the diagrams are summed over.

We now move on to the diagrams that include the gluon condensate to first order, by having one external photon line and two external gluon lines in the full diagram. As we saw in figure 6.1 there are a total of 30 diagrams of this type, however, six of these diagrams do not require integration by the FORM program, as the integration is already done in the partial diagram calculations, and we will therefore start with these.

Our first diagram with gluon condensate will be the one shown in figure 6.42.

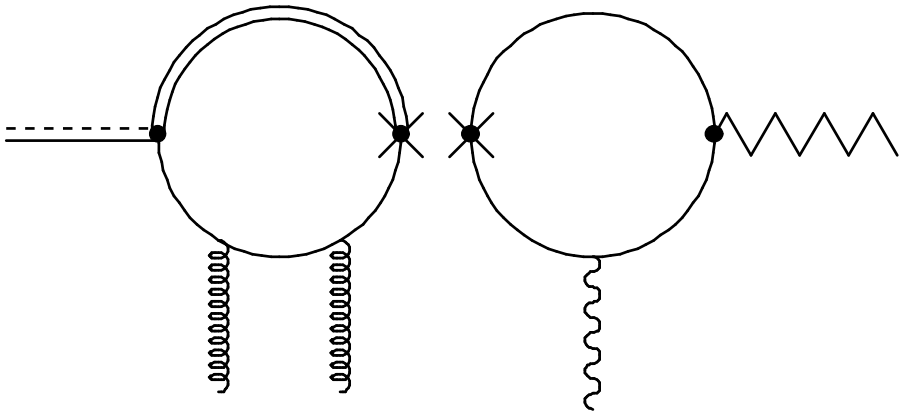

Figure 6.42 A combined diagram for the process $\langle V|\bar{\chi}\Lambda^n\gamma_\mu L\chi|\gamma\rangle\ \langle gg|\bar{q}\gamma^{\mu}LQ_{v_c}|D\rangle$.

This diagram has two gluon lines coupled to the D-meson loop and one photon line coupled to the lower quark in the vector particle loop. The equations for the two partial diagrams are

$$M^{\mu} = \frac{3\pi - 4}{384m^2} G_H \left\langle \frac{\alpha_s}{\pi} G^2 \right\rangle Tr\left[\xi^{\dagger}\gamma^{\mu} LH\right] \tag{6.91}$$

and

$$M^{\mu} = -\frac{ieN_c h_v}{8} Tr_F\left[\Lambda^n V^v\right] Tr\left[\left(\left(\frac{-i}{32\pi^2}\right)(2\gamma_5+1) - I_2\right)\gamma^{\mu}\gamma_v\tilde{Q}_{\xi}^{v}\sigma\cdot F\right] \tag{6.92}$$

respectively. Multiplying these expressions gives us the following

$$\begin{aligned}
\mathrm{DggVf_d} &= -\frac{3\pi-4}{384m^2}\frac{iN_C h_v G_H e}{8}\left\langle\frac{\alpha_s}{\pi}G^2\right\rangle \mathrm{Tr}\left[\xi^\dagger\gamma^\mu LH\right]\times \mathrm{Tr_F}\left[\Lambda^n V^v\right]\mathrm{Tr}\left[\left(\left(\frac{-i}{32\pi^2}\right)(2\gamma_5+1)-I_2\right)\gamma^\mu\gamma_v\tilde{Q}_\xi^v\sigma\cdot F\right] \\
&= -\frac{3\pi-4}{384m^2}\frac{iN_C h_v G_H eQ_u\sqrt{M_D}}{64}\left\langle\frac{\alpha_s}{\pi}G^2\right\rangle \mathrm{Tr}\left[\gamma^\mu(1-\gamma_5)(1+\gamma\cdot v)\gamma_5\right]\times \\
&\quad \mathrm{Tr_F}\left[\Lambda^n V^v\right]\mathrm{Tr}\left[\left(\left(\frac{-i}{32\pi^2}\right)(2\gamma_5+1)-I_2\right)\gamma^\mu\gamma_v\left[\gamma^\alpha,\gamma^\beta\right]\cdot F_{\alpha\beta}\right]
\end{aligned} \tag{6.93}$$

Using FORM to calculate the product of the two traces we get

$$\begin{aligned}
\mathrm{DggVf_d} &= -\frac{3\pi-4}{384m^2}\frac{iN_C h_v G_H eQ_u\sqrt{M_D}}{64}\left\langle\frac{\alpha_s}{\pi}G^2\right\rangle\times \\
&\quad (64*v\cdot y*z\cdot V*I_2+6*v\cdot y*z\cdot V*\frac{i}{\pi^2}-64*v\cdot z*y\cdot V*I_2 \\
&\quad -6*v\cdot z*y\cdot V*\frac{i}{\pi^2}-64*e_(v,y,z,V)*I_2-6*e_(v,y,z,V)*\frac{i}{\pi^2}) \\
&= \frac{3\pi-4}{384m^2}\frac{iN_C h_v G_H eQ_u\sqrt{M_D}}{32}\left\langle\frac{\alpha_s}{\pi}G^2\right\rangle\times\left(32I_2+\frac{3i}{\pi^2}\right)\left(-F_{\mu\nu}v^\mu V^v+e_(v,y,z,V)\right)
\end{aligned} \tag{6.94}$$

Looking now at the diagram in figure 6.43,

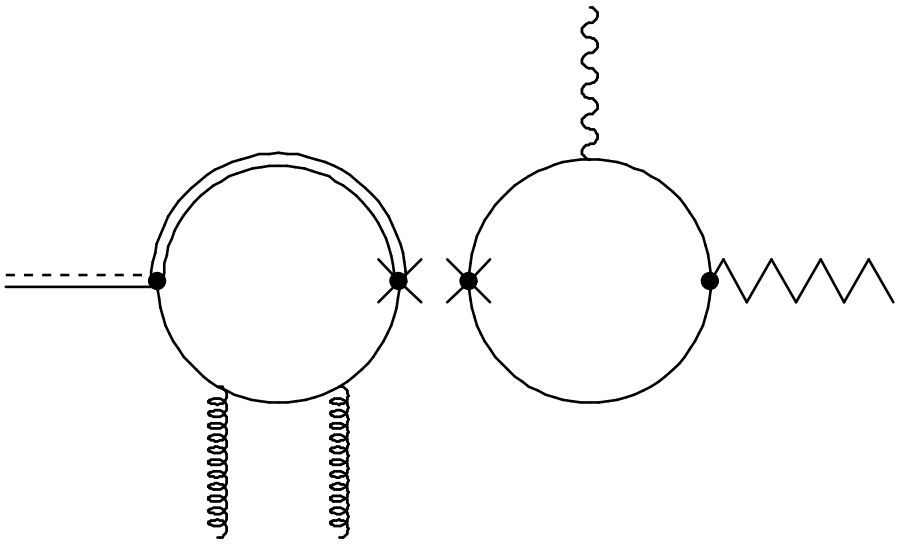

Figure 6.43 A combined diagram for the process $\langle V|\bar{\chi}\Lambda^n\gamma_\mu L\chi|\gamma\rangle\ \langle gg|\bar{q}\gamma^\mu LQ_{v_c}|D\rangle$.

we have the following expression for M for the creation type diagram

$$M^\mu = -\frac{ieN_C h_v}{8}\mathrm{Tr_F}\left[\Lambda^n V^v\right]\mathrm{Tr}\left[\left(\left(\frac{-i}{32\pi^2}\right)(2\gamma_5+1)-I_2\right)\gamma^\mu\tilde{Q}_\xi^v\sigma\cdot F\gamma_v\right] \tag{6.95}$$

Giving us almost the same result as we had in eq. 6.94

$$
\begin{aligned}
\mathrm{DggVf_u} &= -\frac{3\pi-4}{384\mathrm{m}^2}\frac{\mathrm{iN_C h_v G_H e Q_u}\sqrt{\mathrm{M_D}}}{64}\left\langle\frac{\alpha_s}{\pi}\mathrm{G}^2\right\rangle\times \\
&(-64*\mathrm{v}\cdot\mathrm{y}*\mathrm{z}\cdot\mathrm{V}*\mathrm{I}_2-6*\mathrm{v}\cdot\mathrm{y}*\mathrm{z}\cdot\mathrm{V}*\frac{\mathrm{i}}{\pi^2}+64*\mathrm{v}\cdot\mathrm{z}*\mathrm{y}\cdot\mathrm{V}*\mathrm{I}_2 \\
&+6*\mathrm{v}\cdot\mathrm{z}*\mathrm{y}\cdot\mathrm{V}*\frac{\mathrm{i}}{\pi^2}-64*\mathrm{e\_(v,y,z,V)}*\mathrm{I}_2-6*\mathrm{e\_(v,y,z,V)}*\frac{\mathrm{i}}{\pi^2}) \\
&=\frac{3\pi-4}{384\mathrm{m}^2}\frac{\mathrm{iN_C h_v G_H e Q_u}\sqrt{\mathrm{M_D}}}{32}\left\langle\frac{\alpha_s}{\pi}\mathrm{G}^2\right\rangle\times\left(32\mathrm{I}_2+\frac{3\mathrm{i}}{\pi^2}\right)\left(\mathrm{F_{\mu\nu}v^\mu V^\nu}+\mathrm{e\_(v,y,z,V)}\right)
\end{aligned}
\tag{6.96}
$$

Also here the parity breaking terms will cancel when the diagrams are summed over.

Our next diagram in line is shown in figure 6.44.

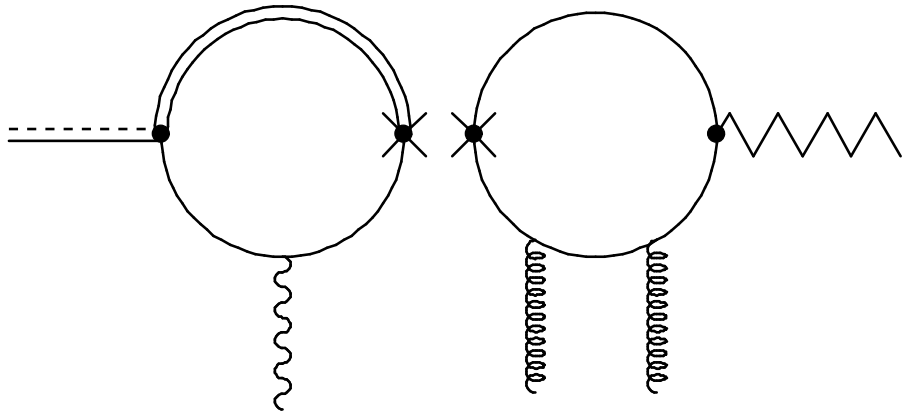

Figure 6.44 A combined diagram for the process $\langle \mathrm{V}|\bar{\chi}\Lambda^{\mathrm{n}}\gamma_\mu \mathrm{L}\chi|\mathrm{gg}\rangle\langle\gamma|\bar{\mathrm{q}}\gamma^\mu \mathrm{LQ}_{\mathrm{v_c}}|\mathrm{D}\rangle$.

Here the annihilation diagram has the following expression for M

$$
\mathrm{M}^\mu=\frac{\mathrm{N_c G_H e}}{4}\mathrm{Tr}\left[\xi^\dagger\gamma^\mu \mathrm{LH}\left(\mathrm{iI}_2\{\gamma\cdot\mathrm{v},\sigma\cdot\mathrm{F}\tilde{\mathrm{Q}}^{\mathrm{V}}_\xi\}+\frac{1}{8\pi}\sigma\cdot\mathrm{F}\tilde{\mathrm{Q}}^{\mathrm{V}}_\xi\right)\right] \tag{6.97}
$$

while M for the creation diagram is given by

$$
\mathrm{M}=-\frac{\mathrm{h_V}}{128\mathrm{m}^2}\left\langle\frac{\alpha}{\pi}\mathrm{G}^2\right\rangle\mathrm{Tr_F}\left[\Lambda^{\mathrm{n}}\mathrm{V}^{\mathrm{v}}\right]\mathrm{g}_{\mu\nu} \tag{6.98}
$$

Multiplying and using FORM as usual gives us the result

$$
\begin{aligned}
\mathrm{DfVg_dg_d} &= \frac{i\pi^2 m^2 N_C h_V G_H e}{4}\left\langle \frac{\alpha}{\pi}G^2\right\rangle\left(\frac{i}{128\pi^2 m^4}\right)\times \\
&\quad \mathrm{Tr}\left[\xi^{\dagger}\gamma^{\mu}\mathrm{LH}\left(iI_2\{\gamma\cdot v,\sigma\cdot F\tilde{Q}_{\xi}^{V}\}+\frac{1}{8\pi}\sigma\cdot F\tilde{Q}_{\xi}^{V}\right)\right]\mathrm{Tr_F}\left[\Lambda^n V^{\nu}\right]g_{\mu\nu} \\
&= \frac{i\pi^2 m^2 N_C h_V G_H e Q_d\sqrt{M_D}}{32}\left\langle \frac{\alpha}{\pi}G^2\right\rangle\left(\frac{i}{128\pi^2 m^4}\right)\times \\
&\quad \left(\frac{2}{\pi}*v\cdot y*z\cdot V-\frac{2}{\pi}*v\cdot z*y\cdot V+32i\cdot I_2*e\_(v,x,y,V)-\frac{2}{\pi}*e\_(v,x,y,V)\right) \\
&= -\frac{N_C h_V G_H e Q_d\sqrt{M_D}}{2048 m^2}\left\langle \frac{\alpha}{\pi}G^2\right\rangle\left(\frac{1}{\pi}F_{\mu\nu}v^{\mu}V^{\nu}+\left(16i\cdot I_2-\frac{1}{\pi}\right)e\_(v,x,y,V)\right)
\end{aligned}
\tag{6.99}
$$

For the diagram in figure 6.45,

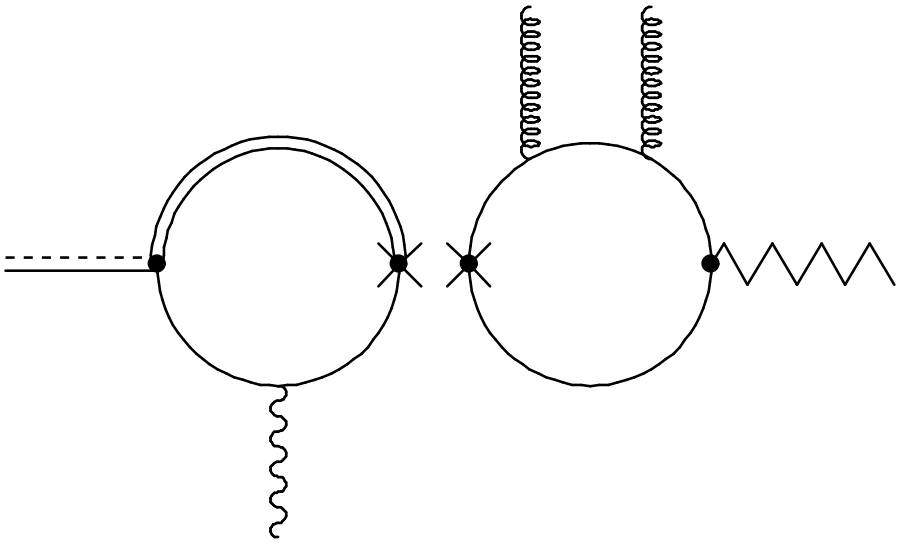

Figure 6.45 A combined diagram for the process $\langle V|\bar{\chi}\Lambda^n\gamma_{\mu}L\chi|gg\rangle\langle\gamma|\bar{q}\gamma^{\mu}LQ_{v_c}|D\rangle$.

where the gluon lines now are couples to the upper light quark, we get the same answer as in the diagram above, since the expression for the creation diagram with two gluon lines coupled to the lower quark is the same as the one with two gluons coupled to the upper quark.

$$
M = -\frac{h_V}{128m^2}\left\langle \frac{\alpha}{\pi}G^2\right\rangle \mathrm{Tr_F}\left[\Lambda^n V^{\nu}\right]g_{\mu\nu} \tag{6.100}
$$

So the Feynman diagram calculation for the diagram in figure 6.45 is simply

$$
\mathrm{DfVg_ug_u} = -\frac{N_C h_V G_H e Q_d\sqrt{M_D}}{2048 m^2}\left\langle \frac{\alpha}{\pi}G^2\right\rangle\left(\frac{1}{\pi}F_{\mu\nu}v^{\mu}V^{\nu}+\left(16i\cdot I_2-\frac{1}{\pi}\right)e\_(v,x,y,V)\right) \tag{6.101}
$$

Next we look at the diagram in figure 6.46.

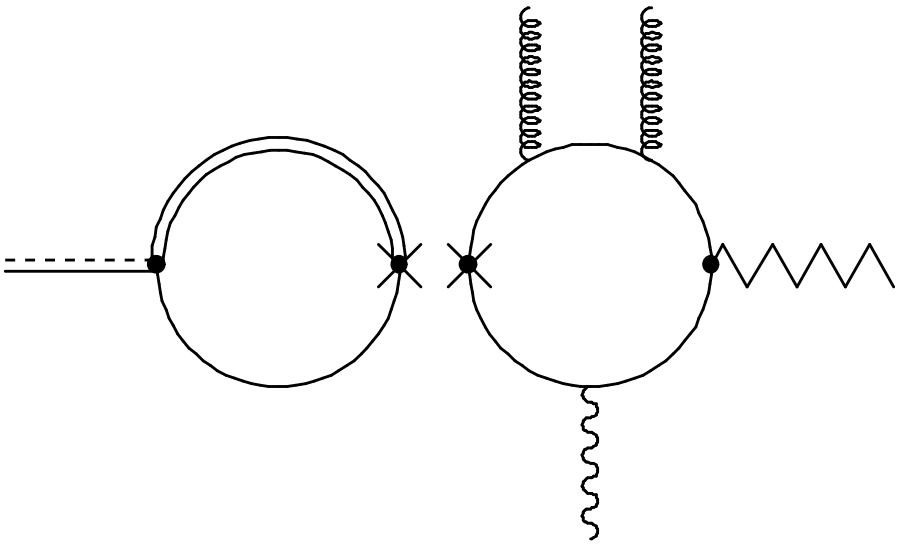

Figure 6.46 A combined diagram for the process $\langle V|\bar{\chi}\Lambda^n\gamma_\mu L\chi|gg\gamma\rangle\langle 0|\bar{q}\gamma^\mu LQ_{v_c}|D\rangle$.

This total diagram has no external lines coupled to the D-meson loop, but two gluon lines coupled to the upper quark and one photon coupled to the lower quark. The expressions for M are here

$$M^\mu = -iN_c G_H [mI_{3/2} - I_1] Tr[\xi^\dagger \gamma^\mu LH] \tag{6.102}$$

for the annihilation diagram, and

$$M^\lambda = -\frac{h_V e}{3840m^4}\left\langle \frac{\alpha}{\pi}G^2 \right\rangle Tr_F\left[\Lambda^n V^\delta\right] Tr\left[(2\gamma_5+1)\gamma^\lambda\gamma_\delta \tilde{Q}_\xi^V \sigma\cdot F\right] \tag{6.103}$$

for the creation diagram. Further calculation gives

$$\begin{aligned}
DVg_u g_u f_d &= \frac{iN_C h_V G_H e}{3840m^4}\left\langle \frac{\alpha}{\pi}G^2 \right\rangle \left[mI_{3/2} - I_1\right] Tr[\xi^\dagger\gamma^\mu LH] \times Tr_F\left[\Lambda^n V^\nu\right] Tr\left[(2\gamma_5+1)\gamma^\mu\gamma_\nu\tilde{Q}_\xi^V\sigma\cdot F\right] \\
&= -\frac{N_C h_V G_H e Q_u \sqrt{M_D}}{15360m^4}\left\langle \frac{\alpha}{\pi}G^2 \right\rangle \left[mI_{3/2} - I_1\right] \times \\
&\quad Tr\left[\gamma^\mu(1-\gamma_5)(1+\gamma\cdot v)\gamma_5\right] Tr_F\left[\Lambda^n V^\nu\right] Tr\left[(2\gamma_5+1)\gamma^\mu\gamma_\nu\sigma\cdot F\right] \\
&= \frac{iN_C h_V G_H e Q_u \sqrt{M_D}}{30720m^4}\left\langle \frac{\alpha}{\pi}G^2 \right\rangle \left[mI_{3/2} - I_1\right] \times \\
&\quad \left(-64*v\cdot y*z\cdot V + 64*v\cdot z*y\cdot V + 128*e_(v,y,z,V)\right) \\
&= \frac{iN_C h_V G_H e Q_u \sqrt{M_D}}{480m^4}\left\langle \frac{\alpha}{\pi}G^2 \right\rangle \left[mI_{3/2} - I_1\right]\left(-F_{\mu\nu}v^\mu V^\nu + 2e_(v,y,z,V)\right)
\end{aligned} \tag{6.104}$$

The next diagram, as shown in figure 6.47, is equal to the one we just calculated, except that the external lines now have switched places, i.e. we have one photon line coupled to the upper quark and two gluons coupled to the lower quark.

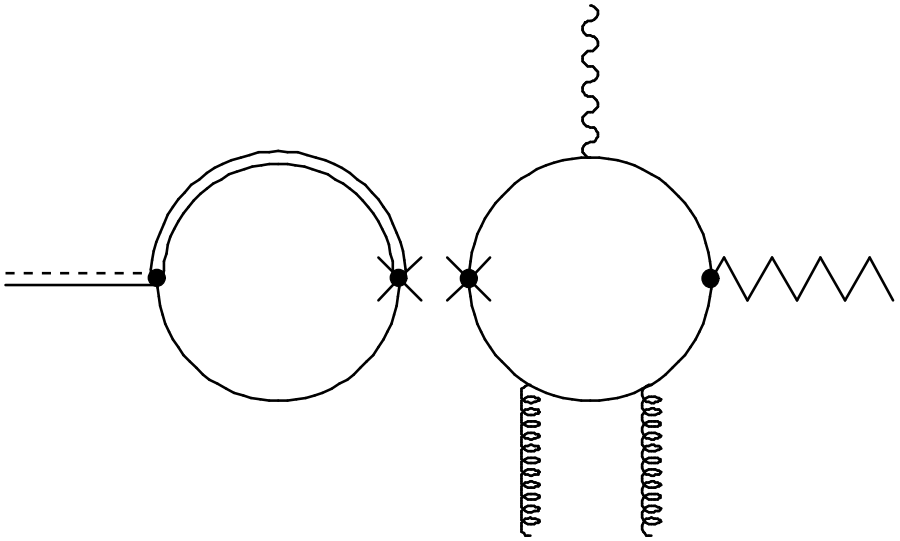

Figure 6.47 A combined diagram for the process $\langle V|\bar{\chi}\Lambda^n\gamma_\mu L\chi|gg\gamma\rangle\langle 0|\bar{q}\gamma^\mu LQ_{v_c}|D\rangle$.

The creation diagram has the following expression for M

$$M^\lambda = -\frac{h_V e}{3840m^4}\left\langle\frac{\alpha}{\pi}G^2\right\rangle \mathrm{Tr}_F\left[\Lambda^n V^\delta\right]\mathrm{Tr}\left[(2\gamma_5+1)\gamma^\lambda\tilde{Q}_\xi^v\sigma\cdot F\gamma_\delta\right] \tag{6.105}$$

So the total expression for the diagram in figure 6.47 becomes

$$\begin{aligned}
DVg_d g_d f_u &= \frac{iN_C h_V e G_H}{3840m^4}\left\langle\frac{\alpha}{\pi}G^2\right\rangle\left[mI_{3/2}-I_1\right]\times\mathrm{Tr}\left[\xi^\dagger\gamma^\mu LH\right]\mathrm{Tr}_F\left[\Lambda^n V^v\right]\mathrm{Tr}\left[(2\gamma_5+1)\gamma^\mu\tilde{Q}_\xi^v\sigma\cdot F\gamma_v\right]\\
&= -\frac{N_C h_V G_H e Q_u\sqrt{M_D}}{15360m^4}\left\langle\frac{\alpha}{\pi}G^2\right\rangle\left[mI_{3/2}-I_1\right]\times\\
&\mathrm{Tr}\left[\gamma^\mu(1-\gamma_5)(1+\gamma\cdot v)\gamma_5\right]\mathrm{Tr}_F\left[\Lambda^n V^v\right]\mathrm{Tr}\left[(2\gamma_5+1)\gamma^\mu\sigma\cdot F\gamma_v\right]\\
&= \frac{iN_C h_V G_H e Q_u\sqrt{M_D}}{30720m^4}\left\langle\frac{\alpha}{\pi}G^2\right\rangle\left[mI_{3/2}-I_1\right]\times\\
&(64*v\cdot y*z\cdot V-64*v\cdot z*y\cdot V+128*e_(v,y,z,V))\\
&= \frac{iN_C h_V G_H e Q_u\sqrt{M_D}}{480m^4}\left\langle\frac{\alpha}{\pi}G^2\right\rangle\left[mI_{3/2}-I_1\right]\left(F_{\mu v}v^\mu V^v+2e_(v,y,z,V)\right)
\end{aligned} \tag{6.106}$$

These were the six total diagrams which did not require integration by FORM. What we have left now are the last 24 diagrams where the trace product has to be integrated in FORM, and therefore requires larger and a bit more complicated programs.

We start by looking at the total diagram shown in figure 6.48.

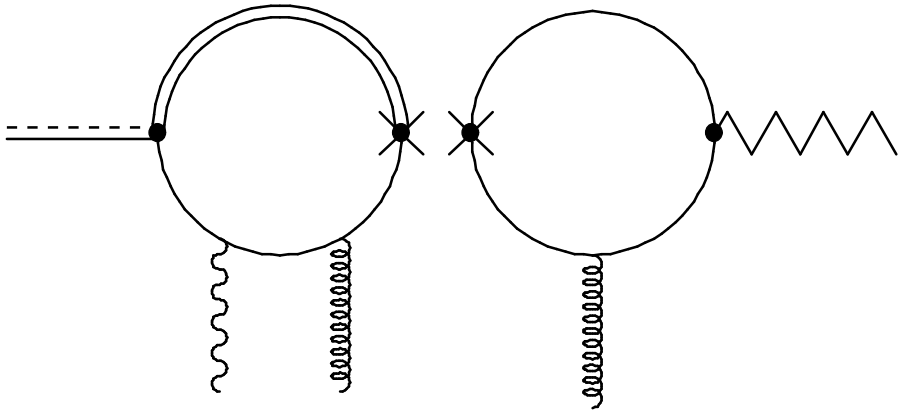

Figure 6.48 A combined diagram for the process $\langle \mathrm{Vg}|\bar{\chi}\Lambda^{n}\gamma_{\mu}t^{b}\mathrm{L}\chi|0\rangle\langle\gamma\mathrm{g}|\bar{q}\gamma^{\mu}\mathrm{L}t^{a}\mathrm{Q}_{v_c}|\mathrm{D}\rangle$.

This is the combination of the annihilation diagram in figure 6.8, having one photon and one gluon coupled to the light quark, and the creation diagram in figure 6.17, having one gluon coupled to the lower quark. The expression for M for each of these diagrams where calculated to be

$$\mathrm{M}^{\lambda} = \mathrm{i}\frac{\mathrm{G_H e g_s}}{8}\int\frac{\mathrm{d}^4\mathrm{p}}{(2\pi)^4}\mathrm{Tr}\left[\xi^{\dagger}\gamma^{\lambda}\mathrm{L}\frac{1}{\mathrm{v}\cdot\mathrm{p}}\mathrm{H}\times\mathrm{QF}_{\mu\nu}\mathrm{G}^{a}_{\alpha\beta}\mathrm{R}^{\mu\nu\alpha\beta}\right] \tag{6.107}$$

and

$$\mathrm{M}^{\mu} = \frac{\mathrm{i}h_{v}g_{s}}{16}\mathrm{Tr}_{\mathrm{F}}\left[\Lambda^{n}\mathrm{V}^{v}\right]\mathrm{Tr}\left[\left(\left(\frac{-\mathrm{i}}{32\pi^2}\right)(2\gamma_5+1)-\mathrm{I}_2\right)\gamma^{\mu}\sigma\gamma_{v}{}^{\alpha\beta}\mathrm{G}_{\alpha\beta}\right] \tag{6.108}$$

respectively. The total M for the diagram in figure 6.48 is as usual a multiplication of these two expressions, i.e. mainly a multiplication of two traces.

$$\begin{aligned}\mathrm{DfgVg_d} &= -\frac{h_{v}\mathrm{G_H e g_s}^{2}}{128}\int\frac{\mathrm{d}^4\mathrm{p}}{(2\pi)^4}\mathrm{Tr}\left[\xi^{\dagger}\gamma^{\lambda}\mathrm{L}\frac{1}{\mathrm{v}\cdot\mathrm{p}}\mathrm{H}\times\mathrm{QF}_{\mu\nu}\mathrm{G}^{a}_{\alpha\beta}\mathrm{R}^{\mu\nu\alpha\beta}\right]\times \\ &\quad \mathrm{Tr}_{\mathrm{F}}\left[\Lambda^{n}\mathrm{V}^{\delta}\right]\mathrm{Tr}\left[\left(\mathrm{m}^2\mathrm{I}_3(2\gamma_5+1)-\mathrm{I}_2\right)\gamma^{\lambda}\gamma_{\delta}\sigma^{\sigma\rho}\mathrm{G}_{\sigma\rho}\right] \\ &= -\frac{h_{v}\mathrm{G_H eQ_d}\sqrt{\mathrm{M_D}}\pi^2}{3072}\left\langle\frac{\alpha}{\pi}\mathrm{G}^2\right\rangle\int\frac{\mathrm{d}^4\mathrm{p}}{(2\pi)^4}\mathrm{Tr}\left[\gamma^{\lambda}(1-\gamma_5)\frac{1}{\mathrm{v}\cdot\mathrm{p}}(1+\gamma\cdot\mathrm{v})\gamma_5\mathrm{F}_{\mu\nu}\mathrm{R}^{\mu\nu\alpha\beta}\right]\times \\ &\quad \mathrm{Tr}_{\mathrm{F}}\left[\Lambda^{n}\mathrm{V}^{\delta}\right]\mathrm{Tr}\left[\left(\left(\frac{-\mathrm{i}}{32\pi^2}\right)(2\gamma_5+1)-\mathrm{I}_2\right)\gamma^{\lambda}\gamma_{\delta}\left[\gamma^{\sigma},\gamma^{\rho}\right]\right]\left(g_{\alpha\sigma}g_{\beta\rho}-g_{\alpha\rho}g_{\beta\sigma}\right)\end{aligned} \tag{6.109}$$

Using FORM to calculate the product of the traces, this expression becomes

$$
\begin{aligned}
\mathrm{DfgVg_d} = & -\frac{h_v G_H e Q_d \sqrt{M_D}\pi^2}{3072}\left\langle \frac{\alpha}{\pi} G^2 \right\rangle \times \\
& \left(-\frac{13}{12m^2\pi^4} * v\cdot y * z\cdot V + \frac{3}{4m^2\pi^3} * v\cdot y * z\cdot V + \frac{40i\cdot I_2}{3m^2\pi^2} * v.y * z.V - \frac{8i\cdot I_2}{m^2\pi} * v\cdot y * z\cdot V\right. \\
& + \frac{13}{12m^2\pi^4} * v\cdot z * y\cdot V * - \frac{3}{4m^2\pi^3} * v\cdot z * y\cdot V - \frac{40i\cdot I_2}{3m^2\pi^2} * v\cdot z * y\cdot V + \frac{8i\cdot I_2}{m^2\pi} * v.z * y.V \\
& \left. - \frac{2}{m^2\pi^4} * e\_(v,y,z,V) - \frac{11}{12m^2\pi^3} * e\_(v,y,z,V) + \frac{16i\cdot I_2}{m^2\pi^2} * e\_(v,y,z,V) + \frac{32i\cdot I_2}{3m^2\pi} * e\_(v,y,z,V)\right) \\
= & -\frac{h_v G_H e Q_d \sqrt{M_D}\pi}{3072m^2}\left\langle \frac{\alpha}{\pi} G^2 \right\rangle \times \left(\left(-\frac{13}{12\pi^3} + \frac{3}{4\pi^2} + \frac{40i\cdot I_2}{3\pi} - 8i\cdot I_2 \right) F_{\mu\nu} v^\mu V^\nu \right. \\
& \left. + \left(-\frac{2}{\pi^3} - \frac{11}{12\pi^2} + \frac{16i\cdot I_2}{\pi} + \frac{32i\cdot I_2}{3} \right) e\_(v,y,z,V)\right)
\end{aligned}
\qquad (6.110)
$$

The next diagram that we will look at, figure 6.49, will give almost the same result, as the only difference from this diagram and the one in figure 6.48 is the position of the gluon line in the V-loop.

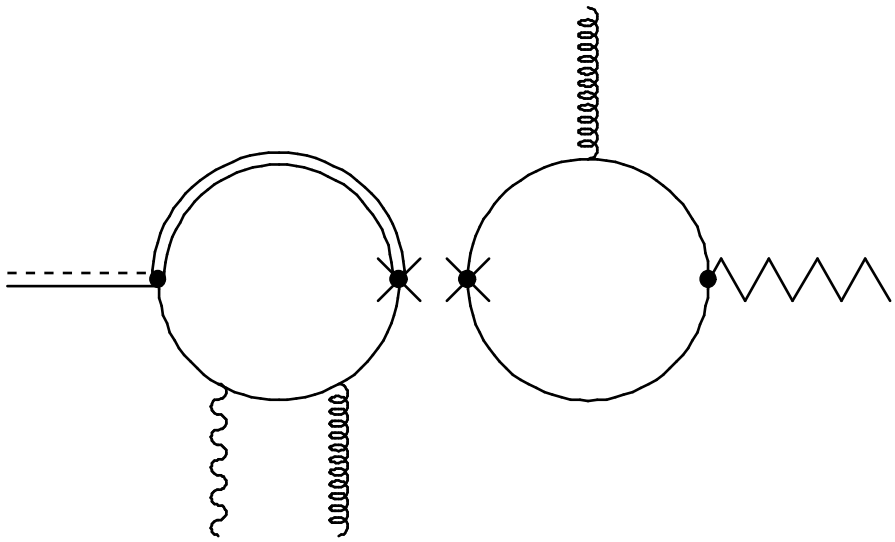

Figure 6.49 A combined diagram for the process $\left\langle \mathrm{Vg}\left|\bar{\chi}\Lambda^n\gamma_\mu t^b L\chi\right|0\right\rangle \left\langle \gamma g\left|\bar{q}\gamma^\mu L t^a Q_{v_c}\right|D\right\rangle$.

The creation diagram had the following expression for M

$$
M^\mu = \frac{ih_v g_s}{16}\mathrm{Tr}_F\left[\Lambda^n V^\nu\right]\mathrm{Tr}\left[\left(\left(\frac{-i}{32\pi^2}\right)(2\gamma_5+1) - I_2\right)\gamma^\mu \sigma^{\alpha\beta} G_{\alpha\beta}\gamma_\nu\right] \qquad (6.111)
$$

which gives the result

$$
\begin{aligned}
\mathrm{DfgVg_u} &= -\frac{h_v G_H e g_s^{\,2}}{128}\int\frac{d^4p}{(2\pi)^4}\mathrm{Tr}\left[\xi^{\dagger}\gamma^{\lambda}L\frac{1}{v\cdot p}H\times QF_{\mu\nu}G^{a}_{\alpha\beta}R^{\mu\nu\alpha\beta}\right]\times \\
&\quad \mathrm{Tr_F}\left[\Lambda^n V^{\delta}\right]\mathrm{Tr}\left[\left(\left(\frac{-i}{32\pi^2}\right)(2\gamma_5+1)-I_2\right)\gamma^{\lambda}\sigma^{\sigma\rho}G_{\sigma\rho}\gamma_{\delta}\right] \\
&= -\frac{h_v G_H e Q_d\sqrt{M_D}\pi^2}{3072}\left\langle\frac{\alpha}{\pi}G^2\right\rangle\int\frac{d^4p}{(2\pi)^4}\mathrm{Tr}\left[\gamma^{\lambda}(1-\gamma_5)\frac{1}{v\cdot p}(1+\gamma\cdot v)\gamma_5 F_{\mu\nu}R^{\mu\nu\alpha\beta}\right]\times \\
&\quad \mathrm{Tr_F}\left[\Lambda^n V^{\delta}\right]\mathrm{Tr}\left[\left(\left(\frac{-i}{32\pi^2}\right)(2\gamma_5+1)-I_2\right)\gamma^{\lambda}\left[\gamma^{\sigma},\gamma^{\rho}\right]\gamma_{\delta}\right]\left(g_{\alpha\sigma}g_{\beta\rho}-g_{\alpha\rho}g_{\beta\sigma}\right)
\end{aligned}
\tag{6.112}
$$

Using FORM we get

$$
\begin{aligned}
\mathrm{DfgVg_u} &= -\frac{h_v G_H e Q_d\sqrt{M_D}\pi^2}{3072}\left\langle\frac{\alpha}{\pi}G^2\right\rangle\times \\
&\quad (-\frac{1}{4m^2\pi^4}*v\cdot y*z\cdot V+\frac{1}{4m^2\pi^3}*v\cdot y*z\cdot V-\frac{40i\cdot I_2}{3m^2\pi^2}*v.y*z.V+\frac{8i\cdot I_2}{m^2\pi}*v\cdot y*z\cdot V \\
&\quad +\frac{1}{4m^2\pi^4}*v\cdot z*y\cdot V*-\frac{1}{4m^2\pi^3}*v\cdot z*y\cdot V+\frac{40i\cdot I_2}{3m^2\pi^2}*v\cdot z*y\cdot V-\frac{8i\cdot I_2}{m^2\pi}*v.z*y.V \\
&\quad -\frac{1}{m^2\pi^4}*e\_(v,y,z,V)-\frac{1}{4m^2\pi^3}*e\_(v,y,z,V)-\frac{16i\cdot I_2}{m^2\pi^2}*e\_(v,y,z,V)-\frac{32i\cdot I_2}{3m^2\pi}*e\_(v,y,z,V)) \\
&= -\frac{h_v G_H e Q_d\sqrt{M_D}\pi}{3072m^2}\left\langle\frac{\alpha}{\pi}G^2\right\rangle\times(\left(-\frac{1}{4\pi^3}+\frac{1}{4\pi^2}-\frac{40i\cdot I_2}{3\pi}+8i\cdot I_2\right)F_{\mu\nu}v^{\mu}V^{\nu} \\
&\quad -\left(\frac{1}{\pi^3}+\frac{1}{4\pi^2}+\frac{16i\cdot I_2}{\pi}+\frac{32i\cdot I_2}{3}\right)e\_(v,y,z,V))
\end{aligned}
\tag{6.113}
$$

The diagram in figure 6.50 is also of the same type as the two total diagrams above, only that here the photon and gluon lines in the annihilation diagram have switched places.

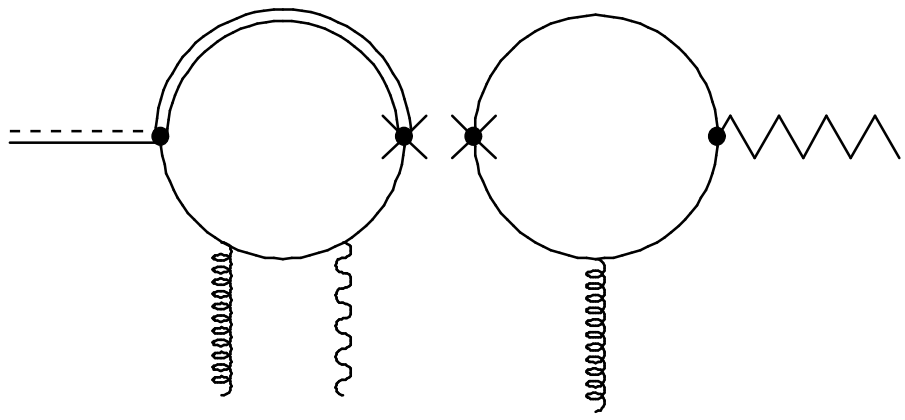

Figure 6.50 A combined diagram for the process $\left\langle \mathrm{Vg}\left|\bar{\chi}\Lambda^n\gamma_{\mu}t^bL\chi\right|0\right\rangle\left\langle g\gamma\left|\bar{q}\gamma^{\mu}Lt^aQ_{v_c}\right|D\right\rangle$.

Here the annihilation diagram has been calculated to be

$$M^{\lambda} = i\frac{G_H e g_s}{8}\int\frac{d^4p}{(2\pi)^4}Tr\left[\xi^{\dagger}\gamma^{\lambda}L\frac{1}{v\cdot p}H\times G^a_{\mu\nu}QF_{\alpha\beta}R^{\mu\nu\alpha\beta}\right] \tag{6.114}$$

while we have already seen the expression for M for the creation diagram (eq. 6.108). A multiplication and calculation by FORM gives

$$\begin{aligned}
DgfVg_d = &-\frac{h_v G_H e g_s^{\,2}}{128}\int\frac{d^4p}{(2\pi)^4}Tr\left[\xi^{\dagger}\gamma^{\lambda}L\frac{1}{v\cdot p}H\times QF_{\alpha\beta}G^a_{\mu\nu}R^{\mu\nu\alpha\beta}\right]\times \\
&Tr_F\left[\Lambda^n V^{\delta}\right]Tr\left[\left(\left(\frac{-i}{32\pi^2}\right)(2\gamma_5+1)-I_2\right)\gamma^{\lambda}\gamma_{\delta}\sigma^{\sigma\rho}G_{\sigma\rho}\right] \\
&= -\frac{h_v G_H e Q_d\sqrt{M_D}\pi^2}{3072}\left\langle\frac{\alpha}{\pi}G^2\right\rangle\times \\
&(-\frac{1}{4m^2\pi^4}*v\cdot y*z\cdot V-\frac{1}{6m^2\pi^3}*v\cdot y*z\cdot V+\frac{88i\cdot I_2}{3m^2\pi^2}*v.y*z.V+\frac{16i\cdot I_2}{3m^2\pi}*v\cdot y*z\cdot V \\
&+\frac{1}{4m^2\pi^4}*v\cdot z*y\cdot V*+\frac{1}{6m^2\pi^3}*v\cdot z*y\cdot V-\frac{88i\cdot I_2}{3m^2\pi^2}*v\cdot z*y\cdot V-\frac{16i\cdot I_2}{3m^2\pi}*v.z*y.V \\
&+\frac{1}{3m^2\pi^3}*e_(v,y,z,V)-\frac{16i\cdot I_2}{m^2\pi^2}*e_(v,y,z,V)-\frac{8i\cdot I_2}{3m^2\pi}*e_(v,y,z,V)) \\
&= -\frac{h_v G_H e Q_d\sqrt{M_D}\pi}{3072m^2}\left\langle\frac{\alpha}{\pi}G^2\right\rangle\times(\left(-\frac{1}{4\pi^3}-\frac{1}{6\pi^2}+\frac{88i\cdot I_2}{3\pi}+\frac{16i\cdot I_2}{3}\right)F_{\mu\nu}v^{\mu}V^{\nu} \\
&+\left(\frac{1}{3\pi^2}-\frac{16i\cdot I_2}{\pi}-\frac{8i\cdot I_2}{3}\right)e_(v,y,z,V))
\end{aligned} \tag{6.115}$$

The calculations for the diagram in figure 6.51 follow almost immediately

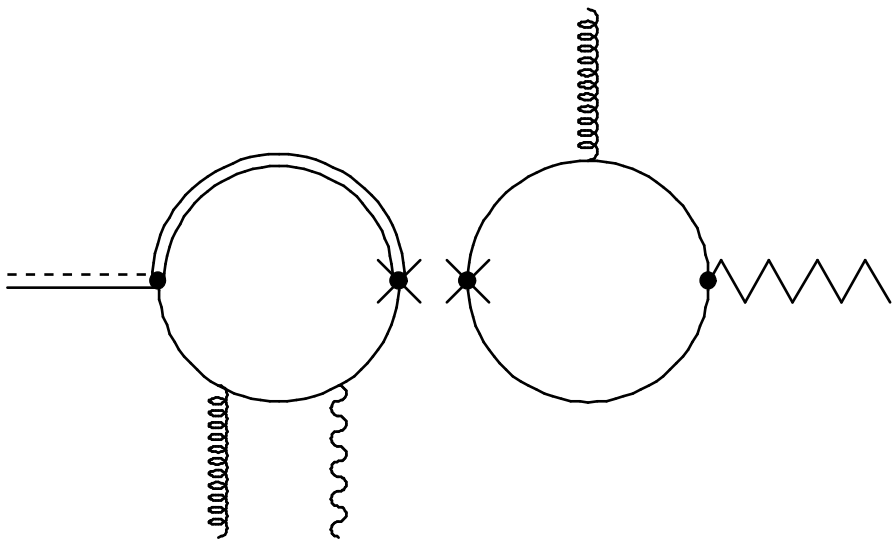

Figure 6.51 A combined diagram for the process $\langle Vg|\bar{\chi}\Lambda^n\gamma_{\mu}t^bL\chi|0\rangle\langle g\gamma|\bar{q}\gamma^{\mu}Lt^aQ_{v_c}|D\rangle$.

$$
\begin{aligned}
\mathrm{DgfVg_u} &= -\frac{h_v G_H e g_s^{\,2}}{128}\int\frac{d^4p}{(2\pi)^4}\mathrm{Tr}\left[\xi^\dagger\gamma^\lambda L\frac{1}{v\cdot p}H\times QF_{\alpha\beta}G^a_{\mu\nu}R^{\mu\nu\alpha\beta}\right]\times \\
&\quad \mathrm{Tr_F}\left[\Lambda^n V^\delta\right]\mathrm{Tr}\left[\left(m^2 I_3\left(2\gamma_5+1\right)-I_2\right)\gamma^\lambda\sigma^{\sigma\rho}G_{\sigma\rho}\gamma_\delta\right] \\
&= -\frac{h_v G_H e Q_d\sqrt{M_D}\pi^2}{3072}\left\langle\frac{\alpha}{\pi}G^2\right\rangle\times \qquad (6.116)\\
&\quad \left(\frac{19}{12m^2\pi^4}*v\cdot y*z\cdot V+\frac{1}{6m^2\pi^3}*v\cdot y*z\cdot V-\frac{88i\cdot I_2}{3m^2\pi^2}*v.y*z.V-\frac{16i\cdot I_2}{3m^2\pi}*v\cdot y*z\cdot V\right. \\
&\quad -\frac{19}{12m^2\pi^4}*v\cdot z*y\cdot V*-\frac{1}{6m^2\pi^3}*v\cdot z*y\cdot V+\frac{88i\cdot I_2}{3m^2\pi^2}*v\cdot z*y\cdot V+\frac{16i\cdot I_2}{3m^2\pi}*v.z*y.V \\
&\quad \left.-\frac{1}{m^2\pi^4}*e\_(v,y,z,V)+\frac{1}{6m^2\pi^3}*e\_(v,y,z,V)+\frac{16i\cdot I_2}{m^2\pi^2}*e\_(v,y,z,V)+\frac{8i\cdot I_2}{3m^2\pi}*e\_(v,y,z,V)\right) \\
&= -\frac{h_v G_H e Q_d\sqrt{M_D}\pi}{3072m^2}\left\langle\frac{\alpha}{\pi}G^2\right\rangle\times\left(\left(\frac{19}{12\pi^3}+\frac{1}{6\pi^2}-\frac{88i\cdot I_2}{3\pi}-\frac{16i\cdot I_2}{3}\right)F_{\mu\nu}v^\mu V^\nu\right. \\
&\quad \left.+\left(-\frac{1}{\pi^3}+\frac{1}{6\pi^2}+\frac{16i\cdot I_2}{\pi}+\frac{8i\cdot I_2}{3}\right)e\_(v,y,z,V)\right)
\end{aligned}
$$

The next of the diagrams with external gluon lines is the one in figure 6.52.

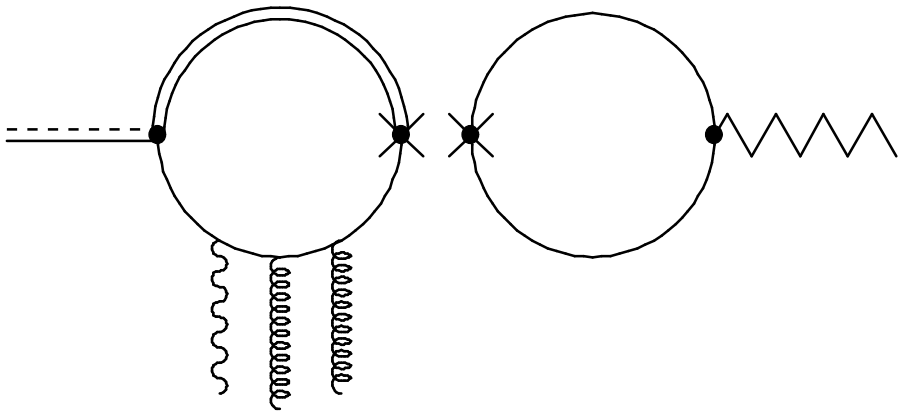

Figure 6.52 A combined diagram for the process $\left\langle V\left|\bar{\chi}\Lambda^n\gamma_\mu L\chi\right|0\right\rangle\left\langle\gamma gg\left|\bar{q}\gamma^\mu LQ_{v_c}\right|D\right\rangle$.

This type of diagram has all three external lines coupled to the annihilation diagram, and we get three diagrams of this type, where the only difference between them is the position of the photon line. Here the annihilation diagram has the following expression for M

$$
M^\lambda = \frac{N_C G_H e}{48}\left\langle\frac{\alpha_s}{\pi}G^2\right\rangle\int\frac{d^4p}{(2\pi)^4}\mathrm{Tr}\left[\xi^\dagger\gamma^\lambda L\frac{1}{v\cdot p}H\times QF_{\mu\nu}\left(g_{\alpha\rho}g_{\beta\sigma}-g_{\alpha\sigma}g_{\beta\rho}\right)T^{\mu\nu\alpha\beta\sigma\rho}\right] \qquad (6.117)
$$

The creation diagram we have already seen has this expression for M

$$
M^\mu = ih_V\mathrm{Tr_F}\left[\Lambda^n V^\nu\right]\left[m^2 I_2 - I_1\right]g_{\mu\nu} \qquad (6.118)
$$

Calculating the product of these two expressions we get

$$\begin{aligned}
\mathrm{DfggV} &= \frac{iN_C h_V G_H e}{48}\left\langle \frac{\alpha_s}{\pi}G^2 \right\rangle \left[m^2 I_2 - I_1 \right] \mathrm{Tr}_F\left[\Lambda^n V^\delta \right] g_{\lambda\delta} \times \\
&\int \frac{d^4p}{(2\pi)^4}\mathrm{Tr}\left[\xi^\dagger \gamma^\lambda L \frac{1}{v\cdot p} H \times Q F_{\mu\nu}\left(g_{\alpha\rho}g_{\beta\sigma} - g_{\alpha\sigma}g_{\beta\rho} \right) T^{\mu\nu\alpha\beta\sigma\rho} \right] \\
&= \frac{N_C h_V G_H e Q_d \sqrt{M_D}}{192}\left\langle \frac{\alpha_s}{\pi}G^2 \right\rangle \left[m^2 I_2 - I_1 \right] \times \\
&\left(-\frac{i}{4m^4\pi} * v\cdot y * z\cdot V + \frac{i}{4m^4\pi} * v\cdot z * y\cdot V + \frac{i}{6m^4\pi^2} * e_(v,y,z,V) + \frac{5i}{16m^4\pi} * e_(v,y,z,V) \right) \\
&= \frac{iN_C h_V G_H e Q_d \sqrt{M_D}}{192m^4}\left\langle \frac{\alpha_s}{\pi}G^2 \right\rangle \left[m^2 I_2 - I_1 \right] \left(-\frac{1}{4\pi} F_{\mu\nu} v^\mu V^\nu + \left(\frac{1}{6\pi^2} + \frac{5}{16\pi} \right) e_(v,y,z,V) \right)
\end{aligned} \tag{6.119}$$

In the next diagram the external photon line has moved in between the gluon lines, giving us the diagram in figure 6.53 below.

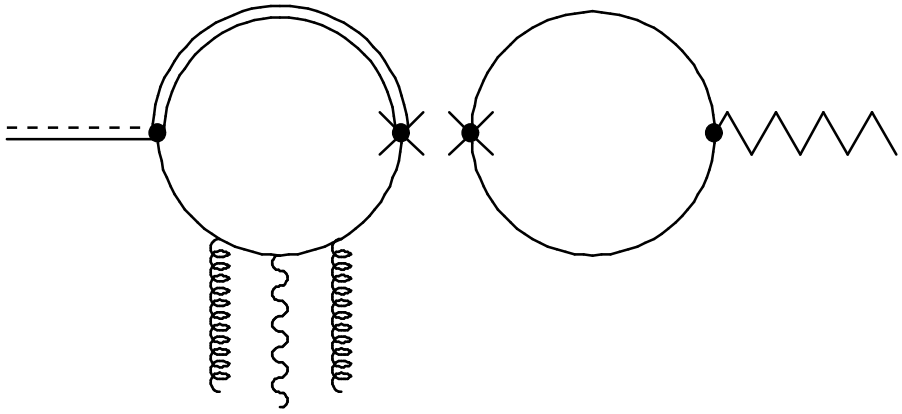

Figure 6.53 A combined diagram for the process $\left\langle V\left|\bar{\chi}\Lambda^n\gamma_\mu L\chi\right|0\right\rangle \left\langle g\gamma g\left|\bar{q}\gamma^\mu L Q_{v_c}\right|D\right\rangle$.

Here the annihilation diagram has this expression for M

$$M^\lambda = \frac{N_C G_H e}{48}\left\langle \frac{\alpha_s}{\pi}G^2 \right\rangle \int \frac{d^4p}{(2\pi)^4}\mathrm{Tr}\left[\xi^\dagger \gamma^\lambda L \frac{1}{v\cdot p} H \times Q F_{\alpha\beta}\left(g_{\mu\rho}g_{\nu\sigma} - g_{\mu\sigma}g_{\nu\rho} \right) T^{\mu\nu\alpha\beta\sigma\rho} \right] \tag{6.120}$$

So the total diagram calculation becomes

$$
\begin{aligned}
\mathrm{DgfgV} &= \frac{iN_C h_V G_H e}{48}\left\langle \frac{\alpha_s}{\pi} G^2 \right\rangle \left[m^2 I_2 - I_1 \right] \mathrm{Tr}_F\left[\Lambda^n V^\delta \right] g_{\lambda\delta} \times \\
&\int \frac{d^4 p}{(2\pi)^4} \mathrm{Tr}\left[\xi^\dagger \gamma^\lambda L \frac{1}{v\cdot p} H \times Q F_{\alpha\beta}\left(g_{\mu\rho} g_{\nu\sigma} - g_{\mu\sigma} g_{\nu\rho} \right) T^{\mu\nu\alpha\beta\sigma\rho} \right] \\
&= \frac{N_C h_V G_H e Q_d \sqrt{M_D}}{192}\left\langle \frac{\alpha_s}{\pi} G^2 \right\rangle \left[m^2 I_2 - I_1 \right] \times \\
&\left(-\frac{i}{8m^4\pi} * v\cdot y * z\cdot V + \frac{i}{8m^4\pi} * v\cdot z * y\cdot V + \frac{i}{8m^4\pi} * e\_(v,y,z,V) \right) \\
&= \frac{iN_C h_V G_H e Q_d \sqrt{M_D}}{192 m^4}\left\langle \frac{\alpha_s}{\pi} G^2 \right\rangle \left[m^2 I_2 - I_1 \right] \times \frac{1}{8\pi}\left(-F_{\mu\nu} v^\mu V^\nu + e\_(v,y,z,V) \right)
\end{aligned}
\tag{6.121}
$$

The last of this type of diagram is show in figure 6.54.

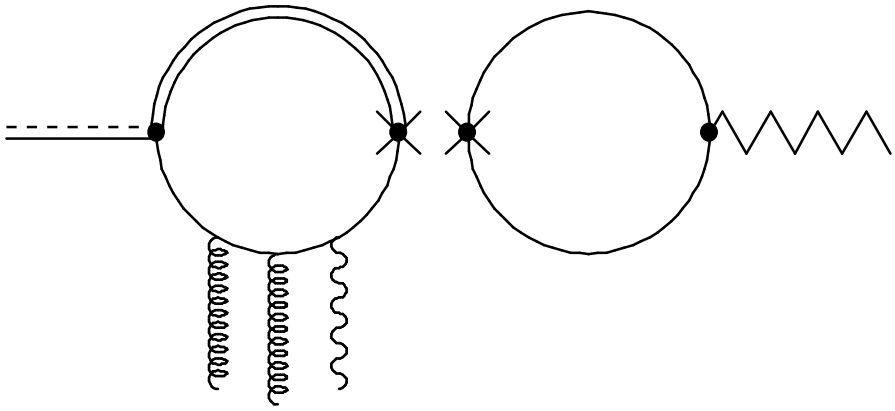

Figure 6.54 A combined diagram for the process $\left\langle V \left| \bar{\chi} \Lambda^n \gamma_\mu L \chi \right| 0 \right\rangle \left\langle gg\gamma \left| \bar{q} \gamma^\mu L Q_{v_c} \right| D \right\rangle$.

The annihilation diagram is here given by

$$
M^\lambda = \frac{N_C G_H e}{48}\left\langle \frac{\alpha_s}{\pi} G^2 \right\rangle \int \frac{d^4 p}{(2\pi)^4} \mathrm{Tr}\left[\xi^\dagger \gamma^\lambda L \frac{1}{v\cdot p} H \times Q F_{\rho\sigma}\left(g_{\mu\alpha} g_{\nu\beta} - g_{\mu\beta} g_{\nu\alpha} \right) T^{\mu\nu\alpha\beta\sigma\rho} \right] \tag{6.122}
$$

which gives a total expression of

$$
\begin{aligned}
\mathrm{DggfV} &= \frac{iN_C h_V G_H e}{48}\left\langle \frac{\alpha_s}{\pi}G^2 \right\rangle \left[m^2 I_2 - I_1 \right] \mathrm{Tr}_F\left[\Lambda^n V^\delta \right] g_{\lambda\delta} \times \\
&\int \frac{d^4p}{(2\pi)^4} \mathrm{Tr}\left[\xi^\dagger \gamma^\lambda L \frac{1}{v\cdot p} H \times Q F_{\rho\sigma}\left(g_{\mu\alpha}g_{\nu\beta} - g_{\mu\beta}g_{\nu\alpha} \right) T^{\mu\nu\alpha\beta\sigma\rho} \right] \\
&= \frac{N_C h_V G_H e Q_d \sqrt{M_D}}{192}\left\langle \frac{\alpha_s}{\pi}G^2 \right\rangle \left[m^2 I_2 - I_1 \right] \times \\
&\left(-\frac{3i}{8m^4\pi} * v\cdot y * z\cdot V + \frac{3i}{8m^4\pi} * v\cdot z * y\cdot V + \frac{i}{2m^4\pi^2} * e\_(v,y,z,V) - \frac{3i}{16m^4\pi} * e\_(v,y,z,V) \right) \\
&= \frac{iN_C h_V G_H e Q_d \sqrt{M_D}}{192m^4}\left\langle \frac{\alpha_s}{\pi}G^2 \right\rangle \left[m^2 I_2 - I_1 \right] \left(-\frac{3}{8\pi} F_{\mu\nu} v^\mu V^\nu + \left(\frac{1}{2\pi^2} - \frac{3}{16\pi} \right) e\_(v,y,z,V) \right)
\end{aligned}
\tag{6.123}
$$

The six diagrams that now follow, are similar to the three just calculated in the respect that all three external lines are coupled to only one quark line. The diagrams themselves and the result of them will not differ much from each other.

Our first of these will be the one given in figure 6.55.

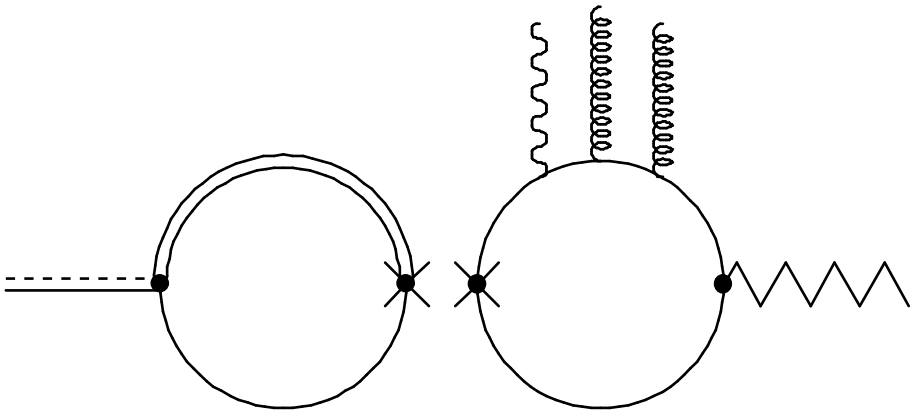

Figure 6.55 A combined diagram for the process $\left\langle V \left| \bar{\chi}\Lambda^n \gamma_\mu L \chi \right| \gamma g g \right\rangle \left\langle 0 \left| \bar{q}\gamma^\mu L Q_{v_c} \right| D \right\rangle$.

Here the annihilation diagram has the following expression for M

$$
M^\mu = -iN_c G_H [m I_{3/2} - I_1] \mathrm{Tr}[\xi^\dagger \gamma^\mu L H] \tag{6.124}
$$

while the creation diagram is given by

$$
M^\lambda = \frac{\pi^2 h_V e}{96}\left\langle \frac{\alpha}{\pi}G^2 \right\rangle \mathrm{Tr}_F\left[\Lambda^n V^\delta \right] \int \frac{d^D p}{(2\pi)^D} \mathrm{Tr}\left[(1+\gamma_5)\gamma^\lambda Q F_{\mu\nu}\left(g_{\alpha\rho}g_{\beta\sigma} - g_{\alpha\sigma}g_{\beta\rho} \right) T^{\mu\nu\alpha\beta\sigma\rho} \gamma_\delta S(p) \right] \tag{6.125}
$$

This gives us the following result when these two expressions are multiplied

$$DVf_u g_u g_u = -\frac{\pi^2 N_C h_V G_H e Q_u \sqrt{M_D}}{384}\left[mI_{3/2} - I_1\right]\left\langle\frac{\alpha}{\pi}G^2\right\rangle \mathrm{Tr}\left[\gamma^\mu(1-\gamma_5)(1+\gamma\cdot v)\gamma_5\right]\times$$
$$\mathrm{Tr}_F\left[\Lambda^n V^\delta\right]\int\frac{d^D p}{(2\pi)^D}\mathrm{Tr}\left[(1+\gamma_5)\gamma^\lambda F_{\mu\nu}T^{\mu\nu\alpha\beta\sigma\rho}\gamma_\delta S(p)\right]\left(g_{\alpha\rho}g_{\beta\sigma} - g_{\alpha\sigma}g_{\beta\rho}\right) \quad (6.126)$$

Using FORM we get

$$DVf_u g_u g_u = -\frac{\pi^2 N_C h_V G_H e Q_u \sqrt{M_D}}{384}\left[mI_{3/2} - I_1\right]\left\langle\frac{\alpha}{\pi}G^2\right\rangle\times$$
$$\left(\frac{13i}{5m^4\pi^2} * v\cdot y * z\cdot V - \frac{13i}{5m^4\pi^2} * v\cdot z * y\cdot V - \frac{13i}{5m^4\pi^2} * e\_(v,y,z,V)\right) \quad (6.127)$$
$$= -\frac{N_C h_V G_H e Q_u \sqrt{M_D}}{384m^4}\left[mI_{3/2} - I_1\right]\left\langle\frac{\alpha}{\pi}G^2\right\rangle\times\frac{13i}{5}\left(F_{\mu\nu}v^\mu V^\nu - e\_(v,y,z,V)\right)$$

For the diagram in figure 6.56

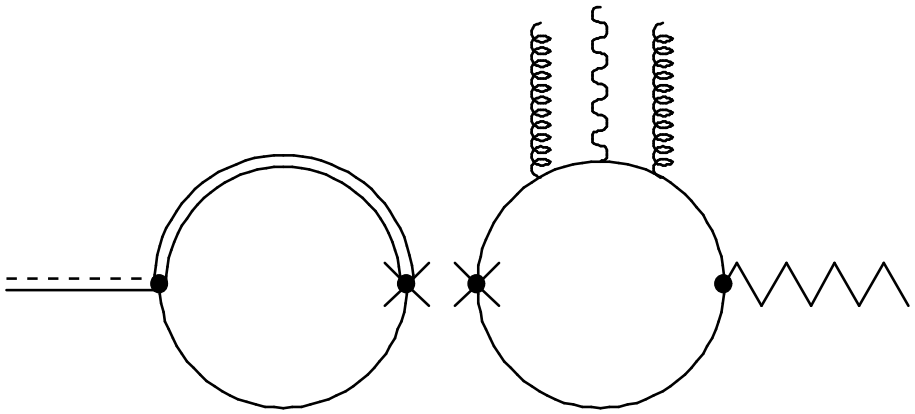

Figure 6.56 A combined diagram for the process $\langle V|\bar{\chi}\Lambda^n\gamma_\mu L\chi|g\gamma g\rangle\langle 0|\bar{q}\gamma^\mu LQ_{v_c}|D\rangle$.

we have a creation diagram with the expression

$$M^\lambda = \frac{\pi^2 h_V e}{96}\left\langle\frac{\alpha}{\pi}G^2\right\rangle \mathrm{Tr}_F\left[\Lambda^n V^\delta\right]\int\frac{d^D p}{(2\pi)^D}\mathrm{Tr}\left[(1+\gamma_5)\gamma^\lambda Q F_{\alpha\beta}\left(g_{\mu\rho}g_{\nu\sigma} - g_{\mu\sigma}g_{\nu\rho}\right)T^{\mu\nu\alpha\beta\sigma\rho}\gamma_\delta S(p)\right] \quad (6.128)$$

This gives the result

$$
\begin{aligned}
DVg_u f_u g_u &= -\frac{\pi^2 N_C h_V G_H e Q_u \sqrt{M_D}}{384}\left[mI_{3/2} - I_1\right]\left\langle \frac{\alpha}{\pi} G^2 \right\rangle \mathrm{Tr}\left[\gamma^\mu (1-\gamma_5)(1+\gamma\cdot v)\gamma_5\right]\times \\
&\quad \mathrm{Tr}_F\left[\Lambda^n V^\delta\right]\int \frac{d^D p}{(2\pi)^D}\mathrm{Tr}\left[(1+\gamma_5)\gamma^\lambda F_{\alpha\beta} T^{\mu\nu\alpha\beta\sigma\rho}\gamma_\delta S(p)\right]\left(g_{\mu\rho}g_{\nu\sigma} - g_{\mu\sigma}g_{\nu\rho}\right) \\
&= -\frac{\pi^2 N_C h_V G_H e Q_u \sqrt{M_D}}{384}\left[mI_{3/2} - I_1\right]\left\langle \frac{\alpha}{\pi} G^2 \right\rangle \times \\
&\quad \left(-\frac{11i}{15m^4\pi^2} * v\cdot y * z\cdot V + \frac{11i}{15m^4\pi^2} * v\cdot z * y\cdot V + \frac{11i}{15m^4\pi^2} * e\_(v,y,z,V)\right) \\
&= -\frac{N_C h_V G_H e Q_u \sqrt{M_D}}{384m^4}\left[mI_{3/2} - I_1\right]\left\langle \frac{\alpha}{\pi} G^2 \right\rangle \times \frac{11i}{15}\left(-F_{\mu\nu} v^\mu V^\nu + e\_(v,y,z,V)\right)
\end{aligned}
\tag{6.129}
$$

In the next diagram, as shown in figure 6.57,

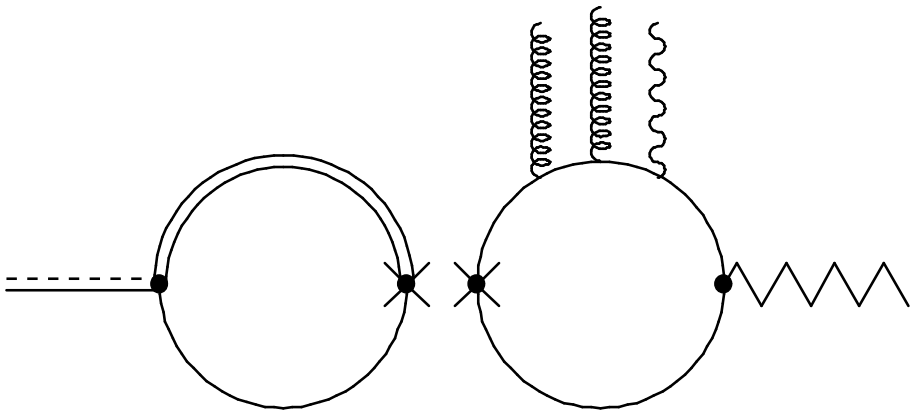

Figure 6.57 A combined diagram for the process $\left\langle V\left|\bar{\chi}\Lambda^n\gamma_\mu L\chi\right|gg\gamma\right\rangle\left\langle 0\left|\bar{q}\gamma^\mu LQ_{v_c}\right|D\right\rangle$.

we have

$$
M^\lambda = \frac{\pi^2 h_V e}{96}\left\langle \frac{\alpha}{\pi} G^2 \right\rangle \mathrm{Tr}_F\left[\Lambda^n V^\delta\right]\int \frac{d^D p}{(2\pi)^D}\mathrm{Tr}\left[(1+\gamma_5)\gamma^\lambda Q F_{\rho\sigma}\left(g_{\mu\alpha}g_{\nu\beta} - g_{\mu\beta}g_{\nu\alpha}\right)T^{\mu\nu\alpha\beta\sigma\rho}\gamma_\delta S(p)\right] \tag{6.130}
$$

for the creation diagram. The result of the multiplication here will be

$$
\begin{aligned}
DVg_u g_u f_u &= -\frac{\pi^2 N_C h_V G_H e Q_u \sqrt{M_D}}{384}\left[m I_{3/2} - I_1 \right]\left\langle \frac{\alpha}{\pi} G^2 \right\rangle \mathrm{Tr}\left[\gamma^\mu (1-\gamma_5)(1+\gamma\cdot v)\gamma_5 \right]\times \\
&\quad \mathrm{Tr}_F\left[\Lambda^n V^\delta \right]\int \frac{d^D p}{(2\pi)^D}\mathrm{Tr}\left[(1+\gamma_5)\gamma^\lambda F_{\rho\sigma} T^{\mu\nu\alpha\beta\sigma\rho}\gamma_\delta S(p) \right]\left(g_{\mu\alpha} g_{\nu\beta} - g_{\mu\beta} g_{\nu\alpha} \right) \\
&= -\frac{\pi^2 N_C h_V G_H e Q_u \sqrt{M_D}}{384}\left[m I_{3/2} - I_1 \right]\left\langle \frac{\alpha}{\pi} G^2 \right\rangle \times \\
&\quad \left(\frac{2i}{m^4\pi^2} * v\cdot y * z\cdot V - \frac{2i}{m^4\pi^2} * v\cdot z * y\cdot V - \frac{2i}{m^4\pi^2} * e\_(v,y,z,V) \right) \\
&= -\frac{N_C h_V G_H e Q_u \sqrt{M_D}}{384 m^4}\left[m I_{3/2} - I_1 \right]\left\langle \frac{\alpha}{\pi} G^2 \right\rangle \times 2i\left(F_{\mu\nu} v^\mu V^\nu - e\_(v,y,z,V) \right)
\end{aligned}
\tag{6.131}
$$

We now move on to the diagram where the external lines are coupled to the lower quark line of the creation loop diagram. The first one of these is given in figure 6.58 below

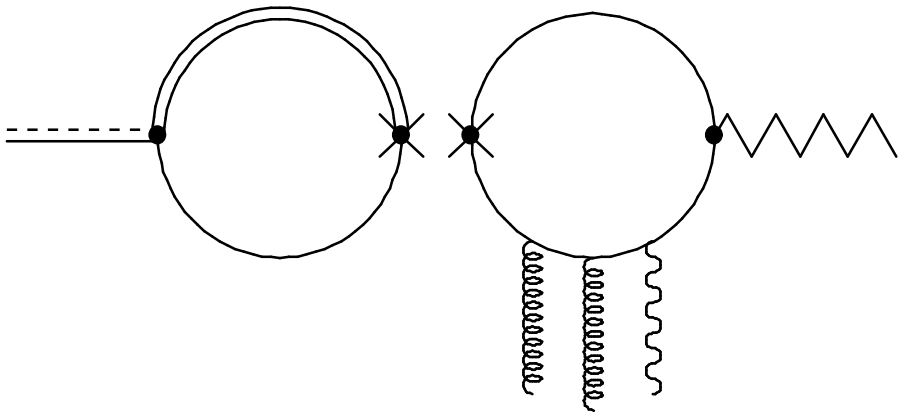

Figure 6.58 A combined diagram for the process $\left\langle V\left|\bar{\chi}\Lambda^n\gamma_\mu L\chi\right|\gamma gg\right\rangle\left\langle 0\left|\bar{q}\gamma^\mu LQ_{v_c}\right|D\right\rangle$.

The creation diagram has here the following expression for M

$$
M^\lambda = \frac{\pi^2 h_V e}{96}\left\langle \frac{\alpha}{\pi} G^2 \right\rangle \mathrm{Tr}_F\left[\Lambda^n V^\delta \right]\int \frac{d^D p}{(2\pi)^D}\mathrm{Tr}\left[(1+\gamma_5)\gamma^\lambda S(p)\gamma_\delta Q F_{\mu\nu}\left(g_{\alpha\rho} g_{\beta\sigma} - g_{\alpha\sigma} g_{\beta\rho} \right) T^{\mu\nu\alpha\beta\sigma\rho} \right] \tag{6.132}
$$

This gives the result

$$
\begin{aligned}
\mathrm{DVf_d g_d g_d} &= -\frac{\pi^2 N_C h_V G_H e Q_u \sqrt{M_D}}{384}\left[\mathrm{mI_{3/2}} - \mathrm{I_1}\right]\left\langle\frac{\alpha}{\pi}G^2\right\rangle \mathrm{Tr}\left[\gamma^\mu(1-\gamma_5)(1+\gamma\cdot v)\gamma_5\right]\times \\
&\quad \mathrm{Tr_F}\left[\Lambda^n V^\delta\right]\int\frac{d^D p}{(2\pi)^D}\mathrm{Tr}\left[(1+\gamma_5)\gamma^\lambda S(p)\gamma_\delta F_{\mu\nu}T^{\mu\nu\alpha\beta\sigma\rho}\right]\left(g_{\alpha\rho}g_{\beta\sigma}-g_{\alpha\sigma}g_{\beta\rho}\right) \\
&= -\frac{\pi^2 N_C h_V G_H e Q_u \sqrt{M_D}}{384}\left[\mathrm{mI_{3/2}} - \mathrm{I_1}\right]\left\langle\frac{\alpha}{\pi}G^2\right\rangle\times \\
&\quad \left(\frac{13i}{5m^4\pi^2} * v\cdot y * z\cdot V - \frac{13i}{5m^4\pi^2} * v\cdot z * y\cdot V - \frac{13i}{5m^4\pi^2} * e\_(v,y,z,V)\right) \\
&= -\frac{N_C h_V G_H e Q_u \sqrt{M_D}}{384m^4}\left[\mathrm{mI_{3/2}} - \mathrm{I_1}\right]\left\langle\frac{\alpha}{\pi}G^2\right\rangle\times\frac{13i}{5}\left(F_{\mu\nu}v^\mu V^\nu - e\_(v,y,z,V)\right)
\end{aligned}
\tag{6.133}
$$

For the diagram in figure 6.59

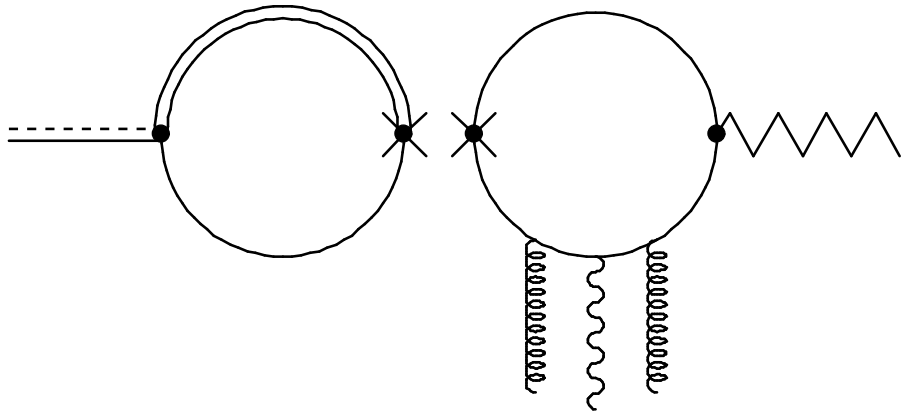

Figure 6.59 A combined diagram for the process $\left\langle V\left|\bar{\chi}\Lambda^n\gamma_\mu L\chi\right|g\gamma g\right\rangle\left\langle 0\left|\bar{q}\gamma^\mu LQ_{v_c}\right|D\right\rangle$.

the creation diagram has the following expression

$$
M^\lambda = \frac{\pi^2 h_V e}{96}\left\langle\frac{\alpha}{\pi}G^2\right\rangle \mathrm{Tr_F}\left[\Lambda^n V^\delta\right]\int\frac{d^D p}{(2\pi)^D}\mathrm{Tr}\left[(1+\gamma_5)\gamma^\lambda S(p)\gamma_\delta Q F_{\alpha\beta}\left(g_{\mu\rho}g_{\nu\sigma}-g_{\mu\sigma}g_{\nu\rho}\right)T^{\mu\nu\alpha\beta\sigma\rho}\right] \tag{6.134}
$$

which gives us the result

$$
\begin{aligned}
DVg_d f_d g_d = &-\frac{\pi^2 N_C h_V G_H e Q_u \sqrt{M_D}}{384}\left[mI_{3/2} - I_1\right]\left\langle\frac{\alpha}{\pi}G^2\right\rangle \mathrm{Tr}\left[\gamma^\mu(1-\gamma_5)(1+\gamma\cdot v)\gamma_5\right]\times \\
&\mathrm{Tr}_F\left[\Lambda^n V^\delta\right]\int\frac{d^D p}{(2\pi)^D}\mathrm{Tr}\left[(1+\gamma_5)\gamma^\lambda S(p)\gamma_\delta F_{\alpha\beta}T^{\mu\nu\alpha\beta\sigma\rho}\right]\left(g_{\mu\rho}g_{\nu\sigma}-g_{\mu\sigma}g_{\nu\rho}\right) \\
= &-\frac{\pi^2 N_C h_V G_H e Q_u \sqrt{M_D}}{384}\left[mI_{3/2} - I_1\right]\left\langle\frac{\alpha}{\pi}G^2\right\rangle\times \\
&\left(-\frac{1\,\mathrm{li}}{15m^4\pi^2}*v\cdot y*z\cdot V+\frac{1\,\mathrm{li}}{15m^4\pi^2}*v\cdot z*y\cdot V+\frac{1\,\mathrm{li}}{15m^4\pi^2}*e\_(v,y,z,V)\right) \\
= &-\frac{N_C h_V G_H e Q_u \sqrt{M_D}}{384m^4}\left[mI_{3/2} - I_1\right]\left\langle\frac{\alpha}{\pi}G^2\right\rangle\times\frac{1\,\mathrm{li}}{15}\left(-F_{\mu\nu}v^\mu V^\nu + e\_(v,y,z,V)\right)
\end{aligned}
\tag{6.135}
$$

Finally, the last one of this type of diagram is shown in figure 6.60.

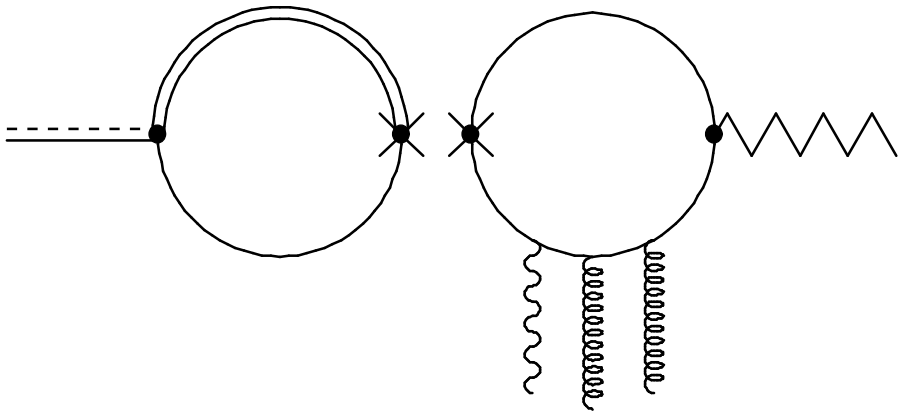

Figure 6.60 A combined diagram for the process $\left\langle V\left|\bar{\chi}\Lambda^n\gamma_\mu L\chi\right|gg\gamma\right\rangle\left\langle 0\left|\bar{q}\gamma^\mu LQ_{v_c}\right|D\right\rangle$.

It has the following expression for the creation diagram

$$
M^\lambda = \frac{\pi^2 h_V e}{96}\left\langle\frac{\alpha}{\pi}G^2\right\rangle \mathrm{Tr}_F\left[\Lambda^n V^\delta\right]\int\frac{d^D p}{(2\pi)^D}\mathrm{Tr}\left[(1+\gamma_5)\gamma^\lambda S(p)\gamma_\delta Q F_{\rho\sigma}\left(g_{\mu\alpha}g_{\nu\beta}-g_{\mu\beta}g_{\nu\alpha}\right)T^{\mu\nu\alpha\beta\sigma\rho}\right] \tag{6.136}
$$

and therefore gets the following result for the total diagram

$$
\begin{aligned}
DVg_d g_d f_d &= -\frac{\pi^2 N_C h_V G_H e Q_u \sqrt{M_D}}{384}\left[mI_{3/2} - I_1\right]\left\langle\frac{\alpha}{\pi}G^2\right\rangle \mathrm{Tr}\left[\gamma^\mu(1-\gamma_5)(1+\gamma\cdot v)\gamma_5\right]\times \\
&\quad \mathrm{Tr}_F\left[\Lambda^n V^\delta\right]\int\frac{d^D p}{(2\pi)^D}\mathrm{Tr}\left[(1+\gamma_5)\gamma^\lambda S(p)\gamma_\delta F_{\rho\sigma}T^{\mu\nu\alpha\beta\sigma\rho}\right]\left(g_{\mu\alpha}g_{\nu\beta}-g_{\mu\beta}g_{\nu\alpha}\right) \\
&= -\frac{\pi^2 N_C h_V G_H e Q_u \sqrt{M_D}}{384}\left[mI_{3/2} - I_1\right]\left\langle\frac{\alpha}{\pi}G^2\right\rangle\times \\
&\quad \left(\frac{2i}{m^4\pi^2}*v\cdot y*z\cdot V - \frac{2i}{m^4\pi^2}*v\cdot z*y\cdot V - \frac{2i}{m^4\pi^2}*e\_(v,y,z,V)\right) \\
&= -\frac{N_C h_V G_H e Q_u \sqrt{M_D}}{384m^4}\left[mI_{3/2} - I_1\right]\left\langle\frac{\alpha}{\pi}G^2\right\rangle\times 2i\left(F_{\mu\nu}v^\mu V^\nu - e\_(v,y,z,V)\right)
\end{aligned}
\tag{6.137}
$$

We see that the results from the diagrams in figure 6.55 and 6.58, figure 6.56 and 6.59, and figure 6.57 and 6.60 are all mutually equal.

In the next four diagrams we will continue to have an annihilation diagram without any external lines, but the creation diagram will now have photon and gluon lines coupled to both the upper and lower quark lines. This we have already seen two examples of in figure 6.46 and 6.47, but there we did not do the integration in the FORM program.

We start with the diagram in figure 6.61.

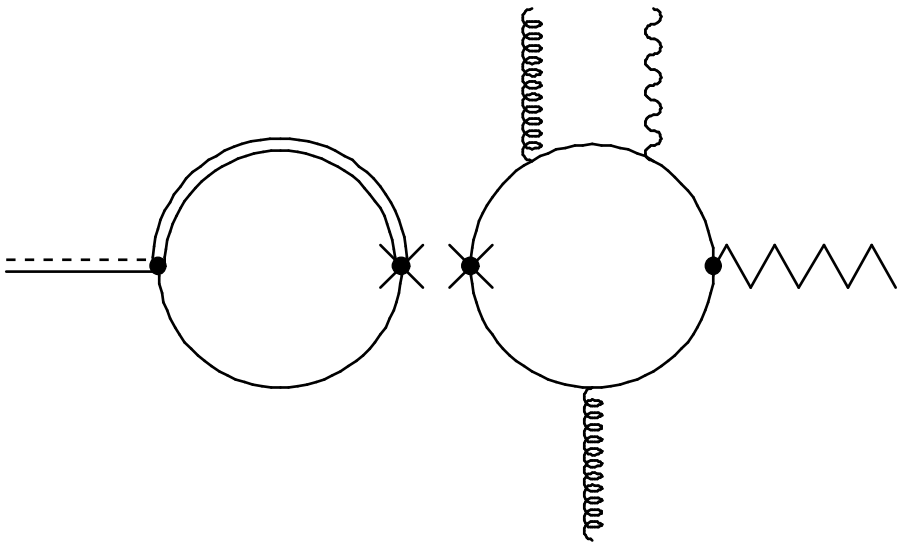

Figure 6.61 A combined diagram for the process $\left\langle V\left|\bar{\chi}\Lambda^n\gamma_\mu L\chi\right|g\gamma g\right\rangle\left\langle 0\left|\bar{q}\gamma^\mu LQ_{v_c}\right|D\right\rangle$.

Here the creation diagram has the following expression for M

$$
\begin{aligned}
M^\lambda &= -\frac{h_V e\pi^2}{384}\left\langle\frac{\alpha_s}{\pi}G^2\right\rangle\left(g_{\mu\sigma}g_{\nu\rho}-g_{\mu\rho}g_{\nu\sigma}\right)\mathrm{Tr}_F\left[\Lambda^n V^\delta\right]\times \\
&\quad \int\frac{d^D p}{(2\pi)^D}\frac{1}{(p^2-m^2)^2}\mathrm{Tr}\left[(1+\gamma_5)\gamma^\lambda Q F_{\alpha\beta}R^{\mu\nu\alpha\beta}\gamma_\delta\left\{\left[\gamma^\sigma,\gamma^\rho\right],(\gamma\cdot p+m)\right\}\right]
\end{aligned}
\tag{6.138}
$$

which gives us the final result for the total diagram

$$
\begin{aligned}
DVg_u f_u g_d &= \frac{i\pi^2 N_C h_V G_H e}{384}\left\langle \frac{\alpha_s}{\pi}G^2\right\rangle\left[mI_{3/2}-I_1\right]\left(g_{\mu\sigma}g_{\nu\rho}-g_{\mu\rho}g_{\nu\sigma}\right)\mathrm{Tr}\left[\xi^{\dagger}\gamma^{\lambda}LH\right]\mathrm{Tr}_F\left[\Lambda^n V^{\delta}\right]\times \\
&\int\frac{d^D p}{(2\pi)^D}\frac{1}{(p^2-m^2)^2}\mathrm{Tr}\left[\left(1+\gamma_5\right)\gamma^{\lambda}QF_{\alpha\beta}R^{\mu\nu\alpha\beta}\gamma_{\delta}\left\{\left[\gamma^{\sigma},\gamma^{\rho}\right],(\gamma\cdot p+m)\right\}\right] \\
&= \frac{\pi^2 N_C h_V G_H e Q_u\sqrt{M_D}}{1536}\left\langle \frac{\alpha_s}{\pi}G^2\right\rangle\left[mI_{3/2}-I_1\right]\left(g_{\mu\sigma}g_{\nu\rho}-g_{\mu\rho}g_{\nu\sigma}\right)\mathrm{Tr}\left[\gamma^{\lambda}\left(1-\gamma_5\right)\left(1+\gamma\cdot v\right)\gamma_5\right]\mathrm{Tr}_F\left[\Lambda^n V^{\delta}\right]\times \\
&\int\frac{d^D p}{(2\pi)^D}\frac{1}{(p^2-m^2)^2}\mathrm{Tr}\left[\left(1+\gamma_5\right)\gamma^{\lambda}QF_{\alpha\beta}R^{\mu\nu\alpha\beta}\gamma_{\delta}\left\{\left[\gamma^{\sigma},\gamma^{\rho}\right],(\gamma\cdot p+m)\right\}\right] \qquad (6.139) \\
&= \frac{\pi^2 N_C h_V G_H e Q_u\sqrt{M_D}}{1536}\left\langle \frac{\alpha_s}{\pi}G^2\right\rangle\left[mI_{3/2}-I_1\right]\times \\
&\left(\frac{12i}{5\pi^2 m^4}*v\cdot y*z\cdot V-\frac{12i}{5\pi^2 m^4}*v\cdot z*y\cdot V-\frac{12i}{5\pi^2 m^4}*e\_(v,y,z,V)\right) \\
&= \frac{iN_C h_V G_H e Q_u\sqrt{M_D}}{640m^4}\left\langle \frac{\alpha_s}{\pi}G^2\right\rangle\left[mI_{3/2}-I_1\right]\left(F_{\mu\nu}v^{\mu}V^{\nu}-e\_(v,y,z,V)\right)
\end{aligned}
$$

The next diagram that we look at is the one in figure 6.62, where the upper external lines have switched places compared to the diagram in figure 6.61.

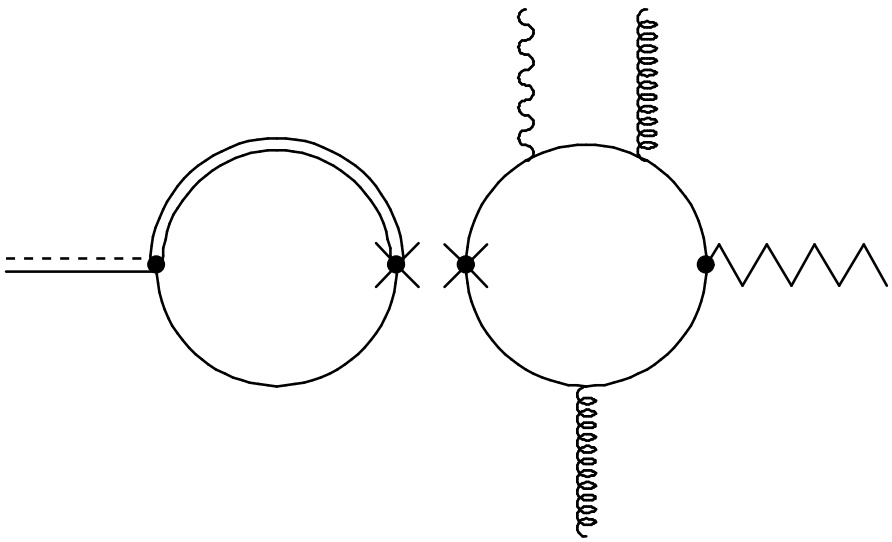

Figure 6.62 A combined diagram for the process $\left\langle V\left|\bar{\chi}\Lambda^n\gamma_\mu L\chi\right|\gamma gg\right\rangle\left\langle 0\left|\bar{q}\gamma^{\mu}LQ_{v_c}\right|D\right\rangle$.

Here we have

$$M^{\lambda} = -\frac{h_V e\pi^2}{384}\left\langle \frac{\alpha_s}{\pi} G^2 \right\rangle \left(g_{\alpha\sigma}g_{\beta\rho} - g_{\alpha\rho}g_{\beta\sigma}\right) \mathrm{Tr}_F\left[\Lambda^n V^{\delta}\right] \times$$
$$\int \frac{d^D p}{(2\pi)^D} \frac{1}{(p^2 - m^2)^2} \mathrm{Tr}\left[\left(1+\gamma_5\right)\gamma^{\lambda} Q F_{\mu\nu} R^{\mu\nu\alpha\beta} \gamma_{\delta} \left\{\left[\gamma^{\sigma}, \gamma^{\rho}\right], (\gamma \cdot p + m)\right\}\right] \tag{6.140}$$

for the creation diagram, giving us the result

$$DVf_u g_u g_d = \frac{i\pi^2 N_C h_V G_H e}{384}\left\langle \frac{\alpha_s}{\pi} G^2 \right\rangle \left[m I_{3/2} - I_1\right] \left(g_{\alpha\sigma}g_{\beta\rho} - g_{\alpha\rho}g_{\beta\sigma}\right) \mathrm{Tr}\left[\xi^{\dagger}\gamma^{\lambda} L H\right] \mathrm{Tr}_F\left[\Lambda^n V^{\delta}\right] \times$$
$$\int \frac{d^D p}{(2\pi)^D} \frac{1}{(p^2 - m^2)^2} \mathrm{Tr}\left[\left(1+\gamma_5\right)\gamma^{\lambda} Q F_{\mu\nu} R^{\mu\nu\alpha\beta} \gamma_{\delta} \left\{\left[\gamma^{\sigma}, \gamma^{\rho}\right], (\gamma \cdot p + m)\right\}\right]$$
$$= \frac{\pi^2 N_C h_V G_H e Q_u \sqrt{M_D}}{1536}\left\langle \frac{\alpha_s}{\pi} G^2 \right\rangle \left[m I_{3/2} - I_1\right] \times \tag{6.141}$$
$$\left(\frac{12i}{5\pi^2 m^4} * v \cdot y * z \cdot V - \frac{12i}{5\pi^2 m^4} * v \cdot z * y \cdot V - \frac{12i}{5\pi^2 m^4} * e\_(v, y, z, V)\right)$$
$$= \frac{i N_C h_V G_H e Q_u \sqrt{M_D}}{640 m^4}\left\langle \frac{\alpha_s}{\pi} G^2 \right\rangle \left[m I_{3/2} - I_1\right] \left(F_{\mu\nu} v^{\mu} V^{\nu} - e\_(v, y, z, V)\right)$$

For the diagram in figure 6.63,

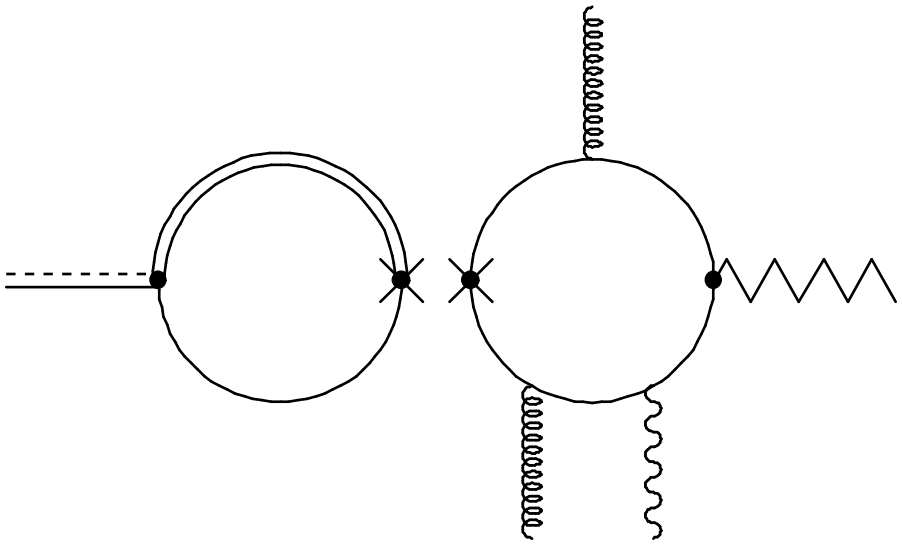

Figure 6.63 A combined diagram for the process $\left\langle V\left|\bar{\chi}\Lambda^n \gamma_{\mu} L \chi\right| g\gamma g\right\rangle \left\langle 0\left|\bar{q}\gamma^{\mu} L Q_{v_c}\right| D\right\rangle$.

we have an expression for M for the creation diagram that goes as follows

$$M^{\lambda} = -\frac{h_V e\pi^2}{384}\left\langle \frac{\alpha_s}{\pi} G^2 \right\rangle \left(g_{\sigma\alpha}g_{\rho\beta} - g_{\sigma\beta}g_{\rho\alpha}\right) \mathrm{Tr}_F\left[\Lambda^n V^{\delta}\right] \times$$
$$\int \frac{d^D p}{(2\pi)^D} \frac{1}{(p^2 - m^2)^2} \mathrm{Tr}\left[\left(1+\gamma_5\right)\gamma^{\lambda} \left\{\left[\gamma^{\sigma}, \gamma^{\rho}\right], (\gamma \cdot p + m)\right\} \gamma_{\delta} Q F_{\mu\nu} R^{\mu\nu\alpha\beta}\right] \tag{6.142}$$

This gives the result

$$
\begin{aligned}
DVg_u f_d g_d = {} & \frac{i\pi^2 N_C h_V G_H e}{384}\left\langle \frac{\alpha_s}{\pi} G^2 \right\rangle \left[mI_{3/2} - I_1 \right] \left(g_{\sigma\alpha} g_{\rho\beta} - g_{\sigma\beta} g_{\rho\alpha} \right) \mathrm{Tr}\left[\xi^{\dagger} \gamma^{\lambda} L H \right] \mathrm{Tr}_F\left[\Lambda^n V^{\delta} \right] \times \\
& \int \frac{d^D p}{(2\pi)^D} \frac{1}{(p^2 - m^2)^2} \mathrm{Tr}\left[(1+\gamma_5) \gamma^{\lambda} \left\{ \left[\gamma^{\sigma}, \gamma^{\rho} \right], (\gamma \cdot p + m) \right\} \gamma_{\delta} Q F_{\mu\nu} R^{\mu\nu\alpha\beta} \right] \\
= {} & \frac{\pi^2 N_C h_V G_H e Q_u \sqrt{M_D}}{1536} \left\langle \frac{\alpha_s}{\pi} G^2 \right\rangle \left[mI_{3/2} - I_1 \right] \times \\
& \left(-\frac{4i}{15\pi^2 m^4} * v \cdot y * z \cdot V + \frac{4i}{15\pi^2 m^4} * v \cdot z * y \cdot V - \frac{4i}{15\pi^2 m^4} * e\_(v, y, z, V) \right) \\
= {} & \frac{i N_C h_V G_H e Q_u \sqrt{M_D}}{4635 m^4} \left\langle \frac{\alpha_s}{\pi} G^2 \right\rangle \left[mI_{3/2} - I_1 \right] \left(-F_{\mu\nu} v^{\mu} V^{\nu} - e\_(v, y, z, V) \right)
\end{aligned}
\tag{6.143}
$$

For the last one of the total diagrams having an annihilation diagram with no external lines, shown in figure 6.64,

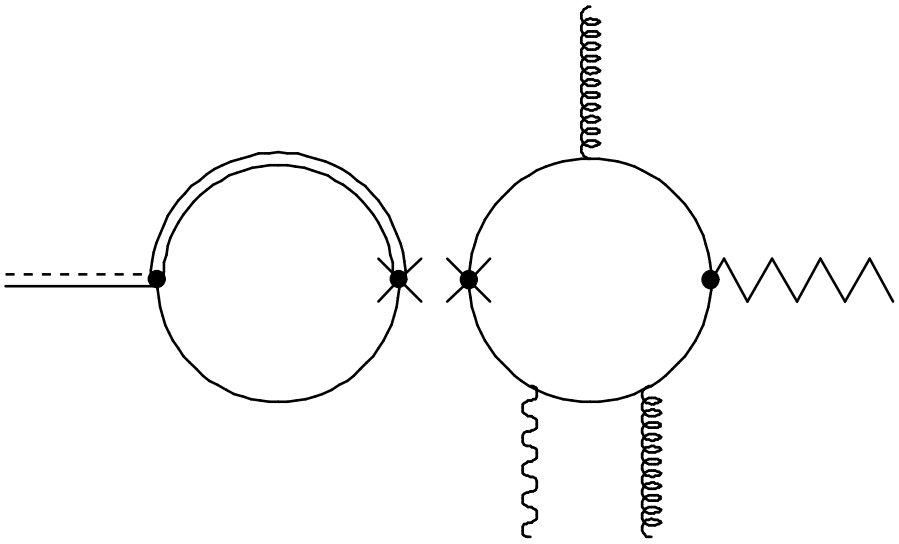

Figure 6.64 A combined diagram for the process $\left\langle V \left| \bar{\chi} \Lambda^n \gamma_{\mu} L \chi \right| gg\gamma \right\rangle \left\langle 0 \left| \bar{q} \gamma^{\mu} L Q_{v_c} \right| D \right\rangle$.

we have an M expression for the creation diagram which is

$$
\begin{aligned}
M^{\lambda} = {} & -\frac{h_V e \pi^2}{384}\left\langle \frac{\alpha_s}{\pi} G^2 \right\rangle \left(g_{\sigma\mu} g_{\rho\nu} - g_{\sigma\nu} g_{\rho\mu} \right) \mathrm{Tr}_F\left[\Lambda^n V^{\delta} \right] \times \\
& \int \frac{d^D p}{(2\pi)^D} \frac{1}{(p^2 - m^2)^2} \mathrm{Tr}\left[(1+\gamma_5) \gamma^{\lambda} \left\{ \left[\gamma^{\sigma}, \gamma^{\rho} \right], (\gamma \cdot p + m) \right\} \gamma_{\delta} Q F_{\alpha\beta} R^{\mu\nu\alpha\beta} \right]
\end{aligned}
\tag{6.144}
$$

This gives

$$
\begin{aligned}
DVg_u g_d f_d &= \frac{i\pi^2 N_C h_V G_H e}{384}\left\langle \frac{\alpha_s}{\pi} G^2 \right\rangle \left[mI_{3/2} - I_1 \right]\left(g_{\sigma\mu} g_{\rho\nu} - g_{\sigma\nu} g_{\rho\mu} \right) Tr\left[\xi^\dagger \gamma^\lambda LH \right] Tr_F\left[\Lambda^n V^\delta \right] \times \\
&\int \frac{d^D p}{(2\pi)^D} \frac{1}{(p^2 - m^2)^2} Tr\left[(1+\gamma_5)\gamma^\lambda \left\{ \left[\gamma^\sigma, \gamma^\rho \right], (\gamma \cdot p + m) \right\} \gamma_\delta Q F_{\alpha\beta} R^{\mu\nu\alpha\beta} \right] \\
&= \frac{\pi^2 N_C h_V G_H e Q_u \sqrt{M_D}}{1536}\left\langle \frac{\alpha_s}{\pi} G^2 \right\rangle \left[mI_{3/2} - I_1 \right] \times \\
&\left(-\frac{4i}{15\pi^2 m^4} * v \cdot y * z \cdot V + \frac{4i}{15\pi^2 m^4} * v \cdot z * y \cdot V - \frac{4i}{15\pi^2 m^4} * e\_(v, y, z, V) \right) \\
&= \frac{i N_C h_V G_H e Q_u \sqrt{M_D}}{4635 m^4}\left\langle \frac{\alpha_s}{\pi} G^2 \right\rangle \left[mI_{3/2} - I_1 \right]\left(-F_{\mu\nu} v^\mu V^\nu - e\_(v, y, z, V) \right)
\end{aligned}
\tag{6.145}
$$

In the next four total diagrams we have an annihilation diagram with one external gluon line, and the other two coupled to one of the quark propagators in the creation diagram loop.

We start with the diagram in figure 6.65.

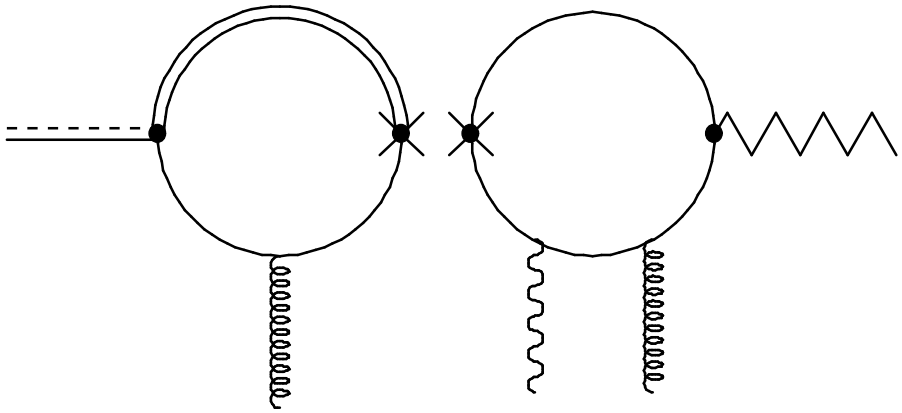

Figure 6.65 A combined diagram for the process $\left\langle V \left| \bar{\chi} \Lambda^n \gamma_\mu t^a L \chi \right| g\gamma \right\rangle \left\langle g \left| \bar{q} \gamma^\mu t^a L Q_{v_c} \right| D \right\rangle$.

The annihilation diagram has the following expression for M

$$
M^\lambda - \frac{G_H g_s}{8} Tr\left[\xi^\dagger \gamma^\lambda LH \left(iI_2 \{ \gamma \cdot v, \sigma \cdot G \} + \frac{1}{8\pi} \sigma \cdot G \right) \right] \tag{6.146}
$$

and the creation diagram has this expression

$$
M^\lambda = \frac{i h_V e g_S}{16} Tr_F\left[\Lambda^n V^\delta \right] \int \frac{d^D p}{(2\pi)^D} Tr\left[(1+\gamma_5)\gamma^\lambda S(p) \gamma_\delta Q F_{\mu\nu} G_{\alpha\beta} R^{\mu\nu\alpha\beta} \right] \tag{6.147}
$$

Combining these as a product we get

$$
\begin{aligned}
DgVg_d f_d = &-\frac{ih_V G_H e g_S^{\,2}}{128}\mathrm{Tr}\left[\xi^{\dagger}\gamma^{\lambda}LH\left(iI_2\{\gamma\cdot v,\sigma\cdot G\}+\frac{1}{8\pi}\sigma\cdot G\right)\right]\times \\
&\mathrm{Tr}_F\left[\Lambda^n V^{\delta}\right]\int\frac{d^D p}{(2\pi)^D}\mathrm{Tr}\left[(1+\gamma_5)\gamma^{\lambda}S(p)\gamma_{\delta}QF_{\mu\nu}G_{\alpha\beta}R^{\mu\nu\alpha\beta}\right] \\
&=-\frac{ih_V G_H e Q_u\sqrt{M_D}\pi^2}{6144}\left\langle\frac{\alpha_s}{\pi}G^2\right\rangle\left(g_{\sigma\alpha}g_{\rho\beta}-g_{\sigma\beta}g_{\rho\alpha}\right)\times \\
&\mathrm{Tr}\left[\gamma^{\mu}(1-\gamma_5)(1+\gamma\cdot v)\gamma_5\left(iI_2\left\{\gamma\cdot v,\left[\gamma^{\sigma},\gamma^{\rho}\right]\right\}+\frac{1}{8\pi}\left[\gamma^{\sigma},\gamma^{\rho}\right]\right)\right]\times \\
&\mathrm{Tr}_F\left[\Lambda^n V^{\delta}\right]\int\frac{d^D p}{(2\pi)^D}\mathrm{Tr}\left[(1+\gamma_5)\gamma^{\lambda}S(p)\gamma_{\delta}F_{\mu\nu}R^{\mu\nu\alpha\beta}\right] \\
&=-\frac{ih_V G_H e Q_u\sqrt{M_D}\pi^2}{6144}\left\langle\frac{\alpha_s}{\pi}G^2\right\rangle\times \\
&\left(\frac{i}{2m^2\pi^3}*v\cdot y*z\cdot V+\frac{8I_2}{3m^2\pi^2}*v\cdot y*z\cdot V-\frac{i}{2m^2\pi^3}*v\cdot z*y\cdot V\right. \\
&\left.-\frac{8I_2}{3m^2\pi^2}*v\cdot z*y\cdot V-\frac{73i}{160m^2\pi^3}*e\_(v,y,z,V)-\frac{69I_2}{20m^2\pi^2}*e\_(v,y,z,V)\right) \\
&=-\frac{ih_V G_H e Q_u\sqrt{M_D}}{6144m^2}\left\langle\frac{\alpha_s}{\pi}G^2\right\rangle\left(\left(\frac{i}{2\pi}+\frac{8I_2}{3}\right)F_{\mu\nu}v^{\mu}V^{\nu}-\left(\frac{73i}{160\pi}+\frac{69I_2}{20}\right)e\_(v,y,z,V)\right)
\end{aligned}
\tag{6.148}
$$

Next we look at the diagram in figure 6.66, in which the external lines in the creation loop now are connected to the upper quark line.

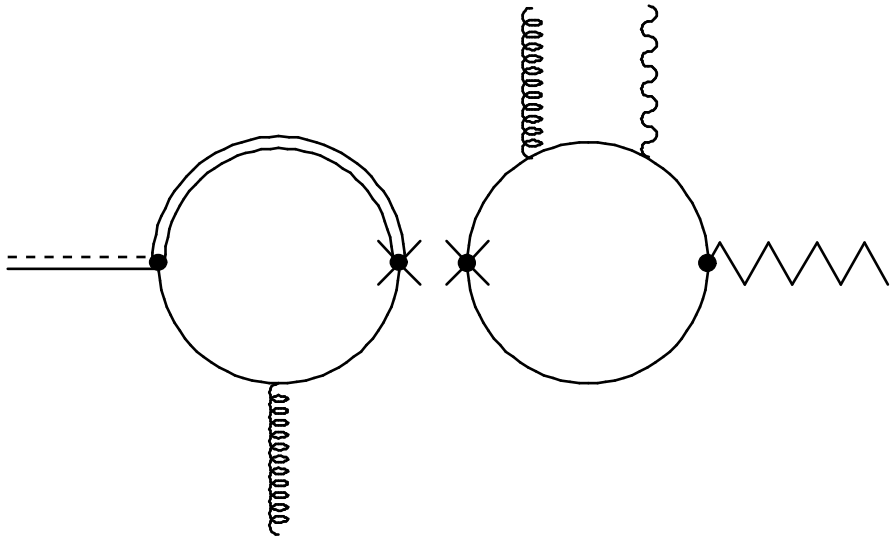

Figure 6.66 A combined diagram for the process $\left\langle V\left|\bar{\chi}\Lambda^n\gamma_{\mu}t^a L\chi\right|g\gamma\right\rangle\left\langle g\left|\bar{q}\gamma^{\mu}t^a LQ_{v_c}\right|D\right\rangle$.

This gives us an expression for the creation diagram that goes as follows

$$M^{\lambda}=\frac{ih_V eg_S}{16}Tr_F\left[\Lambda^n V^{\delta}\right]\int\frac{d^D p}{(2\pi)^D}Tr\left[\left(1+\gamma_5\right)\gamma^{\lambda}QF_{\alpha\beta}G_{\mu\nu}R^{\mu\nu\alpha\beta}\gamma_{\delta}S(p)\right] \tag{6.149}$$

And the final result becomes

$$\begin{aligned}
DgVg_u f_u =& -\frac{ih_V G_H eQ_u\sqrt{M_D}\pi^2}{3072}\left\langle\frac{\alpha_s}{\pi}G^2\right\rangle\left(g_{\sigma\mu}g_{\rho\nu}-g_{\sigma\nu}g_{\rho\mu}\right)\times\\
&Tr\left[\gamma^{\mu}\left(1-\gamma_5\right)\left(1+\gamma\cdot v\right)\gamma_5\left(iI_2\left\{\gamma\cdot v,\left[\gamma^{\sigma},\gamma^{\rho}\right]\right\}+\frac{1}{8\pi}\left[\gamma^{\sigma},\gamma^{\rho}\right]\right)\right]\times\\
&Tr_F\left[\Lambda^n V^{\delta}\right]\int\frac{d^D p}{(2\pi)^D}Tr\left[\left(1+\gamma_5\right)\gamma^{\lambda}F_{\alpha\beta}R^{\mu\nu\alpha\beta}\gamma_{\delta}S(p)\right]\\
=&-\frac{ih_V G_H eQ_u\sqrt{M_D}\pi^2}{6144}\left\langle\frac{\alpha_s}{\pi}G^2\right\rangle\times\\
&(-\frac{3i}{2m^2\pi^3}*v\cdot y*z\cdot V-\frac{40I_2}{3m^2\pi^2}*v\cdot y*z\cdot V+\frac{3i}{2m^2\pi^3}*v\cdot z*y\cdot V\\
&+\frac{40I_2}{3m^2\pi^2}*v\cdot z*y\cdot V+\frac{497i}{240m^2\pi^3}*e_(v,y,z,V)+\frac{763I_2}{60m^2\pi^2}*e_(v,y,z,V))\\
=&-\frac{ih_V G_H eQ_u\sqrt{M_D}}{6144m^2}\left\langle\frac{\alpha_s}{\pi}G^2\right\rangle\left(-\left(\frac{3i}{2\pi}+\frac{40I_2}{3}\right)F_{\mu\nu}v^{\mu}V^{\nu}+\left(\frac{497i}{240\pi}+\frac{763I_2}{60}\right)e_(v,y,z,V)\right)
\end{aligned} \tag{6.150}$$

For the next diagram, figure 6.67,

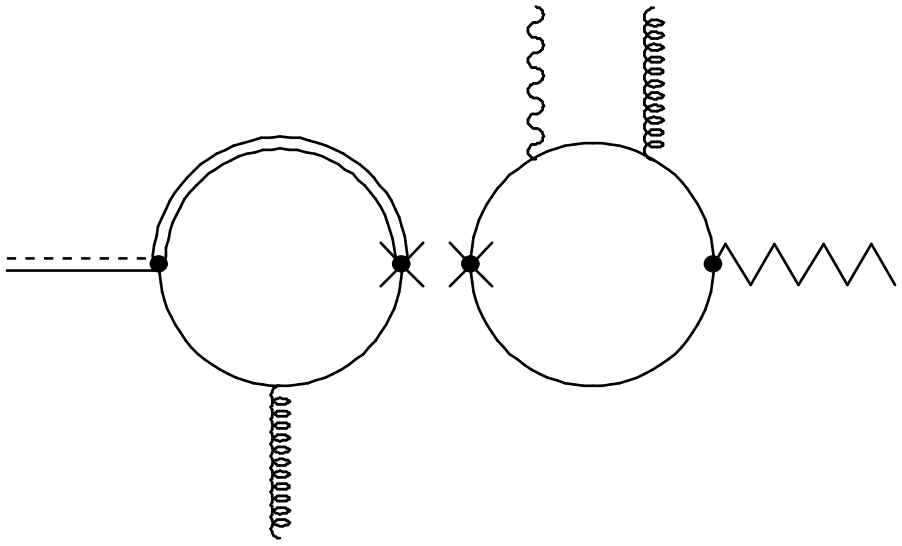

Figure 6.67 A combined diagram for the process $\left\langle V\left|\bar{\chi}\Lambda^n\gamma_{\mu}t^a L\chi\right|\gamma g\right\rangle\left\langle g\left|\bar{q}\gamma^{\mu}t^a LQ_{v_c}\right|D\right\rangle$.

we have

$$M^{\lambda}=\frac{ih_V eg_S}{16}Tr_F\left[\Lambda^n V^{\delta}\right]\int\frac{d^D p}{(2\pi)^D}Tr\left[\left(1+\gamma_5\right)\gamma^{\lambda}QF_{\mu\nu}G_{\alpha\beta}R^{\mu\nu\alpha\beta}\gamma_{\delta}S(p)\right] \tag{6.151}$$

for the creation diagram. This gives the result

$$
\begin{aligned}
DgVf_u g_u &= -\frac{ih_V G_H e Q_u \sqrt{M_D}\pi^2}{6144}\left\langle \frac{\alpha_s}{\pi}G^2\right\rangle\left(g_{\sigma\alpha}g_{\rho\beta}-g_{\sigma\beta}g_{\rho\alpha}\right)\times \\
&\quad \mathrm{Tr}\left[\gamma^\mu\left(1-\gamma_5\right)\left(1+\gamma\cdot v\right)\gamma_5\left(iI_2\left\{\gamma\cdot v,\left[\gamma^\sigma,\gamma^\rho\right]\right\}+\frac{1}{8\pi}\left[\gamma^\sigma,\gamma^\rho\right]\right)\right]\times \\
&\quad \mathrm{Tr}_F\left[\Lambda^n V^\delta\right]\int\frac{d^D p}{(2\pi)^D}\mathrm{Tr}\left[\left(1+\gamma_5\right)\gamma^\lambda Q F_{\mu\nu}R^{\mu\nu\alpha\beta}\gamma_\delta S(p)\right] \\
&= -\frac{ih_V G_H e Q_u \sqrt{M_D}\pi^2}{6144}\left\langle \frac{\alpha_s}{\pi}G^2\right\rangle\times \\
&\quad \left(\frac{i}{2m^2\pi^3}*v\cdot y*z\cdot V+\frac{8I_2}{3m^2\pi^2}*v\cdot y*z\cdot V-\frac{i}{2m^2\pi^3}*v\cdot z*y\cdot V-\frac{8I_2}{3m^2\pi^2}*v\cdot z*y\cdot V\right. \\
&\quad \left.-\frac{73i}{160m^2\pi^3}*e\_(v,y,z,V)-\frac{69I_2}{20m^2\pi^2}*e\_(v,y,z,V)\right) \\
&= -\frac{ih_V G_H e Q_u \sqrt{M_D}}{6144m^2}\left\langle \frac{\alpha_s}{\pi}G^2\right\rangle\left(\left(\frac{i}{2\pi}+\frac{8I_2}{3}\right)F_{\mu\nu}v^\mu V^\nu-\left(\frac{73i}{160\pi}+\frac{69I_2}{20}\right)e\_(v,y,z,V)\right)
\end{aligned}
\tag{6.152}
$$

The diagram in figure 6.68

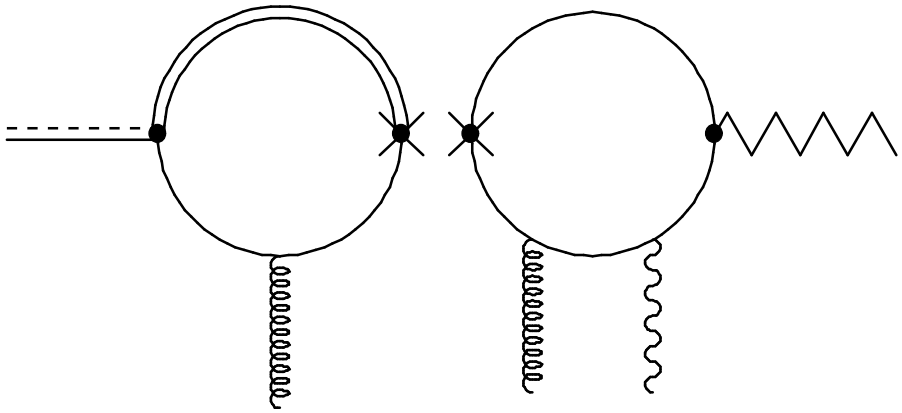

Figure 6.68 A combined diagram for the process $\left\langle V\left|\bar{\chi}\Lambda^n\gamma_\mu t^a L\chi\right|\gamma g\right\rangle\left\langle g\left|\bar{q}\gamma^\mu t^a L Q_{v_c}\right|D\right\rangle$.

has the following expression for the creation diagram

$$
M^\lambda = \frac{ih_V e g_S}{16}\mathrm{Tr}_F\left[\Lambda^n V^\delta\right]\int\frac{d^D p}{(2\pi)^D}\mathrm{Tr}\left[\left(1+\gamma_5\right)\gamma^\lambda S(p)\gamma_\delta Q F_{\alpha\beta}G_{\mu\nu}R^{\mu\nu\alpha\beta}\right] \tag{6.153}
$$

This gives us the result

$$
\begin{aligned}
\mathrm{DgVf_d g_d} &= -\frac{\mathrm{i h_V G_H e Q_u}\sqrt{\mathrm{M_D}}\pi^2}{6144}\left\langle\frac{\alpha_s}{\pi}\mathrm{G}^2\right\rangle\left(\mathrm{g_{\sigma\mu}g_{\rho\nu}}-\mathrm{g_{\sigma\nu}g_{\rho\mu}}\right)\times \\
&\quad \mathrm{Tr}\left[\gamma^\mu\left(1-\gamma_5\right)\left(1+\gamma\cdot\mathrm{v}\right)\gamma_5\left(\mathrm{iI_2}\left\{\gamma\cdot\mathrm{v},\left[\gamma^\sigma,\gamma^\rho\right]\right\}+\frac{1}{8\pi}\left[\gamma^\sigma,\gamma^\rho\right]\right)\right]\times \\
&\quad \mathrm{Tr_F}\left[\Lambda^{\mathrm{n}}\mathrm{V}^\delta\right]\int\frac{\mathrm{d^D p}}{(2\pi)^{\mathrm{D}}}\mathrm{Tr}\left[\left(1+\gamma_5\right)\gamma^\lambda \mathrm{S(p)}\gamma_\delta \mathrm{F}_{\alpha\beta}\mathrm{R}^{\mu\nu\alpha\beta}\right] \\
&= -\frac{\mathrm{i h_V G_H e Q_u}\sqrt{\mathrm{M_D}}\pi^2}{6144}\left\langle\frac{\alpha_s}{\pi}\mathrm{G}^2\right\rangle\times \\
&\quad (-\frac{3\mathrm{i}}{2\mathrm{m}^2\pi^3}*\mathrm{v}\cdot\mathrm{y}*\mathrm{z}\cdot\mathrm{V}-\frac{40\mathrm{I_2}}{3\mathrm{m}^2\pi^2}*\mathrm{v}\cdot\mathrm{y}*\mathrm{z}\cdot\mathrm{V}+\frac{3\mathrm{i}}{2\mathrm{m}^2\pi^3}*\mathrm{v}\cdot\mathrm{z}*\mathrm{y}\cdot\mathrm{V} \\
&\quad +\frac{40\mathrm{I_2}}{3\mathrm{m}^2\pi^2}*\mathrm{v}\cdot\mathrm{z}*\mathrm{y}\cdot\mathrm{V}+\frac{497\mathrm{i}}{240\mathrm{m}^2\pi^3}*\mathrm{e\_(v,y,z,V)}+\frac{763\mathrm{I_2}}{60\mathrm{m}^2\pi^2}*\mathrm{e\_(v,y,z,V)}) \\
&= -\frac{\mathrm{i h_V G_H e Q_u}\sqrt{\mathrm{M_D}}}{6144\mathrm{m}^2}\left\langle\frac{\alpha_s}{\pi}\mathrm{G}^2\right\rangle\left(-\left(\frac{3\mathrm{i}}{2\pi}+\frac{40\mathrm{I_2}}{3}\right)\mathrm{F}_{\mu\nu}\mathrm{v}^\mu\mathrm{V}^\nu+\left(\frac{497\mathrm{i}}{240\pi}+\frac{763\mathrm{I_2}}{60}\right)\mathrm{e\_(v,y,z,V)}\right)
\end{aligned}
\tag{6.154}
$$

Also here we can see that the calculations of the diagrams in figure 6.66 and 6.68, and the calculations of the diagrams in figure 6.65 and 6.67 are mutually equal.

We are almost at the end of this total diagram calculation now, only three diagrams left, and we start with the diagram in figure 6.69. We have

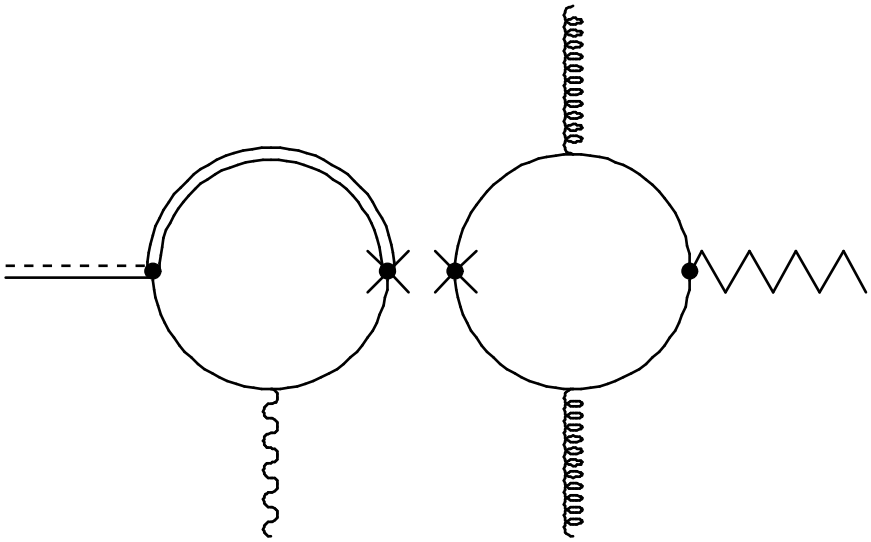

Figure 6.69 A combined diagram for the process $\left\langle \mathrm{V}\left|\bar{\chi}\Lambda^{\mathrm{n}}\gamma_\mu \mathrm{L}\chi\right|\mathrm{gg}\right\rangle\left\langle\gamma\left|\bar{\mathrm{q}}\gamma^\mu \mathrm{LQ_{v_c}}\right|\mathrm{D}\right\rangle$.

$$
\begin{aligned}
\mathrm{M}^\lambda &= -\frac{\mathrm{i}\pi^2\mathrm{h_V}}{768}\left\langle\frac{\alpha_s}{\pi}\mathrm{G}^2\right\rangle\left(\mathrm{g_{\alpha\sigma}g_{\beta\rho}}-\mathrm{g_{\alpha\rho}g_{\beta\sigma}}\right)\mathrm{Tr_F}\left[\Lambda^{\mathrm{n}}\mathrm{V}^\delta\right]\times \\
&\quad \int\frac{\mathrm{d^D p}}{(2\pi)^{\mathrm{D}}}\frac{1}{\left(\mathrm{p}^2-\mathrm{m}^2\right)^4}\mathrm{Tr}\left[\left(1+\gamma_5\right)\gamma^\lambda\left(\left\{\left[\gamma^\alpha,\gamma^\beta\right],\gamma\cdot\mathrm{p}\right\}\gamma_\delta\left\{\left[\gamma^\sigma,\gamma^\rho\right],\gamma\cdot\mathrm{p}\right\}+4\mathrm{m}^2\left[\gamma^\alpha,\gamma^\beta\right]\gamma_\delta\left[\gamma^\sigma,\gamma^\rho\right]\right)\right]
\end{aligned}
\tag{6.155}
$$

for the expression for M for the creation diagram, and

$$M^{\lambda} = \frac{N_c G_H e}{4} \mathrm{Tr}\left[\xi^{\dagger} \gamma^{\lambda} \mathrm{LH}\left(iI_2\{\gamma\cdot v, \sigma\cdot F\tilde{Q}_{\xi}^{V}\} + \frac{1}{8\pi}\sigma\cdot F\tilde{Q}_{\xi}^{V} \right) \right] \tag{6.156}$$

for the annihilation diagram. This gives us

$$\begin{aligned}
\mathrm{DfVg_u g_d} &= -\frac{i\pi^2 N_C h_V G_H e}{3072}\left\langle \frac{\alpha_s}{\pi} G^2 \right\rangle \left(g_{\alpha\sigma}g_{\beta\rho} - g_{\alpha\rho}g_{\beta\sigma}\right) \mathrm{Tr}\left[\xi^{\dagger}\gamma^{\lambda}\mathrm{LH}\left(iI_2\{\gamma\cdot v, \sigma\cdot F\tilde{Q}_{\xi}^{V}\} + \frac{1}{8\pi}\sigma\cdot F\tilde{Q}_{\xi}^{V} \right)\right] \mathrm{Tr_F}\left[\Lambda^n V^{\delta}\right]\times \\
&\int \frac{d^D p}{(2\pi)^D} \frac{1}{\left(p^2 - m^2\right)^4} \mathrm{Tr}\left[(1+\gamma_5)\gamma^{\lambda}\left(\left\{ \left[\gamma^{\alpha},\gamma^{\beta}\right], \gamma\cdot p\right\}\gamma_{\delta}\left\{\left[\gamma^{\sigma},\gamma^{\rho}\right],\gamma\cdot p\right\} + 4m^2\left[\gamma^{\alpha},\gamma^{\beta}\right]\gamma_{\delta}\left[\gamma^{\sigma},\gamma^{\rho}\right]\right)\right] \\
&= -\frac{i\pi^2 N_C h_V G_H e Q_d \sqrt{M_D}}{24576}\left\langle \frac{\alpha_s}{\pi} G^2 \right\rangle \left(g_{\alpha\sigma}g_{\beta\rho} - g_{\alpha\rho}g_{\beta\sigma}\right)\times \\
&\mathrm{Tr}\left[\gamma^{\lambda}(1-\gamma_5)(1+\gamma\cdot v)\gamma_5\left(iI_2\{\gamma\cdot v, \left[\gamma^{\mu},\gamma^{\nu}\right]\cdot F_{\mu\nu}\} + \frac{1}{8\pi}\left[\gamma^{\mu},\gamma^{\nu}\right]\cdot F_{\mu\nu}\right)\right] \mathrm{Tr_F}\left[\Lambda^n V^{\delta}\right]\times \\
&\int \frac{d^D p}{(2\pi)^D} \frac{1}{\left(p^2 - m^2\right)^4} \mathrm{Tr}\left[(1+\gamma_5)\gamma^{\lambda}\left(\left\{ \left[\gamma^{\alpha},\gamma^{\beta}\right], \gamma\cdot p\right\}\gamma_{\delta}\left\{\left[\gamma^{\sigma},\gamma^{\rho}\right],\gamma\cdot p\right\} + 4m^2\left[\gamma^{\alpha},\gamma^{\beta}\right]\gamma_{\delta}\left[\gamma^{\sigma},\gamma^{\rho}\right]\right)\right] \\
&= -\frac{i\pi^2 N_C h_V G_H e Q_d \sqrt{M_D}}{24576}\left\langle \frac{\alpha_s}{\pi} G^2 \right\rangle \times \\
&\left(\frac{16i}{m^2\pi^3} * v\cdot y * z\cdot V - \frac{16i}{m^2\pi^3} * v\cdot z * y\cdot V - \frac{16i}{m^2\pi^3} * e_(v,y,z,V) - \frac{256\cdot I_2}{m^2\pi^2} * e_(v,y,z,V)\right) \\
&= -\frac{iN_C h_V G_H e Q_d \sqrt{M_D}}{1536 m^2}\left\langle \frac{\alpha_s}{\pi} G^2 \right\rangle \left(\frac{i}{\pi} F_{\mu\nu} v^{\mu} V^{\nu} - \left(\frac{i}{\pi} + 16 I_2\right) e_(v,y,z,V)\right)
\end{aligned} \tag{6.157}$$

The next two diagrams has one photon and one gluon line coupled to each of the quark lines in the creation diagram, and one gluon line coupled to the light quark in the annihilation diagram. The first of these diagrams is the one in figure 6.70 below.

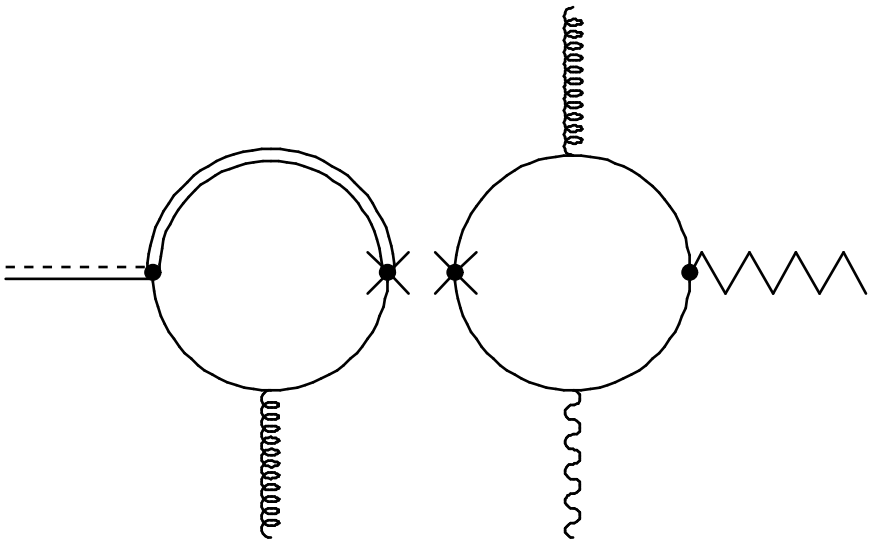

Figure 6.70 A combined diagram for the process $\langle V|\bar{\chi}\Lambda^n\gamma_\mu L\chi|g\gamma\rangle\langle g|\bar{q}\gamma^\mu LQ_{v_c}|D\rangle$.

This diagram has the following expressions for M

$$M^\lambda = -\frac{G_H g_s}{8}\mathrm{Tr}\left[\xi^\dagger\gamma^\lambda LH\left(iI_2\{\gamma\cdot v,\sigma\cdot G\}+\frac{1}{8\pi}\sigma\cdot G\right)\right] \tag{6.158}$$

for the annihilation diagram, and

$$M^\lambda = \frac{ih_V e g_s}{256}\mathrm{Tr}_F\left[\Lambda^n V^\delta\right]\int\frac{d^D p}{(2\pi)^D}\frac{1}{\left(p^2-m^2\right)^4} \tag{6.159}$$
$$\mathrm{Tr}\left[(1+\gamma_5)\gamma^\lambda\left(\left\{\left[\gamma^\alpha,\gamma^\beta\right]G_{\alpha\beta},\gamma\cdot p\right\}\gamma_\delta\left\{\tilde{Q}_\xi^V\left[\gamma^\sigma,\gamma^\rho\right]F_{\sigma\rho},\gamma\cdot p\right\}+4m^2\left[\gamma^\alpha,\gamma^\beta\right]G_{\alpha\beta}\gamma_\delta\tilde{Q}_\xi^V\left[\gamma^\sigma,\gamma^\rho\right]F_{\sigma\rho}\right)\right]$$

for the creation diagram. Combining these as usual gives the result

$$
\begin{aligned}
\mathrm{DgVg_u f_d} &= -\frac{\mathrm{i h_V G_H e g_s^{\,2}}}{2048}\mathrm{Tr}\left[\xi^{\dagger}\gamma^{\lambda}\mathrm{LH}\left(\mathrm{i I_2}\{\gamma\cdot v,\sigma\cdot G\}+\frac{1}{8\pi}\sigma\cdot G\right)\right]\mathrm{Tr_F}\left[\Lambda^n V^{\delta}\right]\int\frac{d^D p}{(2\pi)^D}\frac{1}{\left(p^2-m^2\right)^4}\\
&\mathrm{Tr}\left[(1+\gamma_5)\gamma^{\lambda}\left(\left\{\left[\gamma^{\alpha},\gamma^{\beta}\right]G_{\alpha\beta},\gamma\cdot p\right\}\gamma_{\delta}\left\{\tilde{Q}_{\xi}^{V}\left[\gamma^{\sigma},\gamma^{\rho}\right]F_{\sigma\rho},\gamma\cdot p\right\}+4m^2\left[\gamma^{\alpha},\gamma^{\beta}\right]G_{\alpha\beta}\gamma_{\delta}\tilde{Q}_{\xi}^{V}\left[\gamma^{\sigma},\gamma^{\rho}\right]F_{\sigma\rho}\right)\right]\\
&=-\frac{\mathrm{i h_V G_H e Q_u}\sqrt{M_D}\,g_s^{\,2}}{16384}\mathrm{Tr}\left[\gamma^{\lambda}(1-\gamma_5)(1+\gamma\cdot v)\gamma_5 G_{\mu\nu}\left(\mathrm{i I_2}\{\gamma\cdot v,\left[\gamma^{\mu},\gamma^{\nu}\right]\}+\frac{1}{8\pi}\left[\gamma^{\mu},\gamma^{\nu}\right]\right)\right]\mathrm{Tr_F}\left[\Lambda^n V^{\delta}\right]\times\\
&\int\frac{d^D p}{(2\pi)^D}\frac{1}{\left(p^2-m^2\right)^4}\mathrm{Tr}\left[(1+\gamma_5)\gamma^{\lambda}\left(\left\{\left[\gamma^{\alpha},\gamma^{\beta}\right]G_{\alpha\beta},\gamma\cdot p\right\}\gamma_{\delta}\left\{\left[\gamma^{\sigma},\gamma^{\rho}\right]F_{\sigma\rho},\gamma\cdot p\right\}+4m^2\left[\gamma^{\alpha},\gamma^{\beta}\right]G_{\alpha\beta}\gamma_{\delta}\left[\gamma^{\sigma},\gamma^{\rho}\right]F_{\sigma\rho}\right)\right]\\
&=-\frac{\mathrm{i}\pi^2\mathrm{h_V G_H e Q_u}\sqrt{M_D}}{98304}\left\langle\frac{\alpha_s}{\pi}G^2\right\rangle\left(g_{\mu\alpha}g_{\nu\beta}-g_{\mu\beta}g_{\nu\alpha}\right)\mathrm{Tr}\left[\gamma^{\lambda}(1-\gamma_5)(1+\gamma\cdot v)\gamma_5\left(\mathrm{i I_2}\{\gamma\cdot v,\left[\gamma^{\mu},\gamma^{\nu}\right]\}+\frac{1}{8\pi}\left[\gamma^{\mu},\gamma^{\nu}\right]\right)\right]\times\\
&\mathrm{Tr_F}\left[\Lambda^n V^{\delta}\right]\int\frac{d^D p}{(2\pi)^D}\frac{1}{\left(p^2-m^2\right)^4}\mathrm{Tr}\left[(1+\gamma_5)\gamma^{\lambda}\left(\left\{\left[\gamma^{\alpha},\gamma^{\beta}\right],\gamma\cdot p\right\}\gamma_{\delta}\left\{\left[\gamma^{\sigma},\gamma^{\rho}\right]F_{\sigma\rho},\gamma\cdot p\right\}+4m^2\left[\gamma^{\alpha},\gamma^{\beta}\right]\gamma_{\delta}\left[\gamma^{\sigma},\gamma^{\rho}\right]F_{\sigma\rho}\right)\right]\\
&=-\frac{\mathrm{i}\pi^2\mathrm{h_V G_H e Q_u}\sqrt{M_D}}{98304}\left\langle\frac{\alpha_s}{\pi}G^2\right\rangle\times\left(-\frac{64\mathrm{i}}{m^2\pi^3}*v\cdot y*z\cdot V*-\frac{512\cdot I_2}{m^2\pi^2}*v\cdot y*z\cdot V+\frac{64\mathrm{i}}{m^2\pi^3}*v\cdot z*y\cdot V\right.\\
&\left.+\frac{512\cdot I_2}{m^2\pi^2}*v\cdot z*y\cdot V+\frac{64\mathrm{i}}{m^2\pi^3}*e\_(v,y,z,V)+\frac{512\cdot I_2}{m^2\pi^2}*e\_(v,y,z,V)\right) \qquad (6.160)\\
&=-\frac{\mathrm{i h_V G_H e Q_u}\sqrt{M_D}}{1536m^2}\left\langle\frac{\alpha_s}{\pi}G^2\right\rangle\left(\frac{\mathrm{i}}{\pi}+8I_2\right)\left(-F_{\mu\nu}v^{\mu}V^{\nu}+e\_(v,y,z,V)\right)
\end{aligned}
$$

The last of the total diagrams is shown in figure 6.71.

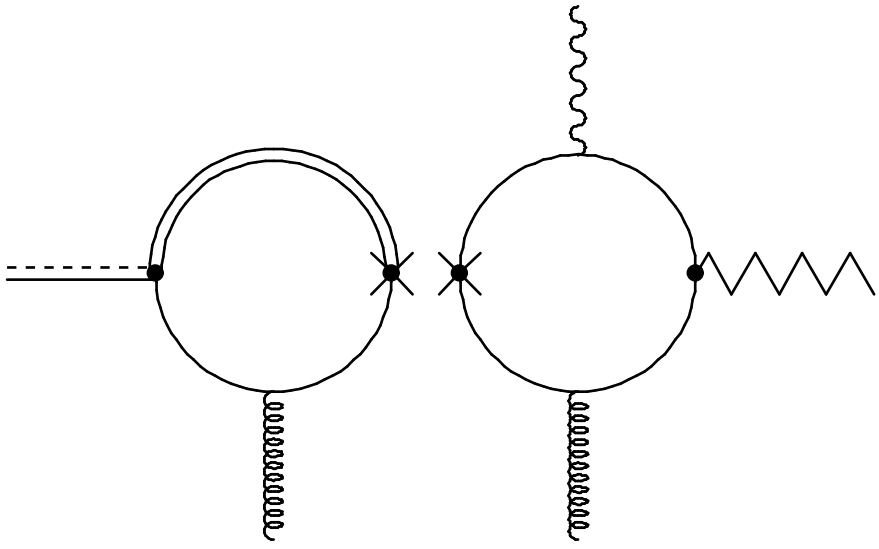

Figure 6.71 A combined diagram for the process $\langle V|\bar{\chi}\Lambda^n\gamma_{\mu}L\chi|g\gamma\rangle\langle g|\bar{q}\gamma^{\mu}LQ_{v_c}|D\rangle$.

The creation diagram is here given by the expression

$$M^{\lambda} = \frac{ih_V e g_s}{256} \mathrm{Tr}_F\left[\Lambda^n V^{\delta}\right] \int \frac{d^D p}{(2\pi)^D} \frac{1}{\left(p^2 - m^2\right)^4} \tag{6.161}$$
$$\mathrm{Tr}\left[(1+\gamma_5)\gamma^{\lambda}\left(\left\{\tilde{Q}_{\xi}^{V}\left[\gamma^{\sigma},\gamma^{\rho}\right]F_{\sigma\rho},\gamma\cdot p\right\}\gamma_{\delta}\left\{\left[\gamma^{\alpha},\gamma^{\beta}\right]G_{\alpha\beta},\gamma\cdot p\right\}+4m^2\tilde{Q}_{\xi}^{V}\left[\gamma^{\sigma},\gamma^{\rho}\right]F_{\sigma\rho}\gamma_{\delta}\left[\gamma^{\alpha},\gamma^{\beta}\right]G_{\alpha\beta}\right)\right]$$

which gives a similar result to the diagram in figure 6.70

$$\begin{aligned}
Dg V g_d f_u &= -\frac{ih_V G_H e g_s^{\,2}}{2048}\mathrm{Tr}\left[\xi^{\dagger}\gamma^{\lambda}LH\left(iI_2\{\gamma\cdot v,\sigma\cdot G\}+\frac{1}{8\pi}\sigma\cdot G\right)\right]\mathrm{Tr}_F\left[\Lambda^n V^{\delta}\right]\int\frac{d^D p}{(2\pi)^D}\frac{1}{\left(p^2-m^2\right)^4}\\
&\mathrm{Tr}\left[(1+\gamma_5)\gamma^{\lambda}\left(\left\{\tilde{Q}_{\xi}^{V}\left[\gamma^{\sigma},\gamma^{\rho}\right]F_{\sigma\rho},\gamma\cdot p\right\}\gamma_{\delta}\left\{\left[\gamma^{\alpha},\gamma^{\beta}\right]G_{\alpha\beta},\gamma\cdot p\right\}+4m^2\tilde{Q}_{\xi}^{V}\left[\gamma^{\sigma},\gamma^{\rho}\right]F_{\sigma\rho}\gamma_{\delta}\left[\gamma^{\alpha},\gamma^{\beta}\right]G_{\alpha\beta}\right)\right]\\
&= -\frac{ih_V G_H e Q_u\sqrt{M_D}\,g_s^{\,2}}{16384}\mathrm{Tr}\left[\gamma^{\lambda}(1-\gamma_5)(1+\gamma\cdot v)\gamma_5 G_{\mu\nu}\left(iI_2\{\gamma\cdot v,\left[\gamma^{\mu},\gamma^{\nu}\right]\}+\frac{1}{8\pi}\left[\gamma^{\mu},\gamma^{\nu}\right]\right)\right]\mathrm{Tr}_F\left[\Lambda^n V^{\delta}\right]\times\\
&\int\frac{d^D p}{(2\pi)^D}\frac{1}{\left(p^2-m^2\right)^4}\mathrm{Tr}\left[(1+\gamma_5)\gamma^{\lambda}\left(\left\{\left[\gamma^{\sigma},\gamma^{\rho}\right]F_{\sigma\rho},\gamma\cdot p\right\}\gamma_{\delta}\left\{\left[\gamma^{\alpha},\gamma^{\beta}\right]G_{\alpha\beta},\gamma\cdot p\right\}+4m^2\left[\gamma^{\sigma},\gamma^{\rho}\right]F_{\sigma\rho}\gamma_{\delta}\left[\gamma^{\alpha},\gamma^{\beta}\right]G_{\alpha\beta}\right)\right]\\
&= -\frac{i\pi^2 h_V G_H e Q_u\sqrt{M_D}}{98304}\left\langle\frac{\alpha_s}{\pi}G^2\right\rangle\left(g_{\mu\alpha}g_{\nu\beta}-g_{\mu\beta}g_{\nu\alpha}\right)\mathrm{Tr}\left[\gamma^{\lambda}(1-\gamma_5)(1+\gamma\cdot v)\gamma_5\left(iI_2\{\gamma\cdot v,\left[\gamma^{\mu},\gamma^{\nu}\right]\}+\frac{1}{8\pi}\left[\gamma^{\mu},\gamma^{\nu}\right]\right)\right]\times\\
&\mathrm{Tr}_F\left[\Lambda^n V^{\delta}\right]\int\frac{d^D p}{(2\pi)^D}\frac{1}{\left(p^2-m^2\right)^4}\mathrm{Tr}\left[(1+\gamma_5)\gamma^{\lambda}\left(\left\{\left[\gamma^{\sigma},\gamma^{\rho}\right]F_{\sigma\rho},\gamma\cdot p\right\}\gamma_{\delta}\left\{\left[\gamma^{\alpha},\gamma^{\beta}\right],\gamma\cdot p\right\}+4m^2\left[\gamma^{\sigma},\gamma^{\rho}\right]F_{\sigma\rho}\gamma_{\delta}\left[\gamma^{\alpha},\gamma^{\beta}\right]\right)\right]\\
&= -\frac{i\pi^2 h_V G_H e Q_u\sqrt{M_D}}{98304}\left\langle\frac{\alpha_s}{\pi}G^2\right\rangle\times\left(\frac{64i}{3m^2\pi^3}*v\cdot y*z\cdot V*+\frac{512\cdot I_2}{3m^2\pi^2}*v\cdot y*z\cdot V-\frac{64i}{3m^2\pi^3}*v\cdot z*y\cdot V\right.\\
&\left.-\frac{512\cdot I_2}{3m^2\pi^2}*v\cdot z*y\cdot V-\frac{64i}{3m^2\pi^3}*e_(v,y,z,V)-\frac{512\cdot I_2}{3m^2\pi^2}*e_(v,y,z,V)\right)\\
&= -\frac{ih_V G_H e Q_u\sqrt{M_D}}{1536m^2}\left\langle\frac{\alpha_s}{\pi}G^2\right\rangle\left(\frac{i}{\pi}+8I_2\right)\left(F_{\mu\nu}v^{\mu}V^{\nu}-e_(v,y,z,V)\right)
\end{aligned} \tag{6.162}$$

This was all the total diagrams, both with and without the gluon condensate to first order, for the process $D \rightarrow V + \gamma$. We will in the next and final chapter sum the results for the full diagrams we now have calculated.

If one studies the answers closely one may notice that they all appear to be real valued, as the divergent integrals (I_1, $I_{3/2}$ and I_2) are having imaginary values. This doesn't seem quite right since what we have been calculating are the M values, which are equal to $i\mathcal{L}$, and we expect the Lagrangian to be real, i.e. M to be imaginary. However, there will appear an i when we include the numerical factors from the Fermi theory making M imaginary, and thereby saves us from ending up with imaginary amplitudes.

Chapter 7

Numerical Results

In this final chapter we will use the results from the last chapter to calculate the amplitudes for the process $D^0 \to \bar{K}^{*0}\gamma$, both with and without the gluon condensate to first order, and also look at the decay width Γ and branching ratios, and compare the results with experimental values. The amplitudes will be calculated and weighted using the expression we gained from Fierz transformation and Fermi theory (eq. 3.18)

$$\begin{aligned}\left\langle \bar{K}^{*0}\gamma \right| \mathcal{L}_{\text{eff}} \left| D^0 \right\rangle = i\frac{G_F}{\sqrt{2}} V^*_{cs} V_{ud} \{ & \left(C_1 + \frac{C_2}{N_C} \right) \cdot \\ & [\left\langle \bar{K}^{*0}\gamma gg \right| (\bar{d}\gamma^\mu(1-\gamma_5)s) \left| 0 \right\rangle \left\langle 0 \right| (\bar{u}\gamma_\mu(1-\gamma_5)c) \left| D^0 \right\rangle \\ & + \left\langle \bar{K}^{*0}\gamma \right| (\bar{d}\gamma^\mu(1-\gamma_5)s) \left| 0 \right\rangle \left\langle gg \right| (\bar{u}\gamma_\mu(1-\gamma_5)c) \left| D^0 \right\rangle \\ & + \left\langle \bar{K}^{*0}gg \right| (\bar{d}\gamma^\mu(1-\gamma_5)s) \left| 0 \right\rangle \left\langle \gamma \right| (\bar{u}\gamma_\mu(1-\gamma_5)c) \left| D^0 \right\rangle \\ & + \left\langle \bar{K}^{*0} \right| (\bar{d}\gamma^\mu(1-\gamma_5)s) \left| 0 \right\rangle \left\langle \gamma gg \right| (\bar{u}\gamma_\mu(1-\gamma_5)c) \left| D^0 \right\rangle] \\ & + 2C_2 [\left\langle \bar{K}^{*0}\gamma g \right| (\bar{d}t^a\gamma^\mu(1-\gamma_5)s) \left| 0 \right\rangle \left\langle g \right| (\bar{u}t^a\gamma_\mu(1-\gamma_5)c) \left| D^0 \right\rangle \\ & + \left\langle \bar{K}^{*0}g \right| (\bar{d}t^a\gamma^\mu(1-\gamma_5)s) \left| 0 \right\rangle \left\langle \gamma g \right| (\bar{u}t^a\gamma_\mu(1-\gamma_5)c) \left| D^0 \right\rangle] \}\end{aligned} \tag{7.1}$$

Note that we have here included the factor i before the weak factor, since we do not want to end up with imaginary values for the amplitudes. As the amplitude expressions seen in this equation may be represented by more then one of the diagrams calculated, we should rewrite it in order to see where each of the calculated diagrams belong. F. ex. the original amplitude $\left\langle \bar{K}^{*0}\gamma gg \right| (\bar{d}\gamma^\mu(1-\gamma_5)s) \left| 0 \right\rangle \left\langle 0 \right| (\bar{u}\gamma_\mu(1-\gamma_5)c) \left| D^0 \right\rangle$ describes no less then twelve different diagrams, after the permutations of one photon and two gluons coupled to the vector particle loop has been considered. In the notation of the diagram calculations this equals $(DVf_u g_u g_u + DVg_u f_u g_u + DVg_u g_u f_u + DVf_d g_d g_d + DVg_d f_d g_d + DVg_d g_d f_d + DVg_u g_u f_d + DVf_u g_d g_d + DVg_u f_u g_d + DVf_u g_u g_d + DVg_u f_d g_d + DVg_u g_d f_d)$. Using this syntax we get an expression for the amplitude which has the following form

$$\begin{aligned}\left\langle \bar{K}^{*0}\gamma\right|\mathcal{L}_{eff}\left|D^{0}\right\rangle = i\frac{G_F}{\sqrt{2}}V^{*}_{cs}V_{ud}\{&\left(C_1+\frac{C_2}{N_C}\right)\cdot\\ &[(DVf_ug_ug_u+DVg_uf_ug_u+DVg_ug_uf_u+DVf_dg_dg_d+DVg_df_dg_d+\\ &DVg_dg_df_d+DVg_ug_uf_d+DVf_ug_dg_d+DVg_uf_ug_d+DVf_ug_ug_d+\\ &DVg_uf_dg_d+DVg_ug_df_d)+(DggVf_u+DggVf_d)+(DfVg_ug_u+\\ &DfVg_dg_d+DfVg_ug_d)+(DfggV+DgfgV+DggfV)]\\ &+2C_2[(DgVg_df_d+DgVg_uf_u+DgVf_ug_u+DgVf_dg_d+DgVg_uf_d+\\ &DgVf_ug_d)+(DgfVg_d+DgfVg_u+DfgVg_d+DfgVg_u)]\}\end{aligned} \tag{7.2}$$

The general expression for the result had the following form

$$\mathcal{L} = A^{(+)}i\varepsilon^{\mu\nu\alpha\beta}\Phi_D v_\mu \varepsilon'_\nu(V)k_\alpha\varepsilon_\beta(\gamma)+A^{(-)}\Phi_D F_{\mu\nu}v^\mu V^\nu \tag{7.3}$$

where Φ_D was the pseudoscalar part of the D-meson field. In our process, where the heavy meson field is given by $H = 1/2\cdot(1+\gamma\cdot v)\left(-iP_5\gamma_5\right)$, Φ_D becomes equal to P_5. In terms of the factors $A^{(\pm)}$ the decay width can be expressed as

$$\Gamma(D\to V\gamma) = \left(\left|A^{(+)}\right|^2+\frac{\left|A^{(-)}\right|^2}{4}\right)\times\frac{M_D^2\left(1-\left(\frac{m_V}{M_D}\right)^2\right)^4}{\frac{72}{\pi}\left(1+\left(\frac{m_V}{M_D}\right)^2\right)} \tag{7.4}$$

So our first task will be to find the factors $A^{(\pm)}$. In order to do this, we will use eq. 7.3 and the results from chapter 6. We have to remember though that what we have calculated in the last chapter is $M = i\mathcal{L}$, so when going from the calculated values for the diagrams to the factors $A^{(\pm)}$, there will be a lot of different i's and other factors being multiplied and divided by. In order to keep track of them all, we show explicitly in the expressions below how one gets from M to $A^{(\pm)}$.

$$A^{(+)} = -i\frac{M^{PC}}{\sqrt{M_D}\cdot e\_(v,y,z,V)} \tag{7.5}$$

$$A^{(-)} = -i\frac{M^{PV}}{\sqrt{M_D}\cdot F_{\mu\nu}v^\mu V^\nu} \tag{7.6}$$

The superscripts PC and PV stands for parity conserving and parity violating, respectively, and represents the parity conserving and violating terms of M. P_5 has been written as $\sqrt{M_D}$, since we substituted P_5 in the momentum space with $\sqrt{M_D}$ in the calculations of the diagrams, and it is this expression that we have used throughout chapter 6.

Table 7.1 on the next page shows the amplitude, the corresponding diagrams and the $A^{(+)}$ and the $A^{(-)}$ factors. We have to remember though that these values has to be weighted with the

Wilson coefficients and multiplied with the Fermi coupling constant and the CKM matrix elements, according to eq. 7.2. That is, the values for $A^{(\pm)}$ in the first four rows (the factorizable part) has to be multiplied with a factor $\left(C_1 + C_2/N_C\right)$, while the factors in the last two rows (the non-factorizable part) has to be multiplied with $2C_2$. Finally they all have to be multiplied with the weak term $i\frac{G_F}{\sqrt{2}}V^*_{cs}V_{ud}$.

Table 7.1 The amplitude, the corresponding diagrams and the $A^{(+)}$ and the $A^{(-)}$ factors for the process $D^0 \to \bar{K}^{*0}\gamma$, including the gluon condensate to first order.

Amplitude	**Diagrams**	$\mathbf{A^{(+)}}$	$\mathbf{A^{(-)}}$
$\left\langle \bar{K}^{*0}\gamma gg\left\vert(\bar{d}\gamma^\mu(1-\gamma_5)s)\right\vert 0\right\rangle \times$ $\left\langle 0\left\vert(\bar{u}\gamma_\mu(1-\gamma_5)c)\right\vert D^0\right\rangle$	$DVf_ug_ug_u + DVg_uf_ug_u +$ $DVg_ug_uf_u + DVf_dg_dg_d +$ $DVg_df_dg_d + DVg_dg_df_d +$ $DVg_ug_uf_d + DVf_ug_dg_d +$ $DVg_uf_ug_d + DVf_ug_ug_d +$ $DVg_uf_dg_d + DVg_ug_df_d$	$\frac{N_C h_V G_H e Q_u}{6592m^4}\times$ $\left[mI_{3/2} - I_1\right]\times$ $\left\langle\frac{\alpha}{\pi}G^2\right\rangle\left(\frac{7391}{45}\right)$	$\frac{N_C h_V G_H e Q_u}{6592m^4}\times$ $\left[mI_{3/2} - I_1\right]\times$ $\left\langle\frac{\alpha}{\pi}G^2\right\rangle(-115)$
$\left\langle \bar{K}^{*0}\gamma\left\vert(\bar{d}\gamma^\mu(1-\gamma_5)s)\right\vert 0\right\rangle \times$ $\left\langle gg\left\vert(\bar{u}\gamma_\mu(1-\gamma_5)c)\right\vert D^0\right\rangle$	$DggVf_u + DggVf_d$	$\frac{3\pi-4}{384m^2}\frac{N_C h_V G_H e Q_u}{16}\times$ $\left\langle\frac{\alpha_s}{\pi}G^2\right\rangle\left(\frac{3i}{\pi^2} - 32I_2\right)$	0
$\left\langle \bar{K}^{*0}gg\left\vert(\bar{d}\gamma^\mu(1-\gamma_5)s)\right\vert 0\right\rangle \times$ $\left\langle \gamma\left\vert(\bar{u}\gamma_\mu(1-\gamma_5)c)\right\vert D^0\right\rangle$	$DfVg_ug_u + DfVg_dg_d +$ $DfVg_ug_d$	$i\frac{N_C h_V G_H e Q_d}{3072m^2}\times$ $\left\langle\frac{\alpha}{\pi}G^2\right\rangle\left(80i\cdot I_2 - \frac{5}{\pi}\right)$	$i\frac{N_C h_V G_H e Q_d}{3072m^2}\times$ $\left\langle\frac{\alpha_s}{\pi}G^2\right\rangle\frac{1}{\pi}$
$\left\langle \bar{K}^{*0}\left\vert(\bar{d}\gamma^\mu(1-\gamma_5)s)\right\vert 0\right\rangle \times$ $\left\langle \gamma gg\left\vert(\bar{u}\gamma_\mu(1-\gamma_5)c)\right\vert D^0\right\rangle$	$DfggV + DgfgV + DggfV$	$\frac{N_C h_V G_H e Q_d}{192m^4}\left\langle\frac{\alpha_s}{\pi}G^2\right\rangle\times$ $\left[m^2I_2 - I_1\right]\left(\frac{2}{3\pi^2} + \frac{1}{4\pi}\right)$	$\frac{N_C h_V G_H e Q_d}{192m^4}\times$ $\left\langle\frac{\alpha_s}{\pi}G^2\right\rangle\left[m^2I_2 - I_1\right]\times$ $\left(-\frac{3}{4\pi}\right)$
$\left\langle \bar{K}^{*0}\gamma g\left\vert(\bar{d}t^a\gamma^\mu(1-\gamma_5)s)\right\vert 0\right\rangle \times$ $\left\langle g\left\vert(\bar{u}t^a\gamma_\mu(1-\gamma_5)c)\right\vert D^0\right\rangle$	$DgVg_df_d + DgVg_uf_u +$ $DgVf_ug_u + DgVf_dg_d +$ $DgVg_uf_d + DgVf_ug_d$	$\frac{h_V G_H e Q_u}{6144m^2}\left\langle\frac{\alpha_s}{\pi}G^2\right\rangle\times$ $\left(\frac{539i}{48\pi} - \frac{1238I_2}{15}\right)$	$\frac{h_V G_H e Q_u}{6144m^2}\left\langle\frac{\alpha_s}{\pi}G^2\right\rangle\times$ $\left(-\frac{2i}{\pi} - \frac{64I_2}{3}\right)$
$\left\langle \bar{K}^{*0}g\left\vert(\bar{u}t^a\gamma^\mu(1-\gamma_5)s)\right\vert 0\right\rangle \times$ $\left\langle \gamma g\left\vert(\bar{d}t^a\gamma_\mu(1-\gamma_5)c)\right\vert D^0\right\rangle$	$DgfVg_d + DgfVg_u +$ $DfgVg_d + DfgVg_u$	$i\frac{h_V G_H e Q_d}{1536m^2}\times$ $\left\langle\frac{\alpha}{\pi}G^2\right\rangle\left(\frac{2}{\pi^2} + \frac{1}{3\pi}\right)$	$-i\frac{h_V G_H e Q_d}{3072m^2}\times$ $\left\langle\frac{\alpha}{\pi}G^2\right\rangle\left(\frac{1}{\pi}\right)$

In the same manner we can look at the diagrams without any gluon condensate, and see what values for $A^{(\pm)}$ this gives. The results are shown in table 7.2. These are factorizable diagrams,

so here we will again weight the factors using the Wilson coefficients $(C_1 + C_2/N_C)$, and we also have to include the Fermi coupling constant and the CKM matrix elements, just as above, when calculating numerical values.

Table 7.2 The amplitude, the corresponding diagrams and the $A^{(+)}$ and the $A^{(-)}$ factors for the process $D^0 \to \bar{K}^{*0}\gamma$, without the gluon condensate.

Amplitude	**Diagrams**	**$A^{(+)}$**	**$A^{(-)}$**
$\langle \bar{K}^{*0} \vert (\bar{d}t^a\gamma^\mu(1-\gamma_5)s)\vert 0\rangle \times$ $\langle \gamma \vert (\bar{u}t^a\gamma_\mu(1-\gamma_5)c)\vert D^0\rangle$	DfV	$\frac{N_c{}^2 G_H h_V e Q_d}{16} \times$ $\left[m^2 I_2 - I_1\right]\left(16i \cdot I_2 - \frac{1}{\pi}\right)$	$\frac{N_c{}^2 G_H h_V e Q_d}{16} \times$ $\left[m^2 I_2 - I_1\right]\left(\frac{1}{\pi}\right)$
$\langle \bar{K}^{*0}\gamma \vert (\bar{d}t^a\gamma^\mu(1-\gamma_5)s)\vert 0\rangle \times$ $\langle 0 \vert (\bar{u}t^a\gamma_\mu(1-\gamma_5)c)\vert D^0\rangle$	$DVf_d + DVf_u$	$-i\frac{N_c{}^2 G_H h_V e Q_u}{16} \times$ $\left[m I_{3/2} - I_1\right]\left(32 I_2 + \frac{3i}{\pi^2}\right)$	0

By writing the diagrams without the gluon condensate to first order separately we can compare the two situations, and see which one of the two that contributes mostly. We also suspect, from eq 3.19, that the non-factorizable diagrams will dominate somewhat (about 7 times) over the factorizable diagrams, i.e. the $A^{(\pm)}$ factors in the last two rows of table 7.1 will dominate over the factors in the other rows.

7.1 Input Parameter Values

In order for us to get some numerical results out of our calculations we need the values of the parameters that have been used. Some of these values are model dependent, while others are constants or physical measurable quantities. Table 7.3 on the next page shows a list of these values, most of which comes from [4].

Table 7.3 Input parameters

Parameter	Value
$\left\langle \frac{\alpha}{\pi} G^2 \right\rangle^{1/4}$	$(0,275 \pm 0,010)$ GeV
$\langle \bar{q}q \rangle$	-(0,240 GeV)^3
G_H	$(6,8 \pm 0,4)$ GeV$^{-1/2}$
g_A	0,6
m	(240 ± 30) MeV
M_{D^0}	(1864,6 ± 0,5) MeV
f_π	93 MeV
h_V	6
C_1	-0,06 ± 0,12
C_2	1,10 ± 0,05

Let us look a little closer at the different parameters and their values. Ideally we should have just one value for the gluon condensate, which can be used both for the pure light vector sector and the heavy-light D-sector. However, to find this value would require that we also took the third, fourth and so on orders of the gluon condensate into account, and that is clearly too complex for this thesis. So instead we will use different values of the gluon condensate depending on where the external gluon lines are connected, i.e. depending on what diagram in table 7.1 and 7.2 we are looking at. When the gluons are only connected to the D-meson loop, we will use the value of the gluon condensate for the D-sector, taken from [4]

$$\left\langle \frac{\alpha}{\pi} G^2 \right\rangle^{1/4} = (0,300 \pm 0,020) \text{ GeV} \tag{7.7}$$

In the pure V-sector we will use the following value for the gluon condensate

$$\left\langle \frac{\alpha}{\pi} G^2 \right\rangle^{1/4} = 0,250 \text{ GeV} \tag{7.8}$$

For the diagrams where gluons are coupled to both loops, we will simply use an average value of the two.

$$\left\langle \frac{\alpha}{\pi} G^2 \right\rangle^{1/4} = (0,275 \pm 0,010) \text{ GeV} \tag{7.9}$$

The value of the quark condensate $\langle \bar{q}q \rangle$ is its standard value, given without uncertainties, and is also taken from [4].

The meson coupling constant G_H has the following value in the D-sector

(7.10)

$$G_D = (6,8 \pm 0,4)\ \text{GeV}^{-1/2}$$

This is the value that we will use since the only place in the Feynman diagrams that this term appear, is in the vertex between the D-meson and the heavy and light quark lines, as was shown in figure 5.1.

The strong axial coupling g_A is introduced through the linear divergent integral $I_{3/2}$, in the form of $\delta g_A = 1 - g_A$ as shown in the appendix. The first factor in the expression for δg_A, the normalization term 1, is originating from the calculations of a Feynman one-loop diagrams of a vector field coupled to the light quark in the heavy-light meson, while the second term, g_A, comes from the same diagram calculations, but with the vector field replaced by an axial vector field. In the D-sector g_A has the value

$$g_A = 0,55 \pm 0,08 \tag{7.11}$$

But this value is taken when m = 220±30, and as one can see from table 7.3, we have a bit higher value for m, which would suggest, from [4], that the value of g_A should be higher. We therefore choose the value

$$g_A = 0,6 \tag{7.12}$$

m is the SU(3) invariant constituent light quark mass, and is a model dependent parameter. For the D → V process that we are looking at, we will get a slightly higher value than the one given in [4], where the value of the mass is (220 ± 30) MeV.

M_{D^0} is the mass of the D^0 meson. It will primarily enter through the factor following the sum of the $A^{(\pm)}$ factors in the expression for the decay width Γ (eq. 7.4). We have specified the D meson to be a D^0 particle here, since this is the particle we have decay data for.

f_π is the bare pion decay constant. It was also introduced earlier when we looked at the chiral quark model in connection with the ξ term in the rotated fields. f_π will for example show up in the expression for the logarithmic divergent integral I_2, as can be seen in the appendix.

As we might recall from chapter 4.1.2 (eq. 4.34), the coefficient h_V was actually expressed through the equation

$$\frac{f^2 h_V^2}{3m^2}\left[1 - \frac{1}{15m^2 f^2}\left\langle \frac{\alpha_S}{\pi} G^2 \right\rangle\right] = 1 \tag{7.13}$$

However, we will not be using this expression to calculate h_V since it would require one specific value for the gluon condensate for all the different diagrams. We know, on the other hand, from [13] that h_V should be roughly 6, so we will use this explicit value for h_V instead. In addition, from the equation above, if the value of the gluon condensate becomes larger than $15m^2f^2$ the value of h_V will become imaginary. This is not physical, since it also would make the Lagrange function imaginary.

Also in table 7.3 are the Wilson coefficients C_1 and C_2. Their values we got from [10] which were the values calculated at a scale μ = 1 GeV and with the number of colours equal to 3. We could not use the so called effective values for C_1 and C_2 (where $1/N_C \to 0$) since in that case the non-factorizable effects are included in the coefficients, as discussed in section 3.2.

In connection to this we also have the weak $\frac{G_F}{\sqrt{2}} V^*_{cs} V_{ud}$ term. The Fermi constant G_F has a value of $1{,}166 \cdot 10^{-5}$ GeV^{-2} [5], while the Cabibbo-Kobayashi-Maskawa matrix gives the following value for the product of the matrix elements $V^*_{cs} V_{ud} = 0{,}9504$. This value we have gained by taking an average value of the values of the matrix elements given in eq. 2.9, and then multiplied them together. (We do not expect this to be a very accurate procedure, but it will give us an estimate of the correct value.) Using this we get the following result for the weak factor in the amplitude

$$\frac{G_F}{\sqrt{2}} V^*_{cs} V_{ud} = 7{,}84 \cdot 10^{-6} \text{ GeV}^{-2} \tag{7.14}$$

Now that we have established numerical values for the parameters, we should be able to calculate terms that in turn are based on these values. This includes the divergent integrals I_1, I_2 and $I_{3/2}$. However, since we will not be using eq. 4.34 to calculate the value of h_V, we will have different values for the gluon condensate depending on which diagram we are studying. From eq. 4.20 and 4.21 we had the following relations for the divergent integrals I_1 and I_2.

$$I_1 = i\frac{\langle \bar{q}q \rangle}{4mN_C} + \frac{i}{48m^2 N_C}\left\langle \frac{\alpha_S}{\pi} G^2 \right\rangle \tag{7.15}$$

$$I_2 = i\frac{f_\pi^2}{4m^2 N_C} - \frac{i}{96m^4 N_C}\left\langle \frac{\alpha_S}{\pi} G^2 \right\rangle \tag{7.16}$$

Since the I_1 and I_2 are dependent on the value of the gluon condensate and will appear in all types of diagrams, we will get different values for these integrals depending on which diagram calculation we are doing. We therefore cannot calculate the numerical values of I_1 and I_2 now, but have to insert the explicit equations for them (eq. 7.15 and 7.16) into our calculations. Another important thing about the divergent integrals I_1 and I_2 is that when we insert the equations for them into our calculations, we will get contributions that are proportional to the square of the gluon condensate. These contributions have to be excluded, because including them would mean that we take into account second order gluon condensate contributions, and not only contributions to first order, which is what we are looking at in this thesis. $I_{3/2}$, on the other hand, does not depend on the gluon condensate and can be calculated now. This gives us

$$I_{3/2} = \frac{3}{4}\frac{i\delta g_A}{G_H^2 N_C} + i\frac{m}{16\pi} = i\left(6{,}94 \cdot 10^{-3}\right) \text{ GeV} \tag{7.17}$$

Now we have found all the values for the parameters used in the calculations, and are ready to start looking at what numerical results our calculations will give. However, it could be useful

to look at some experimental results first, in order to be able to compare our calculated results with these experimental findings.

7.2 Experimental Results

In this section we will primarily look at the experimental decay widths for the process $D^0 \to \overline{K}^{*0}\gamma$, using the data given from the Particle Data Group (PDG) [11]. The PDG has listed the following decay width ratio or branching ratio for this process

$$\Gamma_i/\Gamma < 7,6\cdot 10^{-4} \tag{7.18}$$

and it is given within 90 % confidence limits. Γ is here the total decay width of the D^0 meson and Γ_i is the decay width for the particular process $D^0 \to \overline{K}^{*0}\gamma$. The listed momentum for this process is p = 719 MeV in the rest frame of the D^0 meson, far below the value of ~ 80 GeV listed in eq. 3.10.

In order for us to get some numbers which we later can compare our calculated decay widths with, we need to find the value of the total decay width Γ. The mean lifetime for the D^0 meson is also given by the PDG and has the value

$$\tau_{D^0} = (410,3 \pm 1,5)\cdot 10^{-15}\ \text{s} \tag{7.19}$$

Using the following relation [1] we can estimate the total decay width

$$\Gamma_{D^0} = \frac{\hbar}{\tau_{D^0}} = \frac{6,58211915\cdot 10^{-25}\ \text{GeV s}}{(410,3 \pm 1,5)\cdot 10^{-15}\ \text{s}} = (1,604 \pm 0,0059)\cdot 10^{-12}\ \text{GeV} \tag{7.20}$$

Using this result we can now calculate an upper bound for the decay width for the process $D^0 \to \overline{K}^{*0}\gamma$, by using the branching ratio given in eq. 7.18.

$$\Gamma_i = \Gamma(D^0 \to \overline{K}^{*0}\gamma) < (1,219 \pm 0,045)\cdot 10^{-15}\ \text{GeV} \tag{7.21}$$

The PDG also lists branching ratios for other decay processes, such as $D^0 \to \rho^0\gamma$, $D^0 \to \omega\gamma$ and $D^0 \to \varphi\gamma$.

$$\Gamma_{\rho^0}/\Gamma_{D^0} < 2,4\cdot 10^{-4} \tag{7.22}$$

$$\Gamma_{\omega}/\Gamma_{D^0} < 2,4\cdot 10^{-4} \tag{7.23}$$

$$\Gamma_{\varphi}/\Gamma_{D^0} = \left(2,5^{+0,7}_{-0,6}\right)\cdot 10^{-5} \tag{7.24}$$

We should be able to find decay widths also for these processes by following the same procedure as we have done above. Doing so gives us the following results

$$\Gamma_i = \Gamma\left(D^0 \to \rho^0\gamma\right) < (3{,}850 \pm 0{,}014)\cdot 10^{-16}\ \text{GeV} \tag{7.25}$$

$$\Gamma_i = \Gamma\left(D^0 \to \omega\gamma\right) < (3{,}850 \pm 0{,}014)\cdot 10^{-16}\ \text{GeV} \tag{7.26}$$

$$\Gamma_i = \Gamma\left(D^0 \to \varphi\gamma\right) = (4{,}010 \pm 0{,}28)\cdot 10^{-17}\ \text{GeV} \tag{7.27}$$

Note that the decay width in last process, the decay to a φ-meson, is not an upper limit, but an precise value. This is since the branching ratio given by the PDG is stated as an exact result (with uncertainties of course) and not as a limit. Decay widths for processes involving other D-mesons than the D^0 should also be possible to calculate with the same procedure as above. However, lack of data permits us from doing any further calculations based on experimental findings.

7.3 Calculated Results

Now we are ready to do the calculations of the decay widths for the processes from the diagram calculations in chapter 6. We will do this by using eq. 7.4. However, before we start, we need the numerical values of the factors $A^{(\pm)}$. The general expressions for these factors were given in table 7.1 and 7.2, and the results for the decay process $D^0 \to \bar{K}^{*0}\gamma$ are given in table 7.4 and 7.5, where we have included the weighting of the Wilson coefficients and the factor $i\frac{G_F}{\sqrt{2}}V^*_{cs}V_{ud}$.

Table 7.4 The diagrams with gluon condensate to first order and their corresponding numerical values of the factors $A^{(\pm)}$

Diagrams	$\mathbf{A^{(+)}}$ $(\text{GeV}^{-1/2})$	$\mathbf{A^{(-)}}$ $(\text{GeV}^{-1/2})$
$DVf_ug_ug_u + DVg_uf_ug_u + DVg_ug_uf_u + DVf_dg_dg_d + DVg_df_dg_d + DVg_dg_df_d + DVg_ug_uf_d + DVf_ug_dg_d + DVg_uf_ug_d + DVf_ug_ug_d + DVg_uf_dg_d + DVg_ug_df_d$	$-3{,}41\cdot 10^{-9}$	$2{,}39\cdot 10^{-9}$
$DggVf_u + DggVf_d$	$2{,}15\cdot 10^{-10}$	0
$DfVg_ug_u + DfVg_dg_d + DfVg_ug_d$	$-3{,}56\cdot 10^{-10}$	$6{,}32\cdot 10^{-11}$
$DfggV + DgfgV + DggfV$	$9{,}29\cdot 10^{-11}$	$-1{,}51\cdot 10^{-10}$
$DgVg_df_d + DgVg_uf_u + DgVf_ug_u + DgVf_dg_d + DgVg_uf_d + DgVf_ug_d$	$-7{,}09\cdot 10^{-9}$	$6{,}28\cdot 10^{-10}$
$DgfVg_d + DgfVg_u + DfgVg_d + DfgVg_u$	$4{,}29\cdot 10^{-10}$	$-2{,}21\cdot 10^{-10}$

Table 7.5 The diagrams without gluon condensate and their corresponding numerical values of the factors $A^{(\pm)}$

Diagrams	$\mathbf{A^{(+)}}$ $(\mathrm{GeV}^{-1/2})$	$\mathbf{A^{(-)}}$ $(\mathrm{GeV}^{-1/2})$
DfV	$-4,83\cdot10^{-9}$	$2,96\cdot10^{-9}$
$\mathrm{DVf_d}+\mathrm{DVf_u}$	$-1,54\cdot10^{-8}$	0

The factor following the sum of $A^{(+)}$ and $A^{(-)}$ for the process $D^0\to\bar{K}^{*0}\gamma$ has the value

$$\frac{M_{D^0}^2\left(1-\left(\frac{m_{\bar{K}^{*0}}}{M_{D^0}}\right)^2\right)^4}{\frac{72}{\pi}\left(1+\left(\frac{m_{\bar{K}^{*0}}}{M_{D^0}}\right)^2\right)}=(0,04311\pm0,00014)\ \mathrm{GeV}^2 \tag{7.28}$$

From table 7.4 and 7.5 we can sum all the $A^{(+)}$ and $A^{(-)}$ coefficients together, and this gives us

$$\begin{aligned}A^{(+)}&=-3,03\cdot10^{-8}\ \mathrm{GeV}^{-1/2}\\ A^{(-)}&=5,67\cdot10^{-9}\ \mathrm{GeV}^{-1/2}\end{aligned} \tag{7.29}$$

Now, putting these values, together with the value from eq. 7.28 above, into the expression for the decay width (eq. 7.4), we get the following result

$$\Gamma(D^0\to\bar{K}^{*0}\gamma)=(3,99\pm0,017)\cdot10^{-17}\ \mathrm{GeV} \tag{7.30}$$

The experimental value for this decay was given in eq. 7.21 and had the value

$$\Gamma_{\mathrm{exp}}\left(D^0\to\bar{K}^{*0}\gamma\right)<(1,219\pm0,045)\cdot10^{-15}\ \mathrm{GeV} \tag{7.31}$$

As we can see, our theoretically calculated value is about 30 times lower than the experimental value.

Doing the same calculations for the decay processes $D^0\to\rho^0\gamma$, $D^0\to\omega\gamma$ and $D^0\to\varphi\gamma$ with different values of the $A^{(\pm)}$ factors (since the CKM matrix elements are different) and different values of eq. 7.28, gives us

$$\Gamma\left(D^0\to\rho^0\gamma\right)=(2,87\pm0,011)\cdot10^{-18}\ \mathrm{GeV} \tag{7.32}$$

$$\Gamma\left(D^0\to\omega\gamma\right)=(2,82\pm0,007)\cdot10^{-18}\ \mathrm{GeV} \tag{7.33}$$

$$\Gamma\left(D^0\to\varphi\gamma\right)=(1,34\pm0,004)\cdot10^{-18}\ \mathrm{GeV} \tag{7.34}$$

which ranges from around 137 to 30 times below the experimental results. For ρ^0 and ω we can argue that although the values are low, they are within the range of the decay width. But for φ we had an exact value, so the argument does not hold here. However, the decay process

$D^0 \to \varphi\gamma$ actually has the smallest deviation from the experimental value, so it does have the best fit of all the decay processes we looked at.

Calculating the branching ratios for these processes gives us the following values

$$\frac{\Gamma(D^0 \to \bar{K}^{*0}\gamma)}{\Gamma_{D^0}} = \frac{(3,99 \pm 0,017)\cdot 10^{-17}}{(1,604 \pm 0,0059)\cdot 10^{-12}} \approx (2,49 \pm 0,014)\cdot 10^{-5} \tag{7.35}$$

$$\frac{\Gamma(D^0 \to \rho^0\gamma)}{\Gamma_{D^0}} = \frac{(2,87 \pm 0,011)\cdot 10^{-18}}{(1,604 \pm 0,0059)\cdot 10^{-12}} \approx (1,79 \pm 0,009)\cdot 10^{-6} \tag{7.36}$$

$$\frac{\Gamma(D^0 \to \omega\gamma)}{\Gamma_{D^0}} = \frac{(2,82 \pm 0,007)\cdot 10^{-18}}{(1,604 \pm 0,0059)\cdot 10^{-12}} \approx (1,75 \pm 0,008)\cdot 10^{-6} \tag{7.37}$$

$$\frac{\Gamma(D^0 \to \varphi\gamma)}{\Gamma_{D^0}} = \frac{(1,34 \pm 0,004)\cdot 10^{-18}}{(1,604 \pm 0,0059)\cdot 10^{-12}} \approx (5,70 \pm 0,034)\cdot 10^{-7} \tag{7.38}$$

By comparing these values with the ones given in eq. 7.18 and eq. 7.22 though 7.24, we see that we get values being around 137 to 30 times lower than we would expect from experiment.

7.4 Conclusion

What we have done in this thesis is to look at the general decay process $D \to V\gamma$, and calculated the amplitudes and decay widths for the special cases D = D^0 and V = $\bar{K}^{*0}$, ρ^0, ω and φ, including the gluon condensate to first order. To do this we used the heavy light chiral quark model and the chiral quark model for vector mesons. In doing so we treated the c-quark as a heavy particle, and disregarded terms including $1/m_c$ as these where considered being small in the theory. As the mass of the c-quark is 1,15 – 1,35 GeV and our energy cutoff was chosen to be Λ = 1 GeV, this could give rise to uncertainties and inaccuracies in the theory.

After this general discussion, we turned to the specific process $D^0 \to \bar{K}^{*0}\gamma$. This process we approximated as a point interaction using Fermi theory, and using Wilson coefficients to account for the effects of the heavy particle. From this we found that the non-factorizable part of the decay process was slightly dominating over the factorizable one. We next used the VSA factorization limit to split the $D^0 \to \bar{K}^{*0}\gamma$ process to two parts; one which annihilated the D-meson and one which created the vector meson. We then calculated $M = i\mathcal{L}$ for these two types of diagrams separately, with gluons and photons coupled to them. This gave nine diagrams of the annihilation type and 26 of the creation type. Later these two types of diagrams were combined into the total diagrams, and from these we calculated the amplitudes and decay widths, and compared them to experimental values.

So what can we say about our theoretical findings from the last section? It appears that the decay widths we have found are too small compared to the experimental results. At least this

is true for φ, where we have an exact value, whereas in the other processes we only have upper limits. One reason for these lower results could be that terms of higher order in the gluon condensate gives important contributions which we have not calculated in this thesis (though this is not very likely, since we expect high order contributions to contribute less). Or that the use of the effective field theory for this process gives rise to inaccuracies, since the mass of the c-quark is close to the cutoff. Or it may be that the values used in our calculations are inaccurate.

This latter reason for the deviation is very important in connection with the factor h_V, since the expression for h_V (eq. 4.34) shows that it is dependent on both the value of the gluon condensate and the value of the mass. This really means that we can use the value of h_V only at a certain value of the gluon condensate and the mass. What we have done in the calculations above is to use different values of the gluon condensate, depending on that diagram the gluon lines are connected to, but we have not changed the value of h_V in the same manner.

The fact that we have not used equation 4.34 for h_V in our calculations (and thereby left out the dependence of the condensate and mass) also has a large effect on the behaviour of the decay width as a function of the other parameters. That is, if we try to adjust the other parameters, such as the value of the gluon condensate, the constituent quark mass or the factors $A^{(\pm)}$, in order to get the calculated values of the decay width to agree with the experimental, the results turns out to have values that are not physical for this process.

Let's look at the decay width for $D^0 \to \bar{K}^{*0}\gamma$ as a function of gluon condensate, and use, for simplicity, a single value of the gluon condensate, i.e. the same value of the gluon condensate everywhere. A plot of this with the experimentally correct decay width is shown in figure 7.1 on the next page.

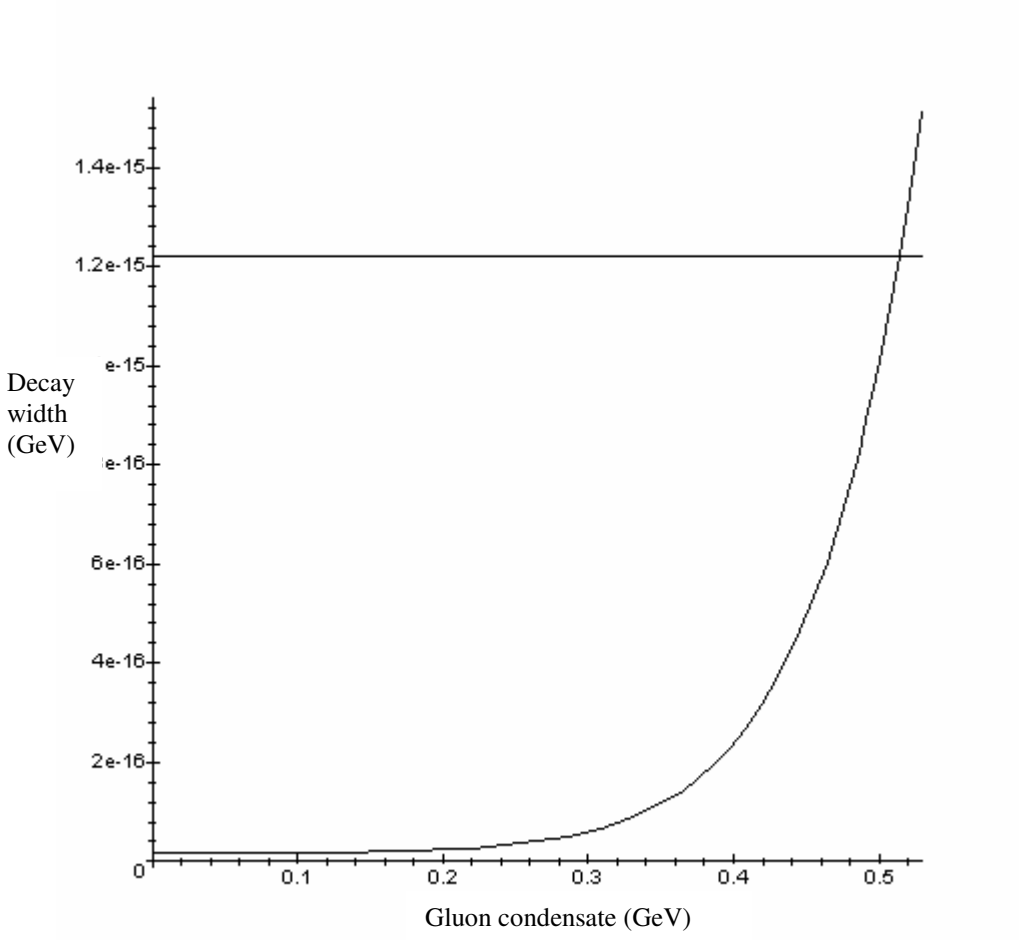

Figure 7.1 The decay width for $D^0 \to \bar{K}^{*0}\gamma$ *as a function of gluon condensate. The strait line is the experimental value of the decay width.*

We find that the value of the gluon condensate that fits our calculated result in section 7.3, when we are using only a single value for the gluon condensate when calculating the decay width, should be $\left\langle \frac{\alpha}{\pi} G^2 \right\rangle^{1/4} = 0,264 \text{ GeV}$. However, should we try to adjust the gluon condensate to fit the experimentally correct value, the condensate becomes 0,514 GeV, which is more than twice as much as the value we have used in our calculations.

Looking at the decay width as a function of the constituent quark mass, and again including the experimentally correct value for the decay width gives us the following plot

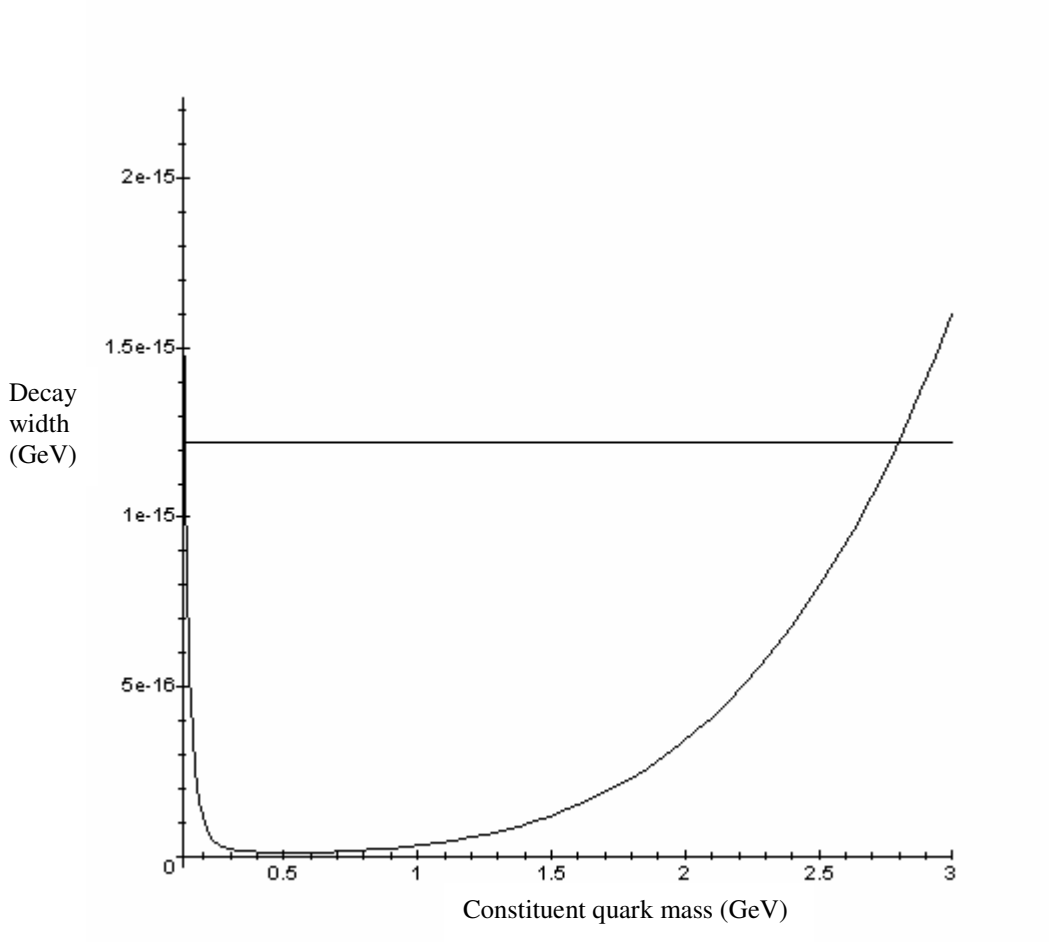

Figure 7.2 The decay width for $D^0 \to \bar{K}^{*0}\gamma$ *as a function of constituent quark mass. The strait line is the experimental value of the decay width.*

We get two crossings here between the calculated and the experimental decay width

$$m = 0{,}130 \text{ GeV} \quad \text{and} \quad m = 2{,}79 \text{ GeV}$$

Both of these values are deviate largely from the value we have used, m = 0,240 GeV, so, again, we cannot adjust the calculated decay width to fit the experimental value simply by a small adjustment of the constituent quark mass.

What if contributions from higher order gluon condensates plays an important role? When including higher order terms, we would get larger values of the $A^{(\pm)}$ factors, so let's look at the decay width as a function of the factors $A^{(\pm)}$. Plotted as a graph together with the experimental correct decay width we get the graphs as shown in figure 7.3.

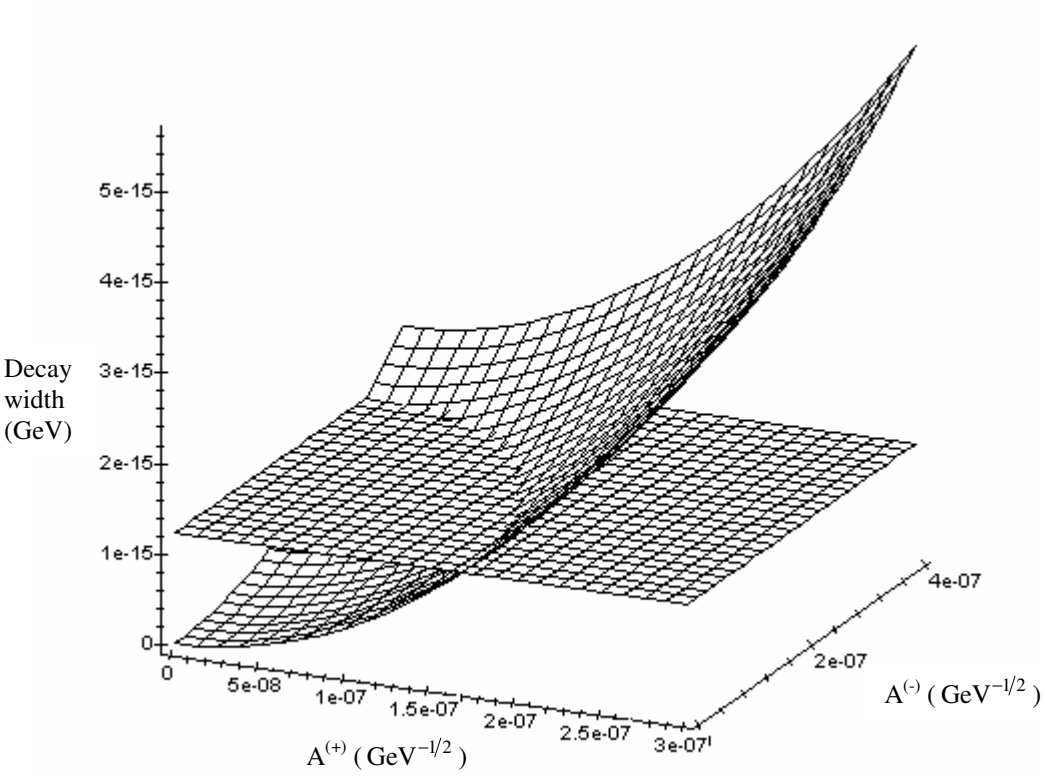

Figure 7.3 The decay width for $D^0 \to \bar{K}^{*0}\gamma$ *as a function of the factors* $A^{(\pm)}$*. The flat plane is the experimental value of the decay width.*

From this figure we can see that the graph showing the decay width as a function of the $A^{(\pm)}$ factors is cutting the experimental correct plane at an ellipse around the origin (figure 7.3 show only the first quadrant of this ellipse). However, in order for the values of $A^{(+)}$ and $A^{(-)}$ to be lying on this ellipse they have to be considerably larger (of order 10^1) than the values given in eq. 7.29. This would mean that contributions from higher order gluon condensates should be dominating considerably over the contributions from the first and zero order, and that we do not expect.

So what values would we get if we where to use eq. 4.34 for h_V in our calculations instead of the value 6? First of all, in order to use this expression we have to use a single value for the gluon condensate, so we choose the average value in eq. 7.9. This gives the value ~9,2 for h_V, which is obviously not 6, but is not a very large deviation either. Looking again specifically at the process $D^0 \to \bar{K}^{*0}\gamma$, we get the following value for the decay width when using the expression for h_V given by eq. 4.34

$$\Gamma(D^0 \to \bar{K}^{*0}\gamma) = (1,06 \pm 0,005)\cdot 10^{-16}\ \text{GeV} \tag{7.39}$$

This value is around 11 times lower than the experimental value; which is less than half of the deviation we had in the calculations where $h_V = 6$. So what do we really gain by using the eq. 4.34 for h_V instead of the value 6, besides an improvement on the decay width? We get the possibility to adjust the gluon condensate to fit the experimentally correct value for the decay width using a value that does not deviate considerably from the value that we have used. By adjusting the gluon condensate to around $\left\langle \frac{\alpha}{\pi} G^2 \right\rangle^{1/4} \approx 0,296$ GeV (which is a value we get by

plotting the decay width as a function of gluon condensate, and reading of where this graph crosses the experimental value), we get the correct value for the decay width for this specific decay process. Using the same value of the gluon condensate and the equation for h_V also for the other processes we have looked at, $D^0 \to \rho^0\gamma$, $D^0 \to \omega\gamma$ and $D^0 \to \varphi\gamma$, we gain a considerably less deviation from the experimental results (of order 10^0). An important note however, is that the decay width becomes very sensitive to the values of the gluon condensate when using eq. 4.34 for h_V. This is due to the factor $15m^2f_\pi^2$ when the gluon condensate approaches this value.

The effect of the constituent quark mass, m, may also be interesting to consider when we use eq. 4.34 for h_V. Using again the average value for the gluon condensate, 0,275 GeV, and adjusting the value of m so that the decay width fits the experimental value, we find that m ~ 0,213 GeV. This value is actually above the lower limit of the uncertainties for m, but it is a lower value than we would expect. This could have to do with the fact that we have not used a correct value for the gluon condensate or h_V.

Can we find a unique value for both the gluon condensate and the constituent quark mass, which gives the experimental correct decay width? The answer seems to be no, because if we plot the decay width as a function of both the gluon condensate and the constituent quark mass we get the graphs shown in figure 7.4 below. The decay width is plotted within the uncertainty ranges of the gluon condensate and the quark mass, and as we can see there are a number of different peaks crossing the experimentally correct value of the decay width (the upper surface).

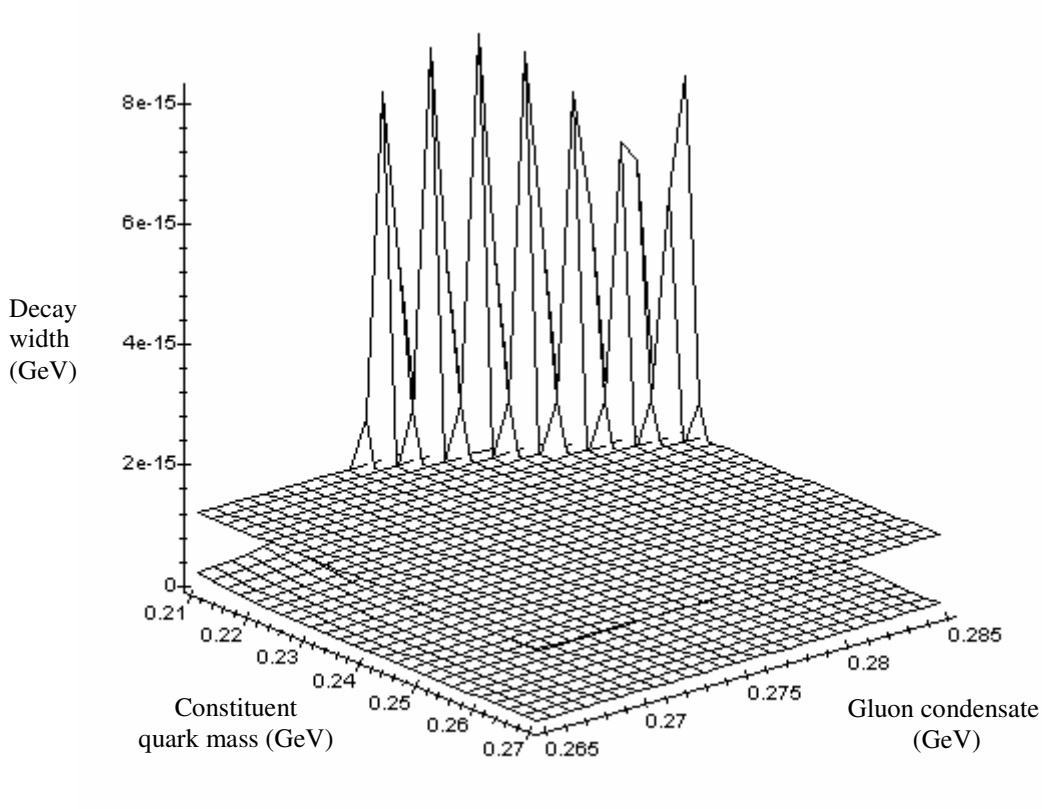

Figure 7.4 The decay width for $D^0 \to \overline{K}^{*0}\gamma$ as a function of constituent quark mass and gluon condensate. The upper flat plane is the experimental value of the decay width.

From figure 7.4 it may look like we have only seven peaks crossing the upper surface, but in fact there are a vast number of peaks crossing the experimentally correct plane (but our limited resolution does not show that in this graph). It therefore seems that we, from our limited data, have to specify either the condensate or the quark mass and then adjust the other parameter if we wish to find the correct value of the decay width, assuming the other parameters are correct. Although we cannot find a specific value for the gluon condensate and the constituent quark mass which makes the decay width agree with the experimental result, we have the ability to adjust these parameters so that the decay width does fit the experimental value, when using eq. 4.34 for h_V. This is not the case when we are using the numerical value 6 for the factor h_V.

Can we say anything about the values of the CKM matrix elements from our results in section 7.3? That would be nice, since these values were only given within 90 % confidence limits. If we plot the decay width as a function of the matrix elements and try to adjust these matrix elements to fit the experimental data, we only end up with matrix elements being larger than one. This is not physical since we know that the matrix elements should be proportional to a probability. We could of course try to use the value of the gluon condensate that we gained above (0,296 GeV) here as well, to get some information about the matrix elements. But then we still have uncertainties in the parameters we are using, especially in the gluon condensate, which makes the decay width very sensitive to changes in this factor. So the values we gain may not give us any more accurate value of the CKM matrix elements than the ones we already have.

If we instead look at the ratio between the decay widths, it would give us ratios between the matrix elements, as is seen from the following

$$\frac{\Gamma_{\vec{K}^{*0}}\left(V_{cs}V_{ud}\right)}{\Gamma_{\varphi}\left(V_{cs}V_{us}\right)} \sim \left(\frac{\left|V_{cs}{}^{*}V_{ud}\right|}{\left|V_{cs}{}^{*}V_{us}\right|}\right)^2 = \left(\frac{\left|V_{ud}\right|}{\left|V_{us}\right|}\right)^2 \tag{7.40}$$

Based on our limited data and the results from the last paragraph, i.e. by using the value 6 for h_V and different values for the gluon condensate, we find

$$\frac{\left|V_{ud}\right|}{\left|V_{us}\right|} = 0,8090 \cdot \sqrt{\frac{\Gamma_{\vec{K}^{*0}}}{\Gamma_{\varphi}}} \approx 4,46 \pm 0,18 \tag{7.41}$$

$$\frac{\left|V_{cd}\right|}{\left|V_{cs}\right|} = 0,8444 \cdot \sqrt{\frac{\Gamma_{\rho^0}}{\Gamma_{\varphi}}} \approx 0,475 \pm 0,009 \tag{7.42}$$

$$\frac{\left|V_{cd}\right|}{\left|V_{cs}\right|} = 0.8589 \cdot \sqrt{\frac{\Gamma_{\omega}}{\Gamma_{\varphi}}} \approx 0,483 \pm 0,009 \tag{7.43}$$

The numerical factor before the square root is a proportionality factor that has been calculated using the values from section 7.3. The experimental values are

$$\frac{\left|V_{ud}\right|}{\left|V_{us}\right|} = 4,43 \pm 0,046 \quad \text{and} \quad \frac{\left|V_{cd}\right|}{\left|V_{cs}\right|} = 0,225 \pm 0,012 \tag{7.44}$$

As we can see, the calculated value in eq. 7.41 does agree quite well with the experimental finding, while the result in eq. 7.42 and eq. 7.43 are twice as large as the experimental value. The reason for this deviation from the experimental result can be that the ρ^0 and ω are not $1/\sqrt{2}\left(-\left|d\bar{d}\right\rangle\right)$ and $1/\sqrt{2}\left(\left|d\bar{d}\right\rangle\right)$ states, as we have approximated them to be when using Fermi theory, giving in reality other values for the CKM matrix elements than the ones we have used. It also appears that calculated values do not change to any great extent, even if we change the value of the gluon condensate to 0,296 GeV. Apparently the change in the two decay widths in the fraction, when we use different values for the gluon condensate, is almost the same. That is, the ratios $\Gamma_{\bar{K}^{*0}}/\Gamma_{\varphi}$, $\Gamma_{\bar{K}^{*0}}/\Gamma_{\rho^0}$ and $\Gamma_{\bar{K}^{*0}}/\Gamma_{\omega}$ seem to be almost independent of what values of the gluon condensate we use.

If we look at the ratio between the non-factorizable diagrams and the factorizable diagrams, we find that the non-factorizable part is to some extent dominating; about a factor 5 over the factorizable diagrams. This domination of the non-factorizable part was what we expected from our discussion in chapter 3.2 and in the beginning of this chapter, and is roughly of the same order as we have calculated (about 7 times over the factorizable diagrams).

We may also look at the contribution from the $A^{(\pm)}$ factors from the diagrams without any gluon condensate as compared to the diagrams with gluon condensate to first order, and see which of the two that contributes mostly. From a strait forward calculation it appears that the diagrams without gluon condensate are contributing mostly, about 2,3 times over the diagrams with the gluon condensate to first order. We expect this to be a general pattern, i.e. we also expect the first order in gluon condensate to be dominant over the second order. Although it could be interesting to see if this is the case and how large the domination then would be, it seems at the moment to be an overwhelmingly task, considering all the different diagrams that we can have.

Bibliography

[1] B. Pohv, K. Rith, C. Scholz and F. Zetsche: Particles and Nuclei An Introduction to the Physical Concepts, Fourth Edition, Springer, 2004, 396 pages

[2] Aksel Hiorth: On Weak Decays of Heavy-Light Mesons Using Quark Models, Heavy Quark- and Chiral-Symmetries, Thesis submitted for the degree of Doctor Scientiarum, Faculty of Mathematics and Natural Sciences, University of Oslo, 2003, 127 pages

[3] J. O. Eeg and Aksel Hiorth: Chiral quark models and their applications. 2004

[4] J. O. Eeg and Aksel Hiorth: Heavy-light chiral quark model. Phys. Rev. D **66**, 2002

[5] John Atle Macdonald Sørensen: The Decay Process $B \to D^* \gamma$ in the $HL\chi QM$, Thesis submitted for the degree of Candidatus Scientiarum, Department of Physics, University of Oslo, 2005, 133 pages

[6] L. Wolfenstein: Parametrization of the Kobayashi-Maskawa Matrix, Phys. Rev. Lett. **51**, 1945-1947, 1983

[7] Michael E. Peskin and Daniel V. Schroeder: An Introduction to Quantum Field Theory, Westview press, 1995, 842 pages

[8] A. J. Buras: QCD factors a_1 and a_2 beyond leading order logarithms versus factorization in non-leptonic heavy meson decays. Nucl. Phys. B **434**, 606-518, 1995

[9] J. A. M. Vermaseren: Symbolic Manipulation with FORM, CAN, 1991, 258 pages

[10] J. O. Eeg, S. Fajfer and J. Zupan: Nonfactorizable contributions to the decay mode $D^0 \to K^0 \overline{K}^0$, Phys. Rev. D **64,** 2001.

[11] S. Eidelman et al. (Particle Data Group), Phys. Lett. B **592**, 1 (2004) (URL: http://pdg.lbl.gov)

[12] G. L. Squires: Practical Physics, Cambridge university press, 2001, 212 pages

[13] A. Deandrea et al.: Semileptonic B→ρ and B→a1 transitions in a quark-meson model, Phys. Rev. D 59, 1999

Other sources of information:

F. Mandl and G. Shaw; Quantum Field Theory, Revised Edition, John Wiley & Sons, 2002, 358 pages

Kenneth S. Krane: Introductory Nuclear Physics, John Wiley & Sons, 1988, 845 pages

John F. Donoghue, Eugene Golowich, Barry R. Holstein; Dynamics of the standard model, Cambridge university press, 1992, 540 pages

C. K. Cheung, G. E. Keough and Michael May; Getting started with Maple, John Wiley & Sons, 1998, 172 pages

Appendix A

Mathematical Formulae

A.1 Divergent Loop Integrals

In the calculations of the diagrams we often end up with divergent loop integrals. For these integrals we use the symbol I_n, where the subscript n represents the power of the denominator in the integral. For n equals 1 we have a quadratically divergent integral and for n equals 2 we have a logarithmic divergent integral.

$$I_1 = \int \frac{d^D p}{(2\pi)^D} \frac{1}{(p^2 - m^2)} \tag{A.1}$$

$$I_2 = \int \frac{d^D p}{(2\pi)^D} \frac{1}{(p^2 - m^2)^2} \tag{A.2}$$

In addition we have also used the linearly divergent integral

$$I_{3/2} = \int \frac{d^D p}{(2\pi)^D} \frac{1}{(v \cdot p)(p^2 - m^2)} \tag{A.3}$$

These integrals can, however, be related to physical quantities. For example, from the pure light sector we can get the relations

$$f_\pi^2 = -4im^2 N_C I_2 + \frac{1}{24m^2} \left\langle \frac{\alpha_S}{\pi} G^2 \right\rangle \tag{A.4}$$

and

$$\langle \bar{q}q \rangle = -4imN_C I_1 - \frac{1}{12m} \left\langle \frac{\alpha_S}{\pi} G^2 \right\rangle \tag{A.5}$$

The heavy-light sector gives us a relation for the linearly divergent integral $I_{3/2}$

$$\delta g_A = 1 - g_A = -\frac{4}{3} i G_H^2 N_C (I_{3/2} - \kappa_0) \tag{A.6}$$

where

$$\kappa_0 = -i\frac{m}{16\pi} \tag{A.7}$$

We can rewrite these expressions to get the following

$$I_1 = i\frac{\langle\bar{q}q\rangle}{4mN_C} + \frac{i}{48m^2N_C}\left\langle\frac{\alpha_S}{\pi}G^2\right\rangle \tag{A.8}$$

$$I_2 = i\frac{f_\pi^2}{4m^2N_C} - \frac{i}{96m^4N_C}\left\langle\frac{\alpha_S}{\pi}G^2\right\rangle \tag{A.9}$$

$$I_{3/2} = \frac{3}{4}\frac{i\delta g_A}{G_H^2N_C} + i\frac{m}{16\pi} \tag{A.10}$$

For $n \geq 3$, the integrals I_n can be calculated using the methods in the next paragraph.

A.2 Dimensional Regularization

The idea of dimensional regularization can be stated as follows: compute the Feynman diagram as an analytical function of the dimensionality of space-time, d. For a sufficiently small d any loop-momentum integral will converge and the Ward identity (a diagrammatic identity that imposes symmetry on quantum mechanical amplitudes, a sort of current conservation statement) will be fulfilled. The final expression for any observable quantity should have a well-defined limit as $d \to 4$.

We look at an example and see how it works. Let space-time have one time-dimension and $d-1$ space-dimensions. We can then Wick-rotate the Feynman integrals over d-dimensional Euclidian space. The Wick rotation is a mathematical trick used in order to remove the minus sign in the Minkowski metric through a rotation of 90° in the p^0 plane (where we have a Euclidian 4-momentum defined as $p_E = \left(p_E^0, \vec{p}_E\right)$, and where $p^0 \equiv ip_E^0$). By changing variables to the Euclidian version, we can evaluate the integral in d-dimensional spherical coordinates. (Had it not been for the minus sign in the metric we could have performed the entire integral in four dimensional spherical coordinates at once.)

We look at the integral

$$\int\frac{d^dp_E}{(2\pi)^d}\frac{1}{({p_E}^2+\Delta)^2} = \int\frac{d\Omega_d}{(2\pi)^d}\cdot\int_0^\infty dp_E\,\frac{{p_E}^{d-1}}{({p_E}^2+\Delta)^2} \tag{A.11}$$

The first factor on the right-hand side of the equal sign contains the area of a unit sphere in d dimensions. In order for us to compute it, we use the following trick

$$\left(\sqrt{\pi}\right)^d = \left(\int dx\ e^{-x^2}\right)^d = \int d^d x\ \exp\left(-\sum_{i=1}^{d} x_i^2\right)$$
$$= \int d\Omega_d \int_0^\infty dx\ x^{d-1} e^{-x^2} = \left(\int d\Omega_d\right) \cdot \frac{1}{2} \int_0^\infty d(x^2)\,(x^2)^{\frac{d}{2}-1} e^{-(x^2)} \qquad \text{(A.12)}$$
$$= \left(\int d\Omega_d\right) \cdot \frac{1}{2}\Gamma\left(d/2\right)$$

This gives us the area of a d-dimensional unit sphere

$$\int d\Omega_d = \frac{2\pi^{d/2}}{\Gamma\left(d/2\right)} \qquad \text{(A.13)}$$

The other factor on the right-hand side of the equation is

$$\int_0^\infty dp_E \frac{{p_E}^{d-1}}{({p_E}^2+\Delta)^2} = \frac{1}{2}\int_0^\infty d({p_E}^2) \frac{({p_E}^2)^{\frac{d}{2}-1}}{({p_E}^2+\Delta)^2}$$
$$= \frac{1}{2}\left(\frac{1}{\Delta}\right)^{2-\frac{d}{2}} \int_0^1 dx x^{1-\frac{d}{2}} (1-x)^{\frac{d}{2}-1} \qquad \text{(A.14)}$$

where we have substituted $x = \Delta/\left({p_E}^2+\Delta\right)$ in the second line. By using the definition of the so called beta-function

$$\int_0^1 dx x^{\alpha-1}(1-x)^{\beta-1} = B(\alpha,\beta) = \frac{\Gamma(\alpha)\Gamma(\beta)}{\Gamma(\alpha+\beta)} \qquad \text{(A.15)}$$

we can evaluate the integral over x. The final result for the d-dimensional integral then becomes

$$\int \frac{d^d p_E}{(2\pi)^d} \frac{1}{({p_E}^2+\Delta)^2} = \frac{1}{(4\pi)^{d/2}} \frac{\Gamma\left(2-\frac{d}{2}\right)}{\Gamma(2)} \left(\frac{1}{\Delta}\right)^{2-\frac{d}{2}} \qquad \text{(A.16)}$$

Since $\Gamma(z)$ has isolated poles at z = 0, -1,-2,…, this integral has isolated poles at d = 4, 6, 8,… We are interested in the situation when $d \to 4$, and we therefore define $\varepsilon = 4 - d$, and uses the approximation

$$\Gamma\left(2-\frac{d}{2}\right) = \Gamma\left(\varepsilon/2\right) = \frac{2}{\varepsilon} - \gamma + \mathcal{O}(\varepsilon) \qquad \text{(A.17)}$$

γ is here a constant called the Euler-Mascheroni constant, and has the approximate value of 0,5772. This constant will, however, cancel for all observable quantities. We get

$$\int \frac{d^d p_E}{(2\pi)^d} \frac{1}{(p_E{}^2+\Delta)^2} \underset{d\to 4}{\to} \frac{1}{(4\pi)^{d/2}} \left(\frac{2}{\varepsilon} - \log\Delta - \gamma + \log(4\pi) + \mathcal{O}(\varepsilon) \right) \tag{A.18}$$

For finite integrals involving both a heavy and a light quark propagator, we first symmetrize the integral, that is we Feynman-parametrize it with λ as an integration variable

$$\begin{aligned} L^{m,\Delta}_{p,q} &\equiv \int \frac{d^d k}{(2\pi)^d} \frac{1}{(k^2-m^2)^p (v\cdot k-\Delta)^q} \\ &= \frac{\Gamma(p+q)}{\Gamma(p)\Gamma(q)} \int_0^\infty d\lambda \int \frac{d^d k}{(2\pi)^d} \frac{2^q \lambda^{q-1}}{(k^2-m^2+2\lambda v\cdot k)^{p+q}} \end{aligned} \tag{A.19}$$

For the integrals we look at we have $\Delta = 0$. After the symmetrization we integrate out the momentum p using the formulas below. First we identify

$$\hat{J} f(p) = \int d^n p \frac{1}{(p^2+2pk+M^2)^\alpha} f(p) \tag{A.20}$$

$$J_0 = \frac{i\pi^{n/2} i^n}{(M^2-k^2)^{\alpha-n/2}\Gamma(\alpha)} \tag{A.21}$$

Then we can use the p integrals below

$$I_0 = \hat{J}_1 = \frac{i\pi^{n/2}}{(M^2-k^2)^{\alpha-n/2}} \frac{\Gamma\left(\alpha-\frac{n}{2}\right)}{\Gamma(\alpha)} = \Gamma\left(\alpha-\frac{n}{2}\right) J_0 \tag{A.22}$$

$$I^\mu = \hat{J} p^\mu = (-k^\mu) I_0 \tag{A.23}$$

$$I_2 = \hat{J} p^2 = J_0 \left\{ k^2 \Gamma\left(\alpha-\frac{n}{2}\right) + \frac{n}{2}\Gamma\left(\alpha-1-\frac{n}{2}\right)(M^2-k^2) \right\} \tag{A.24}$$

$$I^{\mu\nu} = \hat{J} p^\mu p^\nu = J_0 \left\{ k^\mu k^\nu \Gamma\left(\alpha-\frac{n}{2}\right) + \frac{n}{2}\Gamma\left(\alpha-1-\frac{n}{2}\right) g^{\mu\nu}(M^2-k^2) \right\} \tag{A.25}$$

$$\begin{aligned} I^{\mu\nu\lambda} = \hat{J} p^\mu p^\nu p^\lambda = J_0 \{ &-k^\mu k^\nu k^\lambda \Gamma\left(\alpha-\frac{n}{2}\right) - \frac{n}{2}\Gamma\left(\alpha-1-\frac{n}{2}\right)(M^2-k^2)\cdot \\ &(g^{\mu\nu}k^\lambda + g^{\mu\lambda}k^\nu + g^{\nu\lambda}k^\mu) \} \end{aligned} \tag{A.26}$$

$$I_2^\mu = \hat{J} p^2 p^\mu = -J_0 k^\mu \left\{ k^2 \Gamma\left(\alpha-\frac{n}{2}\right) + \frac{n+2}{2}\Gamma\left(\alpha-1-\frac{n}{2}\right)(M^2-k^2) \right\} \tag{A.27}$$

Here $k = \lambda v$, $v\cdot v = 1$ and $n = d = 4$ for us. Our final general integral for calculating the λ integral has the following form

$$\int \frac{x^\beta}{(x^2+m^2)^\alpha} dx = \frac{\Gamma\left(\frac{\beta+1}{2}\right)\Gamma\left(\alpha-\frac{\beta+1}{2}\right)}{2\Gamma(\alpha)(m^2)^{\alpha-\frac{\beta+1}{2}}} \tag{A.28}$$

Using the expressions above we can now calculate specific integrals that appear in the calculations.

A.3 Integrals

Although the procedure for calculating the diagrams is sketched above, we will here give an explicit example of how we can use the equations (eq. A.19 to eq. A.28) in the last paragraph to calculate the integrals. Let's look at the following integral

$$\int \frac{d^4p}{(2\pi)^4} \frac{p^\mu}{(v\cdot p)\left(p^2-m^2\right)^4} \tag{A.29}$$

In order to calculate this integral, we have to use eq. A.19, where $\Delta = 0$.

$$\begin{aligned}\int \frac{d^4p}{(2\pi)^4} \frac{p^\mu}{(v\cdot p)\left(p^2-m^2\right)^4} &= \frac{\Gamma(4+1)}{\Gamma(4)\cdot\Gamma(1)} \int_0^\infty d\lambda \int \frac{d^4k}{(2\pi)^4} \frac{2^1}{\left(k^2-m^2+2\lambda v\cdot k\right)^5}\cdot p^\mu \\ &= 4\cdot \int_0^\infty d\lambda \int \frac{d^4k}{(2\pi)^4} \frac{2^1\cdot p^\mu}{\left(k^2-m^2+2\lambda v\cdot k\right)^5} \\ &= \frac{8}{(2\pi)^4}\cdot \int_0^\infty d\lambda\ \hat{J}f(p)\end{aligned} \tag{A.30}$$

where $f(p) = p^\mu$. We now look at the expression $\hat{J}f(p) = \hat{J}p^\mu$. It is given by eq. A.23 and gives us in our example

$$\begin{aligned}\hat{J}p^\alpha &= (-k^\mu)I_0 \\ &= (-k^\mu)\frac{i\pi^{n/2}}{(M^2-k^2)^{\alpha-n/2}} \frac{\Gamma\left(\alpha-\frac{n}{2}\right)}{\Gamma(\alpha)} \\ &= (-\lambda v^\mu)\Gamma\left(5-\frac{4}{2}\right)J_0 \\ &= -2\lambda v^\mu J_0\end{aligned} \tag{A.31}$$

Here we have used the fact that $k = \lambda v$ from the last paragraph and that n = 4. We also have that $\alpha = 5$ in the integral that we are looking at. We now put our expression back into eq. A.30, which gives

$$
\begin{aligned}
\int \frac{d^4p}{(2\pi)^4}\frac{p^\mu}{(v\cdot p)\left(p^2-m^2\right)^4} &= \frac{8}{(2\pi)^4}\cdot\int_0^\infty d\lambda\ \hat{J}f(p)\\
&= \frac{8}{(2\pi)^4}\cdot\int_0^\infty d\lambda(-2\lambda v^\mu)J_0\\
&= \frac{16v^\mu}{(2\pi)^4}\cdot\int_0^\infty d\lambda(-\lambda)\frac{i\pi^2}{(M^2-k^2)^3\Gamma(5)}\\
&= \frac{16v^\mu}{(2\pi)^4}\cdot\int_0^\infty d\lambda(-\lambda)\frac{i\pi^2}{(-m^2-\left(\lambda v^\alpha\right)^2)^3\Gamma(5)}\\
&= \frac{iv^\mu}{24\pi^2}\cdot\int_0^\infty d\lambda\frac{\lambda}{(m^2+\lambda^2)^3}\\
&= \frac{iv^\mu}{24\pi^2}\frac{\Gamma\left(\frac{1+1}{2}\right)\Gamma\left(3-\frac{1+1}{2}\right)}{2\Gamma(3)(m^2)^{3-\frac{1+1}{2}}}\\
&= \frac{iv^\mu}{96\pi^2m^4}
\end{aligned}
\tag{A.32}
$$

Where we used that $M^2 = -m^2$ and eq. A.28. In the same manner we can calculate other diagrams of the same type. This gives us the following results:

$$\int \frac{d^4p}{(2\pi)^4}\frac{p^\alpha p^\beta}{\left(p^2-m^2\right)^8} = \frac{-ig^{\alpha\beta}}{6720\pi^2m^{10}} \tag{A.33}$$

$$\int \frac{d^4p}{(2\pi)^4}\frac{p^\alpha p^\beta}{\left(p^2-m^2\right)^7} = \frac{ig^{\alpha\beta}}{3840\pi^2m^8} \tag{A.34}$$

$$\int \frac{d^4p}{(2\pi)^4}\frac{p^\alpha p^\beta}{\left(p^2-m^2\right)^6} = \frac{-ig^{\alpha\beta}}{1920\pi^2m^6} \tag{A.35}$$

$$\int \frac{d^4p}{(2\pi)^4}\frac{p^\alpha p^\beta}{\left(p^2-m^2\right)^5} = \frac{ig^{\alpha\beta}}{768\pi^2m^4} \tag{A.36}$$

$$\int \frac{d^4p}{(2\pi)^4}\frac{p^\alpha p^\beta}{\left(p^2-m^2\right)^4} = \frac{-ig^{\alpha\beta}}{192\pi^2m^2} \tag{A.37}$$

$$\int \frac{d^4p}{(2\pi)^4}\frac{p^\alpha}{(v\cdot p)\left(p^2-m^2\right)^5} = \frac{-iv^\alpha}{192\pi^2m^6} \tag{A.38}$$

$$\int \frac{d^4p}{(2\pi)^4}\frac{p^\alpha}{(v\cdot p)\left(p^2-m^2\right)^4} = \frac{iv^\alpha}{96\pi^2m^4} \tag{A.39}$$

$$\int \frac{d^4p}{(2\pi)^4}\frac{p^\alpha}{(v\cdot p)\left(p^2-m^2\right)^3} = \frac{-iv^\alpha}{32\pi^2m^2} \tag{A.40}$$

$$\int \frac{d^4p}{(2\pi)^4}\frac{1}{(v\cdot p)\left(p^2-m^2\right)^5} = \frac{5i}{1024\pi m^7} \tag{A.41}$$

$$\int \frac{d^4p}{(2\pi)^4} \frac{1}{(v\cdot p)\left(p^2-m^2\right)^4} = \frac{-i}{128\pi m^5} \tag{A.42}$$

$$\int \frac{d^4p}{(2\pi)^4} \frac{1}{(v\cdot p)\left(p^2-m^2\right)^3} = \frac{i}{64\pi m^3} \tag{A.43}$$

$$\int \frac{d^4p}{(2\pi)^4} \frac{1}{\left(p^2-m^2\right)^8} = \frac{i}{80640\pi^2 m^{12}} \tag{A.44}$$

$$\int \frac{d^4p}{(2\pi)^4} \frac{1}{\left(p^2-m^2\right)^7} = \frac{-i}{11520\pi^2 m^{10}} \tag{A.45}$$

$$\int \frac{d^4p}{(2\pi)^4} \frac{1}{\left(p^2-m^2\right)^6} = \frac{i}{1920\pi^2 m^8} \tag{A.46}$$

$$\int \frac{d^4p}{(2\pi)^4} \frac{1}{\left(p^2-m^2\right)^5} = \frac{-i}{384\pi^2 m^6} \tag{A.47}$$

$$\int \frac{d^4p}{(2\pi)^4} \frac{1}{\left(p^2-m^2\right)^4} = \frac{i}{96\pi^2 m^4} \tag{A.48}$$

$$\int \frac{d^4p}{(2\pi)^4} \frac{1}{\left(p^2-m^2\right)^3} = \frac{-i}{32\pi^2 m^2} \tag{A.49}$$

These integrals will be used when we calculate the partial diagrams and when we do the integration in the FORM programs.

A.4 Uncertainties

We list here the relations we have used in connection with uncertainty calculations done primarily in chapter 7. These we have taken from [12]. If Z is what we will calculate and ΔZ is the uncertainly in the result, we have the following relations:

$$Z = \begin{cases} A+B \\ A-B \end{cases} \quad \text{gives} \quad \Delta Z = \sqrt{(\Delta A)^2 + (\Delta B)^2} \tag{A.50}$$

and

$$Z = \begin{cases} AB \\ A/B \end{cases} \quad \text{gives} \quad \Delta Z = Z\left(\left(\frac{\Delta A}{A}\right)^2 + \left(\frac{\Delta B}{B}\right)^2\right)^{1/2} \tag{A.51}$$

where ΔA and ΔB are the standard errors in A and B respectively. For a constant k having $\Delta k = 0$ we get

$$\begin{aligned} Z = kA \quad &\text{gives} \quad \Delta Z = k\Delta A \\ Z = \frac{k}{A} \quad &\text{gives} \quad \Delta Z = \frac{k\Delta A}{A^2} \end{aligned} \tag{A.52}$$

Expanding these relations to expressions with more than two independent terms, gives us

$$Z = \begin{cases} A + B + C + ... \\ A - B - C - ... \end{cases} \quad \text{gives} \quad \Delta Z = \sqrt{(\Delta A)^2 + (\Delta B)^2 + (\Delta C)^2 + ...} \tag{A.53}$$

and

$$Z = ABC... \quad \text{gives} \quad \Delta Z = Z\left(\left(\frac{\Delta A}{A}\right)^2 + \left(\frac{\Delta B}{B}\right)^2 + \left(\frac{\Delta C}{C}\right)^2 + ...\right)^{1/2} \tag{A.54}$$

If we have a function of several variables

$$Z = Z(A, B, C, ...) \tag{A.55}$$

The standard error of Z is then given by

$$(\Delta Z)^2 = (\Delta Z_A)^2 + (\Delta Z_B)^2 + (\Delta Z_C)^2 + ... \tag{A.56}$$

where

$$\Delta Z_A = \frac{\partial Z}{\partial A}\Delta A \quad \text{and so on} \tag{A.57}$$

with ΔA being the standard error of A.

Appendix B

FORM program

Here we include the program used in FORM to primarily calculate the product of two traces. We will take the process from figure 6.48 as an example, i.e. where we have one photon and one gluon coupled to the light quark in the diagram for the annihilating D-meson, and one gluon coupled to the lower quark in the V-meson creation diagram. The program will then look like this

```
*
*Program name: DfgVg1.form
*A program to calculate the process (D -> photon + gluon) x (0 -> gluon (lower) + V)
*

Vector p, v, y, z, V;
Indices alpha, beta, sigma, rho, mu, nu, lambda, delta;
Symbol m, Q, Qv, Pi, I2, i;
.global

Nwrite statistics;

Global T=g_(1,p)+m*gi_(1);
Global R(mu?, nu?, alpha?,
beta?)=T*g_(1,beta)*T*g_(1,nu)*T*g_(1,mu)*T*g_(1,alpha)*T+T*g_(1,nu)*T*g_(1,beta)*T*g_(1,mu)*T*
g_(1,alpha)*T+T*g_(1,nu)*T*g_(1,mu)*T*g_(1,beta)*T*g_(1,alpha)*T;
Global F(mu?, nu?)=y(mu)*z(nu)-y(nu)*z(mu);

*
*Multiplication of the traces
*

Global Tr=g_(1,lambda)*g7_(1)*Qv*(gi_(1)+g_(1,v))*g5_(1)*F(mu, nu)*R(mu, nu, alpha,
beta)*V(delta)*(m^2*(-i/(32*Pi^2*m^2))*(2*g5_(2)+gi_(2))-
I2)*g_(2,lambda)*g_(2,delta)*(g_(2,sigma)*g_(2,rho)-g_(2,rho)*g_(2,sigma));
trace4,1;
trace4,2;
.sort;

Global Z1=Q^5*Tr*(d_(alpha, sigma)*d_(beta, rho)-d_(alpha, rho)*d_(beta, sigma));
print Z1;
.sort

*
*Integration
*

Id p.p*Q = 1+m^2*Q;
Id p.v*Qv = 1;
Global Z2=Z1;
print Z2;
```

```
.sort

Id p.y*p.V*Qv =(y.V-y.v*V.v)*p.p*Qv/3;
Id p.z*p.V*Qv =(z.V-z.v*V.v)*p.p*Qv/3;
Id e_(p,v,z,V)*p.y*Qv = e_(y,v,z,V)*p.p*Qv/3;
Id e_(p,v,V,y)*p.z*Qv = e_(z,v,V,y)*p.p*Qv/3;
Id e_(p,v,y,z)*p.V*Qv = e_(V,v,y,z)*p.p*Qv/3;
Global Z3=Z2;
print Z3;
.sort


Id p.p*Q = 1+ m^2*Q;
Global Z4=Z3;
print Z4;
.sort

Id e_(p,V,y,z)*Qv = e_(v,V,y,z);
Id p.y*Qv = y.v;
Id p.z*Qv = z.v;
Global Z5=Z4;
print Z5;
.sort

Id e_(p,V,y,z) = 0;
Id p.y = 0;
Id p.z = 0;
Global Z6=Z5;
print Z6;
.sort


Id Qv*Q^4 = -i/(128*Pi*m^5);
Global Z7=Z6;
Print Z7;
.sort

Id Qv*Q^3 = i/(64*Pi*m^3);
Global Z8=Z7;
print Z8;
.sort

Id Q^4 = i/(96*Pi^2*m^4);
Global Z9=Z8;
print Z9;
.sort

Id Q^3 = -i/(32*Pi^2*m^2);
Global Z10=Z9;
print Z10;
.sort

Id i^2 = -1;
Global sum=Z10;
print sum;

.end;
```

We will not go through in detail all the commands and their meanings in the program, but just look at some of the important concepts used here. For more details on the program structure and the meaning of the different commands, see ref. [9].

However, a few details have to be mentioned. The symbol g_(1,mu) is the same as the gamma matrix γ^μ, where the number 1 refers to the first trace. Since we are multiplying two traces, we have to specify to which trace each matrix belongs, in order for FORM to be able to calculate the product. Also, FORM does not make any difference between γ^μ and γ_μ, so we use the same symbol for both in the program. In addition, we also find symbols like g_(1,p), where p is declared a vector. This symbol means an expression of the type $\gamma \cdot p$, which frequently occurs in our program. Another similar symbol is gi_(1), which is the unit gamma matrix.

The first thing the program does is to implement different variables, such as vectors, indices and symbols. p is the quark energy-momentum 4-vector in the loop, v is the velocity 4-vector of the heavy c-quark, V contains the vector particle polarization 4-vector $\varepsilon(V)$, y is the photon momentum 4-vector (called k in the calculations of the effective propagators) and z is the photon polarization 4-vector. Of the symbols m is the constituent light quark mass, Q is defined to be $Q \equiv \frac{1}{p^2 - m^2}$ and Qv as $Q_v \equiv \frac{1}{v \cdot p}$. The symbol I2 is the logarithmic divergent integral specified in the appendix A.1.

After the implementation of the different variables, there is a declaration of three different functions: T, which is the numerator of the usual propagator S(p), i.e. $T = \gamma \cdot p + m$, R, which is the large sum of propagators given in eq. 5.29, and F, which is the electromagnetic tensor expressed in the photons momentum and polarization vector; $F_{\alpha\beta} = k_\alpha \varepsilon_\beta(\gamma) - k_\beta \varepsilon_\alpha(\gamma)$ $= y(\alpha)z(\beta) - z(\alpha)y(\beta)$, as defined earlier. We have chosen to declare these functions, and not put the expressions directly into the expression for the trace, in order to make the trace expression more easily readable.

Next, the product of the two traces is calculated and printed. Studying the expression closely one can see a number of symbols of the type d_(alpha, sigma). These are defined as d_(alpha, sigma) = $g_{\alpha\sigma}$, giving, in this particular program, an expression of the type $(g_{\alpha\sigma}g_{\beta\rho} - g_{\alpha\rho}g_{\beta\sigma})$.

Often, especially for diagrams which require integration by FORM, the now printed expression is large. In order to shorten it we use of the so called Id-functions. These Id-functions are identity expressions used in order to integrate the trace product. F. ex. the expression Id Qv*Q^4 = -i/(128*Pi*m^5) is the same as

$$\int \frac{d^4p}{(2\pi)^4} \frac{1}{v \cdot p} \frac{1}{\left(p^2 - m^2\right)^4} = -\frac{i}{128\pi m^5} \qquad \text{(B.1)}$$

which is also given in the appendix A.3 (eq. A.43). We use these to eliminate statements like Qv*Q^4 from the original expression for the product of the traces. Caution has to be taken though when we do this, since an Id-function for Qv followed by an Id-function for Q^4

would eliminate the expression Qv*Q^4, but would not give the correct answer, since the product of the two expression is not independent as we do the integral. That is, we cannot separate the two expressions Qv and Q^4 and integrate each expression on its own, but must integrate them as a whole. It is therefore important to print and check the output after each Id operation, thereof so many, seemingly unnecessary, print statements.